This article was downloaded by:
On: *21 January 2011*
Access details: *Access Details: Free Access*
Publisher *Taylor & Francis*
Informa Ltd Registered in England and Wales Registered Number: 1072954 Registered office: Mortimer House, 37-41 Mortimer Street, London W1T 3JH, UK

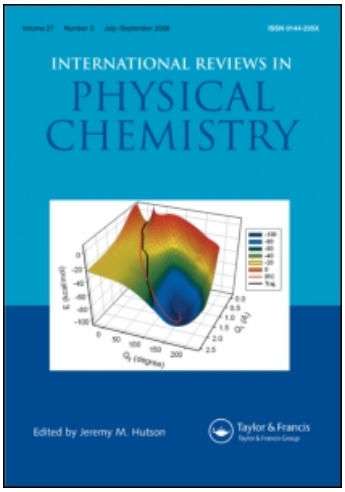

International Reviews in Physical Chemistry
Publication details, including instructions for authors and subscription information:
http://www.informaworld.com/smpp/title~content=t713724383

Recent advances in electronic structure theory: Method of moments of coupled-cluster equations and renormalized coupled-cluster approaches

Piotr Piecuch; Karol Kowalski; Ian S. O. Pimienta; Michael J. Mcguire

Online publication date: 26 November 2010

To cite this Article Piecuch, Piotr , Kowalski, Karol , Pimienta, Ian S. O. and Mcguire, Michael J.(2002) 'Recent advances in electronic structure theory: Method of moments of coupled-cluster equations and renormalized coupled-cluster approaches', International Reviews in Physical Chemistry, 21: 4, 527 — 655
To link to this Article: DOI: 10.1080/0144235021000053811
URL: http://dx.doi.org/10.1080/0144235021000053811

PLEASE SCROLL DOWN FOR ARTICLE

Full terms and conditions of use: http://www.informaworld.com/terms-and-conditions-of-access.pdf

This article may be used for research, teaching and private study purposes. Any substantial or systematic reproduction, re-distribution, re-selling, loan or sub-licensing, systematic supply or distribution in any form to anyone is expressly forbidden.

The publisher does not give any warranty express or implied or make any representation that the contents will be complete or accurate or up to date. The accuracy of any instructions, formulae and drug doses should be independently verified with primary sources. The publisher shall not be liable for any loss, actions, claims, proceedings, demand or costs or damages whatsoever or howsoever caused arising directly or indirectly in connection with or arising out of the use of this material.

INT. REVIEWS IN PHYSICAL CHEMISTRY, 2002
VOL. 21, NO. 4, 527–655

Taylor & Francis
Taylor & Francis Group

Recent advances in electronic structure theory: Method of moments of coupled-cluster equations and renormalized coupled-cluster approaches

PIOTR PIECUCH*†, KAROL KOWALSKI, IAN S. O. PIMIENTA and MICHAEL J. MCGUIRE

Department of Chemistry, Michigan State University, East Lansing, MI 48824, USA

The recently developed new approach to the many-electron correlation problem in atoms and molecules, termed the method of moments of coupled-cluster (CC) equations (MMCC), is reviewed. The ground-state MMCC formalism and its extension to excited electronic states via the equation-of-motion coupled-cluster (EOMCC) approach are discussed. The main principle of all MMCC methods is that of the non-iterative energy corrections which, when added to the ground- and excited-state energies obtained in the standard CC calculations, such as CCSD or EOMCCSD, recover the exact, full configuration interaction (CI) energies. Three types of the MMCC approximations are reviewed in detail: (i) the CI-corrected MMCC methods, which can be applied to ground and excited states; (ii) the renormalized and completely renormalized CC methods for ground states; and (iii) the quasi-variational MMCC approaches for the ground-state problem, including the quadratic MMCC models. It is demonstrated that the MMCC formalism provides a new theoretical framework for designing 'black-box' CC approaches that lead to an excellent description of entire potential energy surfaces of ground- and excited-state molecular systems with an ease of use of the standard single-reference methods. The completely renormalized (CR) CCSD(T) and CCSD(TQ) methods and their quadratic and excited-state MMCC analogues remove the failing of the standard CCSD, CCSD(T), EOMCCSD and similar methods at larger internuclear separations and for states that normally require a genuine multireference description. All theoretical ideas are illustrated by numerical examples involving bond breaking, excited vibrational states, reactive potential energy surfaces and difficult cases of excited electronic states. The description of the existing and well-established variants of the MMCC theory, such as CR-CCSD(T), is augmented by the discussion of future prospects and potentially useful recent developments, including the extension of the black-box CR-CCSD(T) method to excited states.

Downloaded At: 16:32 21 January 2011

Contents

*Author for correspondence; e-mail: piecuch@cem.msu.edu; internet: www.cem.msu.edu/~piecuch/group-web

†Alfred P. Sloan Research Fellow.

International Reviews in Physical Chemistry ISSN 0144–235X print/ISSN 1366–591X online © 2002 Taylor & Francis Ltd
http://www.tandf.co.uk/journals
DOI: 10.1080/0144235021000053811

Downloaded At: 16:32 21 January 2011

1. Introduction

The standard single-reference coupled-cluster (CC) methods [1–5], such as CCSD [6] (CC approach with singles and doubles), and the non-iterative CCSD$+$T(CCSD) = CCSD[T] [7] and CCSD(T) [8] approaches that account for the effect of triexcited clusters using arguments based on the many-body perturbation theory (MBPT), in either the spin-orbital [6–8] and spin-free [9–11] or orthogonally spin-adapted [12–14] forms, are nowadays routinely used in accurate *ab initio* calculations for atomic and molecular systems [15–19]. The idea of adding the *a*

posteriori corrections due to higher-than-doubly excited clusters to CCSD energies, on which the CCSD[T] and CCSD(T) approaches and their more recent CCSD(TQ$_f$) extension [20] are based, is particularly appealing, since it leads to methods that offer the best compromise between high accuracy and relatively low computer cost, as has been demonstrated over and over in numerous molecular applications [15–19]. Although it is nowadays possible to include the triply, quadruply and even pentuply excited clusters in a completely iterative manner (a great new programming strategy developed by Kállay and Surján [21] allows one to write efficient computer codes for CC methods with clusters of any rank), the resulting CCSDT (CC singles, doubles and triples) [22, 23], CCSDTQ (CC singles, doubles, triples and quadruples) [24–27] and CCSDTQP (CC singles, doubles, triples, quadruples and pentuples) [28] approaches appear, at least at the present time, to be far too expensive for routine applications. For example, the full CCSDT and CCSDTQ methods require iterative steps that scale as $n_o^3 n_u^5$ and $n_o^4 n_u^6$, respectively (n_o (n_u) is the number of occupied (unoccupied) orbitals in the molecular orbital basis), which means that the computer time associated with the full CCSDT and CCSDTQ calculations grows as $\mathcal{N}^8$ and $\mathcal{N}^{10}$, respectively, with molecular size ($\mathcal{N}$ is a general measure of the molecular size). This restricts the applicability of these methods to very small systems consisting of $\sim$2–3 light atoms. For comparison, the CCSD(T) method is an $n_o^2 n_u^4$ (or $\mathcal{N}^6$) procedure in the iterative CCSD part and an $n_o^3 n_u^4$ ($\mathcal{N}^7$) procedure in the non-iterative part related to the calculation of the triples (T) correction. In consequence, it is nowadays possible to perform the CCSD(T) calculations for systems with 10–20 atoms. The application of the local correlation formalism of Pulay and Saebø [29–31], within the context of the CC theory [32–35], enabled Schütz and Werner to extend the applicability of the CCSD(T) approach to systems with $\sim$100 atoms [32, 34, 35]. The CCSD(TQ$_f$) method, with its manageable, $\mathcal{N}^7$-type, $n_o^2 n_u^5$ scaling in the non-iterative part related to the calculation of the factorized quadruples (Q$_f$) correction, should become increasingly more popular in the near future, particularly when there is a need to include the combined effect of triples and quadruples in the calculations.

Downloaded At: 16:32 21 January 2011

Unfortunately, it is not possible to apply the CCSD(T), CCSD(TQ$_f$) and similar methods to potential energy surfaces (PESs) involving bond breaking, if the spin-adapted restricted Hartree–Fock (RHF) configuration is used as a reference (cf., for example, [18, 36–49] and references therein). The CCSD method itself, on which the non-iterative CCSD[T], CCSD(T) and CCSD(TQ$_f$) approaches are based, is inadequate for the description of bond breaking, as it neglects the important triply and quadruply excited clusters. The triples and quadruples corrections of the CCSD[T], CCSD(T) and CCSD(TQ$_f$) methods make the situation even worse, since the standard MBPT arguments, on which the non-iterative CC approximations are based, fail owing to the divergent behaviour of the MBPT series at larger internuclear separations. As a result, the PESs produced by the CCSD(T), CCSD(TQ$_f$) and other non-iterative CC approaches are completely unphysical [18, 36–49]. The iterative analogues of the CCSD[T], CCSD(T) and CCSD(TQ$_f$) methods, including the CCSDT-*n* [13, 50–53] and CCSDTQ-1 [54] approaches, and the non-iterative CCSDT + Q(CCSDT) = CCSDT[Q] [54] and CCSDT(Q$_f$) [20] approximations, in which the non-iterative quadruples corrections are added to the CCSDT energies, improve the description of PESs in the bond-breaking region (particularly when the local correlation formalism is employed [35]), but ultimately all of these approaches break down because of the divergent behaviour of the MBPT series at large

internuclear distances (see, for example [36, 39, 40, 45]), particularly when multiple bonds are broken [36, 45].

A very similar failure of the standard CC approximations is observed when we apply them to PESs of excited states. The response CC methods [55–60] and the closely related equation-of-motion CC (EOMCC) approaches [61–64] provide very good results for excited states dominated by single excitations (cf., for example, [61–63, 65–71]), but accurate calculations of excited states of quasi-degenerate systems (particularly excited states having large doubly excited components) and accurate calculations of larger portions of excited-state PESs with the standard response CC and EOMCC approximations, including EOMCCSD [61–63], EOMCCSD(T) [65], EOMCCSD($\tilde{\mathrm{T}}$) [66], EOMCCSD(T') [66], EOMCCSDT-*n* [65, 66], CCSDR(3) [70, 71] and CC3 [68–71], are not possible (see, for example, [63, 65–79]). The magnitude of the problem can be illustrated by the $\sim$2 eV errors in the EOMCCSD results and $\sim$0.9 eV errors in the EOMCCSDT-1 and CC3 results for the lowest $^1\Delta_g$ state of C_2, which is located at $\sim$2 eV above the ground state [71]. The failure of the standard response CC or EOMCC approaches in calculations for excited states dominated by doubles and excited-state PESs can largely be remedied by switching to the full EOMCCSDT (EOMCC singles, doubles and triples) method [75, 76, 80, 81], but, as in the case of the full CCSDT ground-state method, the EOMCCSDT approach represents an expensive iterative $n_o^3 n_u^5$ ($\mathcal{N}^8$) procedure, which can only be applied to small systems [75, 76, 80, 81]. Moreover, as pointed out in [73], there may be situations in which even the full EOMCCSDT scheme breaks down. Clearly, there is a need for new excited-state methods that would account for higher–than–double excitations without invoking the prohibitively expensive steps of the full EOMCCSDT and EOMCCSDTQ (EOMCC singles, doubles, triples and quadruples) approaches.

Downloaded At: 16:32 21 January 2011

The most natural solution to all of the above problems is obtained by switching to the genuine multireference CC (MRCC) formalisms of the state-universal [15, 18, 82–98] or valence-universal [15, 18, 99–102] type, which are specifically designed to handle general open-shell and quasi-degenerate states (including, at least in principle, difficult cases of bond breaking or excited states). However, it is formally much easier to apply the standard single-reference CC or EOMCC methods, which do not suffer from intruder states and multiple, singular, or unphysical solutions that plague the genuine MRCC theories (cf., for example, [85, 90–94, 103, 104]). Moreover, the single-reference CC/EOMCC methods have an ease of application that is not matched by the existing MRCC approaches. The newly developed state-specific MRCC approaches (cf., for example, [105–114]), the similarity-transformed EOMCC method [115–119] and, perhaps, the new MRCC approach combining the MBPT and MRCC ideas [96, 98], which are all based on the genuine multireference formalism, may change this situation, but none of the existing state-specific MRCC methods is simple or general enough to be as widely applicable as the standard CCSD, CCSD(T) or EOMCCSD approaches. Thus, in spite of the tremendous progress in CC theory, which is nowadays routinely used in accurate calculations of many properties of closed-shell and simple open-shell molecular systems, there is a continuing need for new ideas that would extend the applicability of the conventional CC methods to entire molecular PESs and excited electronic states of arbitrary type.

A few approaches have been suggested in recent years with an intention of removing the pervasive failing of the RHF-based single-reference CC approxima-

tions at larger internuclear separations, while avoiding the complexity of the genuine MRCC theory. The representative examples include the reduced multireference CCSD (RMRCCSD) method [18, 120–126], the active-space CC approaches (also known as the SSCC or SSMRCC methods) [27, 37, 39, 40, 44, 74–76, 81, 127–137], the orbital-optimized CC methods [138,139], the non-iterative approaches based on the partitioning of the similarity-transformed Hamiltonian [140–143] (cf. [144] for the original idea) and the renormalized and completely renormalized CC approaches [41–47, 49]. The last of these approaches are based on the more general formalism of the method of moments of CC equations (MMCC) [41–43, 47, 48, 77, 78, 97], which can be applied to ground- and excited-state PESs. All of the above methods focus on improving the description of bond breaking, while retaining the simplicity of the single-reference description based on the spin- and symmetry-adapted references of the RHF type.

At the risk of introducing spin contamination, one can also improve the description of bond breaking (often, significantly) by employing the unrestricted Hartree–Fock (UHF) (see, for example, [36]) or the restricted but 'spin-flipped' [145] reference configurations. In the latter case, one uses the standard EOMCCSD theory to obtain the desired singlet ground state as an excitation from the approximate triplet state resulting from the CCSD calculations with the high-spin, 'spin-flipped', reference. Although the ground electronic states obtained in the so-called Spin-Flip (SF) CCSD calculations are spin contaminated at all internuclear separations (including equilibrium geometries), the resulting PESs involving single bond breaking and the results for molecular systems having diradical character are very good [145, 146]. The SFCC methods can also be used to study singlet–triplet gaps in diradicals [147]. Interestingly enough, the PESs involving single bond breaking obtained in the SFCCSD calculations are considerably better than the PESs obtained in the UHF-based CC calculations [145, 146]. Furthermore, by using the same, 'spin-flipped', high-spin reference at all internuclear geometries, the SFCCSD model and its orbital-optimized SFOD version do not introduce a non-analytic behaviour of the PES in the region of transition between the triplet stable and triplet unstable solutions of the Hartree–Fock equations, observed in the UHF-based CC calculations [36, 148]. On the other hand, it may be quite difficult to generalize the SFCCSD and SFOD methods to PESs involving multiple bond breaking, since breaking multiple bonds will require considering the iterative SFCC (i.e. EOMCC) methods with higher-than-doubly excited clusters. The spin contamination of electronic states obtained in the Spin-Flip and UHF-based CC calculations may cause problems in some applications. The use of the spin–orbital formalism in the SFCC and UHF-based CC methods does not allow for a number of simplifications which are normally possible when the spin and spatial symmetries are present in molecular systems.

In this article, we focus on the single-reference approaches that are based on using the spin- and symmetry-adapted reference configurations. Of all of the approaches of this type, the RMRCCSD method of Paldus and Li [18, 120–126] and the active-space CC or SSCC approaches of Adamowicz, Piecuch and co-workers [27, 37, 39, 40, 44, 74–76, 81, 127–135] are particularly promising. They proved to be successful in describing quasi-degenerate ground states [27, 39, 120, 123, 131], bond breaking [37, 39, 40, 44, 121, 122,124–126, 128, 129, 132, 135], ro-vibrational term values including highly excited states near dissociation [40, 125, 126] and property functions [134]. The RMRCCSD and active-space CC methods largely

Downloaded At: 16:32 21 January 2011

preserve the formal simplicity of the single-reference CC theory and are relatively easy to use, although, in analogy to genuine multireference approaches, they require active orbitals to be chosen, which in some cases may be a difficult thing to do. In addition, the RMRCCSD approach requires that one performs multireference configuration interaction (MRCI) calculations prior to standard CCSD calculations in order to extract information about important triply and quadruply excited clusters (the RMRCCSD approach belongs to a wider category of the externally corrected CC methods, in which non-CC wavefunctions are used to provide information about triply and quadruply excited clusters [13, 14, 18, 149–153]). These MRCI calculations may, in some cases, substantially increase the computer costs of the RMRCCSD calculations. In addition, it is not possible to apply the RMRCCSD method to several electronic states of the same symmetry. The active-space CC or SSCC approaches of Adamowicz, Piecuch and co-workers, in which higher-than-doubly excited components of the cluster operator are selected through active orbitals, have fewer limitations. In particular, the CCSDt and CCSDtq [39, 40, 44] or SSCCSD(T) and SSCCSD(TQ) [27, 127–135] methods are a lot less expensive than their parent CCSDT and CCSDTQ approaches. In addition, the active-space CC approaches can easily be extended to excited states of the same or different symmetries via the EOMCC formalism [74–76, 81] (cf. also the remarks given below). They do not eliminate, however, the need to define active orbitals and they require iterating higher–than–doubly excited clusters, which means that they are technically more complicated than the non-iterative CC approaches of the CCSD(T) type.

Downloaded At: 16:32 21 January 2011

The perturbative approaches based on the partitioning of the similarity-transformed Hamiltonian of Gwaltney and Head-Gordon [140–143] and the renormalized and completely renormalized CC approaches of Kowalski and Piecuch [41–47, 49], in which non-iterative energy corrections are added to the results of standard (e.g. CCSD) calculations, are considerably simpler in this regard. As shown in this work, the completely renormalized CC methods [41–47, 49] and other MMCC approximations [41, 48, 77, 78] are capable of producing PESs of MRCC or MRCI quality with the ease of use of the non-iterative CCSD(T) or CCSD(TQ_f) approximations.

A few new, single-reference-like, methods have also been suggested with an intention of removing the failing of the standard EOMCC approximations for excited states dominated by double excitations and excited-state PESs. The excited-state extensions of the active-space CC approaches mentioned above [74–76, 81] and the excited-state extensions of the MMCC theory [47, 77, 78] (both utilizing the EOMCC formalism) are among the most promising approaches in this area. Other attempts to improve the results of the standard EOMCC calculations, including the EOMCC extensions of the orbital-optimized CC methods [79], have proved to be unsuccessful. As demonstrated in this article, the excited-state extensions of the MMCC theory, in which simple, non-iterative energy corrections of the CCSD(T) or CCSD(TQ_f) type are added to the energies obtained in approximate EOMCC (e.g. EOMCCSD) calculations, remove the failing of the standard EOMCC methods for states dominated by double excitations. They also provide an excellent description of entire excited-state PESs [47, 77, 78].

The main idea of the MMCC formalism and of the related renormalized and completely renormalized CC approaches [41–49, 77, 78] is that of the simple, state-selective, non-iterative energy corrections which, when added to the energies obtained in the standard CC or EOMCC (CCSD, EOMCCSD, etc.) calculations,

recover the exact, full CI, energies of the electronic states of interest. Thus, the MMCC methods and the renormalized and completely renormalized CC approaches preserve the conceptual and computational simplicity of the non-iterative CC methods, such as CCSD(T), CCSD(TQ_f) or EOMCCSD(T), while offering us a new way of controlling the quality of CC or EOMCC results by directly focusing on the quantity of interest, which is the difference between the exact and CC or EOMCC energies. In MMCC calculations, we are not just interested in improving the Hartree–Fock or some other independent-particle-model (IPM) description by adding corrections due to correlation, as we do in the standard quantum chemical approaches, with the hope that the more we add the better the results that are obtained (which, by the way, is not always the case). We are rather dealing with the remanent errors that occur in the standard CC or EOMCC calculations, which we can estimate by using the explicit and non-trivial relationships between the CC or EOMCC and full CI energies defining the MMCC theory. This is particularly important in situations where conventional arguments originating from MBPT, which are often used to design the standard CC approximations, fail owing to divergent behaviour of the MBPT series (as is, for example, the case in studies of quasi-degenerate and excited states, and bond breaking).

In our view, the MMCC theory represents an exciting development in the area of new CC methods for molecular PESs. The MMCC-based completely renormalized CCSD(T), CCSD(TQ) and CCSDT(Q) methods and the EOMCC-based MMCC approaches to excited states provide highly accurate results for ground- and excited-state PESs, while preserving the 'black-box' character and the relatively low computer cost of the non-iterative CC schemes. In this article, we overview the MMCC theory and various approximations that result from it, including the highly promising completely renormalized CC methods, and show examples of successful applications of these new approaches to molecular PESs and vibrational and electronic spectra. The review of the previously published material [41–49, 77, 78] is combined with the examples of new applications. Some very recent methodological developments in the area of the MMCC theory, including the so-called quasi-variational and quadratic MMCC methods, are described as well.

Downloaded At: 16:32 21 January 2011

2. The method of moments of coupled-cluster equations: an overview of the general formalism

As implied by the remarks made in the Introduction, the main idea of the MMCC theory is that of the non-iterative, state-specific, energy corrections

$$\delta_K^{(\mathrm{A})} \equiv E_K - E_K^{(\mathrm{A})} \tag{1}$$

which, when added to the energies of ground and excited states, $E_K^{(\mathrm{A})}$, obtained in the standard CC/EOMCC or MRCC calculations, referred to in this paper as method A, recover the corresponding exact (full CI) energies E_K. Here and elsewhere in this paper, we use a notation in which $K = 0$ represents the ground state and the $K > 0$ values correspond to excited states. The main purpose of all approximate MMCC calculations is to estimate corrections $\delta_K^{(\mathrm{A})}$, such that the resulting MMCC energies, defined as

$$E_K^{\mathrm{MMCC}} = E_K^{(\mathrm{A})} + \delta_K^{(\mathrm{A})}, \tag{2}$$

are close to the corresponding exact energies E_K.

Three types of MMCC theories have been developed so far. In the basic, ground-state formalism (the $K = 0$ case), which leads, in particular, to the renormalized and completely renormalized CC methods, we add corrections $\delta_0^{(A)}$ to the energies obtained in the standard single-reference CC calculations, such as CCSD or CCSDT [41–43, 47, 48]. In the excited-state MMCC formalism (the $K > 0$ case), based on the EOMCC theory, we add corrections $\delta_K^{(A)}$ to the energies of excited states obtained in the standard EOMCC calculations, such as EOMCCSD [47, 77, 78]. Finally, in the MRCC extension of the MMCC theory, which applies to quasi-degenerate ground and excited states, we add corrections $\delta_K^{(A)}$ to the energies obtained in the state-universal MRCC calculations, such as SUMRCCSD [97, 98]. In this article, we focus on the basic ground-state MMCC theory and its extension to excited states via the EOMCC formalism. We begin our discussion with the ground-state theory.

2.1. *The ground-state MMCC theory*

In the single-reference CC theory, the ground-state wavefunction $|\Psi_0\rangle$ of an N-electron system, described by the Hamiltonian H, is defined as follows:

$$|\Psi_0\rangle = \mathrm{e}^T|\Phi\rangle, \tag{3}$$

where T is the cluster operator and $|\Phi\rangle$ is the IPM reference configuration (e.g. the Hartree–Fock determinant) defining the Fermi vacuum. Typically, we truncate the many-body expansion of cluster operator T at a conveniently chosen excitation level. Thus, if A represents the standard single-reference CC approximation and if $m_A < N$ is the excitation level characterizing method A, the formula for cluster operator $T^{(A)}$ defining method A is

$$T^{(A)} = \sum_{n=1}^{m_A} T_n, \tag{4}$$

where T_n, $n = 1, \ldots, m_A$, are the many-body components of $T^{(A)}$. The standard CCSD method is obtained by setting $m_A = 2$ in equation (4). In the CCSDT method, $m_A = 3$, in the CCSDTQ approach, $m_A = 4$, etc.

In all standard CC approximations, the cluster operator $T^{(A)}$ is obtained by solving the system of nonlinear algebraic equations

$$Q^{(A)}\bar{H}^{(A)}|\Phi\rangle = 0, \tag{5}$$

where

$$\bar{H}^{(A)} = \mathrm{e}^{-T^{(A)}} H \mathrm{e}^{T^{(A)}} = (H\mathrm{e}^{T^{(A)}})_C \tag{6}$$

is the similarity-transformed Hamiltonian of the CC theory. We use a notation in which subscript C designates the connected part of the corresponding operator expression and $Q^{(A)}$ is the projection operator onto the subspace of all excited configurations included in $T^{(A)}$, i.e.

$$Q^{(A)} = \sum_{n=1}^{m_A} Q_n, \tag{7}$$

where Q_n is the projection operator onto the subspace of the n-tuply excited configurations relative to reference $|\Phi\rangle$. The system of CC equations, equation (5), is obtained by inserting the CC wavefunction $|\Psi_0\rangle$, equation (3), with $T = T^{(A)}$, into the electronic Schrödinger equation, premultiplying both sides of the Schrödinger

Downloaded At: 16:32 21 January 2011

equation on the left by $e^{-T^{(A)}}$ and projecting the resulting connected cluster form of the Schrödinger equation [3, 4, 15, 18, 41] onto the excited configurations included in $T^{(A)}$ (represented here by the projection operator $Q^{(A)}$). Once the system of equations, equation (5), is solved for $T^{(A)}$, the CC energy is calculated using the formula

$$E_0^{(A)} = \langle \Phi | \bar{H}^{(A)} | \Phi \rangle, \tag{8}$$

obtained by projecting the connected cluster form of the Schrödinger equation on $|\Phi\rangle$.

By analysing the relationships between multiple solutions of the nonlinear equations representing different CC approximations (CCSD, CCSDT, etc.), Piecuch and Kowalski arrived at an interesting expression for the non-iterative correction $\delta_0^{(A)}$ which, when added to the energy obtained in the standard CC calculations, $E_0^{(A)}$, equation (8), gives the full CI ground-state energy E_0. The result of their considerations can be stated as follows [41–43, 47, 48]:

$$\delta_0^{(A)} \equiv E_0 - E_0^{(A)} = \sum_{n=m_A+1}^{N} \sum_{j=m_A+1}^{n} \langle \Psi_0 | Q_n \, C_{n-j}(m_A) \, M_j^{CC}(m_A) | \Phi \rangle / \langle \Psi_0 | e^{T^{(A)}} | \Phi \rangle, \tag{9}$$

where

$$C_{n-j}(m_A) = (e^{T^{(A)}})_{n-j} \tag{10}$$

is the $(n-j)$-body component of the CC wave operator $e^{T^{(A)}}$, defining method A, and where

$$M_j^{CC}(m_A)|\Phi\rangle \equiv Q_j \bar{H}^{(A)} |\Phi\rangle = \sum_J \mathcal{M}_J^{CC,(j)}(m_A) \, |\Phi_J^{(j)}\rangle \tag{11}$$

is the quantity defined through the coefficients

$$\mathcal{M}_J^{CC,(j)}(m_A) = \langle \Phi_J^{(j)} | \bar{H}^{(A)} | \Phi \rangle \tag{12}$$

that represent the projections of the single-reference CC equations of method A on all j-tuply excited configurations $|\Phi_J^{(j)}\rangle$ with $j > m_A$. The $C_{n-j}(m_A)$ quantities are very easy to generate. The zero-body term, $C_0(m_A)$, equals 1, the one-body term, $C_1(m_A)$, equals T_1, the two-body term, $C_2(m_A)$, equals $T_2 + \frac{1}{2}T_1^2$ if $m_A \geq 2$, etc. The $\mathcal{M}_J^{CC,(j)}(m_A)$ quantities, equation (12), represent the generalized moments of CC equations (for a discussion of the relationship between the method of moments of Krylov [154] and the CC theory, see [155]). They can be easily generated for the basic CC approximations, such as CCSD (the $m_A = 2$ case). It should be noted that the generalized moments $\mathcal{M}_J^{CC,(j)}(m_A)$, or their $M_j^{CC}(m_A)|\Phi\rangle$ analogues defined by equation (11), can be viewed as the most fundamental quantities for the standard CC methods. For example, the system of nonlinear equations defining method A, equation (5), can be obtained by imposing the requirement that the $\mathcal{M}_J^{CC,(j)}(m_A)$ moments, with J running over all j-tuply excited configurations with $j = 1, \ldots, m_A$, vanish.

The meaning of equation (9) is as follows. If we want to obtain the exact, full CI, energy by adding the non-iterative correction $\delta_0^{(A)}$ to the energy $E_0^{(A)}$ obtained in the standard CC calculations with method A, we must calculate the generalized moments $\mathcal{M}_J^{CC,(j)}(m_A)$ corresponding to projections of CC equations on all excited configurations that are not included in method A. Thus, if we, for example, want to

Downloaded At: 16:32 21 January 2011

recover the full CI energy by adding the correction $\delta_0^{(A)}$ to the CCSD energy (the $m_A = 2$ case), we have to calculate the generalized moments of the CCSD equations corresponding to projections of these equations on triply, quadruply, pentuply and hextuply excited configurations, i.e.

$$\mathcal{M}^{abc}_{ijk}(2) = \langle \Phi^{abc}_{ijk} | \bar{H}^{\mathrm{CCSD}} | \Phi \rangle, \tag{13}$$

$$\mathcal{M}^{abcd}_{ijkl}(2) = \langle \Phi^{abcd}_{ijkl} | \bar{H}^{\mathrm{CCSD}} | \Phi \rangle, \tag{14}$$

$$\mathcal{M}^{abcde}_{ijklm}(2) = \langle \Phi^{abcde}_{ijklm} | \bar{H}^{\mathrm{CCSD}} | \Phi \rangle, \tag{15}$$

$$\mathcal{M}^{abcdef}_{ijklmn}(2) = \langle \Phi^{abcdef}_{ijklmn} | \bar{H}^{\mathrm{CCSD}} | \Phi \rangle. \tag{16}$$

Here,

$$\bar{H}^{\mathrm{CCSD}} = \mathrm{e}^{-(T_1+T_2)} H \mathrm{e}^{T_1+T_2} = (H \mathrm{e}^{T_1+T_2})_{\mathrm{C}} \tag{17}$$

is the similarity-transformed Hamiltonian of the CCSD approach and $|\Phi^{abc}_{ijk}\rangle$, $|\Phi^{abcd}_{ijkl}\rangle$, $|\Phi^{abcde}_{ijklm}\rangle$ and $|\Phi^{abcdef}_{ijklmn}\rangle$ are the triply, quadruply, pentuply and hextuply excited configurations, respectively. We use the standard notation, in which $i, j, k, l, m, n, \ldots$ represent the spin-orbitals occupied in $|\Phi\rangle$ and $a, b, c, d, e, f, \ldots$ are the unoccupied spin–orbitals. The calculation of the above moments allows us to define quantities $M_j^{\mathrm{CC}}(2)|\Phi\rangle$ with $j = 3$–6,

$$M_3^{\mathrm{CC}}(2)|\Phi\rangle = \sum_{\substack{i<j<k \\ a<b<c}} \mathcal{M}^{abc}_{ijk}(2) |\Phi^{abc}_{ijk}\rangle, \tag{18}$$

$$M_4^{\mathrm{CC}}(2)|\Phi\rangle = \sum_{\substack{i<j<k<l \\ a<b<c<d}} \mathcal{M}^{abcd}_{ijkl}(2) |\Phi^{abcd}_{ijkl}\rangle, \tag{19}$$

$$M_5^{\mathrm{CC}}(2)|\Phi\rangle = \sum_{\substack{i<j<k<l<m \\ a<b<c<d<e}} \mathcal{M}^{abcde}_{ijklm}(2) |\Phi^{abcde}_{ijklm}\rangle, \tag{20}$$

$$M_6^{\mathrm{CC}}(2)|\Phi\rangle = \sum_{\substack{i<j<k<l<m<n \\ a<b<c<d<e<f}} \mathcal{M}^{abcdef}_{ijklmn}(2) |\Phi^{abcdef}_{ijklmn}\rangle, \tag{21}$$

which can be subsequently used to determine the non-iterative correction

$$\delta_0^{\mathrm{CCSD}} = \sum_{n=3}^{N} \sum_{j=3}^{\min(n,6)} \langle \Psi_0 | Q_n \, C_{n-j}(2) \, M_j^{\mathrm{CC}}(2) | \Phi \rangle / \langle \Psi_0 | \mathrm{e}^{T_1+T_2} | \Phi \rangle \tag{22}$$

to the CCSD energy. We do not have to consider the projections of the CCSD equations on higher-than-hextuply excited configurations, since for Hamiltonians containing up to two-body interactions the $M_j^{\mathrm{CC}}(2)|\Phi\rangle$ quantities with $j > 6$ vanish.

The original proof of equation (9), presented by Piecuch and Kowalski in [41], has been based on the so-called Fundamental Theorem of the Formalism of β-Nested equations. This theorem, stated and proved in [41], describes precise mathematical relationships between multiple solutions of the single-reference CC equations representing different CC approximations (CCSD, CCSDT, etc.). An elementary derivation of equation (9), based on applying the resolution of identity to a simple asymmetric energy expression, termed the MMCC functional, i.e.

$$\Lambda^{\mathrm{CC}}[\Psi] = \langle \Psi | (H - E_0^{(\mathrm{A})}) \mathrm{e}^{T^{(\mathrm{A})}} | \Phi \rangle / \langle \Psi | \mathrm{e}^{T^{(\mathrm{A})}} | \Phi \rangle, \tag{23}$$

Downloaded At: 16:32 21 January 2011

introduced for the first time in [42], has been given in appendix A of [42]. The functional $\Lambda^{\mathrm{CC}}[\Psi]$ has the important property that, when $|\Psi\rangle$ in equation (23) is replaced by the exact ground-state wavefunction $|\Psi_0\rangle$, we obtain the exact value of the correction $\delta_0^{(\mathrm{A})}$:

$$\Lambda^{\mathrm{CC}}[\Psi_0] = E_0 - E_0^{(\mathrm{A})} \equiv \delta_0^{(\mathrm{A})}. \tag{24}$$

The elementary derivation of equation (9), based on exploiting the MMCC functional $\Lambda^{\mathrm{CC}}[\Psi]$, equation (23), can also be found in appendix A of this article.

The possibility of applying the MMCC functional of Piecuch and Kowalski in direct calculations of non-iterative corrections to standard CC energies has been investigated in [156, 157]. In our view, it is much better to use the non-iterative corrections $\delta_0^{(\mathrm{A})}$, given by equation (9), or their CCSD counterparts δ_0^{CCSD}, given by equation (22). These equations have a very interesting many-body structure, which allows one to propose a variety of simple approximations that can, in turn, be easily incorporated into the existing electronic structure packages and subsequently applied to relatively large molecular systems and large basis sets by expressing corrections $\delta_0^{(\mathrm{A})}$ in terms of the low-order moments of CC equations (cf., for example, the most recent, highly efficient, implementation [158] of the MMCC-based renormalized and completely renormalized CCSD(T) methods in GAMESS [159]). The direct application of the MMCC functional leads to schemes that are prohibitively expensive for the vast majority of applications. The authors of [156, 157] must have realized this, since they have eventually decided to use the energy formula in terms of the generalized moments of CC equations, which is the same as our equation (9) (cf., for example, [160]). On the other hand, it is interesting to see that the direct application of the MMCC functional of Piecuch and Kowalski leads to considerable improvements in the results of the standard CC calculations for PESs involving bond breaking [156, 157].

Downloaded At: 16:32 21 January 2011

Equation (9) is the basic equation of the ground-state MMCC formalism. The two main elements of equation (9) are the aforementioned generalized moments of CC equations and the wavefunction $|\Psi_0\rangle$. The generalized moments of CC equations can be calculated once we know the corresponding cluster operator $T^{(\mathrm{A})}$. The remaining issue is what we do with the wavefunction $|\Psi_0\rangle$, which in the exact MMCC theory represents the full CI ground state. As we will see in the later sections, it is sufficient to use very simple forms of $|\Psi_0\rangle$, generated in inexpensive MBPT or CI calculations, to obtain excellent results for PESs involving bond breaking. For example, the highly successful completely renormalized CCSD(T), CCSD(TQ) and CCSDT(Q) methods, mentioned in the Introduction, employ the MBPT(2)-like expressions for $|\Psi_0\rangle$ [41–47, 49]. Clearly, depending on the form of $|\Psi_0\rangle$ and depending on the nature of approximations that are used to design the specific form of $\delta_0^{(\mathrm{A})}$, the results of MMCC calculations may not be strictly size extensive. However, all approximate MMCC approaches resulting from equation (9) lead to a correct description of a process of separation of a given N-electron system into fragments consisting of no more than m_{A} electrons each, independent of a specific approximation used to define $|\Psi_0\rangle$ [41, 42]. Thus, each MMCC method in which we correct the CCSD energy using equation (22), or one of its approximate variants described in section 3, provides a correct description of a separation of a given N-electron system into non-interacting electron pairs, independent of the form

of $|\Psi_0\rangle$. An issue of size extensivity of approximate MMCC methods will be addressed in section 3.4.

2.2. *The excited-state MMCC formalism*

As mentioned earlier, the MMCC theory can be extended to excited states via the EOMCC formalism [47, 77, 78]. In this case, the non-iterative, state-specific, energy corrections $\delta_K^{(A)}$, equation (1), are added to the energies of excited states, $E_K^{(A)}$, obtained in the standard EOMCC calculations. Let us recall that in the EOMCC theory the excited states $|\Psi_K\rangle$ are obtained by applying the excitation operator R_K to the CC ground state, i.e.

$$|\Psi_K\rangle = R_K|\Psi_0\rangle, \tag{25}$$

where $|\Psi_0\rangle$ is defined by equation (3). For the consistency of our presentation, the operator R_K is defined as a unit operator for $K = 0$. The excited-state energies E_K and the corresponding excitation operators R_K ($K > 0$) are obtained by diagonalizing the similarity-transformed Hamiltonian $\bar{H} = e^{-T}He^{T}$, where T is the cluster operator obtained in the standard single-reference CC calculations.

In the exact EOMCC theory, the cluster operator T and the excitation operators R_K are sums of all relevant many-body components that can be written for a given N-electron system, including the N-body ones. In the standard EOMCC approximations, such as EOMCCSD, the many-body expansions of T and R_K are truncated at some excitation level. Thus, if A represents the standard EOMCC approximation, in which the many-body expansions of T and R_K are truncated at the m_A-body components with $m_A < N$, we obtain

$$T \simeq T^{(A)} = \sum_{n=1}^{m_A} T_n, \tag{26}$$

$$R_K \simeq R_K^{(A)} = R_{K,0}^{(A)} + R_{K,\mathrm{open}}^{(A)}, \tag{27}$$

where the 'open' part of $R_K^{(A)}$ is defined by

$$R_{K,\mathrm{open}}^{(A)} = \sum_{n=1}^{m_A} R_{K,n}, \tag{28}$$

and T_n and $R_{K,n}$ are the n-body components of operators $T^{(A)}$ and $R_K^{(A)}$, respectively. In the EOMCCSD method, $m_A = 2$, in the EOMCCSDT approach, $m_A = 3$, etc. The cluster operator $T^{(A)}$ is obtained by solving equation (5), as discussed in section 2.1, whereas the excitation operators $R_K^{(A)}$ are obtained by diagonalizing the similarity-transformed Hamiltonian $\bar{H}^{(A)}$, equation (6), in a space spanned by the reference configuration $|\Phi\rangle$ and the excited configurations included in $T^{(A)}$ and $R_K^{(A)}$. The resulting EOMCC equations, defining approximate method A, can be given the following compact form:

$$(P + Q^{(A)})(\bar{H}^{(A)} - E_K^{(A)})R_K^{(A)}|\Phi\rangle = 0, \tag{29}$$

where $\bar{H}^{(A)}$ and $Q^{(A)}$ are defined by equations (6) and (7), respectively, and $P = |\Phi\rangle\langle\Phi|$.

Once the cluster and excitation operators, $T^{(A)}$ and $R_K^{(A)}$, respectively, and the ground- and excited-state energies $E_K^{(A)}$ ($K \geq 0$) are determined by solving the

Downloaded At: 16:32 21 January 2011

relevant CC/EOMCC equations, we calculate the MMCC corrections $\delta_K^{(\mathrm{A})}$, equation (1), by using the following expression [47, 77, 78]:

$$\delta_K^{(\mathrm{A})} = \sum_{n=m_\mathrm{A}+1}^{N} \sum_{j=m_\mathrm{A}+1}^{n} \langle \Psi_K | Q_n \, C_{n-j}(m_\mathrm{A}) M_{K,j}^{\mathrm{EOMCC}}(m_\mathrm{A}) | \Phi \rangle / \langle \Psi_K | R_K^{(\mathrm{A})} \mathrm{e}^{T^{(\mathrm{A})}} | \Phi \rangle, \quad (30)$$

where $C_{n-j}(m_\mathrm{A})$ is defined by equation (10) and

$$M_{K,j}^{\mathrm{EOMCC}}(m_\mathrm{A})|\Phi\rangle = Q_j(\bar{H}^{(\mathrm{A})} R_K^{(\mathrm{A})})|\Phi\rangle. \quad (31)$$

The $M_{K,j}^{\mathrm{EOMCC}}(m_\mathrm{A})|\Phi\rangle$ quantities appearing in equation (30) can be expressed in terms of the generalized moments of the EOMCC equations defining approximation A, i.e. the left-hand side of the EOMCC eigenvalue problem involving $\bar{H}^{(\mathrm{A})}$ (the $(\bar{H}^{(\mathrm{A})} R_K^{(\mathrm{A})})|\Phi\rangle$ term), projected on the j-tuply excited configurations relative to $|\Phi\rangle$:

$$M_{K,j}^{\mathrm{EOMCC}}(m_\mathrm{A})|\Phi\rangle = \sum_J \mathcal{M}_{K,J}^{\mathrm{EOMCC},(j)}(m_\mathrm{A}) \, |\Phi_J^{(j)}\rangle, \quad (32)$$

where

$$\mathcal{M}_{K,J}^{\mathrm{EOMCC},(j)}(m_\mathrm{A}) = \langle \Phi_J^{(j)} | (\bar{H}^{(\mathrm{A})} R_K^{(\mathrm{A})}) | \Phi \rangle \quad (33)$$

are the projections of the $(\bar{H}^{(\mathrm{A})} R_K^{(\mathrm{A})})|\Phi\rangle$ term on the j-tuply excited configurations $|\Phi_J^{(j)}\rangle$. As demonstrated in [77], the generalized moments of the EOMCC equations can be calculated using the following expression:

$$\mathcal{M}_{K,J}^{\mathrm{EOMCC},(j)}(m_\mathrm{A}) = \langle \Phi_J^{(j)} | (\bar{H}_{\mathrm{open}}^{(\mathrm{A})} R_{K,\mathrm{open}}^{(\mathrm{A})})_{\mathrm{C},j} | \Phi \rangle + \sum_{p=m_\mathrm{A}+1}^{j-1} \langle \Phi_J^{(j)} | (\bar{H}_p^{(\mathrm{A})} R_{K,j-p}^{(\mathrm{A})})_{\mathrm{DC}} | \Phi \rangle$$
$$+ r_{K,0}^{(\mathrm{A})} \langle \Phi_J^{(j)} | \bar{H}^{(\mathrm{A})} | \Phi \rangle, \quad (34)$$

where $r_{K,0}^{(\mathrm{A})}$ is the coefficient at the reference configuration $|\Phi\rangle$ in the many-body expansion of $R_K^{(\mathrm{A})}|\Phi\rangle$, subscripts 'open', C and DC refer to open (i.e. having external lines), connected and disconnected parts of a given operator expression and, in general, O_j represents the j-body component of operator O. The computer programs for the MMCC corrections $\delta_K^{(\mathrm{A})}$ are based on equation (34), which is used to derive the explicit formulae for $\mathcal{M}_{K,J}^{\mathrm{EOMCC},(j)}(m_\mathrm{A})$ in terms of matrix elements of $\bar{H}^{(\mathrm{A})}$.

The derivation of equation (30) is similar to the derivation of equation (9). In order to derive equation (30), we have to consider the excited-state extension of the functional $\Lambda^{\mathrm{CC}}[\Psi]$, equation (23), namely

$$\Lambda^{\mathrm{EOMCC}}[\Psi] = \langle \Psi | (H - E_K^{(\mathrm{A})}) R_K^{(\mathrm{A})} \mathrm{e}^{T^{(\mathrm{A})}} | \Phi \rangle / \langle \Psi | R_K^{(\mathrm{A})} \mathrm{e}^{T^{(\mathrm{A})}} | \Phi \rangle. \quad (35)$$

It should be noticed that equation (35) reduces to the ground-state functional $\Lambda^{\mathrm{CC}}[\Psi]$ when $K = 0$ (recall that $R_K^{(\mathrm{A})}$ is a unit operator for $K = 0$). The $\Lambda^{\mathrm{EOMCC}}[\Psi]$ functional, equation (35), satisfies the property

$$\Lambda^{\mathrm{EOMCC}}[\Psi_K] = E_K - E_K^{(\mathrm{A})} \equiv \delta_K^{(\mathrm{A})}. \quad (36)$$

In other words, the functional $\Lambda^{\mathrm{CC}}[\Psi]$ gives us the exact value of $\delta_K^{(\mathrm{A})}$ when $|\Psi\rangle$ in equation (35) is replaced by the exact excited-state ($K > 0$) or ground-state ($K = 0$) wavefunction $|\Psi_K\rangle$. We refer the reader to the original work by Kowalski and Piecuch [77] and to appendix B of this article for the details of the derivation of equation (30), employing the functional $\Lambda^{\mathrm{EOMCC}}[\Psi]$, equation (35).

Downloaded At: 16:32 21 January 2011

Equation (30), with $C_{n-j}(m_A)$ defined by equation (10) and $M^{EOMCC}_{K,j}(m_A)|\Phi\rangle$ defined by equations (32) and (34), is the basic equation of the excited-state MMCC theory. This equation allows us to correct the CC/EOMCC energies (CC energies for $K = 0$ and EOMCC energies for $K > 0$) by calculating the non-iterative corrections $\delta_K^{(A)}$, using the information that can be extracted from the standard CC/EOMCC calculations, i.e. operators $T^{(A)}$ and $R_K^{(A)}$ and matrix elements of $\bar{H}^{(A)}$, and by subsequently adding the resulting corrections $\delta_K^{(A)}$ to the CC/EOMCC energies $E_K^{(A)}$. As in the ground-state MMCC theory, the main elements of equation (30) are the EOMCC equations, in which T is approximated by $T^{(A)}$ and R_K is approximated by $R_K^{(A)}$, projected onto the excited configurations that are not included in method A (the generalized moments of the EOMCC equations defining method A). For example, if we want to recover the exact (full CI) energies E_K by adding corrections $\delta_K^{(A)}$ to the EOMCCSD energies $E_K^{EOMCCSD}$ (the $m_A = 2$ case), we must consider the generalized moments of the EOMCCSD equations, i.e. the EOMCCSD equations projected on triples, quadruples, etc., or

$$\mathcal{M}^{abc}_{K,ijk}(2) = \langle \Phi^{abc}_{ijk} | (\bar{H}^{CCSD} R_K^{CCSD}) | \Phi \rangle, \tag{37}$$

$$\mathcal{M}^{abcd}_{K,ijkl}(2) = \langle \Phi^{abcd}_{ijkl} | (\bar{H}^{CCSD} R_K^{CCSD}) | \Phi \rangle, \tag{38}$$

etc., where $\bar{H}^{CCSD}$ is the similarity-transformed Hamiltonian of the CCSD method defined by equation (17) and

$$R_K^{CCSD} = R_{K,0} + R_{K,1} + R_{K,2} = R_{K,0} + R^{CCSD}_{K,open} \tag{39}$$

is the EOMCCSD excitation operator. Once these moments are determined, we can construct quantities $M^{EOMCC}_{K,j}(2)|\Phi\rangle$ with $j > 2$,

$$M^{EOMCC}_{K,3}(2)|\Phi\rangle = \sum_{\substack{i<j<k \\ a<b<c}} \mathcal{M}^{abc}_{K,ijk}(2) |\Phi^{abc}_{ijk}\rangle, \tag{40}$$

$$M^{EOMCC}_{K,4}(2)|\Phi\rangle = \sum_{\substack{i<j<k<l \\ a<b<c<d}} \mathcal{M}^{abcd}_{K,ijkl}(2) |\Phi^{abcd}_{ijkl}\rangle, \tag{41}$$

etc., which enter the final expression for the non-iterative MMCC corrections

$$\delta_K^{EOMCCSD} = \sum_{n=3}^{N} \sum_{j=3}^{n} \langle \Psi_K | Q_n \, C_{n-j}(2) \, M^{EOMCC}_{K,j}(2) | \Phi \rangle / \langle \Psi_K | R_K^{CCSD} e^{T_1+T_2} | \Phi \rangle \tag{42}$$

to the EOMCCSD energies $E_K^{EOMCCSD}$.

In the exact MMCC theory, the wavefunctions $|\Psi_K\rangle$ are the full CI states. In approximate MMCC methods, we rely on simple estimates of $|\Psi_K\rangle$, provided, for example, by inexpensive CI calculations, although other choices of $|\Psi_K\rangle$, based solely on the information obtained in the standard EOMCC calculations, whose results we are trying to improve by adding corrections $\delta_K^{(A)}$, may be possible too (see section 4). As shown in later sections, it is sufficient to use very simple forms of wavefunctions $|\Psi_K\rangle$ to obtain excellent vertical excitation energies and excited-state PESs. The only requirement that equation (30) imposes on the approximate form of $|\Psi_K\rangle$, to make it usable for the calculation of corrections $\delta_K^{(A)}$, is the presence of higher-than-m_A-tuply excited configurations in $|\Psi_K\rangle$ (e.g. triples in the $m_A = 2$ case).

Before describing the examples of specific MMCC approximations, let us emphasize the state-selective character of the MMCC energy corrections. By having

Downloaded At: 16:32 21 January 2011

some approximate form of the wavefunction $|\Psi_K\rangle$ for a given electronic state, we can determine the correction $\delta_K^{(\mathrm{A})}$ without considering other states. We should also point out that equation (30) represents a natural extension of the ground-state MMCC formula, equation (9), to excited states. Formally, in the ground-state ($K = 0$) case, R_K is a unit operator, $r_{K,0} = 1$, $R_{K,j} = 0$ for $j > 0$ or $R_{K,\mathrm{open}} = 0$, so that (cf. equation (34))

$$\mathcal{M}_{0,J}^{\mathrm{EOMCC},(j)}(m_{\mathrm{A}}) = \langle \Phi_J^{(j)} | \bar{H}^{(\mathrm{A})} | \Phi \rangle \equiv \mathcal{M}_J^{\mathrm{CC},(j)}(m_{\mathrm{A}}), \tag{43}$$

where $\mathcal{M}_J^{\mathrm{CC},(j)}(m_{\mathrm{A}})$ are the generalized moments of the ground-state CC equations (see equation (12)).

3. The ground- and excited-state MMCC($m_{\mathrm{A}}, m_{\mathrm{B}}$) approximations, the renormalized and completely renormalized CC approaches and the quasi-variational MMCC methods: theory and examples of applications

The exact MMCC corrections $\delta_K^{(\mathrm{A})}$, equations (9) and (30), are expressed in terms of the exact wave functions $|\Psi_K\rangle$, which we usually do not know (if we knew the exact $|\Psi_K\rangle$ states, we would not have to perform any calculations!). In approximate MMCC methods, referred to as the MMCC($m_{\mathrm{A}}, m_{\mathrm{B}}$) schemes, wavefunctions $|\Psi\rangle$ are evaluated by using low-order MBPT expressions (in the $K = 0$ case) or by performing limited CI calculations (in the $K = 0$ and $K > 0$ cases). In the MMCC($m_{\mathrm{A}}, m_{\mathrm{B}}$) methods, we limit ourselves to wave functions $|\Psi_K\rangle$ that do not contain higher-than-m_{B}-tuply excited components relative to the $|\Phi\rangle$ reference. This requirement reduces the summation over n in equations (9) and (30) to $\sum_{n=m_{\mathrm{A}}+1}^{m_{\mathrm{B}}}$. The resulting MMCC($m_{\mathrm{A}}, m_{\mathrm{B}}$) energies, $E_K^{\mathrm{MMCC}}(m_{\mathrm{A}}, m_{\mathrm{B}})$, can be given the following form [41–43, 47, 48, 77, 78, 97]:

$$E_K^{\mathrm{MMCC}}(m_{\mathrm{A}}, m_{\mathrm{B}}) = E_K^{(\mathrm{A})} + \delta_K(m_{\mathrm{A}}, m_{\mathrm{B}}), \tag{44}$$

where the formula for the ground-state correction $\delta_0(m_{\mathrm{A}}, m_{\mathrm{B}})$ is

$$\delta_0(m_{\mathrm{A}}, m_{\mathrm{B}}) = \sum_{n=m_{\mathrm{A}}+1}^{m_{\mathrm{B}}} \sum_{j=m_{\mathrm{A}}+1}^{n} \langle \Psi_0 | Q_n \, C_{n-j}(m_{\mathrm{A}}) \, M_j^{\mathrm{CC}}(m_{\mathrm{A}}) | \Phi \rangle / \langle \Psi_0 | \mathrm{e}^{T^{(\mathrm{A})}} | \Phi \rangle \tag{45}$$

and

$$\delta_K(m_{\mathrm{A}}, m_{\mathrm{B}}) = \sum_{n=m_{\mathrm{A}}+1}^{m_{\mathrm{B}}} \sum_{j=m_{\mathrm{A}}+1}^{n} \langle \Psi_K | Q_n \, C_{n-j}(m_{\mathrm{A}}) \, M_{K,j}^{\mathrm{EOMCC}}(m_{\mathrm{A}}) | \Phi \rangle / \langle \Psi_K | R_K^{(\mathrm{A})} \mathrm{e}^{T^{(\mathrm{A})}} | \Phi \rangle \tag{46}$$

is the analogous correction for excited states. Clearly, the non-zero values of corrections $\delta_K^{(\mathrm{A})}$ are obtained only when $m_{\mathrm{B}} > m_{\mathrm{A}}$. When $m_{\mathrm{B}} = N$ and when $|\Psi_K\rangle$ are the exact states, we obtain the exact MMCC theory described in section 2.

In this article, we restrict our discussion to the MMCC($m_{\mathrm{A}}, m_{\mathrm{B}}$) schemes with $m_{\mathrm{A}} = 2$, which can be used to correct the results of the CCSD or EOMCCSD calculations. The MMCC(2, m_{B}) energy expressions can be obtained by setting $m_{\mathrm{A}} = 2$ in equations (44)–(46) or by truncating the summation over n in the exact equations (22) and (42) at $n = m_{\mathrm{B}}$. In this category, two schemes are particularly useful, namely MMCC(2,3) and MMCC(2,4), although we may have to contemplate the higher-order MMCC(2,5) and MMCC(2,6) schemes to obtain the highly

Downloaded At: 16:32 21 January 2011

accurate description of triple bond breaking. We refer the reader to [41, 42, 45, 47] for information about the MMCC$(3,m_{\rm B})$ schemes, which can be used to correct the results of the full CCSDT calculations by adding corrections $\delta_K(3,m_{\rm B})$ to the CCSDT energies.

Depending on the form of $|\Psi_K\rangle$ in the above equations, we divide the existing MMCC$(m_{\rm A},m_{\rm B})$ methods into the following three groups: (i) the CI-corrected MMCC$(m_{\rm A},m_{\rm B})$ schemes [41, 47, 48, 77, 78], which can be applied to ground and excited states; (ii) the renormalized and completely renormalized CC methods for the ground-state problem, which are obtained by inserting the low-order MBPT-like expressions for $|\Psi_0\rangle$ into the MMCC$(m_{\rm A},m_{\rm B})$ formulae [41–47, 49]; and (iii) the most recent quasi-variational MMCC$(m_{\rm A},m_{\rm B})$ approaches to the ground-state problem, including the quadratic MMCC models [161], in which we use the exponential, CC-like, form of $|\Psi_0\rangle$, which we further approximate to reduce the computer cost. It may be possible to extend the completely renormalized CC methods to excited states using the excited-state MMCC$(m_{\rm A},m_{\rm B})$ formulae and EOMCC analogues of the perturbative expressions for $|\Psi_0\rangle$ exploited in the ground-state approaches, but our results in this area, although extremely promising, still have a preliminary character, so that we mention them only at the end, in section 4.

We begin with the CI-corrected MMCC$(m_{\rm A},m_{\rm B})$ schemes. The renormalized and completely renormalized CC methods and the recently formulated quasi-variational MMCC$(m_{\rm A},m_{\rm B})$ approaches [161] are discussed in the following sections. In all cases, the general mathematical and computational concepts are illustrated by examples of applications to molecular systems.

Downloaded At: 16:32 21 January 2011

3.1. *The CI-corrected MMCC$(m_{\rm A},m_{\rm B})$ methods*

In this section, we describe the CI-corrected MMCC$(m_{\rm A},m_{\rm B})$ methods, focusing on the MMCC(2,3) and MMCC(2,4) approximations and their performance in the calculations of ground- and excited-state energies. The higher-order MMCC(2,5) and MMCC(2,6) methods will also be discussed, but only in the context of the ground-state calculations.

3.1.1. *The CI-corrected MMCC(2,3) and MMCC(2,4) approximations: theory*

In the MMCC(2,3) and MMCC(2,4) approaches, we add the relevant corrections $\delta_K^{\rm (A)}$ to the CCSD or EOMCCSD energies. The MMCC(2,3) and MMCC(2,4) energy expressions are obtained by setting $m_{\rm A}$ at 2 and $m_{\rm B}$ at 3 and 4 in equations (44)–(46). We obtain

$$E_0^{\rm MMCC}(2,3) = E^{\rm CCSD} + \langle\Psi_0|Q_3\,M_3^{\rm CC}(2)|\Phi\rangle/\langle\Psi_0|{\rm e}^{T_1+T_2}|\Phi\rangle, \tag{47}$$

$$E_0^{\rm MMCC}(2,4) = E^{\rm CCSD} + \frac{\langle\Psi_0|\{Q_3\,M_3^{\rm CC}(2) + Q_4\,[M_4^{\rm CC}(2) + T_1 M_3^{\rm CC}(2)]\}|\Phi\rangle}{\langle\Psi_0|{\rm e}^{T_1+T_2}|\Phi\rangle}, \tag{48}$$

for the ground-state ($K=0$) case and

$$E_K^{\rm MMCC}(2,3) = E_K^{\rm EOMCCSD} + \langle\Psi_K|Q_3\,M_{K,3}^{\rm EOMCC}(2)|\Phi\rangle/\langle\Psi_K|R_K^{\rm CCSD}{\rm e}^{T_1+T_2}|\Phi\rangle, \tag{49}$$

$$E_K^{\rm MMCC}(2,4) = E_K^{\rm EOMCCSD} + \frac{\langle\Psi_K|\{Q_3\,M_{K,3}^{\rm EOMCC}(2) + Q_4\,[M_{K,4}^{\rm EOMCC}(2) + T_1 M_{K,3}^{\rm EOMCC}(2)]\}|\Phi\rangle}{\langle\Psi_K|R_K^{\rm CCSD}{\rm e}^{T_1+T_2}|\Phi\rangle}, \tag{50}$$

for excited states (the $K > 0$ case). The E^{CCSD} and E_K^{EOMCCSD} energies are the CCSD and EOMCCSD energies, respectively, whereas $M_3^{\mathrm{CC}}(2)|\Phi\rangle$, $M_4^{\mathrm{CC}}(2)|\Phi\rangle$, $M_{K,3}^{\mathrm{EOMCC}}(2)|\Phi\rangle$ and $M_{K,4}^{\mathrm{EOMCC}}(2)|\Phi\rangle$ are the quantities defined in the previous section, which are directly related to the generalized moments of the CCSD and EOMCCSD equations (see equations (18), (19), (40) and (41), respectively). The generalized moments of the CCSD equations that are needed to determine $M_3^{\mathrm{CC}}(2)|\Phi\rangle$ and $M_4^{\mathrm{CC}}(2)|\Phi\rangle$ in equations (47) and (48), $\mathcal{M}_{ijk}^{abc}(2)$ and $\mathcal{M}_{ijkl}^{abcd}(2)$ respectively, are defined by equations (13) and (14). The generalized moments of the EOMCCSD equations that are needed to determine $M_{K,3}^{\mathrm{EOMCC}}(2)|\Phi\rangle$ and $M_{K,4}^{\mathrm{EOMCC}}(2)|\Phi\rangle$ in equations (49) and (50), $\mathcal{M}_{K,ijk}^{abc}(2)$ and $\mathcal{M}_{K,ijkl}^{abcd}(2)$, respectively, are defined by equations (37) and (38). It can be further shown that [77, 78]

$$\mathcal{M}_{K,ijk}^{abc}(2) = \langle \Phi_{ijk}^{abc}|(\bar{H}_2^{\mathrm{CCSD}} R_{K,2})_{\mathrm{C}}|\Phi\rangle + \langle \Phi_{ijk}^{abc}|[\bar{H}_3^{\mathrm{CCSD}}(R_{K,1} + R_{K,2})]_{\mathrm{C}}|\Phi\rangle + \langle \Phi_{ijk}^{abc}|(\bar{H}_4^{\mathrm{CCSD}} R_{K,1})_{\mathrm{C}}|\Phi\rangle + r_{K,0}^{\mathrm{CCSD}} \langle \Phi_{ijk}^{abc}|\bar{H}_3^{\mathrm{CCSD}}|\Phi\rangle \tag{51}$$

and

$$\mathcal{M}_{K,ijkl}^{abcd}(2) = \langle \Phi_{ijkl}^{abcd}|(\bar{H}_3^{\mathrm{CCSD}} R_{K,2})_{\mathrm{C}}|\Phi\rangle + \langle \Phi_{ijkl}^{abcd}|[\bar{H}_4^{\mathrm{CCSD}}(R_{K,1} + R_{K,2})]_{\mathrm{C}}|\Phi\rangle + \langle \Phi_{ijkl}^{abcd}|(\bar{H}_3^{\mathrm{CCSD}} R_{K,1})_{\mathrm{DC}}|\Phi\rangle + r_{K,0}^{\mathrm{CCSD}} \langle \Phi_{ijkl}^{abcd}|\bar{H}_4^{\mathrm{CCSD}}|\Phi\rangle, \tag{52}$$

where, as mentioned earlier, $r_{K,0}^{\mathrm{CCSD}}$ is the coefficient at reference $|\Phi\rangle$ in the many-body expansion of the EOMCCSD eigenvector $R_K^{\mathrm{CCSD}}|\Phi\rangle$, $R_{K,1}$ and $R_{K,2}$ are the singly and doubly excited components of R_K^{CCSD}, and $\bar{H}_j^{\mathrm{CCSD}}$ is the j-body component of the EOMCCSD similarity-transformed Hamiltonian $\bar{H}^{\mathrm{CCSD}}$.

The above expressions immediately imply that the excited-state $\delta_K(2,3)$ corrections are expressed in terms of matrix elements of the EOMCCSD similarity-transformed Hamiltonian that enter the triples–reference (T0), triples–singles (TS) and triples–doubles (TD) blocks of $\bar{H}^{\mathrm{CCSD}}$. The ground-state $\delta_0(2,3)$ correction requires the consideration of only the T0 block of $\bar{H}^{\mathrm{CCSD}}$. The expensive triples–triples (TT) block of $\bar{H}^{\mathrm{CCSD}}$ is not considered in computing corrections $\delta_K(2,3)$, so that the costs of computing corrections $\delta_K(2,3)$ are very similar to the $n_{\mathrm{o}}^3 n_{\mathrm{u}}^4$ costs associated with the popular CCSD(T) [8] ground-state method. Quite similarly, the excited-state corrections $\delta_K(2,4)$ are expressed in terms of the T0, TS and TD blocks of $\bar{H}^{\mathrm{CCSD}}$ in the $\mathcal{M}_{K,ijk}^{abc}(2)$ part and the quadruples–reference (Q0), quadruples–singles (QS) and quadruples–doubles (QD) blocks of $\bar{H}^{\mathrm{CCSD}}$ in the $\mathcal{M}_{K,ijkl}^{abcd}(2)$ part. The ground-state $\delta_0(2,4)$ correction requires the consideration of the T0 and Q0 blocks of $\bar{H}^{\mathrm{CCSD}}$. Again, the most expensive blocks of $\bar{H}^{\mathrm{CCSD}}$, including, for example, the triples–quadruples (TQ), quadruples–triples (QT) and quadruples–quadruples (QQ) blocks, are not considered in the MMCC(2,4) calculations. Those are huge simplifications, particularly if we realize that $\bar{H}^{\mathrm{CCSD}}$ is the similarity-transformed Hamiltonian of the inexpensive CCSD/EOMCCSD approach, i.e. we only have to use the T_1 and T_2 clusters, obtained in the CCSD calculations, to construct it. The most expensive steps of the MMCC(2,4) calculations are very similar to the $n_{\mathrm{o}}^3 n_{\mathrm{u}}^4$ and $n_{\mathrm{o}}^2 n_{\mathrm{u}}^5$ steps seen in calculating the non-iterative triples and quadruples ground-state corrections defining the factorized quadruples CCSD($\mathrm{TQ_f}$) approach of [20].

Further reduction of the computer costs of the CI-corrected MMCC(2,3) and MMCC(2,4) calculations are due to the simple forms of wavefunctions $|\Psi_K\rangle$ used in these calculations. In the CI-corrected MMCC(2,3) calculations, we use the

Downloaded At: 16:32 21 January 2011

wavefunctions $|\Psi_K\rangle$ obtained in the active-space CISDt calculations [41, 47, 48, 77, 78]. In the CI-corrected MMCC(2,4) calculations, we use the wavefunctions $|\Psi_K\rangle$ obtained in the active-space CISDtq calculations [48, 78]. We could also use some other forms of wavefunctions $|\Psi_K\rangle$, resulting from the inexpensive variants of the MRCI method, such as MRDCI [162–164], but in this presentation we will focus on the CISDt and CISDtq schemes as providers of wavefunctions $|\Psi_K\rangle$ for the MMCC calculations, since those have already been tested by us in a number of applications.

In order to define the CISDt and CISDtq wavefunctions for the MMCC(2,3) and MMCC(2,4) calculations, we divide the available spin–orbitals into core spin-orbitals (**i**, **j**, **k**, **l**, ...), active spin–orbitals occupied in reference $|\Phi\rangle$ (**I**, **J**, **K**, **L**, ...), active spin–orbitals unoccupied in $|\Phi\rangle$ (**A**, **B**, **C**, **D**, ...), and virtual spin–orbitals (**a**, **b**, **c**, **d**, ...). Once active orbitals are selected, we define the CISDt and CISDtq wavefunctions as follows [41, 47, 48, 77, 78]:

$$|\Psi_K^{\mathrm{CISDt}}\rangle = (C_{K,0} + C_{K,1} + C_{K,2} + c_{K,3})|\Phi\rangle, \tag{53}$$

$$|\Psi_K^{\mathrm{CISDtq}}\rangle = (C_{K,0} + C_{K,1} + C_{K,2} + c_{K,3} + c_{K,4})|\Phi\rangle, \tag{54}$$

where $C_{K,0}|\Phi\rangle$, $C_{K,1}|\Phi\rangle$ and $C_{K,2}|\Phi\rangle$ are the reference, singly excited and doubly excited components of $|\Psi_K^{\mathrm{CISDt}}\rangle$ and $|\Psi_K^{\mathrm{CISDtq}}\rangle$ and

$$c_{K,3}|\Phi\rangle = \sum_{\substack{\mathbf{I}>j>k \\ a>b>\mathbf{C}}} c_{\mathbf{I}jk}^{ab\mathbf{C}}(K)\,|\Phi_{\mathbf{I}jk}^{ab\mathbf{C}}\rangle, \tag{55}$$

$$c_{K,4}|\Phi\rangle = \sum_{\substack{\mathbf{I}>\mathbf{J}>k>l \\ a>b>\mathbf{C}>\mathbf{D}}} c_{\mathbf{IJ}kl}^{ab\mathbf{CD}}(K)\,|\Phi_{\mathbf{IJ}kl}^{ab\mathbf{CD}}\rangle. \tag{56}$$

Thus, in the CISDt approach, used in the CI-corrected MMCC(2,3) calculations, we construct wavefunctions $|\Psi_K\rangle$ by including all singles and doubles from $|\Phi\rangle$ and a relatively small set of internal and semi-internal triples containing at least one active occupied spin–orbital and at least one active unoccupied spin–orbital index. Similarly, in the CISDtq calculations used to construct wavefunctions $|\Psi_K\rangle$ for the CI-corrected MMCC(2,4) approach, we include all singles and doubles from $|\Phi\rangle$, a relatively small set of internal and semi-internal triples containing at least one active occupied spin–orbital index and at least one active unoccupied spin–orbital index, and a relatively small set of quadruples containing at least two active occupied and at least two active unoccupied spin–orbital indices (cf. equations (55) and (56)). The CI coefficients defining the CISDt and CISDtq wavefunctions are determined variationally. If N_{o} (N_{u}) is the number of active orbitals occupied (unoccupied) in $|\Phi\rangle$, the most expensive steps of the CISDt method scale as $N_{\mathrm{o}}N_{\mathrm{u}}n_{\mathrm{o}}^2n_{\mathrm{u}}^4$, whereas the CISDtq approach is an $N_{\mathrm{o}}^2N_{\mathrm{u}}^2n_{\mathrm{o}}^2n_{\mathrm{u}}^4$ procedure. Since it is sufficient to use rather small active spaces in these calculations, the costs of the CISDt and CISDtq calculations are relatively low. The storage requirements for triples and quadruples characterizing the CISDt and CISDtq methods are relatively small too. The numbers of triples and quadruples considered in the CISDt and CISDtq calculations are $N_{\mathrm{o}}N_{\mathrm{u}}n_{\mathrm{o}}^2n_{\mathrm{u}}^2$ and $N_{\mathrm{o}}^2N_{\mathrm{u}}^2n_{\mathrm{o}}^2n_{\mathrm{u}}^2$, respectively, which is a lot less than the number of all triples and quadruples, if the number of active orbitals is small. In all applications discussed in this work, the number of all triples used in the CISDt-based MMCC(2,3) calculations represented no more than ~30% of all triples. The number of quadruples used in the CISDtq-based MMCC(2,4) calculations represented less

Downloaded At: 16:32 21 January 2011

than 10% (in some cases, 3–4%) of all quadruples (cf., for example, [77, 78] for further details).

The use of the CISDt (the MMCC(2,3) case) and CISDtq (the MMCC(2,4) case) wavefunctions leads to further reductions of the $n_o^3 n_u^4$ and $n_o^2 n_u^5$ costs of constructing the $\delta_K(2,3)$ and $\delta_K(2,4)$ corrections, since we only have to consider the generalized moments of the CCSD/EOMCCSD equations corresponding to projections of these equations on the internal and semi-internal triples and quadruples that are present in the CISDt and CISDtq wavefunctions. For example, once the $|\Psi_K^{\mathrm{CISDt}}\rangle$ wavefunctions are determined by performing the variational CISDt calculations, the costs of constructing the $\delta_K(2,3)$ corrections are $N_o N_u n_o^2 n_u^3$. In practical terms, for the examples of molecular systems and active orbital spaces considered in this article (see sections 3.1.2 and 3.1.3), the actual CPU times required to construct each $\delta_K(2,3)$ correction were comparable with the CPU time of a single CCSD/EOMCCSD iteration. The CPU times needed to construct the $\delta_K(2,4)$ corrections were ~10–30 times larger than the CPU times required to calculate the corresponding $\delta_K(2,3)$ corrections.

The CI-corrected MMCC(2,3) approach represents a useful alternative to the perturbative triples approaches, such as CCSD[T] [7], CCSD(T) [8], EOMCCSD(T) [65], EOMCCSD($\tilde{\mathrm{T}}$) [66], EOMCCSD(T′) [66] and CCSDR(3) [70, 71] and their iterative CCSDT-*n* [13, 50–53], EOMCCSDT-*n* [65, 66] and CC3 [68–71] analogues. The perturbative triples CC/EOMCC or response CC approximations provide an erroneous description of ground- and excited-state PESs [18, 36–49, 72] and fail to describe more complicated excited states, such as the lowest $^1\Delta$ state of the C_2 molecule [71] (see section 3.1.3). The costs of the CI-corrected MMCC(2,3) calculations are similar to the costs of using the non-iterative triples CC/EOMCC methods and yet the results of the CI-corrected MMCC(2,3) calculations for single bond breaking and excited-state PESs are very good [41, 47, 48, 77, 78] (cf. sections 3.1.2 and 3.1.3). Similarly, the CI-corrected MMCC(2,4) approach represents a useful alternative to the perturbative quadruples approaches, such as CCSD(TQ$_f$) [20], which fail to provide a good description of bond breaking [42–48]. As pointed out in [78], the CI-corrected MMCC(2,4) method also represents a very good alternative to the full EOMCCSDT approach [75, 76, 80, 81] to excited states. The EOMCCSDT scheme may fail to provide good results in some cases (see, for example, [73]). The CI-corrected MMCC(2,4) approach appears to be more robust. As shown in [78] (cf. also section 3.1.3), the MMCC(2,4) results for excited states are, on average, considerably better than the results of the full EOMCCSDT calculations. At the same time, the MMCC(2,4) calculations, in which triples as well as quadruples are accounted for in an approximate manner, are often faster than the full EOMCCSDT calculations, in which quadruples are neglected. Because of the use of the CI wavefunctions in constructing the $\delta_K(2,3)$ and $\delta_K(2,4)$ corrections in the CI-corrected MMCC(2,3) and MMCC(2,4) schemes, it is rather easy to adapt the MMCC(2,3) and MMCC(2,4) approaches to the spin and spatial symmetries (something very difficult to accomplish at the EOMCCSDT level).

3.1.2. *The CI-corrected MMCC(2,3) and MMCC(2,4) approximations: examples of applications to ground-state PESs involving bond breaking*

Let us begin with examples of the CI-corrected MMCC(2,3) and MMCC(2,4) benchmark calculations for the ground-state PESs of the HF and H_2O molecules [48]. We used a double zeta (DZ) basis set [165], for which the exact, full CI energies

Downloaded At: 16:32 21 January 2011

Table 1. A comparison of various standard CC, completely renormalized CCSD[T], CCSD(T) and CCSD(TQ), and CI-corrected MMCC(2,3) and MMCC(2,4) ground-state energies with the corresponding full CI, CISDt and CISDtq results obtained for a few internuclear separations R of the HF molecule with the DZ basis set.[a]

Method	$R = R_e$[b]	$R = 2R_e$	$R = 3R_e$	$R = 5R_e$
Full CI[c]	−100.160 300	−100.021 733	−99.985 281	−99.983 293
CCSD	1.634	6.047	11.596	12.291
CCSDT[c]	0.173	0.855	0.957	0.431
CCSD[T][d]	−0.070	−2.725	−38.302	−75.101
CCSD(T)[d]	0.325	0.038	−24.480	−53.183
CCSD(TQ$_f$)[e]	0.218	−0.081	−18.351	−35.078
CR-CCSD[T][d,f]	0.163	0.700	2.508	3.820
CR-CCSD(T)[d,g]	0.500	2.031	2.100	1.650
CR-CCSD(TQ),a[e,h]	0.053	0.396	0.425	0.454
CR-CCSD(TQ),b[i]	0.060	0.299	0.316	0.689
CISDt[e,j]	5.783	16.000	29.238	33.627
CISDtq[e,j]	5.466	6.730	7.456	7.468
MMCC(2,3)[e,j]	1.195	2.708	3.669	3.255
MMCC(2,4)[e,j]	1.207	2.225	3.015	3.066

[a] The full CI total energies are in hartree. The CC, CI and MMCC energies are in millihartree relative to the corresponding full CI energy values.
[b] The equilibrium H–F bond length, R_e, equals 1.7328 bohr.
[c] From [37].
[d] From [41, 42].
[e] From [48].
[f] The completely renormalized CCSD[T] method (see section 3.2).
[g] The completely renormalized CCSD(T) method (see section 3.2).
[h] The 'a' variant of the completely renormalized CCSD(TQ) method (see section 3.2).
[i] The 'b' variant of the completely renormalized CCSD(TQ) method (see section 3.2). The results obtained in the present work.
[j] The active space consisted of the 3σ, 1π, 2π, and 4σ orbitals.

Downloaded At: 16:32 21 January 2011

[37, 166, 167] and many other useful results, including the full CCSDT and CCSDTQ energies [22, 25, 37] and their standard, renormalized and completely renormalized CCSD[T], CCSD(T) and CCSD(TQ) analogues [42], are available. As in all other MMCC calculations overviewed in this work, the ground-state RHF determinant was used as a reference.

The CI-corrected MMCC(2,3) and MMCC(2,4) results for HF and H_2O, obtained in [48], are shown in tables 1 and 2, respectively. They are compared with the exact, full CI, results and a variety of CC results, including the completely renormalized CCSD[T], CCSD(T) and CCSD(TQ) results [41, 42, 48], which are discussed in section 3.2.2. We also compare the MMCC(2,3) and MMCC(2,4) energies with the energy values obtained in the CISDt and CISDtq calculations, which provide the wavefunctions $|\Psi_0\rangle$ for calculating corrections $\delta_0(2,3)$ and $\delta_0(2,4)$. The latter comparison shows how much the results improve when the relatively poor (at best, qualitative) CISDt and CISDtq wavefunctions are inserted into the MMCC(2,3) and MMCC(2,4) energy expressions.

In the case of HF (see table 1), there is a 1.634 millihartree difference between the CCSD and full CI energies at the equilibrium geometry, $R = R_e$ (R is the H–F

Table 2. A comparison of various standard CC, completely renormalized CCSD[T], CCSD(T) and CCSD(TQ), and CI-corrected MMCC(2,3) and MMCC(2,4) ground-state energies with the corresponding full CI, CISDt and CISDtq results obtained for the equilibrium and two displaced geometries of the H_2O molecule with the DZ basis set.[a]

Method	$R = R_e$[b]	$R = 1.5R_e$[c]	$R = 2R_e$[c]
Full CI	−76.157 866[b]	−76.014 521[c]	−75.905 247[c]
CCSD	1.790	5.590	9.333
CCSDT[d]	0.434	1.473	−2.211
CCSDTQ[e]	0.015	0.141	0.108
CCSD[T][f]	0.362	0.751	−11.220
CCSD(T)[f]	0.574	1.465	−7.699
CCSD(TQ_f)[f]	0.166	0.094	−5.914
CR-CCSD[T][f,g]	0.560	2.053	1.163
CR-CCSD(T)[f,h]	0.738	2.534	1.830
CR-CCSD(TQ),a[f,i]	0.195	0.905	1.461
CR-CCSD(TQ),b[j]	0.195	0.836	2.853
CISDt[k,l]	7.229	19.205	50.341
CISDt[l,m]	6.922	18.884	49.948
CISDtq[k,l]	5.844	6.294	8.251
CISDtq[l,m]	2.702	2.919	5.638
MMCC(2,3)[k,l]	1.137	2.710	1.911
MMCC(2,3)[l,m]	0.811	2.407	1.631
MMCC(2,4)[k,l]	1.071	1.634	3.127
MMCC(2,4)[l,m]	0.501	0.942	2.416

[a] The full CI total energies are in hartree. The CC, CI and MMCC energies are in millihartree relative to the corresponding full CI energy values.
[b] The equilibrium geometry and full CI result from [166].
[c] The geometry and full CI result from [167].
[d] From [22].
[e] From [25].
[f] From [42].
[g] The completely renormalized CCSD[T] method (see section 3.2).
[h] The completely renormalized CCSD(T) method (see section 3.2).
[i] The 'a' variant of the completely renormalized CCSD(TQ) method (see section 3.2).
[j] The 'b' variant of the completely renormalized CCSD(TQ) method (see section 3.2). The results obtained in the present work.
[k] The active space consisted of the $3a_1$, $1b_2$, $4a_1$ and $2b_2$ orbitals.
[l] From [48].
[m] The active space consisted of the $1b_1$, $3a_1$, $1b_2$, $4a_1$, $2b_1$ and $2b_2$ orbitals.

Downloaded At: 16:32 21 January 2011

internuclear separation), which increases to 12.291 millihartree at $R = 5R_e$ (for all practical purposes, $R = 5R_e$ can be regarded as a dissociation limit). The large differences between the CCSD and full CI energies at larger values of R are primarily caused by the absence of the connected T_3 clusters in the CCSD wavefunction. The full CCSDT method, which includes these clusters, reduces large errors in the CCSD results, relative to full CI, to as little as 0.173 millihartree at $R = R_e$ and 0.431 millihartree at $R = 5R_e$.

The standard CCSD[T], CCSD(T) and CCSD(TQ_f) approaches fail at large internuclear distances R. The very small errors in the CCSD[T], CCSD(T) and CCSD(TQ_f) results at $R = R_e$ become very large for large values of R. This is well

illustrated by the 75.101, 53.183 and 35.078 millihartree unsigned errors in the CCSD[T], CCSD(T) and CCSD(TQ$_f$) results, respectively, at $R = 5R_e$. As shown in [41–43, 47, 97], the CCSD[T] and CCSD(T) potential energy curves lie significantly below the full CI curve at larger internuclear separations and are characterized by an unphysical hump in the region of intermediate R values. A similar hump is present on the CCSD(TQ$_f$) curve (cf., for example, [46]).

The CI-based MMCC(2,3) and MMCC(2,4) results, shown in table 1, correspond to a choice of the highest occupied and lowest unoccupied σ orbitals, 3σ and 4σ, respectively, and the valence π orbitals as active orbitals in the related CISDt and CISDtq calculations. This is a natural choice of active space for the description of the single bond breaking in HF. In particular, this choice guarantees that the description of the potential energy curve of HF by the CISDt and CISDtq methods is qualitatively correct. However, the CISDt and CISDtq results (particularly the former ones) are quantitatively rather poor at all internuclear separations. Indeed, at the equilibrium geometry, both methods give the >5 millihartree errors relative to full CI and the situation only worsens as we approach the dissociation region. For example, the error in the CISDt result at $R = 5R_e$ is 33.627 millihartree. In the case of the CISDtq method, the error increase is less dramatic, but the 7.468 millihartree error in the CISDtq result at $R = 5R_e$ is still quite large.

Downloaded At: 16:32 21 January 2011

In spite of the relatively poor performance of the CISDt and CISDtq methods and in spite of the large errors in the CCSD results at larger R values, the CISDt-based MMCC(2,3) results and their CISDtq-based MMCC(2,4) analogues are very good. The errors in the MMCC(2,3) results vary between 1.195 millihartree at $R = R_e$ and 3.669 millihartree at $R = 3R_e$. The fact that we can use an inexpensive CISDt method to construct the correction $\delta_0(2,3)$ and reduce, in this way, the 33.627 and 12.291 millihartree errors in the CISDt and CCSD results, respectively, at $R = 5R_e$ to 3.255 millihartree is clearly very encouraging. The use of the better CISDtq wavefunction in the MMCC (MMCC(2,4)) calculations gives a slightly better description of the potential energy curve of HF than that provided by the CISDt-based MMCC(2,3) approach. However, we are not gaining a lot more in this case by performing the more expensive MMCC(2,4) calculations, since the H–F bond is a single bond. Both MMCC potential energy curves (particularly the MMCC(2,4) one) are virtually parallel to the full CI curve.

One of the main reasons for the excellent performance of the CI-based MMCC approaches at large internuclear separations, in spite of the relatively poor description of the potential energy curve of HF by the CISDt and CISDtq methods, is the presence of the $\langle \Psi_0 | e^{T_1+T_2} | \Phi \rangle$ denominators in the expressions for the ground-state MMCC(2,3) and MMCC(2,4) energies, equations (47) and (48), respectively. Those denominators increase their values from $\sim$1.0 at $R = R_e$ to 2.3–2.4 at $R = 5R_e$, damping the corrections due to triples (in the MMCC(2,3) case) or triples and quadruples (in the MMCC(2,4) case), which are considerably overestimated by the traditional CCSD[T], CCSD(T) and CCSD(TQ$_f$) approaches. The increase in the values of the $\langle \Psi_0 | e^{T^{(A)}} | \Phi \rangle$ denominators with stretching chemical bonds is one of the primary characteristics of all MMCC calculations.

Very similar remarks about the performance of the CI-corrected MMCC approximations apply to the case of the simultaneous breaking of both O–H bonds in water (see table 2). This is a challenging case, where both the T_3 clusters and their T_4 counterparts become sizeable. Indeed, when both O–H bonds in H_2O are simultaneously stretched by a factor of 2 (the $R = 2R_e$ case; R is the O–H bond

length), the small, −1.356 and −0.419 millihartree, effects due to T_3 and T_4 at the equilibrium geometry, $R = R_e$ (obtained by forming the CCSDT − CCSD and CCSDTQ − CCSDT energy differences), increase, in absolute value, to −11.544 and 2.319 millihartree, respectively.

It is difficult to describe these large T_3 and T_4 effects for larger values of R with the standard non-iterative CC approximations. The multireference nature of the ground-state wavefunction of H_2O for larger values of R leads to the failure of the CCSD[T], CCSD(T) and CCSD(TQ_f) methods. At $R = 2R_e$, the unsigned errors in the CCSD[T], CCSD(T) and CCSD(TQ_f) results, relative to full CI, are 11.220, 7.699 and 5.914 millihartree, respectively. Even the full CCSDT approach gives a negative, −2.211 millihartree, error at $R = 2R_e$, which is, very likely, the first sign of the breakdown of the CCSDT approximation, which lacks important T_4 clusters, for large values of R. The complete inclusion of T_4 clusters via the CCSDTQ method improves the situation considerably, reducing the 2.211 millihartree error in the CCSDT result at $R = 2R_e$ to 0.108 millihartree (see table 2).

In view of the failure of the standard CCSD[T], CCSD(T) and CCSD(TQ_f) methods at stretched geometries of H_2O, it is remarkable to see that the simple CI-corrected MMCC(2,3) and MMCC(2,4) approximations provide a very good description of the simultaneous breaking of both O–H bonds. This is particularly true for the CISDt-corrected MMCC(2,3) method, which requires a very small computer effort to construct the relevant correction $\delta_0(2,3)$. Already with the minimum set of active orbitals that provide a qualitatively correct description of the simultaneous breaking of both O–H bonds in water (the highest-energy occupied orbitals, $3a_1$ and $1b_2$, and the two lowest-energy unoccupied orbitals, $4a_1$ and $2b_2$; cf. [132]), the CISDt-corrected MMCC(2,3) approach is capable of reducing the 5.590 and 9.333 millihartree errors in the CCSD results at $R = 1.5R_e$ and $R = 2R_e$, and almost equally large (at $R = 2R_e$) unsigned errors in the CCSD[T], CCSD(T) and CCSD(TQ_f) results, to 2.710 and 1.911 millihartree, respectively. With the somewhat better choice of active orbitals, which guarantees a more uniform description of the equilibrium and bond-breaking regions (the three highest-energy occupied orbitals, $1b_1$, $3a_1$ and $1b_2$, and the three lowest-energy unoccupied orbitals, $4a_1$, $2b_1$ and $2b_2$), we obtain even better results. Interestingly enough, the CISDt method, on which the calculation of the MMCC(2,3) correction $\delta_0(2,3)$ is based, provides a poor description of bond breaking in H_2O (cf., for example, the huge, ~19 millihartree, errors in the CISDt results at $R = 1.5R_e$ and even bigger, ~50 millihartree, errors in the CISDt energies at $R = 2R_e$). One of the major strengths of the MMCC(2,3), MMCC(2,4) and similar methods is the ability of these approaches to produce excellent results even when the ground-state wavefunctions $|\Psi_0\rangle$, used to construct the relevant energy corrections, are themselves rather poor. The CISDt-corrected MMCC(2,3) results for the H_2O molecule are a clear demonstration of this principle.

The CISDtq-based MMCC(2,4) results at $R = 2R_e$ seem to be slightly worse than the corresponding CISDt-based MMCC(2,3) results, but the MMCC(2,4) approach offers a more balanced description of the simultaneous breaking of both O–H bonds in H_2O. Indeed, the small, 0.5–1 millihartree, errors in the MMCC(2,4) results at $R = R_e$ slowly and monotonically increase with R, whereas the errors in the MMCC(2,3) results initially increase, as we go from the $R = R_e$ region to $R = 1.5R_e$, and then decrease, as we approach the $R > 1.5R_e$ region. This might be the first sign of the breakdown of the MMCC(2,3) approximation at very large distances R, although we have no solid proof that would support this statement at

Downloaded At: 16:32 21 January 2011

this time. What is well understood is the fact that the simultaneous breaking of both O–H bonds leads to increasingly large T_4 effects and those cannot be described by the simple, non-iterative triples-like, MMCC(2,3) approximation.

There are several factors that are responsible for the superb performance of the CISDtq-based MMCC(2,4) approach in the calculations for bond breaking in H_2O. One of them is the fact that the CISDtq method provides a much better description of the simultaneous breaking of both O–H bonds in H_2O than the CISDt method used in the MMCC(2,3) calculations (see table 2). The incorporation of the quadruply excited moments of the CCSD equations in the MMCC(2,4) calculations is responsible for some improvements, too, particularly in the $R \approx 1.5R_e$ region. However, the bulk of the improvements in the CCSD results obtained by the MMCC theory is already achieved at the lowest MMCC(2,3) level, which uses a relatively poor CISDt wavefunction to construct the corresponding correction $\delta_0(2,3)$. This is related to the dominant role of T_3 clusters in describing the O–H bond breaking in H_2O, which are included in an approximate manner in the MMCC(2,3) calculations. As in the case of the HF molecule, another factor that helps to improve the MMCC(2,3) and MMCC(2,4) results at larger values of R is the presence of the $\langle \Psi_0|e^{T_1+T_2}|\Phi\rangle$ denominators in the MMCC(2,3) and MMCC(2,4) energy expressions. In the case of bond breaking in H_2O, those denominators increase their values from ~1.0 at $R = R_e$ to 1.5–1.7 at $R = 2R_e$. Without the presence of the $\langle \Psi_0|e^{T_1+T_2}|\Phi\rangle$ denominators in equations (47) and (48), the MMCC(2,3) and MMCC(2,4) results would be much worse.

Downloaded At: 16:32 21 January 2011

The small, 0.501, 0.942 and 2.416 millihartree, errors in the CISDtq-based MMCC(2,4) results at $R = R_e$, $1.5R_e$ and $2R_e$, respectively, obtained with the active space consisting of only six valence orbitals, and the fact that the MMCC(2,4) and full CI potential energy curves are almost parallel are very encouraging from the point of view of applications of the CI-based MMCC methods to PESs involving bond breaking. Even if the CISDt-corrected MMCC(2,3) approach breaks down for O–H distances $R \gg 2R_e$, the fact that this simple and inexpensive approach provides 1–3 millihartree errors for all R values ranging between R_e and $2R_e$ is very promising too. Finally, it is very encouraging to see that the CI-corrected MMCC(2,3) and MMCC(2,4) approaches provide energies that are invariably above the full CI energies. This is actually true for bond breaking in water and HF and for many other examples of bond breaking, except for the most complicated types of multiple bond breaking, for which we must go beyond the MMCC(2,4) approximation (see section 3.1.4). The CI-corrected MMCC approximations are capable of eliminating the non-variational behaviour (energies considerably below the full CI energies) of the CCSD[T], CCSD(T) and CCSD(TQ_f) methods. As we will see in Section 3.2, the same is true for other MMCC methods, including the completely renormalized CCSD[T], CCSD(T) and CCSD(TQ) approaches.

3.1.3. *The CI-corrected MMCC(2,3) and MMCC(2,4) approximations: examples of applications to excited states*

Let us now turn our attention to the CI-corrected MMCC(2,3) and MMCC(2,4) methods for excited states. We used those methods to calculate the ground- and excited-state PESs of CH^+ [77,78] and the vertical excitation energies in H_2O, N_2 and C_2 [47, 78]. Here, we overview the results for CH^+, N_2 and C_2, starting with CH^+.

The results of our MMCC calculations for CH^+ are shown in tables 3 and 4 and figure 1. We used the [5s3p1d/3s1p] basis set of Olsen *et al.* [168], for which the full

Downloaded At: 16:32 21 January 2011

Table 3. Vertical excitation energies (in eV) of CH^+, N_2 and C_2.[a] The full CI values represent the excitation energies, whereas all remaining values are the deviations from the full CI results. The $n\,^1X$ energy is the vertical excitation energy from the ground state ($1\,^1\Sigma^+$ for CH^+ and $1\,^1\Sigma_g^+$ for N_2 and C_2) to the nth singlet state of symmetry X.

Molecule	State	Full CI[a]	EOMCCSD	CC3[b]	EOMCCSDt[c,d]	EOMCCSDT[e]	MMCC(2,3)[d,f]	MMCC(2,4)[d,f]	CISDt[d,f]	CISDtq[d,f]
CH^+	$2\,^1\Sigma^+$	8.549	0.560	0.230	0.092	0.074	0.084	0.023	0.882	0.041
	$3\,^1\Sigma^+$	13.525	0.055	0.016	0.000	0.001	0.000	−0.001	0.116	0.133
	$4\,^1\Sigma^+$	17.217	0.099	0.026	0.012	−0.002	0.015	0.008	0.599	0.552
	$1\,^1\Pi$	3.230	0.031	0.012	0.003	−0.003	0.007	0.010	−0.005	0.033
	$2\,^1\Pi$	14.127	0.327	0.219	0.094	0.060	0.105	0.037	0.504	0.380
	$1\,^1\Delta$	6.964	0.924	0.318	0.057	0.040	0.051	0.031	0.605	0.052
	$2\,^1\Delta$	16.833	0.856	0.261	0.016	−0.038	0.006	0.061	0.789	0.431
N_2[g]	$1\,^1\Pi_g$	9.584	0.081	0.033	0.029	0.009	0.092	0.080	0.246	0.162
	$1\,^1\Sigma_u$	10.329	0.136	0.007	−0.005	0.004	0.008	0.032	−0.190	0.080
	$1\,^1\Delta_u$	10.718	0.180	0.009	0.001	0.008	0.024	0.039	−0.151	0.090
	$1\,^1\Pi_u$	13.609	0.400	0.177	0.090	0.052	0.246	0.085	1.047	0.401
C_2[g]	$1\,^1\Pi_u$	1.385	0.089	−0.068	−0.047	0.034	−0.078	−0.044	−0.627	−0.238
	$1\,^1\Delta_g$	2.293	2.054	0.859	0.285	0.407	0.130	0.011	1.182	−0.306
	$1\,^1\Sigma_u^+$	5.602	0.197	−0.047	0.088	0.113	−0.032	−0.039	0.004	0.310
	$1\,^1\Pi_g$	4.494	1.708	0.496	0.075	0.088	−0.026	0.057	1.309	0.145

[a] The full CI results and basis set for CH^+ taken from [168] (see also [79]). The full CI results and basis sets for N_2 and C_2 taken from [71]. The equilibrium bond lengths in CH^+, N_2 and C_2 are 2.13713, 2.068 and 2.348 bohr, respectively.
[b] The CC3 results for CH^+ taken from [69]. The CC3 results for N_2 and C_2 taken from [71].
[c] From [75, 76, 81]. For N_2, the Cartesian d functions were used, instead of the spherical d functions that were used in the remaining calculations for this molecule.
[d] For CH^+, the active space consisted of the 3σ, $1\pi_x \equiv 1\pi$, $1\pi_y \equiv 2\pi$ and 4σ orbitals. For N_2, the active space consisted of the $3\sigma_g$, $1\pi_u$, $2\pi_u$, $1\pi_g$, $2\pi_g$ and $3\sigma_u$ orbitals. For C_2, the active space consisted of the $1\pi_u$, $2\pi_u$, $3\sigma_g$, $3\sigma_u$, $1\pi_g$ and $2\pi_g$ orbitals.
[e] From [76] (CH^+) and [81] (N_2 and C_2).
[f] From [78] (see also [77]).
[g] The lowest-energy core orbitals, $1\sigma_g$ and $1\sigma_u$, were kept frozen.

Downloaded At: 16:32 21 January 2011

Table 4. Mean absolute errors in the calculated vertical excitation energies relative to the corresponding full CI values for CH^+, N_2 and C_2. Three different geometries of CH^+, corresponding to the equilibrium geometry, $R_{C\text{-}H} = R_e = 2.137\,13$ bohr, and two stretched geometries, $R_{C\text{-}H} = 1.5R_e$ and $2R_e$, are considered (based on the data included in table 3 and figure 1; see the text and [77, 78] for further details). Units are eV.

	Mean absolute error							
Molecule	EOMCCSD	CC3	EOMCCSDt	EOMCCSDT	MMCC(2,3)	MMCC(2,4)	CISDt	CISDtq
$CH^+(R_{C\text{-}H} = R_e)$	0.407	0.155	0.039	0.031	0.038	0.024	0.500	0.232
$CH^+(R_{C\text{-}H} = 1.5R_e)$	0.704		0.047	0.037	0.048	0.022	0.467	0.134
$CH^+(R_{C\text{-}H} = 2R_e)$	1.062		0.070	0.066	0.047	0.016	0.348	0.112
N_2	0.199	0.055	0.031	0.018	0.093	0.059	0.409	0.183
C_2	1.012	0.368	0.124	0.161	0.067	0.038	0.781	0.250

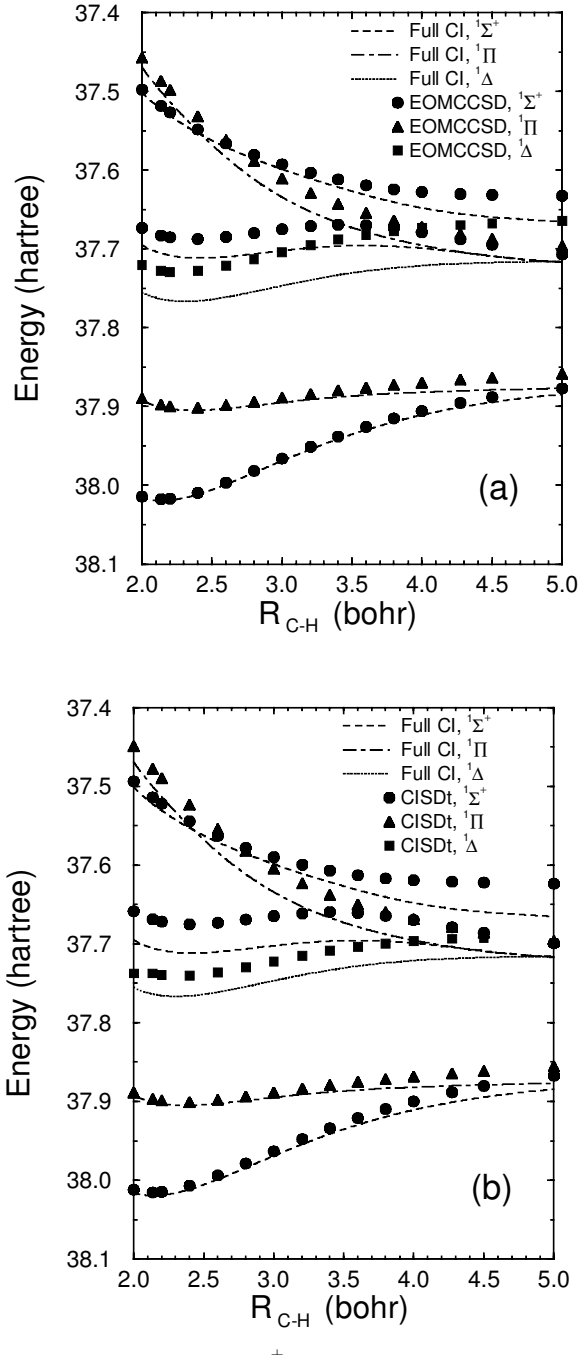

Figure 1. Potential energy curves for the CH^+ ion (energies in hartree and the C–H distance $R_{C\text{-}H}$ in bohr). The results include the ground state and the two lowest excited states of $^1\Sigma^+$ symmetry, for which the full CI curves are indicated by the dashed curves and other results by ●, the two lowest $^1\Pi$ states, for which the full CI curves are indicated by the dashed-dotted curves and other results by ▲ and the lowest $^1\Delta$ state, for which the full CI curve is indicated by the dotted curves and other results by ■. (*a*) A comparison of the EOMCCSD and full CI results. (*b*) A comparison of the CISDt and full CI results. (*Continued*)

Downloaded At: 16:32 21 January 2011

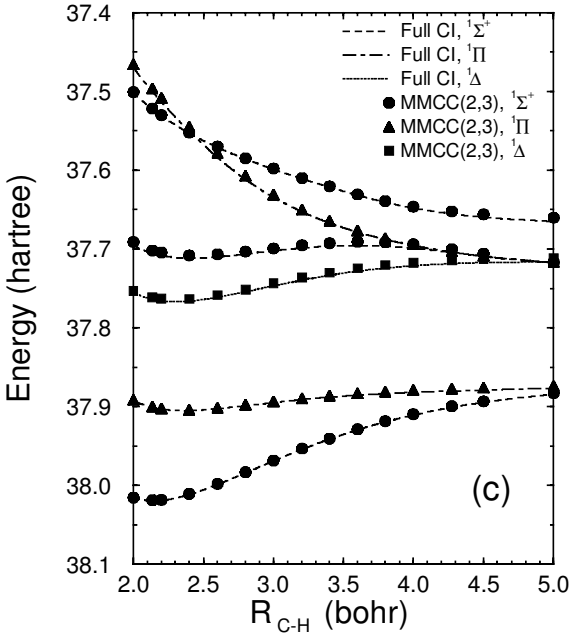

Figure 1 (*continued*). (*c*) A comparison of the CISDt-corrected MMCC(2,3) and full CI results (see [77] for the original numerical data).

Downloaded At: 16:32 21 January 2011

CI results at the equilibrium, $R_{C\text{-}H} = R_e = 2.13713$ bohr, geometry and several stretched geometries can be found in [79, 168]. The MMCC(2,3) and MMCC(2,4) results are compared with the full CI data as well as with the results of the EOMCCSD, full EOMCCSDT [75, 76], CC3 [69] and full EOMCCSDt [75, 76] calculations. Let us recall that the CC3 approach represents one of the most successful perturbative triples response CC models developed by the Jørgensen Aaarhus group [68–71] (for other results for CH^+, obtained with other perturbative triples EOMCC or response CC approaches developed by the Jørgensen and Bartlett groups, see [65, 66, 69, 70]). The EOMCCSDt method is the recently formulated [74–76] excited-state extension of the active-space CCSDt [39, 40, 44] and SSCCSD(T) [27, 128–135] approaches, in which the triexcited components of the cluster operator T and excitation operator R_K are selected with the help of active orbitals using the same triples selection scheme as used in the CISDt method (cf. equations (53) and (55)). When all orbitals are active, the EOMCCSDt approach and the full EOMCCSDT method become completely equivalent. As we will see below, the non-iterative MMCC(2,3) and MMCC(2,4) methods provide results which are considerably better than those obtained with the iterative CC3 approach and comparable with the results of the full EOMCCSDt and EOMCCSDT calculations.

In the case of the CH^+ system, in calculating the CISDt and CISDtq wavefunctions that enter the CI-corrected MMCC(2,3) and MMCC(2,4) approximations, we employed a small active space consisting of the highest-energy occupied orbital, 3σ, and three lowest-energy unoccupied orbitals, $1\pi_x \equiv 1\pi$, $1\pi_y \equiv 2\pi$ and 4σ. As explained in considerable detail in [77] (cf. also [74, 75]), this choice of active space is based on the information about orbital excitations defining the valence excited states of CH^+. The same active space was used in the EOMCCSDt

calculations, whose results are included in tables 3 and 4 [75, 76, 81]. The CISDt and CISDtq excitation energies for CH^+ can be found in tables 3 and 4. The CISDt potential energy curves are shown in figure 1(*b*).

We begin our discussion of the MMCC(2,3) and MMCC(2,4) calculations for CH^+ with the results for $R_{C\text{-}H} = R_e$. For transitions to states that have a predominantly biexcited nature (the first-excited $^1\Sigma^+$ state and the lowest two $^1\Delta$ states) and for the second $^1\Pi$ state that has a significant biexcited component, the errors in the vertical excitation energies at the equilibrium value of $R_{C\text{-}H}$, obtained with the non-iterative MMCC(2,3) approach, are 0.00–0.10 eV. This should be compared with the much larger 0.33–0.92 eV errors in the EOMCCSD results and with the 0.22–0.32 eV errors obtained with the CC3 approach. The only methods that provide competitive results are the iterative EOMCCSDt and EOMCCSDT approaches. Interestingly enough, the CISDt method, which is used to construct the MMCC(2,3) corrections $\delta_K(2,3)$, provides poor excitation energies. However, in spite of the large, 0.50–0.88 eV, errors in the CISDt results for states having large doubly excited components, the CISDt-corrected MMCC(2,3) approximation provides high-quality results. Similar remarks apply to the remaining excited states of CH^+ listed in table 3 (the third and fourth $^1\Sigma^+$ states and the lowest $^1\Pi$ state). Those states are dominated by single excitations, so that the EOMCCSD results are much better in this case, offering us relatively small, 0.03–0.10 eV, errors, but the MMCC(2,3) method provides considerable improvements, reducing the errors in the EOMCCSD results to as little as 0.00–0.02 eV. The MMCC(2,3) results for the third and fourth $^1\Sigma^+$ states and the lowest $^1\Pi$ state are again similar to the results of the EOMCCSDt and EOMCCSDT calculations.

Downloaded At: 16:32 21 January 2011

In view of the excellent performance of the CI-corrected MMCC(2,3) approximation, one might think that it may be hard to make further improvements by applying the MMCC formalism. It is, therefore, somewhat surprising and certainly very encouraging to observe that the CISDtq-corrected MMCC(2,4) results for the first-excited $^1\Sigma^+$ state, the lowest $^1\Delta$ state and the second $^1\Pi$ state are considerably better than those provided by the EOMCCSDT or MMCC(2,3) approaches. For example, the 0.023 and 0.037 eV errors in the MMCC(2,4) results for the first-excited $^1\Sigma^+$ state and the second $^1\Pi$ state, respectively, are 2–3 times smaller than the errors obtained with the MMCC(2,3) and full EOMCCSDT approximations. The MMCC(2,4) results for states dominated by singles (the third and fourth $^1\Sigma^+$ states and the lowest $^1\Pi$ state) are excellent too. The very small errors in the MMCC(2,4) results for the excitation energies corresponding to these three states of 0.001, 0.008 and 0.010 eV, respectively, are very similar to the errors obtained in the MMCC(2,3), EOMCCSDt and full EOMCCSDT calculations. It is useful to learn that the MMCC(2,4) method behaves in a systematic manner, improving most of the MMCC(2,3) results for states having significant doubly excited components and leaving the excellent MMCC(2,3) results for states dominated by singles virtually unchanged.

Let us next discuss the MMCC(2,3) and MMCC(2,4) results for the selected stretched nuclear geometries ($R_{C\text{-}H} = 1.5R_e$ and $2R_e$; cf. table 4 and [77, 78]) and let us also analyse the performance of the MMCC(2,3) method in calculations of entire PESs (see figure 1(*c*)). As the CH^+ ion dissociates into $C^+(2p\ ^2P)$ and $H(1s\ ^2S)$, the full CI expansion of the ground-state wavefunction becomes a mixture of mainly three configurations: the RHF configuration and the singly and doubly excited determinants corresponding to the HOMO $\rightarrow$ LUMO ($3\sigma \rightarrow 4\sigma$) excitations. The

multiconfigurational character of the ground-state wavefunction at larger C–H separations leads to large errors in the results of the CCSD calculations for the ground electronic state. For example, at $R_{C\text{-}H} = 5.0$ bohr, the difference between the CCSD and full CI values of the ground-state energy is 7.517 millihartree, compared with 1.969 millihartree at $R_{C\text{-}H} = R_e$ [76]. This in itself creates a challenging situation for the non-iterative MMCC(2,3) and MMCC(2,4) approximations, in which we use the CCSD T_1 and T_2 cluster components to calculate the $\delta_0(2,3)$ and $\delta_0(2,4)$ corrections to the CCSD energy.

The complicated multiconfigurational structure of the excited states of CH^+ at larger C–H distances $R_{C\text{-}H}$ increases the challenge even further. As the C–H distance increases, all excited states of CH^+ listed in table 3 gain large biexcited components and, in addition, the second $^1\Delta$ state gains a considerable triexcited component [75, 77]. For example, the coefficients in the normalized full CI wavefunction representing the first-excited $^1\Sigma^+$ state at the configuration state functions corresponding to the RHF ground-state determinant and the $3\sigma^2 \rightarrow 1\pi^2$, $3\sigma^2 \rightarrow 4\sigma^2$ and $3\sigma \rightarrow 4\sigma$ excitations are 0.233, −0.679, 0.322 and −0.544, respectively. The lowest $^1\Pi$ state, which at $R_{C\text{-}H} = R_e$ is dominated by singles, becomes a mixture of the singly excited configurations of the $3\sigma \rightarrow 1\pi_{x(y)}$ type and doubly excited configurations of the $3\sigma^2 \rightarrow 4\sigma 1\pi_{x(y)}$ type. A similar remark applies to the second $^1\Pi$ state. The third $^1\Sigma^+$ state, which at $R_{C\text{-}H} = R_e$ is dominated by singles, gains considerable doubly excited components of the $3\sigma^2 \rightarrow 1\pi^2$ and $3\sigma^2 \rightarrow 4\sigma^2$ type. The lowest $^1\Delta$ state does not change its biexcited character and remains dominated by the $3\sigma^2 \rightarrow 1\pi^2$ configurations for all values of $R_{C\text{-}H}$, but the second $^1\Delta$ state, which is also dominated by doubles at $R_{C\text{-}H} = R_e$, gains significant triexcited components of the $2\sigma 3\sigma^2 \rightarrow 4\sigma 1\pi^2$ type. All of this leads to a complete failure of the EOMCCSD approach at larger C–H separations. The errors in the EOMCCSD excitation energies, relative to full CI, for the three lowest excited states of the $^1\Sigma^+$ symmetry, the two lowest $^1\Pi$ states and the two lowest $^1\Delta$ states are 0.668, 0.124, 0.256, 0.109, 0.564, 1.114 and 2.095 eV, respectively, for $R_{C\text{-}H} = 1.5R_e$ and 0.299, 0.532, 0.771, 0.234, 0.467, 1.178 and 3.950 eV, respectively, for $R_{C\text{-}H} = 2R_e$ [76–78]. This implies that the description of the ground- and excited-state PESs of CH^+ constitutes a serious challenge to all kinds of *ab initio* methods, including our non-iterative MMCC(2,3) and MMCC(2,4) approximations.

The results summarized in table 4 and figure 1(*c*) (cf. [77, 78] for further details) show that the MMCC(2,3) and MMCC(2,4) approaches handle this challenge very well. In spite of using a very small active space in the corresponding CISDt and CISDtq calculations and in spite of the failure of the CCSD and EOMCCSD methods at larger internuclear separations, the mean errors in the excitation energies corresponding to all seven states listed in table 3, obtained with the MMCC(2,3) and MMCC(2,4) methods, are as little as 0.048 and 0.022 eV, respectively, at $R_{C\text{-}H} = 1.5R_e$ and 0.047 and 0.016 eV, respectively, at $R_{C\text{-}H} = 2R_e$. The maximum unsigned errors in the MMCC(2,3) and MMCC(2,4) results at $R_{C\text{-}H} = 1.5R_e$ are only 0.086 and 0.046 eV, respectively. At $R_{C\text{-}H} = 2R_e$, those maximum errors are 0.079 and 0.029 eV, respectively [77, 78]. This should be compared with the huge 1.114 and 2.095 eV errors in the EOMCCSD results for the lowest two $^1\Delta$ states at $R_{C\text{-}H} = 1.5R_e$ and with 1.178 and 3.950 eV errors in the EOMCCSD results for the same states at $R_{C\text{-}H} = 2R_e$ [77,78]. The MMCC(2,3) non-iterative corrections $\delta_K(2,3)$ reduce the 0.704 and 1.062 eV mean errors in the EOMCCSD results at $R_{C\text{-}H} = 1.5R_e$ and $2R_e$ by an impressive factor of 15–22 (see table 4). The

Downloaded At: 16:32 21 January 2011

MMCC(2,4) corrections $\delta_K(2,4)$ reduce those errors further, offering us 32 and 66 times smaller mean errors at $R_{C\text{-}H} = 1.5R_e$ and $2R_e$ than the EOMCCSD approach. A similar reduction of errors by a factor of 2–3, when switching from the basic MMCC(2,3) approximation to its higher-order MMCC(2,4) analogue, is also observed in other calculations (cf., for example, the results for the N_2 and C_2 molecules in tables 3 and 4). The fact that the mean absolute errors characterizing the MMCC(2,3) and MMCC(2,4) approximations are as little as 0.04–0.05 and ~0.02 eV, respectively, independent of the nuclear geometry, is another interesting finding. For example, the mean absolute errors characterizing the expensive and iterative full EOMCCSDT method not only are larger than those characterizing the MMCC(2,4) method but also increase with $R_{C\text{-}H}$, from 0.031 eV at $R_{C\text{-}H} = R_e$ to 0.066 eV at $R_{C\text{-}H} = 2R_e$ (see table 4). At the latter C–H distance, the EOMCCSDT method provides worse results than both MMCC(2,3) and MMCC(2,4) approximations.

As in the $R_{C\text{-}H} = R_e$ case, the CISDt approach provides us with a poor description of the electronic states of CH^+ for larger $R_{C\text{-}H}$ values. At $R_{C\text{-}H} = 2R_e$, the errors in the excitation energies corresponding to transitions to the three lowest excited states of the $^1\Sigma^+$ symmetry, two lowest $^1\Pi$ states and two lowest $^1\Delta$ states are 0.351, 0.591, 0.286, 0.082, 0.342, 0.334 and 0.450 eV, respectively [77, 78]. When the CISDt wavefunctions, giving these relatively large errors, are inserted into the formula for the MMCC(2,3) corrections $\delta_K(2,3)$, the errors decrease to 0.007–0.079 eV. On average, we observe a ~10-fold reduction in the mean errors when the CISDt approximation is replaced by the CISDt-corrected MMCC(2,3) approach (see table 4). A similar reduction of errors is observed when we compare the CISDtq results with the CISDtq-based MMCC(2,4) results. The mean absolute errors in the CISDtq results for CH^+ range between 0.112 and 0.232 eV, which should be compared with the 0.016–0.024 eV mean absolute errors in the corresponding MMCC(2,4) results (see table 4).

Downloaded At: 16:32 21 January 2011

As in the case of the ground-state calculations for HF and H_2O, an improvement in the results for the excitation energies of CH^+ offered by the higher-order MMCC(2,4) approach is a consequence of the following two factors: (i) the incorporation of quadruple excitations in the MMCC formalism by the explicit consideration of the $M_{K,4}^{\mathrm{EOMCC}}(2)|\Phi\rangle$ terms or the quadruply excited moments $\mathcal{M}_{K,ijkl}^{abcd}(2)$ in calculating the MMCC(2,4) energies (cf. equations (50) and (41)); (ii) the use of the CISDtq method in determining the wavefunctions $|\Psi_K\rangle$ that enter the MMCC(2,4) energy corrections. Clearly, the CISDtq method provides better results for excited states than the CISDt approach, used to calculate the MMCC(2,3) correction $\delta_K(2,3)$. This has a positive effect on the calculated MMCC(2,4) excitation energies. We must emphasize, however, that the CISDtq method alone is not a great method for excited states. The errors in the CISDtq results can be, in some cases, very small (cf. the 0.015 eV error in the CISDtq energy of the first-excited $^1\Sigma^+$ state at $R_{C\text{-}H} = 2R_e$ [78]), but usually they exceed 0.3 eV [78] (see also table 3).

The high quality of the MMCC(2,3) PESs and the poor quality of the EOMCCSD and CISDt PESs can also be seen in figure 1. The MMCC(2,3) results are so good that it is, in fact, hard to distinguish between the MMCC(2,3) and full CI curves in figure 1(*c*). As shown in [77], the huge (often >1 eV) errors in the EOMCCSD and CISDt results for the entire excited-state PESs of CH^+ (cf. figures 1(*a*) and 1(*b*)) decrease in our MMCC(2,3) calculations to 0.00–0.10 eV. As in the case of the vertical excitation energies, the MMCC(2,4) approach provides further

improvements. Moreover, the MMCC(2,3) and MMCC(2,4) approximations are capable of providing the correct asymptotic behaviour of the potential energy curves of CH^+, restoring, for example, the degeneracy of the second $^1\Sigma^+$ state, the second $^1\Pi$ state and the lowest $^1\Delta$ state in the $R_{C\text{-}H} = \infty$ limit, which is broken by all doubles models, including the EOMCCSD approach (see figure 1 (*a*)) and the so-called VOO-CCD method advocated by Head-Gordon and co-workers [79]. These three states should be exactly degenerate in the $R_{C\text{-}H} = \infty$ limit, since they describe the dissociation of the excited CH^+ ion into $C(2p^2\ ^1D)$ and H^+. For example, the full CI energies of the second $^1\Sigma^+$ state, the second $^1\Pi$ state and the lowest $^1\Delta$ state differ by less than 0.027 eV for $R_{C\text{-}H} = 5.0$ bohr [79]. However, the EOMCCSD energies of these states do not approach the same value when $R_{C\text{-}H}$ approaches ∞ (see figure 1 (*a*)). For $R_{C\text{-}H} = 5.0$ bohr, the difference between the EOMCCSD energies of the second $^1\Sigma^+$ and lowest $^1\Delta$ states is 1.163 eV. The difference between the EOMCCSD energies of the lowest $^1\Delta$ and second $^1\Pi$ states is 0.865 eV [76, 77]. The MMCC(2,3) and MMCC(2,4) methods correct this problem (see figure 1(*c*)). For example, the MMCC(2,3) energies of the second $^1\Sigma^+$ and lowest $^1\Delta$ states differ only by 0.136 eV for $R_{C\text{-}H} = 5.0$ bohr [77]. The MMCC(2,3) energies of the second $^1\Sigma^+$ and second $^1\Pi$ states differ by 0.008 eV at the same C–H distance. The analogous differences between the MMCC(2,4) energies are even smaller.

Downloaded At: 16:32 21 January 2011

The excellent performance of the MMCC(2,3) and MMCC(2,4) approaches in studies of excited states of CH^+ has been confirmed in a number of other calculations, including the calculations for N_2 and C_2 [78]. The N_2 and C_2 molecules provide us with examples of excited states that have significant singly or doubly excited components in a situation where the CCSD method gives a poor description of the ground state. This immediately creates a very demanding situation for the EOMCC and MMCC approaches, since both methods use the similarity-transformed Hamiltonian, which is based on the results of the single-reference CC calculations for the ground electronic state. The C_2 molecule is particularly complicated, since it has low-lying excited states dominated by doubles in a challenging situation where the T_3 and T_4 clusters are large and where the CCSD approach provides a poor description of the ground electronic state.

In order to test the MMCC methods in these demanding cases, we applied the MMCC(2,3) and MMCC(2,4) approaches to the lowest $^1\Pi_g$, $^1\Sigma_u^-$, $^1\Delta_u$ and $^1\Pi_u$ states of N_2 and the lowest $^1\Pi_u$, $^1\Delta_g$, $^1\Sigma_u^+$ and $^1\Pi_g$ states of C_2 [78] (see tables 3 and 4). The corresponding full CI excitation energies were obtained by Christiansen *et al.* [71], who used the cc-pVDZ basis set [169] for N_2 and the modified aug-cc-pVDZ basis set [169, 170] for C_2 (for further information about basis sets and equilibrium nuclear geometries used in these full CI calculations, see [71]; we used the same basis sets and geometries in our MMCC calculations; see also table 3).

The active orbitals used in the CI-corrected MMCC(2,3) and MMCC(2,4) calculations were the $3\sigma_g$, $1\pi_u$, $2\pi_u$, $1\pi_g$, $2\pi_g$ and $3\sigma_u$ orbitals (the three highest occupied and three lowest unoccupied orbitals) in the case of N_2 and the $1\pi_u$, $2\pi_u$, $3\sigma_g$, $3\sigma_u$, $1\pi_g$ and $2\pi_g$ orbitals (the two highest occupied and four lowest unoccupied orbitals) in the case of C_2. This choice of active orbitals is justified by the dominant role of the corresponding orbital excitations in describing the valence excited states of N_2 and C_2 listed in table 3.

As in the case of CH^+, the CI-corrected MMCC(2,3) and MMCC(2,4) results for N_2 and C_2 are compared with the results of the EOMCCSD, CC3 [71], EOMCCSDt [75, 81], EOMCCSDT [81] and full CI [71] calculations. In the EOMCCSDt

calculations reported in [75, 81], we used the same small active spaces as employed in the MMCC(2,3)/CISDt and MMCC(2,4)/CISDtq calculations. We also compare the MMCC results with the results of the CISDt and CISDtq calculations, which are needed to obtain the wavefunctions $|\Psi_K\rangle$ that are used to construct the MMCC corrections $\delta_K(2,3)$ and $\delta_K(2,4)$.

Before discussing the performance of the MMCC(2,3) and MMCC(2,4) approaches for the excited states of the N_2 and C_2 molecules, let us mention that the ground electronic states of N_2 and C_2 are characterized by large T_3 contributions. For N_2, the difference between the CCSD and full CI ground-state energies is 13.465 millihartree and most of this difference is due to T_3 [71]. The effect of T_4 and higher-order clusters, although not negligible, is significantly smaller in this case (for example, the difference between the CCSDT and full CI ground-state energies is only 1.627 millihartree [75]). The correlation effects characterizing the ground state of C_2 are even more complex. They are, in fact, largely non-dynamic, which is reflected in huge T_3 and relatively large T_4 contributions (26.324 and 2.651 millihartree, respectively [39]).

The large role of T_3 and, in the case of C_2, T_4 clusters creates a very challenging situation for all CC theories of the CCSD type. This situation is further aggravated by the complicated multiconfigurational structure of some low-lying states of N_2 and C_2. This is particularly true for the lowest $^1\Delta_g$ and $^1\Pi_g$ states of the C_2 molecule, which are dominated by two-electron excitations [71]. In this case, we observe a complete breakdown of the EOMCCSD and perturbative triples EOMCC or response CC models, such as CC3 (see table 3). For the lowest $^1\Delta_g$ state of C_2, the EOMCCSD and CC3 methods give 2.054 and 0.859 eV errors, respectively. Even the full EOMCCSDT approach gives a 0.407 eV error for this state. The EOMCCSDt method gives a smaller, 0.285 eV, error, which is probably due to the fortuitous cancellation of errors in the ground- and excited-state calculations. The 1.708 and 0.496 eV errors in the EOMCCSD and CC3 calculations for the lowest $^1\Pi_g$ state are not as large as in the case of the $^1\Delta_g$ state, but they are still sizeable. As a matter of fact, the large error in the results of the EOMCCSD calculations is also observed for the lowest $^1\Pi_u$ state of N_2, which has a partially biexcited character (see table 3). In this case, the 0.400 eV error in the EOMCCSD result is considerably reduced by the CC3 and EOMCCSDt methods, which give 0.177 and 0.090 eV errors, respectively. The full EOMCCSDT approach gives a small, 0.052 eV, error for this state.

In view of the above problems encountered in the EOMCCSD, CC3 and, to some extent, full EOMCCSDT calculations, it is remarkable to observe the improvements in the quality of results for the lowest $^1\Delta_g$ and $^1\Pi_g$ states of C_2 and the lowest $^1\Pi_u$ state of N_2, offered by the MMCC(2,3) and MMCC(2,4) approximations. The CISDt-based MMCC(2,3) method reduces the 2.054, 1.708 and 0.400 eV errors in the EOMCCSD results for the lowest $^1\Delta_g$ and $^1\Pi_g$ states of C_2 and the lowest $^1\Pi_u$ state of N_2 to as little as 0.130, 0.026 and 0.246 eV, respectively. Those are remarkable improvements, particularly when we take into account the low cost and the non-iterative character of the MMCC(2,3) calculations. The 0.130 and 0.026 eV errors in the MMCC(2,3) results for the lowest $^1\Delta_g$ and $^1\Pi_g$ states of C_2 are particularly impressive, considering the huge, $\sim$2 eV, errors in the EOMCCSD results and 0.5–0.9 eV errors in the results of the iterative triples CC3 calculations. The MMCC(2,4) method reduces the relatively small, 0.130, 0.026 and 0.246 eV, errors in the MMCC(2,3) results for the lowest $^1\Delta_g$ and $^1\Pi_g$ states of C_2 and the

Downloaded At: 16:32 21 January 2011

lowest $^1\Pi_u$ state of N_2 even further (cf. table 3). This is particularly true for the lowest $^1\Pi_u$ state of N_2, in which case the 0.246 eV error obtained with the MMCC(2,3) approach is reduced to 0.085 eV. Although the very small, 0.011 eV, error, obtained with the CISDtq-corrected MMCC(2,4) method for the lowest $^1\Delta_g$ state of C_2, may be a consequence of the fortuitous cancellation of errors, the fact of the matter remains that the MMCC(2,4) approximation offers systematic improvements in the overall quality of the MMCC calculations for the excited states of N_2 and C_2 having significant biexcited components. This can be seen by analysing the mean absolute errors in the results of the MMCC(2,3) and MMCC(2,4) calculations for N_2 and C_2 shown in table 4.

In the above description, we focused on the most complicated states of N_2 and C_2, which have large biexcited components, but similarly encouraging remarks apply to the performance of the MMCC(2,3) and MMCC(2,4) approaches in the calculations for other excited states. All of the remaining states of the N_2 and C_2 molecules, listed in table 3, namely the lowest $^1\Pi_g$, $^1\Sigma_u^-$ and $^1\Delta_u$ states of N_2 and the lowest $^1\Pi_u$ and $^1\Sigma_u^+$ states of C_2, are dominated by singles, so that reasonably accurate results are already obtained with the EOMCCSD and CC3 approximations, but even in this case the MMCC(2,3) and MMCC(2,4) methods may offer considerable improvements. The best example is provided here by the lowest $^1\Delta_u$ state of N_2 and the lowest $^1\Sigma_u^+$ state of C_2. For the vertical excitation energy corresponding to the transition from the ground state to the lowest $^1\Sigma_u^+$ state of C_2, the EOMCCSD approach gives a relatively large, 0.197 eV, error. This is a consequence of the aforementioned fact that the CCSD method is incapable of providing good results for the ground state of C_2. In spite of the fact that the MMCC(2,3) and MMCC(2,4) corrections $\delta_K(2,3)$ and $\delta_K(2,4)$ are calculated using the T_1 and T_2 clusters of the CCSD theory, the MMCC(2,3) and MMCC(2,4) approaches reduce the 0.197 eV error in the results of the EOMCCSD calculations for the lowest $^1\Sigma_u^+$ state of C_2 to as little as 0.032 and 0.039 eV, respectively.

Downloaded At: 16:32 21 January 2011

As in all other cases considered in this paper, the CISDt and CISDtq approaches alone, which are used to generate the wavefunctions $|\Psi_K\rangle$ for the construction of the MMCC corrections $\delta_K(2,3)$ and $\delta_K(2,4)$, are not sufficient to provide very good results for the excited states of N_2 and C_2. Only the insertion of the CISDt and CISDtq wavefunctions $|\Psi_K\rangle$ into the formulae for $\delta_K(2,3)$ and $\delta_K(2,4)$ guarantees excellent results. For example, the 1.182 and 0.306 eV errors in the CISDt and CISDtq results for the lowest $^1\Delta_g$ state decrease to 0.130 and 0.011 eV, respectively, when the CISDt and CISDtq wavefunctions $|\Psi_K\rangle$ are inserted into the expressions for corrections $\delta_K(2,3)$ and $\delta_K(2,4)$. On average, we observe a reduction of the mean absolute errors in the CISDt and CISDtq results for C_2 by a factor of 7–12 when the CISDt and CISDtq methods are combined with the non-iterative MMCC(2,3) and MMCC(2,4) approximations (see table 4). The reduction of mean absolute errors in the CISDt and CISDtq results for N_2 is less spectacular, although the reduction of errors by a factor of 3–4, when going from the CISDt and CISDtq to the MMCC(2,3) and MMCC(2,4) approximations, respectively, is still quite remarkable.

The results for N_2 and C_2 reported in table 3 and the corresponding mean absolute errors listed in table 4 indicate that the MMCC(2,3) and MMCC(2,4) methods provide the results that are similar or, in some cases, better than those provided by the successful full EOMCCSDt and EOMCCSDT models. This is particularly true for the MMCC(2,4) approach and for the excited states dominated by two-electron transitions (e.g. the lowest $^1\Delta_g$ and $^1\Pi_g$ states of C_2, where there is

the greatest challenge). Interestingly enough, even the simplest MMCC(2,3) approximation, which is a relatively inexpensive $N_o N_u n_o^2 n_u^4$ procedure in the CISDt part and an $n_o^3 n_u^4$ (or $N_o N_u n_o^2 n_u^3$) procedure in the non-iterative part related to the calculation of $\delta_K(2,3)$, provides the results of the full EOMCCSDt/EOMCCSDT or higher quality. For molecular examples described in this section, once the CISDt wavefunctions were calculated, the CPU time required to construct each $\delta_K(2,3)$ correction was comparable with the CPU time of a single EOMCCSD iteration. This is a lot less than in the case of the EOMCCSDT approach, which also requires the determination and storage of the three-body components of the cluster operator T and excitation operator R_K. The MMCC(2,3) and MMCC(2,4) calculations are based on using only the one- and two-body components of T and R_K.

We can summarize the results of the CI-corrected MMCC calculations presented in this and the previous sections by stating that the CISDt-based MMCC(2,3) and CISDtq-based MMCC(2,4) methods provide great improvements in the results of the standard CCSD, CCSD[T], CCSD(T), CCSD(TQ$_f$), EOMCCSD and CC3 calculations. The fact that we can obtain excellent results for a variety of ground and excited states, including several cases of bond breaking and complicated excited states dominated by doubles, in spite of using the relatively poor CISDt and CISDtq wavefunctions $|\Psi_K\rangle$ in constructing corrections $\delta_K(2,3)$ and $\delta_K(2,4)$ ($K \geq 0$), implies that the MMCC theory is a robust formalism, in which very good results can be obtained with the relatively poor wavefunctions $|\Psi_K\rangle$. The robustness of the MMCC theory will become even more transparent when we show the results of calculations with the completely renormalized CCSD(T) and CCSD(TQ) calculations and their quadratic MMCC analogue (cf. sections 3.2.2 and 3.3.2). The completely renormalized CCSD(T) and CCSD(TQ) methods and the quadratic MMCC theory use the relatively inexpensive MBPT-like expressions to design the ground-state wavefunction $|\Psi_0\rangle$ in the calculations of the corrections $\delta_0(2, m_B)$ ($m_B \geq 3$).

Downloaded At: 16:32 21 January 2011

3.1.4. *The CI-corrected MMCC(2,5) and MMCC(2,6) methods and their performance*

Our experience with the CI-corrected MMCC schemes is telling us that the CISDt-corrected MMCC(2,3) method and the CISDtq-corrected MMCC(2,4) approach, described in sections 3.1.1–3.1.3, provide very good results for single and double bond breaking in the ground electronic state [41, 48, 77, 78] and an excellent description of a large variety of excited states [47, 77, 78] (cf. sections 3.1.2 and 3.1.3). However, the results of the CI-corrected MMCC(2,3) and MMCC(2,4) calculations are less impressive when triple bonds (e.g. in N_2) are broken. This is illustrated in table 5, where we show the CISDtq-corrected MMCC(2,4) results for the ground-state PES of the N_2 molecule. The relatively small (a few millihartree) errors in the CISDtq-corrected MMCC(2,4) results for the N–N separations $R < 1.5R_e$ ($R = R_e$ is the equilibrium N–N bond length) become relatively large (> 10 millihartree) for $R \geq 1.5R_e$. At large internuclear separations, such as $R = 2R_e$, the CISDtq-corrected MMCC(2,4) approach suffers from non-variational collapse, similar to that plaguing the CCSD(T) approximation, although the $\lesssim 30$ millihartree absolute errors for $R \leq 2.25R_e$ are, more or less, an order of magnitude smaller than the analogous errors characterizing the CCSD(T), CCSD(TQ$_f$) and CCSDT(Q$_f$) results (cf. table 5; we will return to N_2 in the discussion below). In cases like this, we have to consider the MMCC(2,6) method, in which, in addition to moments $\mathcal{M}_{ijk}^{abc}(2)$ and $\mathcal{M}_{ijkl}^{abcd}(2)$, equations (13) and (14), we calculate moments

Downloaded At: 16:32 21 January 2011

Table 5. A comparison of various standard CC, completely renormalized CCSD(TQ), and CI-corrected MMCC(2,4), MMCC(2,5) and MMCC(2,6) ground-state energies with the corresponding full CI, CISDtq, CISDtqp and CISDtqph results obtained for a few internuclear separations R of the N_2 molecule with the DZ basis set.[a]

Method	$0.75R_e$	R_e[b]	$1.25R_e$	$1.5R_e$	$1.75R_e$	$2R_e$	$2.25R_e$
Full CI[c]	0.549 027	1.105 115	1.054 626	0.950 728	0.889 906	0.868 239	0.862 125
CCSD	3.132	8.289	19.061	33.545	17.714	−69.917	−120.836
CCSDT[d]	0.580	2.107	6.064	10.158	−22.468	−109.767	−155.656
CCSD(T)[c]	0.742	2.156	4.971	4.880	−51.869	−246.405	−387.448
CCSD(TQ_f)[c]	0.226	0.323	0.221	−2.279	−14.243	92.981	334.985
CCSDT(Q_f)[d]	0.047	−0.010	−0.715	−4.584	3.612	177.641	426.175
CR-CCSD(TQ),a[c,e]	0.448	1.106	2.474	5.341	1.498	−40.784	−69.259
CR-CCSD(TQ),b[c,f]	0.451	1.302	3.617	8.011	13.517	25.069	14.796
CISDtq[g]	5.101	7.233	10.651	18.003	30.226	41.978	51.126
CISDtqp[g]	5.401	6.969	8.880	12.086	20.037	28.161	34.276
CISDtqph[g]	5.390	6.799	7.558	6.707	7.189	7.777	8.372
MMCC(2,4)[g]	1.242	2.354	5.363	11.639	10.831	−16.086	−30.720
MMCC(2,5)[g]	1.220	2.089	3.527	5.493	1.631	−24.410	−39.124
MMCC(2,6)[g]	1.217	2.022	2.909	3.186	4.048	4.443	4.552

[a] The full CI total energies E, reported as $-(E + 108)$, are in hartree. The CC, CI and MMCC energies are in millihartree relative to the corresponding full CI energy values. The lowest two occupied and the highest two unoccupied orbitals were frozen in correlated calculations.
[b] The equilibrium bond length, $R_e = 2.068$ bohr.
[c] From [43].
[d] From [45].
[e] The 'a' variant of the completely renormalized CCSD(TQ) method (see section 3.2).
[f] The 'b' variant of the completely renormalized CCSD(TQ) method (see section 3.2).
[g] From [171]. The active space consisted of the $3\sigma_g$, $1\pi_u$, $2\pi_u$, $1\pi_g$, $2\pi_g$ and $3\sigma_u$ orbitals.

$\mathcal{M}^{abcde}_{ijklm}(2)$ and $\mathcal{M}^{abcdef}_{ijklmn}(2)$, corresponding to projections of the CCSD equations on pentuply and hextuply excited configurations (cf. equations (15) and (16)). The CI-corrected MMCC(2,5) approximation does not seem to be sufficiently accurate for the triple bond breaking in the region of larger internuclear separations (see table 5), although the situation dramatically changes when we consider the quadratic version of the quasi-variational MMCC(2,5) theory described in section 3.3.

The formulae defining the ground-state MMCC(2,5) and MMCC(2,6) methods are as follows [171]:

$$E_0^{\mathrm{MMCC}}(2,5) = E^{\mathrm{CCSD}} + \langle \Psi_0 | \{ Q_3 M_3^{\mathrm{CC}}(2) + Q_4 [M_4^{\mathrm{CC}}(2) + T_1 M_3^{\mathrm{CC}}(2)] + Q_5 [M_5^{\mathrm{CC}}(2) + T_1 M_4^{\mathrm{CC}}(2) + (T_2 + \tfrac{1}{2} T_1^2) M_3^{\mathrm{CC}}(2)] \} | \Phi \rangle / \langle \Psi_0 | \mathrm{e}^{T_1 + T_2} | \Phi \rangle, \tag{57}$$

$$E_0^{\mathrm{MMCC}}(2,6) = E^{\mathrm{CCSD}} + \langle \Psi_0 | \{ Q_3 M_3^{\mathrm{CC}}(2) + Q_4 [M_4^{\mathrm{CC}}(2) + T_1 M_3^{\mathrm{CC}}(2)] + Q_5 [M_5^{\mathrm{CC}}(2) + T_1 M_4^{\mathrm{CC}}(2) + (T_2 + \tfrac{1}{2} T_1^2) M_3^{\mathrm{CC}}(2)] + Q_6 [M_6^{\mathrm{CC}}(2) + T_1 M_5^{\mathrm{CC}}(2) + (T_2 + \tfrac{1}{2} T_1^2) M_4^{\mathrm{CC}}(2) + (T_1 T_2 + \tfrac{1}{6} T_1^3) M_3^{\mathrm{CC}}(2)] \} | \Phi \rangle / \langle \Psi_0 | \mathrm{e}^{T_1 + T_2} | \Phi \rangle, \tag{58}$$

where the quantities $M_j^{\mathrm{CC}}(2)|\Phi\rangle$, $j = 3\text{–}6$, are defined by equations (18)–(21). Similar equations can be given for the excited-state MMCC(2,5) and MMCC(2,6) energies, although we have not yet implemented or tested the excited-state MMCC(2,m_{B}) schemes with $m_{\mathrm{B}} > 4$.

In analogy to the CI-corrected MMCC(2,3) and MMCC(2,4) schemes, in the CI-corrected MMCC(2,5) and MMCC(2,6) approaches we calculate wavefunctions $|\Psi_0\rangle$ by solving the CISDtqp and CISDtqph equations, although other choices of $|\Psi_0\rangle$ are clearly possible. The ground-state CISDtqp wavefunction, used instead of $|\Psi_0\rangle$ in the CI-corrected MMCC(2,5) energy formula, equation (57), is obtained by solving the CI eigenvalue problem with all singles and doubles, internal and semi-internal triply and quadruply excited configurations defined by equations (55) and (56) and internal and semi-internal pentuply excited configurations defined by the excitation operator

$$c_{K,5}|\Phi\rangle = \sum_{\substack{\mathbf{I}>\mathbf{J}>\mathbf{K}>l>m \\ a>b>\mathbf{C}>\mathbf{D}>\mathbf{E}}} c^{ab\mathbf{CDE}}_{\mathbf{IJK}lm}(K)\, |\Phi^{ab\mathbf{CDE}}_{\mathbf{IJK}lm}\rangle, \tag{59}$$

where $K = 0$ in the ground-state case. The ground-state CISDtqph wavefunction, used to determine $|\Psi_0\rangle$ in the CI-corrected MMCC(2,6) method (cf. equation (58)), is obtained by solving the CI eigenvalue problem with all singles and doubles, internal and semi-internal triply and quadruply excited configurations defined by equations (55) and (56), internal and semi-internal pentuply excited configurations defined by equation (59) and internal and semi-internal hextuply excited configurations defined by the excitation operator

$$c_{K,6}|\Phi\rangle = \sum_{\substack{\mathbf{I}>\mathbf{J}>\mathbf{K}>\mathbf{L}>m>n \\ a>b>\mathbf{C}>\mathbf{D}>\mathbf{E}>\mathbf{F}}} c^{ab\mathbf{CDEF}}_{\mathbf{IJKL}mn}(K)\, |\Phi^{ab\mathbf{CDEF}}_{\mathbf{IJKL}mn}\rangle, \tag{60}$$

where, again, $K = 0$ in the ground-state calculations. As in the case of the MMCC(2,3) and MMCC(2,4) theories, the use of active orbitals in defining the selected pentuples and hextuples entering equations (59) and (60) significantly

Downloaded At: 16:32 21 January 2011

reduces the computer costs of the CI-corrected MMCC(2,5) and MMCC(2,6) energy corrections, since we do not have to determine all $\mathcal{M}^{abcde}_{ijklm}(2)$ and $\mathcal{M}^{abcdef}_{ijklmn}(2)$ moments. It is sufficient to calculate the moments $\mathcal{M}^{ab\mathbf{CDE}}_{\mathbf{IJK}lm}(2)$ and $\mathcal{M}^{ab\mathbf{CDEF}}_{\mathbf{IJKL}mn}(2)$, corresponding to projections of the CCSD equations on a relatively small set of internal and semi-internal pentuply and hextuply excited configurations of the $|\Phi^{ab\mathbf{CDE}}_{\mathbf{IJK}lm}\rangle$ and $|\Phi^{ab\mathbf{CDEF}}_{\mathbf{IJKL}mn}\rangle$ types. Our experience with these methods indicates that those are the only types of pentuply and hextuply excited configurations that are needed to obtain the excellent description of triple bond breaking. This can be seen by analysing the results of the CI-corrected MMCC(2,5) and MMCC(2,6) calculations for the triple bond breaking in the ground-state N_2 molecule (see table 5 and figure 2).

The N_2 molecule is characterized by large T_3 and T_4 effects and, for stretched nuclear geometries, by the sizeable contributions due to higher-than-quadruply excited clusters, in addition to huge T_3 and T_4 effects. At the equilibrium geometry ($R = R_e$) and for the DZ basis set [165] used in this example, the effect of T_3 clusters, as estimated by forming the difference of the CCSDT and CCSD energies, is -6.182 millihartree (see table 5). The effect of T_4 clusters, as estimated by forming the difference of the full CCSDTQ and CCSDT energies, is -1.912 millihartree [43]. The full CCSDTQ method is virtually exact in this case. The T_5 clusters seem to be responsible for almost the entire 0.195 millihartree effect that constitutes the difference between the CCSDTQ and full CI energies at $R = R_e$ [172]. For the geometries near the equilibrium, the T_3 and T_4 effects are very accurately described by the perturbative CCSD(T) and CCSD(TQ_f) approaches. For example, the

Downloaded At: 16:32 21 January 2011

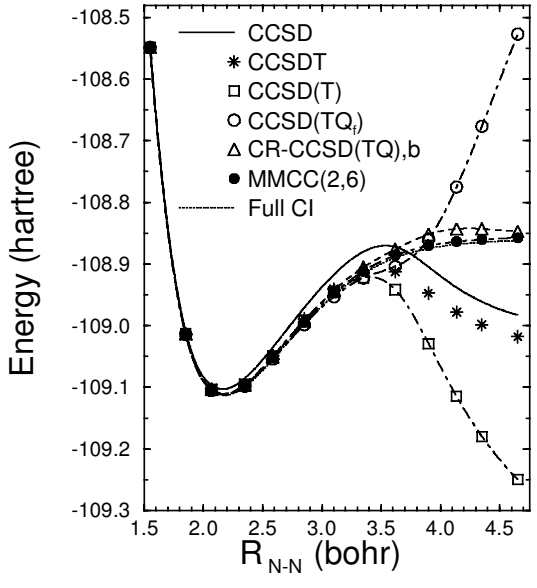

Figure 2. Potential energy curves for the DZ model of the N_2 molecule (energies in hartree and the N–N separation $R_{N\text{-}N}$ in bohr). A comparison of the results obtained with the CR-CCSD(TQ),b and CISDtqph-corrected MMCC(2,6) methods, designated by △ and ●, respectively, with the results of the CCSD, CCSDT, CCSD(T), CCSD(TQ_f) and full CI calculations, designated by the solid curve, *, □, ○ and the dotted curve, respectively (see [43, 171] for the original numerical data).

−6.133 millihartree difference between the CCSD(T) and CCSD energies at $R = R_e$ is virtually identical to a −6.182 millihartree difference between the CCSDT and CCSD energies. The difference between the CCSD(TQ_f) and CCSD(T) energies at $R = R_e$ is −1.833 millihartree, which is practically identical to the difference between the CCSDTQ and CCSDT energies.

The situation becomes a lot more complicated when the N–N bond is stretched. The combined effect of higher–than–doubly excited clusters, as estimated by forming the difference between the full CI and CCSD energies, rapidly increases, from 8.289 millihartree at $R = R_e$ to 33.545 millihartree at $R = 1.5R_e$ (see table 5). At $R \approx 1.75R_e$, the CCSD potential energy curve has an unphysical hump and for the N–N distances greater than 3.74 bohr the CCSD potential energy curve goes significantly below the exact, full CI curve (see table 5 and figure 2). The orbital optimization at the CC doubles level via the so-called VOO-CCD approach [138, 139] does not help: the VOO-CCD potential energy curve for N_2 is as bad as the CCSD curve [139]. Even the full CCSDT method fails to provide a realistic description of the ground-state PES of N_2. The CCSDT curve has a hump for the intermediate values of R, and for larger values of R is located significantly below the exact and CCSD curves (see table 5 and figure 2; note that at $R = 2.25R_e$ the absolute value of the difference between the CCSDT and full CI energies of 155.656 millihartree is greater than the 120.836 millihartree difference between the CCSD and full CI energies). This implies the need for T_4 clusters in this case. It is almost certain that higher–than–quadruply excited clusters play an important role when R becomes large, since triple bond breaking in N_2 requires at least some hextuple excitations (in a CI sense) [18, 122]. This can be seen by comparing the CISDtqph and CISDtqp energies. The CISDtqp approach, which neglects the hextuple excitations altogether, provides a significantly worse description of bond breaking in N_2 than the CISDtqph method (see table 5). It can also be shown that the difference between the CISDTQ (CI with all singles, doubles, triples, and quadruples) and full CI energies at $R = 2R_e$ is almost 40 millihartree [122].

Downloaded At: 16:32 21 January 2011

The inclusion of the triply and quadruply excited clusters via non-iterative perturbative CCSD(T) and CCSD(TQ_f) approximations leads to completely erroneous results at larger internuclear separations (cf. table 5 and figure 2). The relatively small, 2.156 millihartree, difference between the CCSD(T) and full CI energies at $R = R_e$ increases (in absolute value) to 51.869 millihartree at $R = 1.75R_e$, 246.405 millihartree at $R = 2R_e$ and 387.448 millihartree at $R = 2.25R_e$. The CCSD(TQ_f) approach fails, too, giving the 92.981 and 334.985 millihartree errors at $R = 2R_e$ and $2.25R_e$, respectively. As shown in figure 2, the potential energy curves obtained in the CCSD(T) and CCSD(TQ_f) calculations are completely pathological: at larger internuclear separations the CCSD(T) curve is located significantly below the full CI curve and there is a well-pronounced hump on the CCSD(T) curve for the intermediate values of R. The CCSD(TQ_f) potential energy curve is located significantly above the full CI curve. As a matter of fact, an attempt to correct the results by adding the non-iterative correction due to T_4 clusters to the CCSDT energies, as is done in the CCSDT(Q_f) calculations [20], fails too (see table 5). In other words, none of the standard single-reference methods of improving the poor CCSD and CCSDT results at larger N–N separations, based on adding the non-iterative corrections due to triples and quadruples to the RHF-based CCSD or CCSDT energies, leads to a satisfactory description of bond breaking in N_2. The failure of the CCSD(T), CCSD(TQ_f) and CCSDT(Q_f) approaches at larger N–N

distances is a consequence of the divergent nature of the MBPT series and the failure of the CCSD and CCSDT methods to provide reasonable information about the T_1, T_2 and (in the case of CCSDT) T_3 cluster amplitudes, which are used to construct the relevant (T) and (Q_f) corrections. We have tried to design the analogues of the CCSD(T), CCSD(TQ_f) and CCSDT(Q_f) methods that would account for the T_5 and T_6 clusters, using standard arguments originating from MBPT, but none of the resulting methods provided us with reasonable potential energy curves of N_2 [161]. Clearly, a correct description of the bond breaking in N_2 and other triply bonded molecules by the single-reference CC theory requires a different approach.

The MMCC formalism provides us with two different ways of removing the failing of the standard single-reference CC approximations at larger N–N separations in N_2. Excellent results for the triple bond breaking in N_2 can be obtained either by using the CISDtqph-corrected MMCC(2,6) method [171] or by employing the quadratic MMCC approximation [161] described in section 3.3. Reasonably good results can also be obtained with the completely renormalized CCSD(TQ) and CCSDT(Q) approaches [43, 45] (for a discussion of the completely renormalized CCSD(TQ) results, see section 3.2.2), but the quadratic MMCC results discussed in section 3.3.2 and the results of the CISDtqph-corrected MMCC(2,6) calculations discussed in this section are better than the results of the completely renormalized CCSD(TQ) and CCSDT(Q) calculations in the asymptotic region. The quadratic MMCC method [161], discussed in section 3.3, is, in our view, the best solution to date, since it retains the 'black-box' character of the standard methods of the CCSD(T) type, while providing an excellent description of the entire PES of N_2 and other molecules, but the CISDtqph-corrected MMCC(2,6) approach is promising too. This can be seen by analysing the results of the CISDtqph-corrected MMCC(2,6) calculations shown in table 5 and figure 2. In all CI-corrected MMCC calculations reported in table 5 and figure 2 (taken from [171]) and in all relevant active-space CI calculations that were used to generate wavefunctions $|\Psi_0\rangle$ in the MMCC energy expressions, the active space consisted of the $3\sigma_g$, $1\pi_u$, $2\pi_u$, $1\pi_g$, $2\pi_g$ and $3\sigma_u$ valence orbitals. This is the most natural choice of active orbitals for the triple bond breaking in N_2.

The CISDtqph-corrected MMCC(2,6) approach reduces the huge errors in the results of the CCSD, CCSD(T) and similar calculations at larger N–N distances R to as little as 4.443 millihartree at $R = 2R_e$ and 4.552 millihartree at $R = 2.25R_e$. The fact that the errors in the MMCC(2,6) calculations, which are based on the generalized moments of the completely failing CCSD approach, range between 1.217 and 4.552 millihartree in the entire $R = 0.75R_e - 2.25R_e$ region for the complicated case of N_2 clearly demonstrates that the MMCC formalism can handle all kinds of problems, including the most difficult problem of triple bond breaking. In spite of the unphysical shape of the CCSD PES at the intermediate and larger N–N distances, the MMCC(2,6) corrections to the CCSD energies lead to an excellent potential energy curve, which is located only slightly above the exact, full CI, curve (see figure 2). The dissociation energy D_e, defined here as the difference of energies at $R = 2.25R_e$ and $R = R_e$, resulting from the MMCC(2,6) calculations, is 6.68 eV, in excellent agreement with the full CI value of 6.61 eV. The results listed in table 5 show that it is essentially impossible to calculate D_e for other RHF-based single-reference CC methods, owing to the completely unphysical shapes of potential energy curves resulting from the standard single-reference CC calculations. It is, therefore, very encouraging that the MMCC(2,6) method employing the RHF

Downloaded At: 16:32 21 January 2011

reference is capable of providing an accurate representation of the PES of N_2, even at larger N–N separations, where essentially all standard CC approximations fail. The 2.022 millihartree error in the MMCC(2,6) result at $R = R_e$ is not as small as the 0.323 or ~1 millihartree errors in the standard and completely renormalized CCSD(TQ) results (cf. table 5), but the overall performance of the CISDtqph-corrected MMCC(2,6) approximation is much better than the performance of the CCSD(T) or CCSD(TQ)-type methods. The only non-iterative CC method, based on the cluster amplitudes obtained in the CCSD calculations, that can provide the results that are comparable with or better than the results of the MMCC(2,6) calculations, is the aforementioned quadratic MMCC approach discussed in section 3.3.

A comparison of the CISDtqph-corrected MMCC(2,6) results with the results of the CISDtq-corrected MMCC(2,4) and CISDtqp-corrected MMCC(2,5) calculations (all taken from [171]) clearly indicates that the MMCC(2,4) and MMCC(2,5) levels of the MMCC theory are not sufficient to obtain an accurate description of the triple bond breaking in N_2, if the limited CI wavefunctions are used as the wavefunctions $|\Psi_0\rangle$ in constructing the relevant corrections $\delta_0(2, m_B)$. For the DZ basis set used here, the CI-corrected MMCC(2,4) and MMCC(2,5) results are good for $R \leq 1.75R_e$. In this region, the errors in the MMCC(2,4) and MMCC(2,5) energies do not exceed a few millihartree (see table 5). However, for $R \geq 2R_e$, the energies obtained in the CI-corrected MMCC(2,4) and MMCC(2,5) calculations are significantly smaller than the corresponding full CI energies. In other words, at larger N–N separations, the CI-corrected MMCC(2,4) and MMCC(2,5) approaches suffer from a non-variational collapse similar to that characterizing the CCSD and CCSD(T) approximations. On the other hand, there is a considerable difference between the performance of the CCSD, CCSD(T) and other non-iterative CC methods and the CI-corrected MMCC(2,4) and MMCC(2,5) approaches: the negative errors relative to full CI in the results of the CI-corrected MMCC(2,4) and MMCC(2,5) calculations for larger values of R, which for $R = 2R_e$ are, approximately, -20 millihartree, are a lot smaller (in absolute value) than the errors in the CCSD, CCSD(T), CCSD(TQ_f) and CCSDT(Q_f) results. We can definitely conclude that the CI-corrected MMCC(2,4) and MMCC(2,5) methods provide significant improvements in the results of the standard single-reference calculations for triple bond breaking in N_2. The only problem is that the improvements offered by the MMCC(2,4) and MMCC(2,5) approximations at larger N–N separations are not as great as we would like in the asymptotic region. This behaviour of the CI-corrected MMCC methods is in sharp contrast to the behaviour of the quadratic MMCC approximations discussed in section 3.3. As we will see in section 3.3.2, the quadratic MMCC approaches of the MMCC(2,5) type are capable of providing very small, at most a few millihartree, errors in the entire $R = 0.75R_e$–$2.25R_e$ region of the PES of N_2. As a matter of fact, the most expensive moments of the CCSD theory, i.e. $\mathcal{M}^{abcde}_{ijklm}(2)$ and $\mathcal{M}^{abcdef}_{ijklmn}(2)$, can be ignored in the quadratic MMCC calculations for N_2 without significant loss of accuracy at larger N–N separations. It seems to us that the CI-corrected MMCC methods are less flexible in this regard, since the only level of the CI-corrected MMCC theory that guarantees very good results for the triple bond breaking in N_2 is the MMCC(2,6) level.

The main factor that explains the patterns observed in the CI-corrected MMCC calculations for N_2 is the quality of the CI wavefunction $|\Psi_0\rangle$, which is used to construct the MMCC energy corrections. The results in table 5 imply that the CI

Downloaded At: 16:32 21 January 2011

wavefunction $|\Psi_0\rangle$ must provide a qualitatively correct description of bond breaking if we are to obtain both the correct shape and very small errors in the CI-corrected MMCC calculations. Clearly, the CISDtqph method provides a qualitatively correct representation of the potential energy curve of N_2 (see table 5). In consequence, the CISDtqph-corrected MMCC(2,6) results are excellent at all N–N separations. The CISDtqph-corrected MMCC(2,6) approximation reduces the 5.390–8.372 millihartree errors in the bare CISDtqph results for N_2 by a factor of 2–4. The CISDtq and CISDtqp wavefunctions lack important contributions from the hextuply excited configurations and this results in a poorer performance of the CISDtq and CISDtqp methods and their CI-corrected MMCC(2,4) and MMCC(2,5) analogues at larger N–N separations.

The triple bond breaking in N_2 represents a very severe test of accuracy for all MMCC methods, so that not all CI-corrected MMCC approximations perform equally well. In this case, the CISDtqph-corrected MMCC(2,6) method (or, very likely, the MRCI-corrected MMCC(2,6) approach) is essentially the only approach among the CI-corrected MMCC approximations that provides excellent and well-balanced results for smaller and larger N–N distances. For simpler types of bond breaking, including various examples of single and double bond breaking, very good results can already be obtained with the MMCC(2,3) and MMCC(2,4) approximations, whose performance was discussed in section 3.1.2. In those cases, the CISDtqp-corrected MMCC(2,5) method and its CISDtqph-corrected MMCC(2,6) counterpart provide further improvements in the already very good results of the CI-corrected MMCC(2,3) and MMCC(2,4) calculations. For example, the CISDtqp-corrected MMCC(2,5) approach reduces the relatively small, 0.501–2.416 millihartree, errors in the CISDtq-corrected MMCC(2,4) results for the case of the simultaneous breaking of both O–H bonds in the H_2O molecule (discussed earlier in section 3.1.2) to 0.421–0.730 millihartree [171] (see table 6). The CISDtqph-corrected MMCC(2,6) method reduces those very small errors in the CISDtqp-corrected MMCC(2,5) results even further, by 0.004 millihartree at $R = R_e$, by 0.107 millihartree at $R = 1.5R_e$ and by 0.192 millihartree at $R = 2R_e$ (cf. table 6).

Downloaded At: 16:32 21 January 2011

Clearly, the very small, 0.4–0.7 millihartree, errors in the CI-corrected MMCC(2,5) and MMCC(2,6) results for the water molecule are a consequence of the relatively good description of the simultaneous breaking of both O–H bonds in H_2O by the CISDtqp and CISDtqph methods that are used to generate wavefunctions $|\Psi_0\rangle$ for constructing the MMCC(2,5) and MMCC(2,6) corrections $\delta_0(2,5)$ and $\delta_0(2,6)$. The CISDtqph method is particularly good in this case, giving the 1.922–2.600 millihartree errors in the entire $R = R_e$–$2R_e$ region. It is interesting to observe, however, that the MMCC theory is capable of reducing the small, 2.628–3.732 millihartree, errors in the CISDtqp results and even smaller, 1.922–2.600 millihartree, errors in the CISDtqph results by a rather large factor of 4–6, once the CISDtqp and CISDtqph wavefunctions $|\Psi_0\rangle$ are inserted into the MMCC(2,5) and MMCC(2,6) energy expressions. One might think that, once we decide to use the high-quality wavefunction $|\Psi_0\rangle$ in the MMCC calculations, the additional improvements offered by the MMCC theory after inserting this $|\Psi_0\rangle$ into the MMCC energy expressions should no longer be big. Clearly, the reduction of errors in the CISDtqp and CISDtqph results for the double dissociation of H_2O by a factor of 4–6 is not as impressive as the reduction of errors in the CISDt results, when the relatively poor CISDt wavefunction $|\Psi_0\rangle$ is inserted into the MMCC(2,3) energy formula (cf. tables 2 and 6), but the reduction of the $\sim$2–4 millihartree errors in the CISDtqp and

Table 6. A comparison of the CI-corrected MMCC(2,5) and MMCC(2,6) ground-state energies with their MMCC(2,3) and MMCC(2,4) counterparts and with the corresponding full CI, CISDt, CISDtq, CISDtqp and CISDtqph results obtained for the equilibrium and two displaced geometries of the H_2O molecule with the DZ basis set.[a]

Method	$R = R_e$[b]	$R = 1.5R_e$[c]	$R = 2R_e$[c]
Full CI	−76.157866[b]	−76.014521[c]	−75.905247[c]
CISDt[d,e]	6.922	18.884	49.948
CISDtq[d,e]	2.702	2.919	5.638
CISDtqp[e,f]	2.628	2.578	3.732
CISDtqph[e,f]	2.600	2.187	1.922
MMCC(2,3)[d,e]	0.811	2.407	1.631
MMCC(2,4)[d,e]	0.501	0.942	2.416
MMCC(2,5)[e,f]	0.421	0.584	0.730
MMCC(2,6)[e,f]	0.417	0.477	0.538

[a] The full CI total energies are in hartree. The CC, CI and MMCC energies are in millihartree relative to the corresponding full CI energy values.
[b] The equilibrium geometry and full CI result from [166].
[c] The geometry and full CI result from [167].
[d] From [48].
[e] The active space consisted of the $1b_1$, $3a_1$, $1b_2$, $4a_1$, $2b_1$, and $2b_2$ orbitals.
[f] From [171].

Downloaded At: 16:32 21 January 2011

CISDtqph results to as little as 0.4–0.7 millihartree is very encouraging. The results in tables 5 and 6 and the earlier results in tables 1 and 2 show that the MMCC formalism always offers considerable improvements in the results of the limited CI calculations that are used to provide wavefunctions $|\Psi_0\rangle$ for constructing the MMCC corrections $\delta_0(m_A, m_B)$, equation (45). As mentioned in section 3.1.3, a very similar remark applies to excited states: the MMCC theory offers significant improvements in the results of the limited CI calculations of excited states that are used to generate wavefunctions $|\Psi_K\rangle$ for constructing the MMCC corrections $\delta_K(m_A, m_B)$, equation (46).

We should also emphasize the very systematic behaviour of the CI-corrected MMCC approximations. The results for bond breaking in N_2 and H_2O listed in tables 5 and 6 clearly show that the CI-corrected MMCC energies systematically improve when we go from the basic MMCC(2,3) approach through the intermediate MMCC(2,4) and MMCC(2,5) levels to the highest-level MMCC(2,6) approximation. A comparison of the MMCC(2,3) and MMCC(2,4) results in tables 3 and 4 implies that the same should be true for excited states, although we have not yet tested the higher-level MMCC(2,5) and MMCC(2,6) methods in excited-state calculations. The systematic improvements in the results of the CI-corrected MMCC calculations in a sequence of the MMCC$(2,3) \rightarrow$ MMCC$(2,4) \rightarrow$ MMCC$(2,5) \rightarrow$ MMCC$(2,6)$ approximations are a consequence of the fact that, along with incorporating higher and higher moments of the CCSD equations, we are also systematically improving the quality of the CI wavefunctions that enter the MMCC$(2,m_B)$, $m_B = 2$–6, expressions (from CISDt in the MMCC(2,3) case to CISDtqph in the MMCC(2,6) case).

Let us summarize the results discussed in this section and in the earlier sections 3.1.2 and 3.1.3. The CI-corrected MMCC methods are capable of providing very good results for bond breaking [41, 47, 48, 171], but in our view these methods can be particularly useful for excited states, which are often described or characterized through the dominant orbital excitations ($\sigma \rightarrow \sigma$, $\sigma \rightarrow \pi$, etc.; cf. [47, 77, 78]). The *a priori* information about the dominant orbital excitations defining excited states of interest can then be used to select active orbitals for the CISDt, CISDtq or some other relatively inexpensive MRCI-like calculations of the wavefunctions $|\Psi_K\rangle$ that enter the MMCC(2,3) and MMCC(2,4) energy expressions, equations (49) and (50) [47, 77, 78]. The choice of active orbitals for the ground-state calculations with the CI-corrected MMCC methods is usually straightforward, too, since we often know which valence orbitals are involved in the bond-breaking process under consideration, but clearly it would be very useful to be able to describe PESs involving bond breaking without having to select active orbitals. Undoubtedly, it would be desirable to have robust approaches, which combine the simplicity of the 'black-box' non-iterative CC methods, such as CCSD(T), with the efficiency with which active-space or MRCC and MRCI approaches describe quasi-degenerate states and bond breaking. The non-iterative single-reference CC approaches which are flexible and powerful enough that they can handle at least some types of bond breaking, in spite of using elements of MBPT, would be particularly desirable in situations where it is not easy to define the appropriate active space. The completely renormalized CCSD(T) and CCSD(TQ) methods described in the next subsection and the quasi-variational MMCC approaches described in section 3.3 are good candidates for such methods.

Downloaded At: 16:32 21 January 2011

3.2. *The renormalized and completely renormalized CC methods*

The renormalized and completely renormalized CC methods are obtained when the low-order MBPT expressions are used to define the ground-state wavefunction $|\Psi_0\rangle$ in the MMCC(m_A, m_B) energy formulae [41–47, 49]. The renormalized and completely renormalized CCSD[T], CCSD(T) and CCSD(TQ) methods, discussed in this section, are based on the idea of combining the MBPT(2)-like (second-order MBPT-like) wavefunctions $|\Psi_0\rangle$ with the ground-state MMCC(2,3) and MMCC(2,4) approximations introduced in section 3.1 (cf. equations (47) and (48)). As their standard CCSD[T], CCSD(T) and CCSD(TQ_f) counterparts, the renormalized and completely renormalized CCSD[T], CCSD(T) and CCSD(TQ) approaches can be used to correct the results of the CCSD calculations (for single bond breaking, using the renormalized and completely renormalized CCSD[T] and CCSD(T) methods, and, for multiple bond breaking, using the renormalized and completely renormalized CCSD(TQ) approach). The more expensive renormalized and completely renormalized CCSDT(Q) methods, which can be used to correct the CCSDT results by employing the MMCC(3,4) approximation [41, 42, 45, 47], are not discussed here.

3.2.1. *The renormalized and completely renormalized CCSD[T], CCSD(T) and CCSD(TQ) methods: theory*

The completely renormalized CCSD[T] and CCSD(T) methods (the CR-CCSD[T] and CR-CCSD(T) approaches) are examples of the MMCC(2,3) scheme. Thus, if T_1 and T_2 are the cluster operators obtained by solving the CCSD equations, then the energy formulae defining the CR-CCSD[T] and CR-CCSD(T) methods are [41–44, 46, 47, 49]

$$E^{\text{CR-CCSD[T]}} = E^{\text{CCSD}} + \langle \Psi^{\text{CCSD[T]}} | Q_3 \, M_3^{\text{CC}}(2) | \Phi \rangle / \langle \Psi^{\text{CCSD[T]}} | e^{T_1+T_2} | \Phi \rangle, \quad (61)$$

$$E^{\text{CR-CCSD(T)}} = E^{\text{CCSD}} + \langle \Psi^{\text{CCSD(T)}} | Q_3 \, M_3^{\text{CC}}(2) | \Phi \rangle / \langle \Psi^{\text{CCSD(T)}} | e^{T_1+T_2} | \Phi \rangle, \quad (62)$$

where E^{CCSD} is the CCSD energy and $M_3^{\text{CC}}(2)|\Phi\rangle$ is a quantity that can be expressed in terms of moments $\mathcal{M}_{ijk}^{abc}(2)$ according to equation (18). The $|\Psi^{\text{CCSD[T]}}\rangle$ and $|\Psi^{\text{CCSD(T)}}\rangle$ wavefunctions, entering equations (61) and (62), are defined by the very simple, MBPT(2)[SDT]-like, expressions

$$|\Psi^{\text{CCSD[T]}}\rangle = (1 + T_1 + T_2 + T_3^{[2]})|\Phi\rangle, \quad (63)$$

$$|\Psi^{\text{CCSD(T)}}\rangle = |\Psi^{\text{CCSD[T]}}\rangle + Z_3|\Phi\rangle, \quad (64)$$

where the

$$T_3^{[2]}|\Phi\rangle = R_0^{(3)}(V_N T_2)_{\text{C}}|\Phi\rangle \quad (65)$$

term in equation (63) is a CCSD analogue of the connected triples contribution to the MBPT(2) wavefunction and

$$Z_3|\Phi\rangle = R_0^{(3)} V_N T_1|\Phi\rangle \quad (66)$$

is the disconnected triples correction that distinguishes the [T] and (T) corrections. In the above expressions, $R_0^{(3)}$ designates the three-body component of the MBPT reduced resolvent and V_{N} represents the two-body part of the Hamiltonian in the normal-ordered form.

The renormalized CCSD[T] and CCSD(T) methods (the R-CCSD[T] and R-CCSD(T) approaches) are obtained by replacing the $\mathcal{M}_{ijk}^{abc}(2)$ moments in the CR-CCSD[T] and CR-CCSD(T) formulae, equations (61) and (62), respectively, with their lowest-order estimates, i.e. $\langle \Phi_{ijk}^{abc} | (V_{\text{N}} T_2)_{\text{C}} | \Phi \rangle$. Thus, the R-CCSD[T] and R-CCSD(T) energies are calculated as follows [41–44, 46, 47, 49]:

$$E^{\text{R-CCSD[T]}} = E^{\text{CCSD}} + \langle \Psi^{\text{CCSD[T]}} | Q_3 \, (V_N T_2)_{\text{C}} | \Phi \rangle / \langle \Psi^{\text{CCSD[T]}} | e^{T_1+T_2} | \Phi \rangle, \quad (67)$$

$$E^{\text{R-CCSD(T)}} = E^{\text{CCSD}} + \langle \Psi^{\text{CCSD(T)}} | Q_3 \, (V_N T_2)_{\text{C}} | \Phi \rangle / \langle \Psi^{\text{CCSD(T)}} | e^{T_1+T_2} | \Phi \rangle. \quad (68)$$

Although calculations of entire PESs involving single bond breaking require using the CR-CCSD[T] and CR-CCSD(T) methods rather than the R-CCSD[T] and R-CCSD(T) approaches [41, 42, 44, 46, 47, 49], the R-CCSD[T] and R-CCSD(T) methods can help us to understand the relationship between the standard and completely renormalized CC approaches. Moreover, the R-CCSD[T] and R-CCSD(T) methods provide a superior description of moderately stretched chemical bonds, when compared with the conventional CCSD[T] and CCSD(T) approaches [41, 42, 44, 46, 47, 49].

In deriving the above expressions for the R-CCSD[T], R-CCSD(T), CR-CCSD[T] and CR-CCSD(T) energies, we used an idea of replacing the 'trial' wavefunction $|\Psi_0\rangle$ in the general MMCC(2,3) formula, equation (47), by the MBPT(2)[SDT]-like expressions (63) and (64). An alternative derivation of the R-CCSD[T], R-CCSD(T), CR-CCSD[T] and CR-CCSD(T) formulae and their slightly modified variants, employing the energy-dependent form of the CCSDT-1 equations, has been presented in [173]. The original derivation of the R-CCSD[T], R-CCSD(T), CR-CCSD[T] and CR-CCSD(T) expressions by Piecuch and Kowalski [42] has an advantage over the method used one year later in [173] that, by relating the

Downloaded At: 16:32 21 January 2011

R-CCSD[T], R-CCSD(T), CR-CCSD[T] and CR-CCSD(T) methods to the MMCC(m_A, m_B) approximations, we can easily extend the R-CCSD[T], R-CCSD(T), CR-CCSD[T] and CR-CCSD(T) approaches to higher-than-triple excitations, such as quadruples, for which we can use the general MMCC(2,4) formula, equation (48), as the starting point (cf. the description of the renormalized and completely renormalized CCSD(TQ) approaches given below). In addition, the reasoning used by Piecuch and Kowalski in their original work [42] to derive the R-CCSD[T], R-CCSD(T), CR-CCSD[T] and CR-CCSD(T) methods and their higher-order extensions can be applied to develop other types of successful CC 'black boxes' for bond breaking, including the quadratic MMCC approaches discussed in section 3.3. None of this is possible if we want to follow the reasoning presented in [173], although the rederivation of the R-CCSD[T], R-CCSD(T), CR-CCSD[T] and CR-CCSD(T) expressions of Piecuch and Kowalski presented in [173] represents an interesting contribution to our MMCC theory, which once again demonstrates how much can be gained by resigning from the conventional arguments of the single-reference CC formalism.

Let us discuss the relationship between the standard and renormalized or completely renormalized CCSD[T] and CCSD(T) methods. The above definitions of the $|\Psi^{\mathrm{CCSD[T]}}\rangle$ and $|\Psi^{\mathrm{CCSD(T)}}\rangle$ wavefunctions, equations (63) and (64), respectively, allow us to rewrite equations (61), (62), (67) and (68) in the following compact form:

$$E^{\mathrm{CR\text{-}CCSD[T]}} = E^{\mathrm{CCSD}} + N^{\mathrm{CR[T]}}/D^{\mathrm{[T]}}, \tag{69}$$

$$E^{\mathrm{CR\text{-}CCSD(T)}} = E^{\mathrm{CCSD}} + N^{\mathrm{CR(T)}}/D^{\mathrm{(T)}}, \tag{70}$$

$$E^{\mathrm{R\text{-}CCSD[T]}} = E^{\mathrm{CCSD}} + N^{\mathrm{[T]}}/D^{\mathrm{[T]}}, \tag{71}$$

$$E^{\mathrm{R\text{-}CCSD(T)}} = E^{\mathrm{CCSD}} + N^{\mathrm{(T)}}/D^{\mathrm{(T)}}. \tag{72}$$

The $N^{\mathrm{CR[T]}}$, $N^{\mathrm{CR(T)}}$, $N^{\mathrm{[T]}}$ and $N^{\mathrm{(T)}}$ numerators entering the above expressions are defined as

$$N^{\mathrm{CR[T]}} = \langle \Phi | (T_3^{[2]})^\dagger M_3^{\mathrm{CC}}(2) | \Phi \rangle, \tag{73}$$

$$N^{\mathrm{CR(T)}} = N^{\mathrm{CR[T]}} + \langle \Phi | (Z_3)^\dagger M_3^{\mathrm{CC}}(2) | \Phi \rangle, \tag{74}$$

$$N^{\mathrm{[T]}} = \langle \Phi | (T_3^{[2]})^\dagger (V_{\mathrm{N}} T_2)_{\mathrm{C}} | \Phi \rangle, \tag{75}$$

$$N^{\mathrm{(T)}} = N^{\mathrm{[T]}} + \langle \Phi | (Z_3)^\dagger (V_{\mathrm{N}} T_2)_{\mathrm{C}} | \Phi \rangle, \tag{76}$$

where the $T_3^{[2]}$ and Z_3 operators are defined by equations (65) and (66) respectively. The $D^{\mathrm{[T]}}$ and $D^{\mathrm{(T)}}$ denominators entering equations (69)–(72) represent the relevant overlaps between $|\Psi^{\mathrm{CCSD[T]}}\rangle$ and $|\Psi^{\mathrm{CCSD(T)}}\rangle$ and the CCSD ground state. We have

$$D^{\mathrm{[T]}} = \langle \Psi^{\mathrm{CCSD[T]}} | \mathrm{e}^{T_1+T_2} | \Phi \rangle, \tag{77}$$

$$D^{\mathrm{(T)}} = \langle \Psi^{\mathrm{CCSD(T)}} | \mathrm{e}^{T_1+T_2} | \Phi \rangle. \tag{78}$$

The $N^{\mathrm{[T]}}$ and $N^{\mathrm{(T)}}$ numerators defining the R-CCSD[T] and R-CCSD(T) energies (cf. equations (71) and (72)) are directly related to the non-iterative energy corrections

$$E_{\mathrm{T}}^{[4]} = \langle \Phi | (T_3^{[2]})^\dagger (V_{\mathrm{N}} T_2)_{\mathrm{C}} | \Phi \rangle \tag{79}$$

Downloaded At: 16:32 21 January 2011

and

$$E_{\mathrm{ST}}^{[5]} = \langle \Phi | (Z_3)^{\dagger} (V_{\mathrm{N}} T_2)_{\mathrm{C}} | \Phi \rangle \tag{80}$$

that define the standard CCSD[T] and CCSD(T) energies [7, 8],

$$E^{\mathrm{CCSD[T]}} = E^{\mathrm{CCSD}} + E_{\mathrm{T}}^{[4]} \tag{81}$$

and

$$E^{\mathrm{CCSD(T)}} = E^{\mathrm{CCSD[T]}} + E_{\mathrm{ST}}^{[5]} = E^{\mathrm{CCSD}} + E_{\mathrm{T}}^{[4]} + E_{\mathrm{ST}}^{[5]}, \tag{82}$$

respectively. We have

$$N^{\mathrm{[T]}} = E_{\mathrm{T}}^{[4]}, \tag{82}$$

$$N^{\mathrm{(T)}} = E_{\mathrm{T}}^{[4]} + E_{\mathrm{ST}}^{[5]}. \tag{84}$$

It can also be shown that the explicit equations for the $D^{\mathrm{[T]}}$ and $D^{\mathrm{(T)}}$ denominators can be given the following form:

$$D^{\mathrm{[T]}} = 1 + \langle \Phi | T_1^{\dagger} T_1 | \Phi \rangle + \langle \Phi | T_2^{\dagger} \left(T_2 + \tfrac{1}{2} T_1^2 \right) | \Phi \rangle + \langle \Phi | (T_3^{[2]})^{\dagger} (T_1 T_2 + \tfrac{1}{6} T_1^3) | \Phi \rangle, \tag{85}$$

$$D^{\mathrm{(T)}} = D^{\mathrm{[T]}} + \langle \Phi | Z_3^{\dagger} (T_1 T_2 + \tfrac{1}{6} T_1^3) | \Phi \rangle. \tag{86}$$

The above equations allow us to see that the R-CCSD[T] and R-CCSD(T) approaches that are obtained by simplifying the CR-CCSD[T] and CR-CCSD(T) energy formulae reduce to the standard CCSD[T] and CCSD(T) methods when the $D^{\mathrm{[T]}}$ and $D^{\mathrm{(T)}}$ denominators in equations (67) and (68) or (71) and (72) are replaced by 1 [41, 42]. Indeed, by replacing the $D^{\mathrm{[T]}}$ denominator in equation (71) by 1, we obtain the formula for the CCSD[T] energy $E^{\mathrm{CCSD[T]}}$, equation (81). Similarly, by replacing the $D^{\mathrm{(T)}}$ denominator in equation (72) by 1, we obtain the CCSD(T) energy $E^{\mathrm{CCSD(T)}}$, equation (82). As explained in [41, 42], approximation of the $D^{\mathrm{[T]}}$ and $D^{\mathrm{(T)}}$ denominators by 1 is a justified step from the point of view of MBPT, since both denominators equal 1 plus terms which are at least of the second order in the perturbation V_{N}. This becomes clear when we look at the explicit equations for $D^{\mathrm{[T]}}$ and $D^{\mathrm{(T)}}$, equations (85) and (86), respectively, and when we realize that the leading $T_2^{\dagger} T_2$ term in these expressions (excluding, of course, 1) is at least of the second order in V_{N}.

The above analysis implies that the R-CCSD[T], R-CCSD(T), CR-CCSD[T] and CR-CCSD(T) methods can be viewed as the MMCC-based extensions of the standard CCSD[T] and CCSD(T) approaches. The idea of renormalizing the CCSD[T] and CCSD(T) methods via the MMCC formalism can easily be extended to the CCSD(TQ) case. The completely renormalized CCSD(TQ) (CR-CCSD(TQ)) methods are examples of the MMCC(2,4) scheme, in which we improve the results of the standard CCSD calculations by adding the non-iterative corrections $\delta_0(2,4)$, defined in terms of moments $\mathcal{M}_{ijk}^{abc}(2)$ and $\mathcal{M}_{ijkl}^{abcd}(2)$, to the CCSD energies. Two variants of the CR-CCSD(TQ) method, labelled by extra letters 'a' and 'b', are particularly useful. The corresponding CR-CCSD(TQ),a and CR-CCSD(TQ),b energies are calculated in the following way [41–44, 46, 47]:

Downloaded At: 16:32 21 January 2011

$$E^{\text{CR-CCSD(TQ),x}} = E^{\text{CCSD}} + \langle \Psi^{\text{CCSD(TQ),x}} | Q_3 M_3^{\text{CC}}(2) + Q_4 [T_1 M_3^{\text{CC}}(2) + M_4^{\text{CC}}(2)] | \Phi \rangle / \langle \Psi^{\text{CCSD(TQ),x}} | e^{T_1+T_2} | \Phi \rangle \quad (\text{x} = \text{a}, \text{b}), \tag{87}$$

where

$$|\Psi^{\text{CCSD(TQ),a}}\rangle = |\Psi^{\text{CCSD(T)}}\rangle + \tfrac{1}{2} T_2 T_2^{(1)} |\Phi\rangle \tag{88}$$

and

$$|\Psi^{\text{CCSD(TQ),b}}\rangle = |\Psi^{\text{CCSD(T)}}\rangle + \tfrac{1}{2} T_2^2 |\Phi\rangle, \tag{89}$$

with $T_2^{(1)}$ representing the first-order MBPT estimate of T_2 and $|\Psi^{\text{CCSD(T)}}\rangle$ given by equation (64). The $M_3^{\text{CC}}(2)|\Phi\rangle$ and $M_4^{\text{CC}}(2)|\Phi\rangle$ quantities have been defined in section 2.1 (cf. equations (18) and (19) respectively). As in the case of the CR-CCSD[T] and CR-CCSD(T) methods, the above definitions of the $|\Psi^{\text{CCSD(TQ),a}}\rangle$ and $|\Psi^{\text{CCSD(TQ),b}}\rangle$ wavefunctions, equations (88) and (89), respectively, allow us to rewrite the CR-CCSD(TQ),a and CR-CCSD(TQ),b energies, equation (87), in the following compact form:

$$E^{\text{CR-CCSD(TQ),x}} = E^{\text{CCSD}} + N^{\text{CR(TQ),x}} / D^{\text{(TQ),x}} \quad (\text{x} = \text{a}, \text{b}), \tag{90}$$

where

$$N^{\text{CR(TQ),a}} = N^{\text{CR(T)}} + \tfrac{1}{2} \langle \Phi | T_2^{\dagger} (T_2^{(1)})^{\dagger} [T_1 M_3^{\text{CC}}(2) + M_4^{\text{CC}}(2)] | \Phi \rangle, \tag{91}$$

$$N^{\text{CR(TQ),b}} = N^{\text{CR(T)}} + \tfrac{1}{2} \langle \Phi | (T_2^{\dagger})^2 [T_1 M_3^{\text{CC}}(2) + M_4^{\text{CC}}(2)] | \Phi \rangle, \tag{92}$$

$$D^{\text{(TQ),a}} = D^{\text{(T)}} + \tfrac{1}{2} \langle \Phi | T_2^{\dagger} (T_2^{(1)})^{\dagger} (\tfrac{1}{2} T_2^2 + \tfrac{1}{2} T_1^2 T_2 + \tfrac{1}{24} T_1^4) | \Phi \rangle, \tag{93}$$

$$D^{\text{(TQ),b}} = D^{\text{(T)}} + \tfrac{1}{2} \langle \Phi | (T_2^{\dagger})^2 (\tfrac{1}{2} T_2^2 + \tfrac{1}{2} T_1^2 T_2 + \tfrac{1}{24} T_1^4) | \Phi \rangle, \tag{94}$$

with $N^{\text{CR(T)}}$ and $D^{\text{(T)}}$ defined by equations (74) and (86) respectively.

In analogy to the CR-CCSD[T] and CR-CCSD(T) methods and their R-CCSD[T] and R-CCSD(T) counterparts, we can simplify the CR-CCSD(TQ),x (x = a, b) energy expressions by considering the lowest-order estimates of the $\mathcal{M}_{ijk}^{abc}(2)$ and $\mathcal{M}_{ijkl}^{abcd}(2)$ moments, which enter the $M_3^{\text{CC}}(2)|\Phi\rangle$ and $M_4^{\text{CC}}(2)|\Phi\rangle$ quantities via equations (18) and (19), and by dropping the higher-order $T_1 M_3(2)$ term in equation (87) or in equations (91) and (92). This leads to the renormalized R-CCSD(TQ)-1,x and R-CCSD(TQ)-2,x (x = a, b) methods [41–43]. In the R-CCSD(TQ)-1,x methods, we replace $\mathcal{M}_{ijk}^{abc}(2)$ by $\langle \Phi_{ijk}^{abc} | (V_{\text{N}} T_2)_{\text{C}} | \Phi \rangle$ and $\mathcal{M}_{ijkl}^{abcd}(2)$ by $\langle \Phi_{ijkl}^{abcd} | [V_{\text{N}} (\frac{1}{2} T_2^2 + T_3^{[2]})]_{\text{C}} | \Phi \rangle$, where $T_3^{[2]}$ is the estimate for the T_3 cluster component defined by equation (65). In the R-CCSD(TQ)-2,x methods, we replace $\mathcal{M}_{ijk}^{abc}(2)$ by $\langle \Phi_{ijk}^{abc} | [V_{\text{N}} (T_2 + \frac{1}{2} T_2^2)]_{\text{C}} | \Phi \rangle$ and $\mathcal{M}_{ijkl}^{abcd}(2)$ by $\langle \Phi_{ijkl}^{abcd} | (\frac{1}{2} V_{\text{N}} T_2^2)_{\text{C}} | \Phi \rangle$. For example, the R-CCSD(TQ)-1,x energies, x = a, b, can be given the following form:

$$E^{\text{R-CCSD(TQ)-1,x}} = E^{\text{CCSD}} + N^{\text{(TQ)-1,x}} / D^{\text{(TQ),x}} \quad (\text{x} = \text{a}, \text{b}), \tag{95}$$

where

$$N^{\text{(TQ)-1,a}} = N^{\text{(T)}} + \tfrac{1}{2} \langle \Phi | T_2^{\dagger} (T_2^{(1)})^{\dagger} [V_{\text{N}} (\tfrac{1}{2} T_2^2 + T_3^{[2]})]_{\text{C}} | \Phi \rangle \tag{96}$$

and

$$N^{\text{(TQ)-1,b}} = N^{\text{(T)}} + \tfrac{1}{2} \langle \Phi | (T_2^{\dagger})^2 [V_{\text{N}} (\tfrac{1}{2} T_2^2 + T_3^{[2]})]_{\text{C}} | \Phi \rangle, \tag{97}$$

with $N^{\text{(T)}}$ and $T_3^{[2]}$ defined by equations (76) and (65), respectively.

Downloaded At: 16:32 21 January 2011

As explained in [42], all R-CCSD(TQ) and CR-CCSD(TQ) approaches have a similar physical content. For example, they contain all of the terms of the CCSD(T) approach and the fifth-order-type $E_{\rm QQ}^{[5]}$ contributions due to T_4 clusters (or their approximate variants obtained by replacing one of the $T_2^\dagger$ components in equations (92) or (97) by the first-order $(T_2^{(1)})^\dagger$ estimate; cf. equations (91) and (96)). The $E_{\rm QQ}^{[5]}$ contributions are defined as follows:

$$E_{\rm QQ}^{[5]} = \tfrac{1}{4}\langle\Phi|(T_2^\dagger)^2(V_{\rm N}T_2^2)_{\rm C}|\Phi\rangle \tag{98}$$

(cf. [174–176] for a discussion of all $E^{[5]}$ terms). In addition, the R-CCSD(TQ)-1,x (x = a,b) methods include the fifth-order-type $E_{\rm QT}^{[5]}$ term, which is defined as

$$E_{\rm QT}^{[5]} = \tfrac{1}{2}\langle\Phi|(T_2^\dagger)^2(V_{\rm N}T_3^{[2]})_{\rm C}|\Phi\rangle \tag{99}$$

or (in the R-CCSD(TQ)-1,a case) its approximate version obtained by replacing one of the $T_2^\dagger$ components in equation (97) by $(T_2^{(1)})^\dagger$. Indeed, the $N^{\rm (TQ)\text{-}1,b}$ numerator, equation (97), defining the R-CCSD(TQ)-1,b energy, can be written as

$$N^{\rm (TQ)\text{-}1,b} = N^{\rm (T)} + E_{\rm QQ}^{[5]} + E_{\rm QT}^{[5]}. \tag{100}$$

The R-CCSD(TQ)-2,x and, naturally, CR-CCSD(TQ),x approaches contain the

$$E_{\rm TQ}^{[5]} = \tfrac{1}{2}\langle\Phi|(T_3^{[2]})^\dagger(V_{\rm N}T_2^2)_{\rm C}|\Phi\rangle \tag{101}$$

term, which is very similar to $E_{\rm QT}^{[5]}$ (although we should recognize that $E_{\rm QT}^{[5]}$ represents part of the fifth-order effect due to T_4, whereas $E_{\rm TQ}^{[5]}$ represents one of the fifth-order terms due to T_3). Essentially, all of these terms enter the CCSD(TQ$_{\rm f}$) scheme of Kucharski and Bartlett [20], where the energy is calculated as follows:

$$\begin{aligned} E^{\rm CCSD(TQ_f)} &= E^{\rm CCSD} + E_{\rm T}^{[4]} + E_{\rm ST}^{[5]} + \tfrac{1}{2}\langle\Phi|T_2^\dagger(T_2^{(1)})^\dagger[V_{\rm N}(\tfrac{1}{2}T_2^2 + T_3^{[2]})]_{\rm C}|\Phi\rangle \\ &\approx E^{\rm CCSD(T)} + E_{\rm QQ}^{[5]} + E_{\rm QT}^{[5]}. \end{aligned} \tag{102}$$

We should remember, however, that unlike in the CCSD(TQ$_{\rm f}$) method, the T_3 and T_4 energy corrections included in the R-CCSD(TQ)-1,2,x and CR-CCSD(TQ),x (x = a,b) methods are divided by the corresponding $D^{\rm (TQ),x}$ denominators, equations (93) and (94). As explained below, the presence of these denominators significantly improves the description of the ground-state PESs at larger internuclear separations, where the CCSD(TQ$_{\rm f}$) approach fails.

In analogy to the R-CCSD[T] and R-CCSD(T) approaches and their standard CCSD[T] and CCSD(T) counterparts, it can be shown that the R-CCSD(TQ)-1,a scheme, obtained by simplifying the CR-CCSD(TQ),x (x = a,b) equations, reduces to the factorized CCSD(TQ$_{\rm f}$) approach of Kucharski and Bartlett [20], when the $D^{\rm (TQ),a}$ denominator in the R-CCSD(TQ)-1,a energy expression, equation (95), is replaced by 1. Indeed, the CCSD(TQ$_{\rm f}$) energy, equation (102), can be given the following form (cf. equations (84) and (96)):

$$E^{\rm CCSD(TQ_f)} = E^{\rm CCSD} + N^{\rm (TQ)\text{-}1,a}, \tag{103}$$

where $N^{\rm (TQ)\text{-}1,a}$ is defined by equation (96). Clearly, we can obtain equation (103) from the R-CCSD(TQ)-1,a energy formula, equation (95), by replacing $D^{\rm (TQ),a}$ in the latter equation by 1. This very simple relationship between the R-CCSD(TQ)-1,a and CCSD(TQ$_{\rm f}$) methods, combined with the similarity of the physical contents of all R-CCSD(TQ) approximations and the fact that the R-CCSD(TQ) energies are

Downloaded At: 16:32 21 January 2011

obtained by simplifying the CR-CCSD(TQ) energy expressions, implies that the R-CCSD(TQ) and CR-CCSD(TQ) approaches can be viewed as the MMCC extensions of the standard CCSD(TQ$_f$) approach (cf. [41–43] for additional comments).

For the closed-shell molecules at or near their equilibrium geometries, where the MBPT series usually converges, the $D^{[T]}$ and $D^{(T)}$ denominators, equations (77) or (85) and (78) or (86), respectively, defining the (C)R-CCSD[T] and (C)R-CCSD(T) approximations, and the $D^{(TQ),x}$ denominators, equations (93) and (94), defining the (C)R-CCSD(TQ),x (x = a, b) approximations, are close to 1, so that the renormalized and completely renormalized CCSD[T], CCSD(T) and CCSD(TQ) approaches give results that are almost identical to those obtained with the standard CCSD[T], CCSD(T) and CCSD(TQ$_f$) methods. In the region of stretched nuclear geometries, where the MBPT series is manifestly divergent, the $D^{[T]}$, $D^{(T)}$ and $D^{(TQ),x}$ denominators can be much larger than 1 [42, 43]. This is the main reason for the excellent performance of the CR-CCSD[T], CR-CCSD(T) and CR-CCSD(TQ),x approaches at larger internuclear separations. The overlaps of the $|\Psi^{CCSD[T]}\rangle$, $|\Psi^{CCSD(T)}\rangle$ and $|\Psi^{CCSD(TQ),x}\rangle$ (x = a, b) wavefunctions, equations (63), (64), (88) and (89), respectively, with the CCSD wavefunction $e^{T_1+T_2}|\Phi\rangle$, defining those denominators, play a role of natural damping factors, which damp the excessively large and, thus, completely unphysical values of the non-iterative triples and quadruples corrections at larger internuclear separations. Because of the use of intermediate normalization, no such denominators are present in the conventional CCSD[T], CCSD(T) and CCSD(TQ$_f$) energy expressions. In consequence, the standard CCSD[T], CCSD(T) and CCSD(TQ$_f$) methods give completely unphysical PESs when chemical bonds are stretched or broken, whereas the CR-CCSD[T], CR-CCSD(T) and CR-CCSD(TQ),x approaches provide a correct PES description at large internuclear distances [41–47, 49, 158].

Downloaded At: 16:32 21 January 2011

The above simple relationship between the renormalized and completely renormalized CCSD[T], CCSD(T) and CCSD(TQ) methods and their standard counterparts implies that costs of the R-CCSD[T], R-CCSD(T), CR-CCSD[T], CR-CCSD(T), R-CCSD(TQ)-n,x and CR-CCSD(TQ),x (n = 1, 2, x = a, b) calculations are essentially identical to the costs of the standard CCSD[T], CCSD(T) and CCSD(TQ$_f$) calculations. In analogy to the standard CCSD[T] and CCSD(T) methods, the R-CCSD[T], R-CCSD(T), CR-CCSD[T] and CR-CCSD(T) approaches are $n_o^3 n_u^4$ procedures in the non-iterative steps involving triples and $n_o^2 n_u^4$ procedures in the iterative CCSD steps. The memory and disk storage requirements characterizing the R-CCSD[T], R-CCSD(T), CR-CCSD[T] and CR-CCSD(T) methods are essentially identical to those characterizing the standard CCSD[T] and CCSD(T) approaches (see [158] for details). In complete analogy to the non-iterative triples corrections, the cost of the R-CCSD(TQ)-n,x calculations is identical to the cost of the CCSD(TQ$_f$) calculations (the CCSD(TQ$_f$) method is an $n_o^3 n_u^4$ procedure in the triples part and an $n_o^2 n_u^5$ procedure in steps involving T_4 contributions). The CR-CCSD(TQ),x approaches are only twice as expensive as the CCSD(TQ$_f$) method in the steps involving the non-iterative corrections to the CCSD energy.

These relatively low computer costs, combined with the ease of use of the completely renormalized CCSD[T], CCSD(T) and CCSD(TQ) methods that can only be matched by the standard CCSD[T], CCSD(T) and CCSD(TQ$_f$) approaches and with the fact that the CR-CCSD[T], CR-CCSD(T) and CR-CCSD(TQ),x approaches remove the pervasive failing of the standard methods at larger internuclear separations, make the CR-CCSD[T], CR-CCSD(T) and CR-CCSD(TQ),x

approaches attractive alternatives to the existing multireference methods, such as MRCI. The latter methods describe bond breaking correctly, but the effort involved is significantly larger and one has to think about elements such as reference configurations, active orbitals, etc. to set up multireference calculations. None of these elements has to be considered in the CR-CCSD[T], CR-CCSD(T) and CR-CCSD(TQ),x calculations. As we will see in section 3.2.2, the CR-CCSD[T], CR-CCSD(T) and CR-CCSD(TQ),x methods provide results of MRCI quality with an effort similar to the standard CCSD[T], CCSD(T) and CCSD(TQ_f) calculations [41–44, 46, 47, 49, 158]. Similar remarks apply to the R-CCSD[T], R-CCSD(T) and R-CCSD(TQ)-*n*,x approaches, which often improve the results of standard calculations for the intermediate stretches of chemical bonds. We must remember, however, that the R-CCSD[T], R-CCSD(T) and R-CCSD(TQ)-*n*,x methods fail at larger distances [41–44, 46, 47, 49]. For this reason, the CR-CCSD[T], CR-CCSD(T) and CR-CCSD(TQ),x methods are the recommended choices, although the R-CCSD[T], R-CCSD(T) and R-CCSD(TQ)-*n*,x methods can be very useful in some cases too (cf. section 3.2.2).

3.2.2. *The renormalized and completely renormalized CCSD[T], CCSD(T) and CCSD(TQ) methods: examples of applications*

Downloaded At: 16:32 21 January 2011

3.2.2.1. *Benchmark calculations for bond breaking in diatomics and small polyatomics.* We begin the discussion of examples of the renormalized and completely renormalized CCSD[T], CCSD(T) and CCSD(TQ) calculations by examining the results that we obtained for the DZ models of the HF, H_2O, N_2 and C_2 molecules, for which the exact, full CI, potential energy curves and many other data are available (see tables 1, 2 and 5 and figures 2–4). The major characteristics of the DZ model of HF, H_2O and N_2 have been discussed in sections 3.1.2 and 3.1.4. The information about the DZ model of C_2 can be found in [47]. The original R-CCSD[T], R-CCSD(T), CR-CCSD[T] and CR-CCSD(T) data for HF, H_2O, N_2 and C_2 are taken from [41–43, 47]. Another interesting benchmark, discussed in this section, is provided by the F_2 molecule, as described by the cc-pVDZ basis set [169], for which the full CCSDT method provides a virtually exact description of the potential energy curve [44]. Two other benchmarks discussed in this section involve the unimolecular dissociations of ethane and methyl fluoride, studied with the cc-pVDZ basis set by Schütz [35]. In this case, we can compare the performance of the CR-CCSD(T) method with the results of the accurate MRCI calculations employing the complete active-space self-consistent-field (CASSCF) reference [35]. As in all CC calculations discussed in this work, the ground-state RHF configuration was used as a reference in the renormalized and completely renormalized CCSD[T], CCSD(T) and CCSD(TQ) calculations reported in this section.

The most remarkable result is the fact that, unlike the standard CCSD[T], CCSD(T) and CCSD(TQ_f) methods, their MMCC-based CR-CCSD[T], CR-CCSD(T) and CR-CCSD(TQ) counterparts provide highly accurate results at large internuclear separations, in spite of the apparent failure of the underlying CCSD approximation, which provides the T_1 and T_2 cluster components for calculating the relevant non-iterative energy corrections, and in spite of the presence of the MBPT-like terms in the CR-CCSD[T], CR-CCSD(T) and CR-CCSD(TQ) expressions (cf. equations (61) or (69), (62) or (70) and (87) or (90)). The presence of the analogous

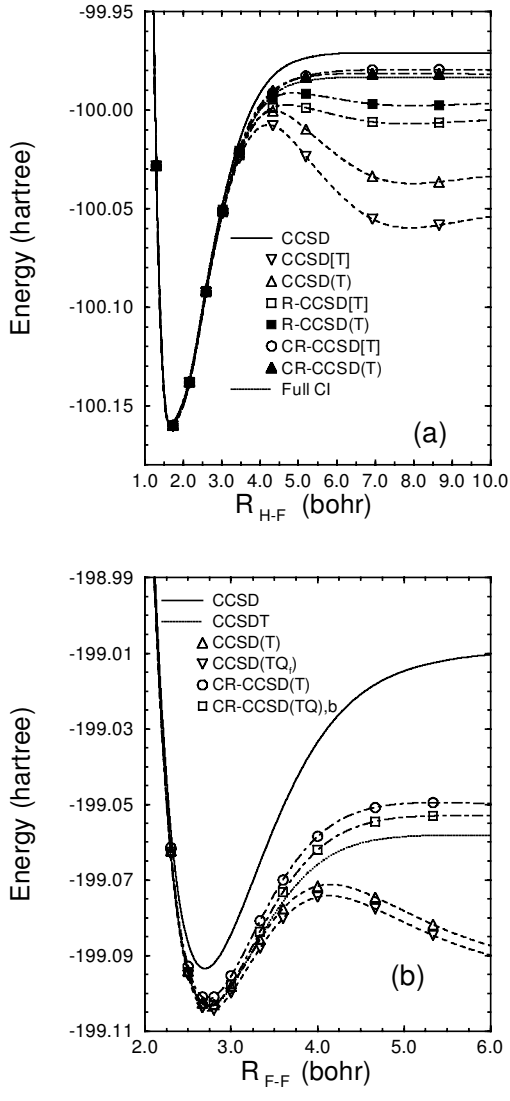

Downloaded At: 16:32 21 January 2011

Figure 3. Potential energy curves for (*a*) the H–F bond breaking in the HF molecule, (*b*) the F–F bond breaking in the F_2 molecule, (*c*) the C–C bond breaking in ethane and (*d*) the C–F bond breaking in methyl fluoride (energies in hartree and the corresponding internuclear separations in bohr). The results for the HF molecule were obtained with the DZ basis set, whereas the results for F_2, C_2H_6 and CH_3F were obtained with the cc-pVDZ basis set. The results for HF ((*a*); taken from [42]) include a comparison of the R-CCSD[T], R-CCSD(T), CR-CCSD[T] and CR-CCSD(T) potential energy curves (designated by □, ■, ○ and ▲, respectively) with curves obtained with the CCSD (solid curve), CCSD[T] (▽), CCSD(T) (△) and full CI (dotted curve) methods. The results for F_2 ((*b*); taken from [44]) include a comparison of the CR-CCSD(T) and CR-CCSD(TQ),b potentials (designated by ○ and □, respectively) with potential energy curves obtained in the CCSD (solid curve), CCSDT (dotted curve), CCSD(T) (△) and CCSD(TQ_f) (▽) calculations. The results for ethane (*c*) and methyl fluoride (*d*) include a comparison of the CR-CCSD(T) potential energy curves (designated by ■ and obtained in the present work) with the CCSD and CCSD(T) curves (designated by the solid curve and ●, respectively, and obtained in this work) and CASPT2 (○), MRCI (△) and MRCI(Q) (▽) potentials obtained by Schütz [35].

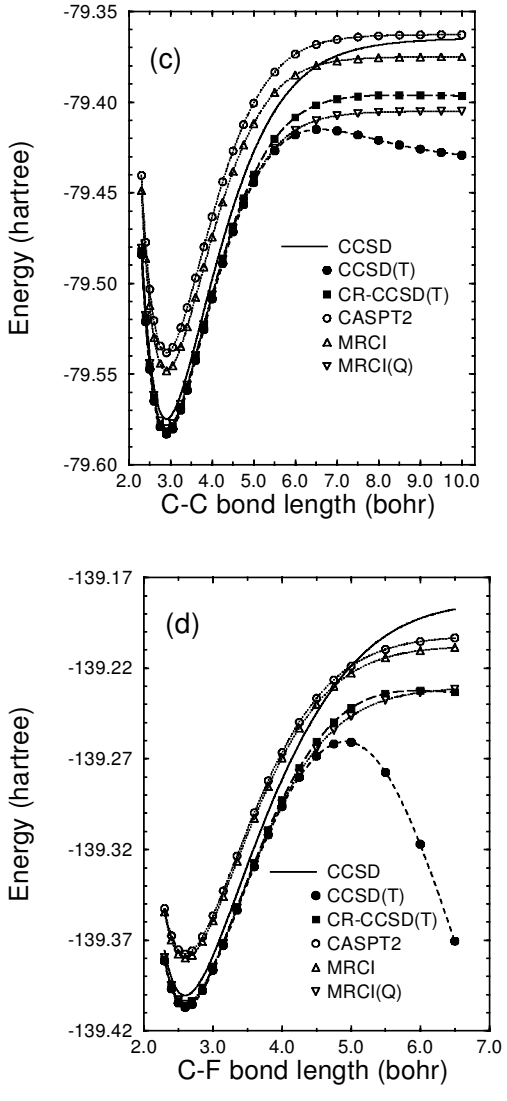

Figure 3(*c*) and 3(*d*).

terms in the conventional CCSD[T], CCSD(T) and CCSD(TQ_f) energy formulae results in a completely erroneous description of the ground-state PESs by the CCSD[T], CCSD(T) and CCSD(TQ_f) approximations owing to the divergent behaviour of the MBPT series at large internuclear separations [18, 36–49] (see tables 1, 2 and 5 and figures 2–4).

As shown in table 1 and figure 3(*a*), already the simple CR-CCSD[T] and CR-CCSD(T) methods completely eliminate the unphysical humps on the ground-state PESs of the HF molecule obtained with the standard CCSD[T], CCSD(T) and CCSD(TQ_f) approaches at intermediate internuclear separations R. The CR-CCSD[T] and CR-CCSD(T) methods provide a variational, accurate and well-balanced description of the entire PES of HF, including very large internuclear

Downloaded At: 16:32 21 January 2011

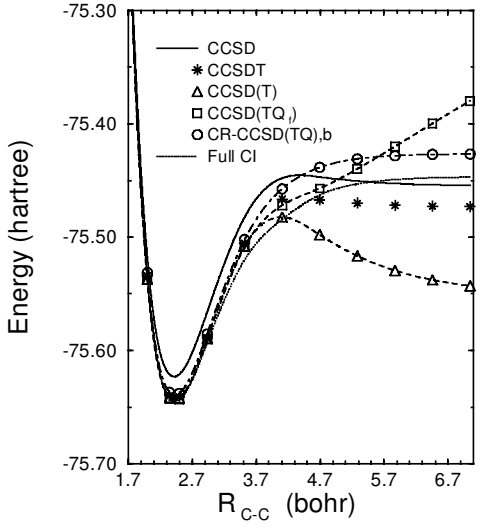

Figure 4. Potential energy curves for the DZ model of the C_2 molecule (energies in hartree and the C–C separation $R_{C\text{-}C}$ in bohr). A comparison of the results obtained with the CR-CCSD(TQ),b method, designated by ○, with the results of the CCSD, CCSDT, CCSD(T), CCSD(TQ_f) and full CI calculations, designated by the solid curve, *, △, □ and the dotted curve, respectively (see [47] for the original numerical data).

Downloaded At: 16:32 21 January 2011

distances R (as large as $5R_e$; as usual, R_e is the equilibrium bond length). Indeed, the ground-state potential energy curves obtained in the CR-CCSD[T] and CR-CCSD(T) calculations are located above the exact, full CI, curve and the errors in the CR-CCSD[T] and CR-CCSD(T) results do not exceed, respectively, 3.8 and 2.1 millihartree in the entire $R \leq 5R_e$ region (see table 1). For the considerably larger aug-cc-pVTZ basis set [169, 170], the errors in the CR-CCSD(T) energies, relative to full CCSDT (the full CCSDT approach is almost exact for single bond breaking [37, 39]), do not exceed 3.9 millihartree [46] (cf. section 3.2.2.2 for further discussion of this case). The CR-CCSD(TQ),a and CR-CCSD(TQ),b methods provide further improvements in the results, reducing the maximum errors relative to full CI for the DZ basis set in the entire $R \leq 5R_e$ region to 0.5 and 0.7 millihartree, respectively.

The CR-CCSD[T], CR-CCSD(T) and CR-CCSD(TQ) methods are particularly effective at larger internuclear separations. For example, the large positive, 11.596 millihartree, error in the CCSD result and the large negative −38.302, −24.480 and 18.351 millihartree errors in the CCSD[T], CCSD(T) and CCSD(TQ_f) results, respectively, at $R = 3R_e$ decrease to 2.508, 2.100, 0.425 and 0.316 millihartree when the CR-CCSD[T], CR-CCSD(T), CR-CCSD(TQ),a and CR-CCSD(TQ),b methods are employed (cf. table 1). As shown in table 1, the reduction of errors in the CCSD[T], CCSD(T) and CCSD(TQ_f) results at $R = 5R_e$, offered by the CR-CCSD[T], CR-CCSD(T) and CR-CCSD(TQ) methods, is even more impressive. The CR-CCSD[T], CR-CCSD(T), CR-CCSD(TQ),a and CR-CCSD(TQ),b results for geometries near the equilibrium ($R \approx R_e$), where the conventional CCSD[T], CCSD(T) and CCSD(TQ_f) methods provide very small errors, are as good as the CCSD[T], CCSD(T) and CCSD(TQ_f) results. For example, the standard CCSD(T) method gives a 0.325 millihartree error at $R = R_e$, which should be compared with a 0.500 millihartree error obtained with the CR-CCSD(T) approach (see table 1). Even

for geometries near the equilibrium, the behaviour of the completely renormalized CC methods can be viewed as somewhat more stable than the behaviour of the standard non-iterative approaches. For example, the standard CCSD[T] method gives a small negative, -0.070 millihartree, error at $R = R_e$, in spite of the fact that the full CCSDT approach gives a positive, 0.173 millihartree, error in this case. The CR-CCSD[T] approach fixes this problem, providing an energy which is slightly (0.163 millihartree) above the corresponding full CI energy (see table 1).

Although we do not particularly advocate the renormalized (R) CCSD[T] and CCSD(T) methods (as opposed to completely renormalized (CR) approaches), which differ from the standard CCSD[T] and CCSD(T) approaches only by the presence of the $D^{[T]}$ and $D^{(T)}$ denominators, equations (77) and (78), respectively, in the corresponding energy expressions (cf. equations (71) and (72)), the R-CCSD[T] and R-CCSD(T) approaches offer considerable improvements in the description of PES of HF in the region of intermediate values of R (see figure 3(*a*) and [41, 42]). This may lead to great improvements in the calculated vibrational term values, as we will see later on (see section 3.2.2.2). We must remember, however, that the R-CCSD[T] and R-CCSD(T) approaches and their R-CCSD(TQ)-*n*,x ($n = 1, 2$; x = a, b) counterparts described in section 3.2.1 cannot completely eliminate the humps on the PESs involving bond breaking (see figure 3(*a*)).

Downloaded At: 16:32 21 January 2011

The example of HF shows that the CR-CCSD[T] and CR-CCSD(T) methods are sufficient for studies of single bond breaking. The CR-CCSD(TQ),x (x = a, b) methods provide further (very nice) improvements, but their use is not necessary to obtain a very good description of the PES involving a dissociation of a single chemical bond. We confirmed this by performing the calculations for several other cases of single bond breaking, including the B–H bond in BH [44], the F–F bond in F_2 [44], the C–C bond in ethane and the C–F bond in methyl fluoride. The results for F_2, ethane and methyl fluoride are shown in figures 3(*b*)–3(*d*), respectively. In all three cases, we used the cc-pVDZ basis set [169] and froze the molecular orbitals correlating with the 1s orbitals of the F and C atoms in the CC calculations.

The F_2 molecule (see figure 3(*b*)) represents a particularly challenging type of single bond breaking for the single-reference RHF-based CC approaches owing to the unusually large non-dynamic correlation effects, even for relatively small stretches of the F–F bond (cf. [36]). For example, the RHF-based CCSD approach produces a potential well which is almost twice as deep as that provided by the highly accurate (virtually exact in this case) full CCSDT approach. The standard CCSD(T) and CCSD(TQ_f) methods fail too. They give the well-pronounced humps for intermediate values of the F–F internuclear separation R and energies at large R values that are almost identical to the energy at the equilibrium geometry [44]. It is, therefore, quite remarkable that the CR-CCSD(T) and CR-CCSD(TQ) methods, which can be viewed as the MMCC-based modifications of the existing CCSD(T) and CCSD(TQ_f) approaches, are capable of providing high-quality potential energy curves, which have correct shapes and which are very close to the curve obtained with the full CCSDT approach (see figure 3(*b*)). For the cc-pVDZ basis set, used here, the reference CCSDT value of the dissociation energy D_e is 1.22 eV (the experimental value of D_e is 1.66 eV [177, 178]). The CCSD calculation gives 2.30 eV, which is approximately twice the full CCSDT value. The CR-CCSD(T), CR-CCSD(TQ),a and CR-CCSD(TQ),b methods give 1.40, 1.35 and 1.36 eV, respectively, in very good agreement with the CCSDT value of D_e of 1.22 eV. Even the simplest R-CCSD(T) method gives 1.31 eV for D_e [44], which is probably a

coincidence, but all of this shows that the renormalized and, particularly, the completely renormalized CCSD(T) and CCSD(TQ) methods provide considerable improvements in the results of the standard CCSD, CCSD(T) and CCSD(TQ_f) calculations (in all of the above estimates of the D_e values, we ignored the presence of a very small, 2.7 millihartree deep, hump on the R-CCSD(T) curve and even smaller, 1.9–2.0 millihartree deep, humps on the CR-CCSD(T) and CR-CCSD(TQ),x curves at $R \approx 2R_e$). Although the CR-CCSD(T) and CR-CCSD(TQ) values of D_e obtained with the cc-pVDZ basis set are also in reasonable agreement with the experimental dissociation energy of 1.66 eV, a comparison with the experimental value of D_e is not very meaningful when a small basis set of the cc-pVDZ quality is employed. Very recently, we performed several calculations for F_2 using the much larger aug-cc-pVQZ basis set [158]. In this case, the CCSD value of D_e is 3.18 eV, which is almost twice as much as the experimental value of D_e. The CR-CCSD(T) method gives 2.03 eV, in much better agreement with the experimental value of 1.66 eV. We must re-emphasize the fact that our CR-CCSD(T) method produces these great potential energy curves and D_e values with the ease of use and the relatively low computer cost of the standard CCSD(T) calculations, which generate completely unrealistic potentials.

Downloaded At: 16:32 21 January 2011

As clearly shown in figure 3(*b*), the CR-CCSD(T) method provides an adequate description of the bond breaking in F_2. The CR-CCSD(TQ) results are, perhaps, somewhat better, but, as in the case of the HF molecule, it is not necessary to use the CR-CCSD(TQ) approach, which requires a consideration of the non-iterative triples as well as quadruples, to obtain a very good description of the potential energy curve of F_2. This should be contrasted with the performance of the recently proposed and more expensive VOD(2) and OD(2) approximations [140–143], in which non-iterative corrections due to a combined effect of T_3 and T_4 clusters, resulting from the partitioning and subsequent perturbative analysis of the CCSD similarity-transformed Hamiltonian, are added to the CCSD energies. For the cc-pVDZ basis set used here, these methods give 1.44 and 1.43 eV, respectively, for the dissociation energy D_e [141], which is somewhat worse than what we can obtain with the much simpler R-CCSD(T) and CR-CCSD(T) approaches that use only T_3 corrections and that do not require additional orbital optimization needed in VOD(2) and OD(2) calculations, when we compare the results with the CCSDT value of D_e. Very similar remarks apply to the equilibrium bond lengths in F_2, which for the cc-pVDZ basis set are 2.73 and 2.74 bohr for the (C)R-CCSD(T) and full CCSDT methods, respectively [44], and ~2.8 bohr for the OD(2) and VOD(2) approaches [141]. All of these remarks are quite important, since the non-iterative $n_o^3n_u^4$ steps of the R-CCSD(T) and CR-CCSD(T) approaches are significantly less expensive than the $n_o^2n_u^5$ or n_u^6 steps of the VOD(2) and OD(2) methods, particularly when the large basis sets are employed. The fact that we can avoid using the CR-CCSD(TQ) approach for F_2 and other cases of single bond breaking is good news too, since the non-iterative $n_o^2n_u^5$ steps of the CR-CCSD(TQ) method and its standard CCSD(TQ_f) analogue, although much less expensive than the iterative $n_o^3n_u^5$ and $n_o^4n_u^6$ steps of the full CCSDT and CCSDTQ approaches, are considerably more expensive than the $n_o^3n_u^4$ steps of the standard, renormalized and completely renormalized methods of the CCSD(T) type.

The adequacy of the CR-CCSD(T) approach in describing a dissociation of a single chemical bond is not limited to diatomics. In figures 3(*c*) and 3(*d*), we show the results of the standard CCSD and CCSD(T) calculations and the MMCC-based CR-

CCSD(T) calculations for the C–C bond breaking in ethane and the C–F bond breaking in methyl fluoride. A comparison is made in this case with the results of various multireference calculations performed recently by Schütz [35], who used a cc-pVDZ basis set and the MOLPRO package [179] to perform them. Those multi-reference calculations include, among others, the calculations employing the internally contracted MRCI methods of Werner and Knowles [180, 181], based on the CASSCF reference (referred to as the MRCI and MRCI(Q) approaches), and the calculations employing the CASSCF-based second-order multireference MBPT approach (CASPT2) [182–190], as implemented in MOLPRO by Werner [191].

It is clear from figures 3(*c*) and 3(*d*) that the standard CCSD and CCSD(T) methods provide an inadequate description of the C–C bond breaking in ethane and the C–F bond breaking in methyl fluoride. In both cases, the CCSD approach provides potential wells which are much too deep, when compared with the results of multireference calculations, whereas the CCSD(T) curves, having the well-pronounced humps at the intermediate C–C and C–F separations, are completely erroneous. The failure of the standard CCSD and CCSD(T) methods is particularly dramatic for the CH_3F molecule (see figure 3(*d*)). In this case, the CCSD value of the dissociation energy D_e, defined by forming the difference between the CCSD energies at the largest stretch of the C–F bond used by us and Schütz [35], i.e. $R_{C\text{-}F} = 6.5$ bohr, and at the approximate value of the optimum C–F distance, i.e. $R_{C\text{-}F} = 2.6$ bohr, is 5.80 eV. A similar calculation of D_e with the CASPT2, MRCI and MRCI(Q) methods gives completely different results, namely 4.74, 4.66 and 4.72 eV, respectively, showing the failure of the CCSD approximation. For the C–F internuclear separations up to 4.25 bohr, the standard CCSD(T) energies agree with the results of the MRCI(Q) calculations, in which the internally contracted MRCI approach is approximately corrected for the effect of higher-than-doubly excited configurations from the multidimensional reference space, to within 2 millihartree. Unfortunately, for $R_{C\text{-}F} \geq 4.5$ bohr, the differences between CCSD(T) and MRCI(Q) results rapidly increase with $R_{C\text{-}F}$ owing to the non-variational collapse of the CCSD(T) theory. For example, the difference between the CCSD(T) and MRCI(Q) energies at $R_{C\text{-}F} = 6.5$ bohr is -138.898 millihartree. The failure of the CCSD(T) method for C–C bond breaking in ethane is not as dramatic (see figure 3(*c*)), but the difference between the CCSD(T) and MRCI(Q) energies at $R_{C\text{-}C} = 10.0$ bohr of -24.176 millihartree is clearly much larger in absolute value than the small, 1–2 millihartree, differences between the MRCI(Q) and CCSD(T) energies for $R_{C\text{-}C} \leq 6.0$ bohr. Again, there is a significant difference between the values of dissociation energies resulting from the single-reference CCSD and multi-reference calculations (the CCSD approach gives 5.70 eV, whereas the CASPT2, MRCI and MRCI(Q) methods give 4.77, 4.71 and 4.76 eV, respectively).

In view of the poor performance of the standard CCSD and CCSD(T) methods in describing the C–C bond breaking in ethane and the C–F bond breaking in methyl fluoride, it is remarkable to observe the excellent agreement between the CR-CCSD(T) and MRCI(Q) potential energy curves (see figures 3(*c*) and 3(*d*)). As in the case of HF and F_2, the CR-CCSD(T) method restores the correct shapes of the potential energy curves for ethane and methyl fluoride, eliminating the humps produced by the CCSD(T) approach for the intermediate C–C and C–F distances. For C–C distances in ethane less than 5.0 bohr, the CR-CCSD(T) and MRCI(Q) energies agree to within 1–2 millihartree. For $R_{C\text{-}C} \geq 5.0$ bohr, the differences between the CR-CCSD(T) and MRCI(Q) energies do not exceed 8.5 millihartree.

Downloaded At: 16:32 21 January 2011

This should be compared with the large positive, ~40 millihartree, differences between the CCSD and MRCI(Q) energies or the large negative, *ca.* −20 millihartree, differences between the CCSD(T) and MRCI(Q) energies for larger values of $R_{C\text{-}C}$. The situation for methyl fluoride is essentially the same. For C–F distances in CH_3F less than or equal to 4.0 bohr, the differences between the CR-CCSD(T) and MRCI(Q) energies do not exceed 1–2 millihartree. They are similarly small for $R_{C\text{-}F} > 5.5$ bohr. Only for $R_{C\text{-}F} \approx 5.0$ bohr are the differences between the CR-CCSD(T) and MRCI(Q) energies ~4.5 millihartree. This should be compared with the large negative, *ca.* −100 millihartree, differences between the CCSD(T) and MRCI(Q) energies for larger values of $R_{C\text{-}F}$. The CR-CCSD(T) dissociation energies D_e, defined by forming the differences between the CR-CCSD(T) energies at the largest C–C and C–F distances considered here ($R_{C-C} = 10.0$ bohr for ethane and $R_{C-F} = 6.5$ bohr for methyl fluoride) and at the approximate equilibrium values of those distances in ethane and methyl fluoride ($R_{C-C} = 2.9$ bohr for ethane and $R_{C-F} = 2.6$ bohr for CH_3F), are 5.04 eV for ethane and 4.72 eV for CH_3F. Thus, the CR-CCSD(T) approach is capable of reducing the ~1 eV errors in the CCSD values of the dissociation energies D_e, relative to the CASPT2, MRCI or MRCI(Q) values of D_e, to ~0.3 eV in the case of ethane and ~0.1 eV in the methyl fluoride case. These results, combined with the well-balanced and accurate description of the potential energy curves of both molecules, and the fact that the CR-CCSD(T) curves are located invariably above the highly accurate MRCI(Q) curves, clearly demonstrate that the CR-CCSD(T) method can be regarded as a viable alternative to the existing multireference methods in cases of single bond stretching or breaking.

Downloaded At: 16:32 21 January 2011

The CR-CCSD[T] and CR-CCSD(T) methods are also sufficiently accurate for cases involving a simultaneous stretching of two single bonds, but one cannot use those methods safely to study multiple bond breaking. A good example of the former situation is provided by the double dissociation of H_2O (see table 2). When both O–H bonds in the H_2O molecule, described here by the DZ basis set, are simultaneously stretched to $R = 2R_e$, the T_3 and T_4 effects become relatively large and difficult to describe and the standard CCSD[T], CCSD(T) and CCSD(TQ_f) methods that are normally used to describe those effects completely fail (cf. section 3.1.2 and table 2). As shown in table 2, the CR-CCSD[T], CR-CCSD(T) and CR-CCSD(TQ),x (x = a, b) methods reduce the large negative, −11.220, −7.699 and −5.914 millihartree, errors in the CCSD[T], CCSD(T) and CCSD(TQ_f) results at $R = 2R_e$ to relatively small positive errors (1.163 millihartree for CR-CCSD[T], 1.830 millihartree for CR-CCSD(T), 1.461 millihartree for CR-CCSD(TQ),a and 2.853 millihartree for CR-CCSD(TQ),b). At the same time, the CR-CCSD[T], CR-CCSD(T) and CR-CCSD(TQ),x (x = a, b) energies at the equilibrium geometry ($R = R_e$) are virtually identical to the highly accurate energy values provided by the standard CCSD[T], CCSD(T) and CCSD(TQ_f) approaches (see table 2). The fact that the CR-CCSD[T] and CR-CCSD(T) methods give energies that differ by less than 2–2.5 millihartree from the corresponding full CI values in the entire $R = R_e$–$2R_e$ region of the doubly dissociating water molecule clearly shows that there is no apparent need to use the higher-level CR-CCSD(TQ),x (x = a, b) methods in cases like this. On the other hand, the CR-CCSD(TQ),x (x = a, b) approaches provide a more stable description of the double dissociation of H_2O, when compared with the CR-CCSD[T] and CR-CCSD(T) methods. For example, the initially small, 0.560 millihartree, error in the CR-CCSD[T] result at $R = R_e$ increases to 2.053 millihartree at $R = 1.5R_e$, finally to decrease again to 1.163 millihartree at $R = 2R_e$ (see

table 2). A similar behaviour is observed for the CR-CCSD(T) approach. Those non-monotonic error changes are the first signs of the eventual breakdown of the CR-CCSD[T] and CR-CCSD(T) methods in the $R > 2R_e$ region. The CR-CCSD(TQ),x (x = a, b) methods behave much better in this regard, since the small errors in the CR-CCSD(TQ),x energies, relative to full CI, monotonically increase with the O–H separation (we can, in fact, use the CR-CCSD(TQ),x (x = a, b) approaches to describe the $R > 2R_e$ region).

Although one may apply the CR-CCSD[T] and CR-CCSD(T) approaches to a simultaneous stretching of two single bonds, the breaking of multiple bonds requires using higher-order MMCC theories, such as CR-CCSD(TQ),b. For example, when we apply the CR-CCSD(T) method to triple bond breaking in the N_2 molecule, discussed earlier in section 3.1.4, we obtain a potential energy curve which is characterized by the hump at $R \approx 1.75R_e$ and which is located below the full CI curve for large N–N separations [43]. The CR-CCSD(T) results are much better than the results of the standard CCSD(T) calculations, but they are far too poor to be used in the quantitative applications that need information about the N_2 electronic energies for stretched nuclear geometries. For example, when the DZ basis set is employed, the unsigned error in the CR-CCSD(T) results relative to full CI at $R = 2.25R_e$ is 133.313 millihartree [43]. This is better than the 387.448 and 334.985 millihartree errors in the CCSD(T) and CCSD(TQ_f) results, but undoubtedly we cannot use the potential energy curve characterized by errors of an order of 100 millihartree in any meaningful applications.

Downloaded At: 16:32 21 January 2011

As already explained in section 3.1.4, the N_2 molecule is characterized by large T_3 and T_4 effects, even at $R = R_e$. It is quite possible that higher–than–quadruply excited clusters play an important role when the N–N internuclear separation R becomes large. Because of the apparent importance of the higher-order clusters in the N_2 case, which cannot be easily approximated using the conventional MBPT or CC arguments, the standard CCSD, CCSD(T) and CCSD(TQ_f) methods and their higher-level CCSDT and CCSDT(Q_f) analogues completely fail at large N–N distances (see section 3.1.4, table 5 and figure 2). As shown in section 3.1.4, the appropriate level of the MMCC theory that provides an excellent description of the entire potential energy curve of N_2 is MMCC(2,6). It is, therefore, interesting to examine whether the lower-order approximations of the CR-CCSD(TQ) (i.e. MMCC(2,4)) type can provide reasonable results in this case.

The results of the CR-CCSD(TQ),a and CR-CCSD(TQ),b calculations for the DZ model of N_2 are shown in table 5 and figure 2. It is quite remarkable to observe the great improvements in the results offered by those two methods, particularly when variant 'b' of the CR-CCSD(TQ) approach is employed. As shown in table 5 and figure 2, the CR-CCSD(TQ),b method, which is a rather simple modification of the conventional CCSD(TQ_f) approach and which uses, as the latter method, the elements of MBPT to estimate the T_3 and T_4 effects, provides a potential energy curve which is quite close to the exact, full CI, curve. A huge, 334.985 millihartree, error in the CCSD(TQ_f) result at $R = 2.25R_e$ decreases to 14.796 millihartree, when the CR-CCSD(TQ),b method is employed (see table 5). The CR-CCSD(TQ),b curve is located above the full CI curve in the entire $R = 0.75R_e$–$2.25R_e$ region and almost all pathologies observed in the standard single-reference CC calculations are eliminated when the CR-CCSD(TQ),b method is employed. The huge humps on the CCSD, CCSD(T) and CCSDT curves and a nearly singular behaviour of the CCSD(TQ_f) and CCSDT(Q_f) approaches at large R values (cf. table 5 and figure

2) are almost entirely eliminated by the CR-CCSD(TQ),b approach. Although there is a hump on the CR-CCSD(TQ),b curve, the size of this hump, as measured by the difference between the CR-CCSD(TQ),b energies at the maximum corresponding to the hump and at $R = 2.25R_e$, is small (~4.9 millihartree [43]). Although there are 10–25 millihartree differences between the CR-CCSD(TQ),b and full CI energies at the intermediate values of R (those differences will be addressed in section 3.3.2), the fact that we can obtain a reasonably accurate potential energy curve for the triply bonded N_2 molecule, which is also located above the full CI curve in the entire $R = 0.75R_e$–$2.25R_e$ region, with the ease of use characterizing the standard non-iterative CC 'black boxes' of the CCSD(TQ_f) type, is a truly intriguing finding. Further improvements in the CR-CCSD(TQ),b description of the triple bond breaking in N_2 can be obtained when we use the quadratic MMCC approach discussed in section 3.3 or the CISDtqph-corrected MMCC(2,6) theory described in section 3.1.4. Although the quadratic MMCC method is, at this time, our preferred computational strategy, it might be useful to mention here that we can also improve the description of the ground-state PES of N_2 in the region of intermediate R values with the completely renormalized versions of the CCSDT(Q_f) approach (see [41, 42] for details). For example, variant 'b' of the CR-CCSDT(Q) method [41, 42], in which the completely renormalized corrections due to T_4 clusters are added to the CCSDT energies, provides a curve for N_2 which is characterized by errors relative to full CI that do not exceed 7.6 millihartree in the $R = 0.75R_e$–$2.25R_e$ region and that are as small as 0.719 millihartree at $R = R_e$ and 1.161 millihartree at $R = 2R_e$ [45, 47].

When we use the higher-order MMCC theories, such as CR-CCSD(TQ),x, it is not completely immaterial how we treat wavefunctions $|\Psi\rangle$ that enter the MMCC energy expressions. The evidence provided in tables 1, 2, 5 and 6 indicates that we can use wavefunctions that themselves lead to rather inaccurate description of bond breaking, so an issue is not so much in using the high-quality wavefunctions $|\Psi\rangle$. Our experience with the MMCC methods is telling us that a lot more attention has to be paid to the way we handle the T_1 and T_2 clusters that enter the MMCC expressions. As shown in table 5 for the DZ model of N_2, this is particularly true for the MMCC(2,4)-based CR-CCSD(TQ) case. The CR-CCSD(TQ),b approach provides a rather well-balanced description of the triple bond breaking in N_2, but the CR-CCSD(TQ),a method, which differs from the CR-CCSD(TQ),b approach only by the treatment of T_2 clusters in the formula for $|\Psi\rangle$ (cf. equations (88) and (89)), is only applicable to the N–N separations that do not exceed $1.75R_e$. As shown in table 5, the CR-CCSD(TQ),a method suffers from the non-variational collapse in the $R > 1.75R_e$ region. The errors in the CR-CCSD(TQ),a results are not nearly as big as the errors in the CCSD(T) or CCSD(TQ_f) calculations, but they are considerably bigger than the errors obtained in the CISDtq-corrected MMCC(2,4) calculations, in spite of the fact that the CR-CCSD(TQ),a approach also belongs to the family of the MMCC(2,4) approximations (see section 3.2.1). The CR-CCSD(TQ),a method provides significantly worse results for large N–N separations than the CR-CCSD(TQ),b approach, since variant 'a' of the CR-CCSD(TQ) theory uses the first-order MBPT estimate of T_2 in the definition of $|\Psi\rangle$ (cf. equation (88)), which in our view is not a good idea at larger internuclear separations. The CR-CCSD(TQ),b approach uses only the CCSD values of the T_2 cluster amplitudes in the definition of $|\Psi\rangle$ (cf. equation (89)) and this alone leads to considerable improvements in the description of the $R > 1.75R_e$ region by the CR-CCSD(TQ) approximation. If one decides to apply the CR-CCSD(TQ) method to a case of multiple bond breaking,

Downloaded At: 16:32 21 January 2011

our recommendation at this time is to use the CCSD values of the T_2 cluster amplitudes in the definition of $|\Psi\rangle$ (not their MBPT estimates), as is done in the CR-CCSD(TQ),b approach. The principle of using the converged CCSD values of T_1 and T_2 clusters in designing the higher-level MMCC approximations is also used in the quadratic MMCC theory and other quasi-variational MMCC methods discussed in section 3.3.

The final example in this section is the C_2 molecule, as described by the DZ basis set [47] (see figure 4). In analogy to N_2, the multiply bonded C_2 molecule is characterized by the large T_n, $n > 2$, effects, already at the equilibrium geometry. For the DZ basis set used here, the effect of T_3 clusters at $R = R_e$, as measured by the difference between the CCSDT and CCSD energies, is 18.593 millihartree. The difference between the CCSDT and full CI energies at $R = R_e$ is 2.091 millihartree, which indicates that T_4 clusters are quite important too. As in the N_2 case, all standard single-reference CC approaches, including the iterative CCSD and CCSDT methods and their perturbative CCSD(T), CCSD(TQ_f) and CCSDT(Q_f) extensions, fail to provide a correct description of the potential energy curve of C_2 [47] (see figure 4). The CCSD, CCSD(T) and full CCSDT curves have big humps for the intermediate values of R. At $R = 3R_e$, the unsigned errors in the CCSD(T), CCSD(TQ_f) and CCSDT(Q_f) energies, relative to full CI, are 96.055, 67.237 and 94.229 millihartree, respectively, when a DZ basis set is employed. The CR-CCSD(TQ),b approach reduces these large errors to 20.282 millihartree. Although in this paper we focus on the MMCC-based corrections to the CCSD energies, it may be worth mentioning that the aforementioned variant 'b' of the CR-CCSDT(Q) method reduces this error even further, to 10.052 millihartree [47]. As shown in figure 4, the CR-CCSD(TQ),b potential energy curve of C_2 is considerably better than the curves provided by all standard CC methods.

Downloaded At: 16:32 21 January 2011

Before proceeding to the next section, where we describe the examples of applications of the R-CCSD(T), CR-CCSD(T) and CR-CCSD(TQ) methods to vibrational term values of small molecules, let us point out that, in analogy to the CI-corrected MMCC approximations, one of the main reasons of the excellent performance of the CR-CCSD[T], CR-CCSD(T) and CR-CCSD(TQ) approaches is the presence of the $\langle\Psi|e^{T_1+T_2}|\Phi\rangle$ denominators in the corresponding energy expressions. Those denominators play the role of natural damping factors, which damp the corrections due to triples (in the CR-CCSD[T] and CR-CCSD(T) cases) or triples and quadruples (in the CR-CCSD(TQ) case) that are grossly overestimated by the conventional CCSD[T], CCSD(T) and CCSD(TQ_f) approaches at larger internuclear separations. For example, for the DZ model of HF, the $\langle\Psi|e^{T_1+T_2}|\Phi\rangle$ denominators $D^{[T]}$ and $D^{(T)}$, defining the CR-CCSD[T] and CR-CCSD(T) methods (cf. equations (77) and (78)), increase their values from *ca.* 1.0 at $R = R_e$ to *ca.* 2.4 at $R = 5R_e$. For the DZ model of the water molecule, the denominators $D^{[T]}$, $D^{(T)}$, $D^{(TQ),a}$ and $D^{(TQ),b}$, equations (77), (78), (93) and (94), respectively, that define the CR-CCSD[T], CR-CCSD(T), CR-CCSD(TQ),a and CR-CCSD(TQ),b methods increase their values from *ca.* 1.0 at $R = R_e$ to *ca.* 1.6 at $R = 2R_e$. For the most complicated case of the triple bond breaking in N_2, as described by the DZ basis set, the $D^{(TQ),a}$ and $D^{(TQ),b}$ denominators of the CR-CCSD(TQ),a and CR-CCSD(TQ),b theories increase their values from *ca.* 1.0 at $R = R_e$ to 7.8 and 12.9, respectively, at $R = 2.25R_e$. The increase of the value of $D^{(TQ),a}$ is not sufficient to damp the triples and quadruples corrections at larger N–N separations, which is one of the reasons why the CR-CCSD(TQ),a approximation fails to provide a very good description of

the $R > 1.75R_e$ region in N_2. The CR-CCSD(TQ),b method is much better in this regard, since the corresponding $\langle\Psi|e^{T_1+T_2}|\Phi\rangle$ denominator $D^{(TQ),b}$, equation (94), increases its value more dramatically. It should be emphasized that no such denominators are present in the standard CCSD[T], CCSD(T) and CCSD(TQ_f) energy formulae and, in consequence, the CCSD[T], CCSD(T) and CCSD(TQ_f) non-iterative corrections due to triples and quadruples overestimate the T_3 and T_4 effects, producing completely unphysical potential energy curves at larger internuclear separations.

3.2.2.2. *Vibrational term values*. An interesting way of testing the accuracy of the electronic structure methods that are aimed at the accurate description of PESs involving bond breaking is provided by calculating vibrational term values, including highly excited vibrational states near dissociation. The calculated vibrational term values can then be compared with the experimental or, in the case of diatomics, RKR [192–195] data. Since vibrational term values are very sensitive to the details of the PES, we can learn a lot about the ability of a given method to provide correct information about the PES topology by performing such calculations. This, in particular, applies to the CR-CCSD[T], CR-CCSD(T) and CR-CCSD(TQ) methods discussed in this paper.

Downloaded At: 16:32 21 January 2011

In this section, we focus on two examples of calculations of vibrational term values. The first example, taken from [46, 47], deals with the vibrational term values of the HF molecule, as described by the fairly realistic aug-cc-pVTZ basis set [169, 170] (see table 7 and figure 5(*a*)). The second example, taken from our more recent study [196], involves the vibrational term values of the F_2 molecule, also described by the aug-cc-pVTZ basis set (see table 8 and figure 5(*b*)). We begin our discussion with the results for the HF molecule.

The CCSD, CCSDT, CCSD(T), CCSD(TQ_f), CR-CCSD(T) and CR-CCSD(TQ),b potential energy curves resulting from our calculations for the aug-cc-pVTZ model of HF are shown in figure 5(*a*). We do not show the CR-CCSD(TQ),a curve, since there is practically no difference between the CR-

Table 7. Selected vibrational energies $G(v)$ (in cm^{-1}; v is the vibrational quantum number) and dissociation energies D_e (in eV) of the HF molecule as described by the aug-cc-pVTZ basis set. The RKR values (taken from [197]) represent total energies and all theoretically computed energies (taken from [46, 47]) represent errors relative to RKR. The $v = 0$ values are the zero-point energies, whereas the $v > 0$ values are the excitation energies relative to the $v = 0$ level.

v	RKR	CCSD	CCSDT	CCSD(T)	CCSD(TQ_f)	R-CCSD(T)	CR-CCSD(T)	CR-CCSD(TQ),b
0	2 051	15	−7	−7	−7	−4	−3	−6
1	6 012	52	−19	−18	−17	−9	−4	−16
2	9 802	96	−28	−25	−23	−9	−2	−22
3	13 424	144	−36	−32	−29	−9	2	−27
5	20 182	252	−54	−47	−43	−6	12	−37
10	34 363	623	−116	−136	−124	1	49	−70
11	36 738	728	−131	−175	−159	1	60	−77
12	38 955	850	−148	−232	−211	−2	72	−84
13	41 007	993	−166			−9	87	−91
15	44 576	1 370	−207			−55	123	−109
19	49 027	2 881	−325				227	−159
D_e	6.120	0.725	−0.056				0.026	0.019

Downloaded At: 16:32 21 January 2011

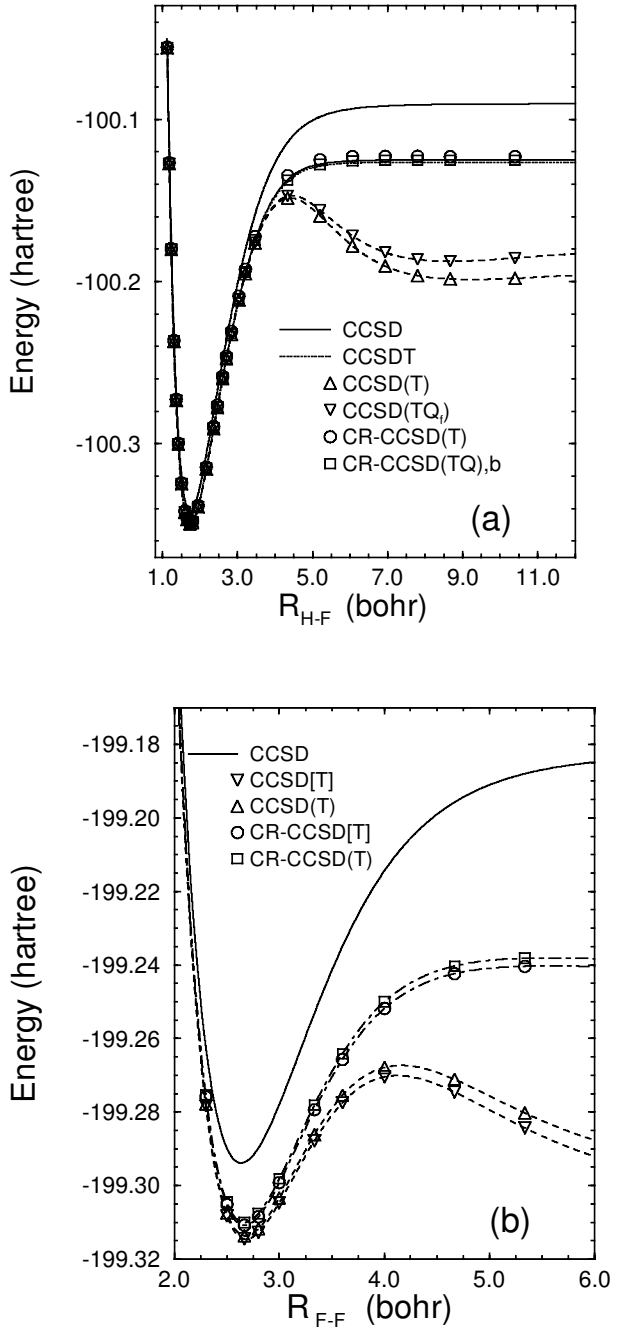

Figure 5. Potential energy curves of the (*a*) HF and (*b*) F_2 molecules obtained with the aug-cc-pVTZ basis set. The results for HF ((*a*); see [46] for the original numerical data) include a comparison of the CR-CCSD(T) and CR-CCSD(TQ),b potential energy curves (designated by ○ and □, respectively) with curves obtained in the CCSD (solid curve), CCSDT (dotted curve), CCSD(T) (△) and CCSD(TQ_f) (▽) calculations. The results for F_2 ((*b*); taken from [196]) include a comparison of the CR-CCSD[T] (○) and CR-CCSD(T) (□) potentials with potential energy curves obtained with the CCSD (solid curve), CCSD[T] (▽) and CCSD(T) (△) methods.

Table 8. Selected vibrational energies $G(v)$ (in cm^{-1}; v is the vibrational quantum number) and approximate dissociation energies D_e (in eV) of the F_2 molecule as described by the aug-cc-pVTZ basis set. The RKR values (taken from [178]) represent total energies and all theoretically computed energies (taken from [196]) represent errors relative to RKR. The $v = 0$ values are the zero-point energies, whereas the $v > 0$ values are the excitation energies relative to the $v = 0$ level.

v	RKR	CCSD	CCSD[T]	CCSD(T)	R-CCSD[T]	R-CCSD(T)	CR-CCSD[T]	CR-CCSD(T)
0	456	47	−5	−1	9	12	13	15
1	894	98	−9	−2	21	26	27	32
2	1 764	202	−20	−6	43	53	57	67
3	2 610	312	−33	−11	66	82	89	104
4	3 432	427	−48	−17	92	113	123	143
5	4 227	549	−66	−27	119	146	159	185
6	4 997	679	−88	−39	148	181	198	230
7	5 740	816	−115	−55	179	219	240	278
8	6 455	961			212	259	285	330
9	7 142	1 116			247	302	334	385
10	7 798	1 280			286	348	386	445
12	9 019	1 643			371	450	504	579
14	10 108	2 056			469	567	643	734
16	11 054	2 529			579	701	805	916
18	11 843	3 075			703	853	996	1 129
20	12 453	3 713			840	1 026	1 225	1 384
22	12 830	4 497					1 529	1 718
D_e	1.658	1.392					0.262	0.301

Downloaded At: 16:32 21 January 2011

CCSD(TQ),a and CR-CCSD(TQ),b potentials in this case. As in the case of the DZ basis set, discussed in the previous section, the CR-CCSD(T) and CR-CCSD(TQ),b (or CR-CCSD(TQ),a) methods eliminate the well-pronounced humps on the CCSD(T) and CCSD(TQ_f) curves and provide considerable improvements in the calculated dissociation energies D_e when the aug-cc-pVTZ basis set is employed. As shown in table 7, the CR-CCSD(T) and CR-CCSD(TQ),b methods reduce the 0.725 eV error in the CCSD result for D_e to 0.026 and 0.019 eV, respectively (the experimental value of D_e is 6.120 eV [177,197]). The CR-CCSD(TQ),a method provides a very similar result (a 0.023 eV error [46]). Clearly, the CCSD(T) and CCSD(TQ_f) values of D_e cannot be defined because of the presence of the humps on the CCSD(T) and CCSD(TQ_f) curves (cf. figure 5(*a*)). It is interesting to note that the CR-CCSD(T) and CR-CCSD(TQ),x (x = a, b) values of D_e are better than the D_e value resulting from the full CCSDT calculations, which give a 0.056 eV error with a considerably greater effort.

Because of the presence of the humps on the CCSD(T) and CCSD(TQ_f) potential energy curves of HF, the CCSD(T) and CCSD(TQ_f) potentials do not support bound vibrational states with $v > 12$. Moreover, errors in the CCSD(T) and CCSD(TQ_f) vibrational term values, relative to the experimental or RKR data [197], rapidly increase, from 7 cm^{-1} for $v = 0$ to more than 210 cm^{-1} for $v = 12$ (see table 7). The CCSD curve for HF has no humps and supports bound states with $v > 12$, but the CCSD method overbinds the HF molecule by more than 0.7 eV, which results in a fast increase of errors in the calculated vibrational term values, from 15 cm^{-1} for $v = 0$ to 2881 cm^{-1} for the highest experimentally observed $v = 19$ state. Although the simplest way of renormalizing the CCSD(T) method, via the R-CCSD(T) approach, does not lead to a complete elimination of the hump on the

CCSD(T) potential energy curve of HF (cf. section 3.2.2.1), the R-CCSD(T) approach provides considerable improvements in the poor CCSD results. Indeed, vibrational term values resulting from the R-CCSD(T) calculations differ from the RKR values [197] by as little as 1–9 cm^{-1} for $v \leq 13$ (the energy of the $v = 13$ level is $\sim$41 000 cm^{-1}) and, more importantly, we can use the R-CCSD(T) approach to study vibrational states with v as high as 16 (cf. table 7 and [46]). As shown in [46], similar remarks apply to other renormalized (R) methods, including the R-CCSD(TQ)-n,x ($n = 1, 2$; x = a, b) approaches discussed in section 3.2.1.

The CR-CCSD(T) and CR-CCSD(TQ),x (x = a, b) methods provide somewhat worse vibrational term values, when compared with the R-CCSD(T) and R-CCSD(TQ)-n,x vibrational energy levels with $v \leq 15$, but, on the other hand, we can calculate the entire vibrational spectrum of the HF molecule, including the highest experimentally observed $v = 19$ state, with these approaches. Most importantly, the CR-CCSD(T) and CR-CCSD(TQ),x (x = a, b) methods enable us to obtain a highly accurate and well-balanced description of the vibrational spectrum of HF with the ease of use characterizing standard methods of the CCSD(T) type. With an exception of a few low-lying states resulting from the CR-CCSD(T) calculations, the small, a few cm^{-1}, errors in the CR-CCSD(T) and CR-CCSD(TQ),x results for the $v = 0$ level systematically increase with v, without ever exceeding 230 cm^{-1}, when the aug-cc-pVTZ basis set is employed. The CR-CCSD(T) method reduces the 2881 cm^{-1} and 325 cm^{-1} errors in the CCSD and full CCSDT results, respectively, for the $v = 19$ state of HF (the energy of this highest observed state is 49 027 cm^{-1}) to 227 cm^{-1} (see table 7). The CR-CCSD(TQ),b approach provides further improvements in the overall description of the vibrational spectrum of HF, reducing the error in the results for the $v = 19$ state to 159 cm^{-1}. The CR-CCSD(TQ),a method gives a 135 cm^{-1} error for this state [46]. Interestingly enough, the CR-CCSD(TQ),b potential predicts the existence of the $v = 20$ energy level to be located 28 cm^{-1} below the corresponding dissociation limit. The most accurate potential function for HF to date, obtained using the hybrid RKR-based theoretical approach (RKR plus improved long-range plus very accurate and expensive *ab initio* calculations), produces the $v = 20$ level with an energy of 23 cm^{-1} below the dissociation limit [198, 199]. Clearly, none of the existing *ab initio* approaches can provide the results of similar quality with the ease of use characterizing the CR-CCSD(T) and CR-CCSD(TQ),x methods. For example, it would not be easy to obtain the results of this high quality with the MRCI approaches, which are a lot more demanding and a lot more complicated.

The HF molecule is characterized by a large binding energy and large non-dynamic correlation effects at large H–F separations, but there are many examples of singly bonded molecules which are more challenging than HF. The F_2 molecule is one of them. The F_2 molecule is known to be a relatively weakly bound system ($D_e = 1.658$ eV [177, 178]), which can be characterized by a large degree of non-dynamic correlation and big T_3 contributions for the relatively small stretches of the F–F bond. In spite of its single-bond character, F_2 creates severe problems for many *ab initio* approaches. For example, the F_2 molecule is not bound in the UHF description and, as pointed out in the previous section, the CCSD approach employing the RHF reference overbinds it by a factor close to 2 (see figure 5(*b*) and table 8). In consequence, the vibrational term values of F_2 resulting from the CCSD calculations are very poor, even for states with the small values of the vibrational quantum number v. This can be seen in table 8, which shows that errors

Downloaded At: 16:32 21 January 2011

in the CCSD results for the vibrational term values of F_2 obtained with the aug-cc-pVTZ basis set, relative to the RKR values reported in [178], rapidly increase with v, from 47 cm^{-1} for $v = 0$ to 549 cm^{-1} for $v = 5$, to 1280 cm^{-1} for $v = 10$ and to 4497 cm^{-1} for the highest experimentally observed $v = 22$ level, whose exact energy of 12 830 cm^{-1} is very close to the dissociation energy D_0, estimated by Colbourn *et al.* as 12 920 $\pm$ 50 cm^{-1} [178]. The standard CCSD[T] and CCSD(T) methods reduce the large errors in the CCSD results to a few cm^{-1} for $v = 0$ and 66 and 27 cm^{-1}, respectively, for $v = 5$ (cf. table 8), but states with $v > 7$ cannot be determined in any meaningful manner using the CCSD[T] and CCSD(T) potentials owing to the presence of the well-pronounced humps on the CCSD[T] and CCSD(T) potential energy curves (see figure 5(*b*)). It is, therefore, worthwhile to examine the performance of the CR-CCSD(T) and similar methods in calculations of vibrational term values using F_2 as an example.

The R-CCSD[T], R-CCSD(T), CR-CCSD[T] and CR-CCSD(T) results for the vibrational term values and dissociation energy D_e of the F_2 molecule, as described by the aug-cc-pVTZ basis set, are shown in table 8. The CR-CCSD[T] and CR-CCSD(T) potential energy curves are shown in figure 5(*b*). Those results are taken from our recent work [196], where we used the highly efficient computer codes [158] incorporated in the GAMESS package [159]. We have not yet performed the CR-CCSD(TQ),x (x = a, b) calculations for F_2 with larger basis sets, such as aug-cc-pVTZ, since our pilot CR-CCSD(TQ),x codes are too inefficient for the large-scale calculations of this type. Thus, in this discussion we focus on the R-CCSD[T], R-CCSD(T), CR-CCSD[T] and CR-CCSD(T) results.

Downloaded At: 16:32 21 January 2011

As shown in table 8, the CR-CCSD[T] and CR-CCSD(T) methods provide considerable improvements in the calculated vibrational term values. The 47, 549, 1280 and 4497 cm^{-1} errors in the CCSD results for the $v = 0$, $v = 5$, $v = 10$ and $v = 22$ states of F_2 decrease to 13, 159, 386 and 1529 cm^{-1}, respectively, when the CR-CCSD[T] method is employed. The CR-CCSD(T) approach provides equally remarkable improvements (see table 8). On average, the CR-CCSD[T] and CR-CCSD(T) methods reduce the large errors in the CCSD results for the vibrational term values of F_2 by a factor of 3. Significant improvements in the results offered by the CR-CCSD[T] and CR-CCSD(T) approaches are mainly a consequence of the considerably better description of the intermediately stretched and asymptotic regions of the F_2 potential energy curve by the CR-CCSD[T] and CR-CCSD(T) methods (see figure 5(*b*)). Indeed, the CR-CCSD[T] and CR-CCSD(T) approaches reduce the 1.4 eV error in the CCSD value of the dissociation energy D_e to $\sim$0.3 eV (see table 8). On the basis of our experiences with the CR-CCSD(TQ),x (x = a, b) methods, including the CR-CCSD(TQ),x calculations for a DZ model of F_2 discussed in section 3.2.2.1, we would expect that further improvements in the results should be obtained with the CR-CCSD(TQ),x approaches. We will verify the validity of this statement once our CR-CCSD(TQ),x codes are more efficient.

The CR-CCSD[T] and CR-CCSD(T) results for the low-lying states are somewhat worse than those provided by the standard CCSD[T] and CCSD(T) methods, but we must keep in mind that the standard CCSD[T] and CCSD(T) approaches produce unphysical shapes of the potential energy curve of F_2, which do not allow us to determine the vibrational term values with $v > 7$. As a matter of fact, the R-CCSD[T] and R-CCSD(T) results are also better than the CR-CCSD[T] and CR-CCSD(T) results, but, again, the R-CCSD[T] and R-CCSD(T) approaches do not eliminate the humps on the CCSD[T] and CCSD(T) potentials as effectively as the

CR-CCSD[T] and CR-CCSD(T) approaches [196], so that we cannot obtain any meaningful information about the highest experimentally observed $v = 22$ level using the R-CCSD[T] and R-CCSD(T) methods (cf. table 8). On the other hand, the R-CCSD[T] and R-CCSD(T) methods, which differ from the standard CCSD[T] and CCSD(T) approaches only by the presence of the $D^{[T]} = \langle \Psi^{CCSD[T]} | e^{T_1+T_2} | \Phi \rangle$ and $D^{(T)} = \langle \Psi^{CCSD(T)} | e^{T_1+T_2} | \Phi \rangle$ denominators in the corresponding energy expressions (cf. equations (67) or (71) and (68) or (72) with equations (81) and (82)), provide great improvements in the CCSD results. For example, the R-CCSD[T] method reduces the 47, 549, 1280 and 3713 cm^{-1} errors in the CCSD results for the $v = 0$, $v = 5$, $v = 10$ and $v = 20$ states of F_2 to 9, 119, 286 and 840 cm^{-1}, respectively (see table 8). The R-CCSD[T] and R-CCSD(T) methods reduce the well-pronounced humps on the CCSD[T] and CCSD(T) curves so much that we can even obtain some information about the high-lying $v = 20$ state with the R-CCSD[T] and R-CCSD(T) approaches. Although in principle we do not recommend using the R-CCSD[T] and R-CCSD(T) methods (the CR-CCSD[T] and CR-CCSD(T) approaches are significantly better in the asymptotic region), our calculations of the vibrational term values for the HF and F_2 molecules show that the R-CCSD[T] and R-CCSD(T) approaches may represent a viable alternative in calculations of molecular PESs as long as we are only interested in the moderate stretches of single chemical bonds.

Downloaded At: 16:32 21 January 2011

3.2.2.3. *The renormalized and completely renormalized CCSD(T) calculations of potential energy surfaces for exchange chemical reactions: a comparison of the CCSD, CCSD(T), R-CCSD(T), CR-CCSD(T) and full CI or MRCI results for the collinear BeFH system.* One of the main goals of the research described in this paper is the development of the simple and yet very accurate 'black-box' CC methods that could be routinely used to calculate the entire molecular PESs or large portions of those for chemical reactions. All of the examples described in the previous two sections have dealt with various types of unimolecular dissociation. However, none of the examples discussed in sections 3.2.2.1 and 3.2.2.2 has included the calculation of the entire PES for an exchange chemical reaction of the $A + BC \rightarrow AB + C$ type, where the B–C bond is broken and the A–B bond is formed. A non-trivial application of the R-CCSD(T) and CR-CCSD(T) methods to an exchange chemical reaction is discussed in this section.

An example included in this section involves a prototypical case of the $Be + HF \rightarrow BeF + H$ reaction, which has been studied by several authors using many theoretical techniques, ranging from the *ab initio* [200–202], density-functional [202] and diatomics-in-molecules [203–205] calculations of the ground-state PES to fitting the PES to various functional forms [200, 201, 206–208] and dynamical calculations [200, 207]. In the absence of the independent experimental results for the $Be + HF \rightarrow BeF + H$ reaction that would enable us to evaluate critically the accuracy of the existing theoretical PESs, we performed two sets of calculations. In the first set of calculations, reported in [49], we compared the PESs resulting from the R-CCSD(T) and CR-CCSD(T) calculations with the exact PES obtained with the full CI approach. In this case, we used a small basis set MIDI [209], consisting only of 14 contracted Gaussian functions, so that we could perform full CI calculations for a large number of nuclear geometries representing the ground-state PES of the BeFH system. In the second set of calculations, whose details will be reported elsewhere [210], we compared the R-CCSD(T) and CR-CCSD(T) PESs with the PES obtained using the internally contracted MRCI(Q) approach [180, 181]

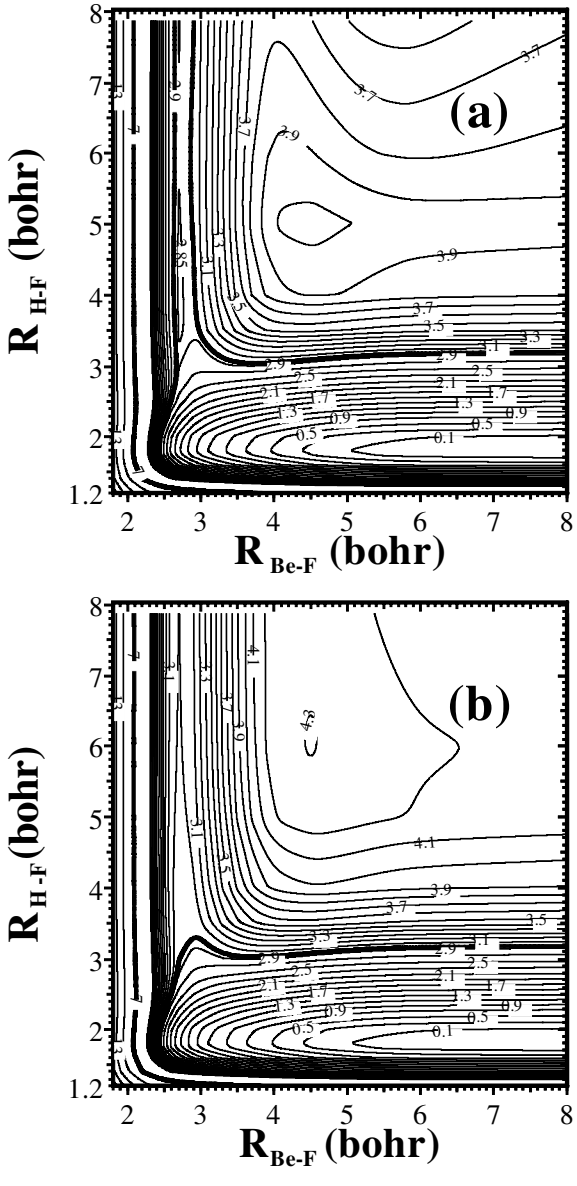

Downloaded At: 16:32 21 January 2011

Figure 6. Contour plots of the ground-state PESs of the collinear BeFH system obtained in the (*a*) CCSD(T), (*b*) R-CCSD(T), (*c*) CR-CCSD(T) and (*d*) full CI calculations with the MIDI basis set (based on the numerical data reported in [49]). The Be–F and H–F distances, $R_{Be\text{-}F}$ and $R_{H\text{-}F}$, respectively, are in bohr. In each case, the energies E are reported in eV relative to the energy of the Be + HF reactants, defined by the nuclear geometry $R_{Be\text{-}F} = 8.0$ bohr and $R_{H\text{-}F} = 1.7325$ bohr. The thick contour line corresponding to $E = 2.9$ eV separates the region where the contour spacing is 0.2 eV from the region where the contour spacing is 0.1 eV. The thick contour line corresponding to $E = 7.0$ eV separates the high-energy part of the PES where the contour spacing is 3 eV from the region where the contour spacing is 0.1 eV. An extra contour line corresponding to $E = 2.85$ eV has been added to emphasize the presence of an artificial barrier and exaggerated potential well in the product valley on the CCSD(T) PES (and absence of those features on the R-CCSD(T), CR-CCSD(T) and full CI PESs).

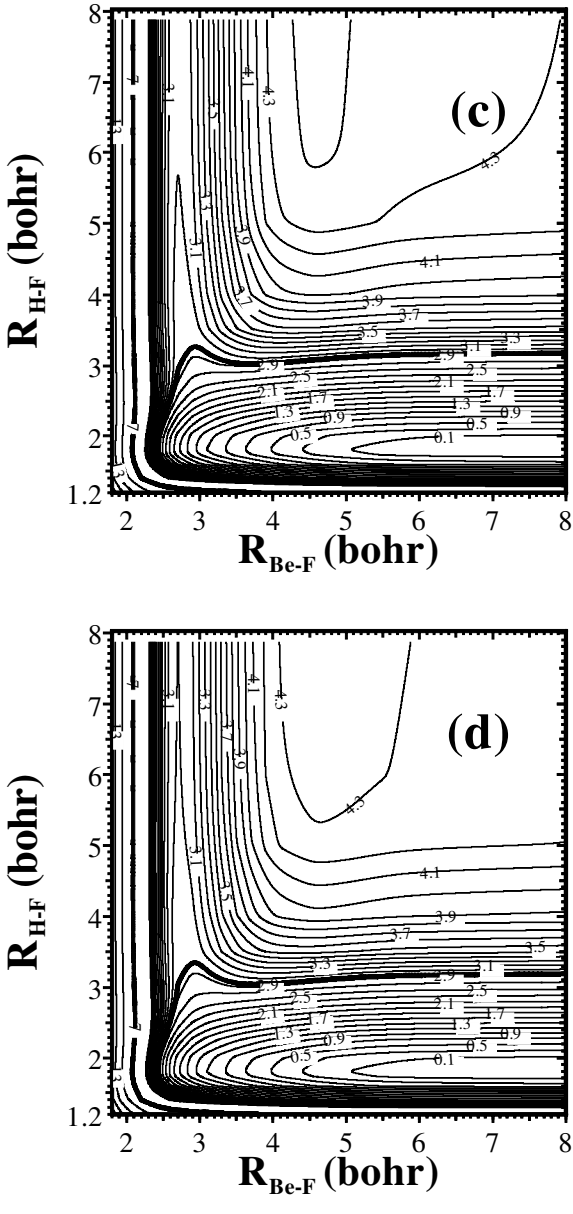

Figure 6(*c*) and 6(*d*).

Downloaded At: 16:32 21 January 2011

employing CASSCF reference, as implemented in MOLPRO [179]. In this case, we used a considerably larger cc-pVTZ basis set [169], consisting of 85 contracted Gaussian functions. As is usually done, the core orbital correlating with the 1s shell of the F atom was frozen in all of the above calculations.

In view of the methodological nature of this review, in this section we focus on the results for the collinear arrangement of the Be, F and H atoms, with the Be atom approaching the HF molecule from the fluorine side. A more complete discussion of

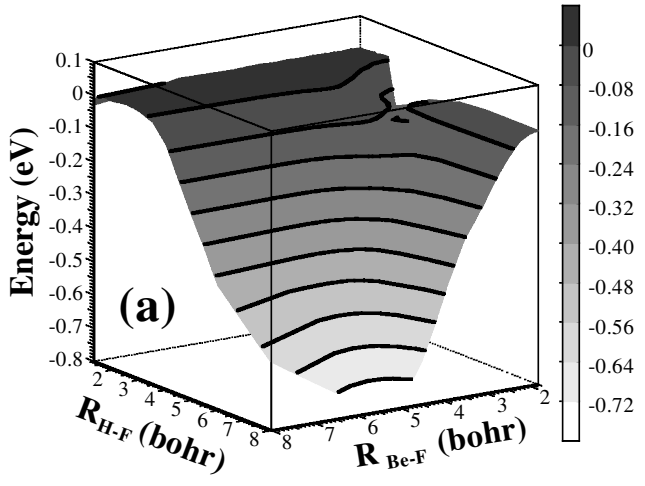

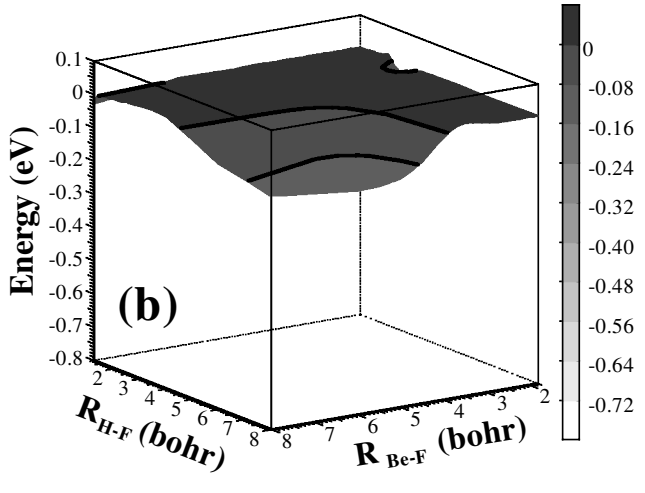

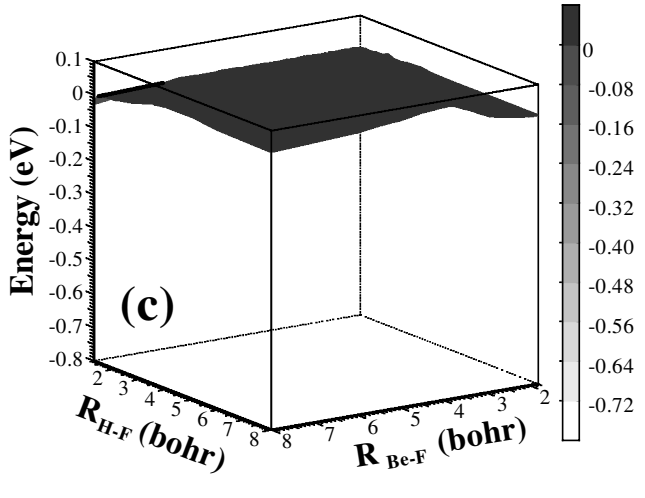

Downloaded At: 16:32 21 January 2011

the ground-state PES of the BeFH system, including several values of the Be–F–H angle, the process of insertion of the Be atom into the H–F bond, and the case of the Be atom approaching HF from the H side, will be presented elsewhere [210].

For the collinear arrangement of the Be, F and H atoms, the ground electronic state of the BeFH system is a $^1\Sigma^+$ state correlating with the $Be(2s^2\ ^1S)+HF(X\ ^1\Sigma^+)$ state of reactants, the $BeF(X\ ^2\Sigma^+)+H(1s^1\ ^2S)$ state of products and the $Be(2s^2\ ^1S)+F(2p^5\ ^2P)+H(1s^1\ ^2S)$ state of non-interacting atoms. The $Be(2s^2\ ^1S)+HF(X\ ^1\Sigma^+)$ reactants are reasonably well approximated by the ground-state RHF configuration $1\sigma^2 2\sigma^2 3\sigma^2 4\sigma^2 1\pi^4 5\sigma^2$, so that basically all RHF-based CC methods are capable of providing accurate results in this region. The situation dramatically changes when the $BeF(X\ ^2\Sigma^+)+H(1s^1\ ^2S)$ product channel and the non-interacting atom limit are examined. In those two cases, the ground-state RHF configuration is a very poor reference for the correlated calculations. In consequence, the standard RHF-based CC methods completely fail in the BeF + H and Be + F + H regions.

Normally, the BeF + H product channel, corresponding to the breaking of the H–F bond and making of the Be–F bond, requires a genuinely multireference description involving, among other configurations, the RHF ground state $1\sigma^2 2\sigma^2 3\sigma^2 4\sigma^2 1\pi^4 5\sigma^2$, the doubly excited configuration $1\sigma^2 2\sigma^2 3\sigma^2 4\sigma^2 1\pi^4 6\sigma^2$ and the singly excited configuration of the $1\sigma^2 2\sigma^2 3\sigma^2 4\sigma^2 1\pi^4 5\sigma^1 6\sigma^1$ type. Similar remarks apply to the Be + F + H region, which corresponds to a simultaneous breaking of the H–F and Be–F bonds. In this case, which is even more challenging for the standard single-reference CC methods, the ground-state wavefunction of the BeFH system is a mixture of several configurations, including the RHF configuration $1\sigma^2 2\sigma^2 3\sigma^2 1\pi^4 4\sigma^2 5\sigma^2$, the singly excited $1\sigma^2 2\sigma^2 3\sigma^2 1\pi^4 4\sigma^1 5\sigma^2 6\sigma^1$ configuration and three doubly excited configurations, namely $1\sigma^2 2\sigma^2 3\sigma^2 1\pi^4 4\sigma^2 6\sigma^2$, $1\sigma^2 2\sigma^2 3\sigma^2 1\pi^4 4\sigma^1 5\sigma^1 6\sigma^2$ and $1\sigma^2 2\sigma^2 3\sigma^2 1\pi^4 5\sigma^2 6\sigma^2$. In general, in order to obtain a uniformly accurate zero-order description of the ground-state PES of the BeFH system, including the aforementioned BeF + H and Be + F + H regions and other product channels, such as BeH + F, we must use a CASSCF-based multireference formalism involving at least eight active electrons and at least eight active orbitals correlating with the 2s and 2p shells of the Be atom (cf., for example, the well-known problem of the 2s–2p orbital quasi-degeneracy in Be), the 2p shell of the F atom and the 1s shell of the H atom. This is exactly what we did in our MRCI(Q) calculations with the cc-pVTZ basis set employing the CASSCF reference [210]. It is interesting to examine how this genuine multireference description of the ground-state PES of BeFH compares with the results of the much simpler, single-reference, RHF-based, R-CCSD(T) and CR-CCSD(T) calculations.

The results of our calculations for the collinear BeFH system are shown in figures 6 and 7 and table 9 (calculations with the MIDI basis set) and in figures 8 and 9 and table 10 (calculations with the cc-pVTZ basis set). In both cases, we used the following basic grid of 345 nuclear geometries, obtained by combining 23 Be–F distances $R_{Be\text{-}F}$ with the 15 H–F distances $R_{H\text{-}F}$, to represent the ground-state PES

Figure 7. The dependence of the differences between the (*a*) CCSD(T), (*b*) R-CCSD(T) and (*c*) CR-CCSD(T) energies and the full CI energies (in eV) for the collinear BeFH system, as described by the MIDI basis set, on the H–F and Be–F internuclear separations, $R_{H\text{-}F}$ and $R_{Be\text{-}F}$, respectively, (in bohr). For the original numerical data, see [49].

Downloaded At: 16:32 21 January 2011

of BeFH: $R_{Be-F} = 1.8$, 1.9, 2.0, 2.2, 2.4, 2.5, 2.5719, 2.6, 2.7, 2.9, 3.1, 3.3, 3.5, 3.7, 3.9, 4.1, 4.5, 4.7, 5.0, 5.2, 5.5, 6.0 and 8.0 bohr; $R_{H-F} = 1.2$, 1.4, 1.6, 1.7325, 1.8, 2.0, 2.25, 2.5, 2.75, 3.0, 3.5, 4.0, 5.0, 6.0 and 8.0 bohr. The presence of the equilibrium bond lengths for BeF ($R_{Be-F} = 2.5719$ bohr) and HF ($R_{H-F} = 1.7325$ bohr) among the values of R_{Be-F} and R_{H-F} should be noted. Additional points were considered whenever we wanted to obtain a more detailed information about a given region of the PES (e.g. the saddle-point region). The reader is referred to the original work [49, 210] for further details.

Let us begin our discussion with the results obtained with the MIDI basis set. A comparison of the CCSD(T) contour plot in figure 6(*a*) and the full CI contour plot in figure 6(*d*) immediately shows that the RHF-based CCSD(T) approach provides a PES which has a completely wrong topology. The differences between the CCSD(T) and full CI PESs are particularly large when both the Be–F and the H–F bonds are stretched. Those differences are greater than 10 millihartree (0.272 eV) in the entire $R_{Be-F} \geq 3.9$ bohr and $R_{H-F} \geq 6.0$ bohr region and for $R_{Be-F} \geq 3.3$ bohr and $R_{H-F} = 8.0$ bohr. They are greater than 5 millihartree (0.136 eV) in the $R_{Be-F} > 3.0$ bohr and $R_{H-F} \geq 5.0$ bohr region and for $R_{Be-F} = 1.8$–2.0 bohr and $R_{H-F} = 2.75$–3.0 bohr. As shown in figure 7(*a*), the PES obtained in the CCSD(T) calculations can be characterized by a highly non-uniform distribution of errors, with the relatively small differences between the CCSD(T) and full CI energies observed at smaller Be–F and H–F distances and larger differences between the CCSD(T) and full CI energies in the region defined by larger R_{Be-F} and R_{H-F} values. The PES obtained in the CCSD calculations is also characterized by large errors relative to full CI. For example, the differences between the CCSD and full CI energies are greater than 10 millihartree (0.272 eV) in the entire $R_{Be-F} \geq 3.3$ bohr and $R_{H-F} \geq 5.0$ bohr region. The only essential difference between the CCSD and CCSD(T) PESs is the fact that the PES obtained in the CCSD calculations is located above the exact, full CI, PES, whereas the CCSD(T) PES is, in its most part, located below the full CI PES. Otherwise, we can regard the CCSD and CCSD(T) PESs as equally poor. For example (cf. table 9), the maximum error in the CCSD results, relative to full CI, is 16.287 millihartree (0.443 eV; at $R_{Be-F} = 3.9$ bohr and $R_{H-F} = 8.0$ bohr). The maximum error in the CCSD(T) results is 28.605 millihartree (0.778 eV; at $R_{Be-F} = 5.5$ bohr and $R_{H-F} = 8.0$ bohr).

The CR-CCSD(T) method reduces the above maximum errors in the CCSD and CCSD(T) results to 3.122 millihartree (0.085 eV). As a matter of fact, there are only four geometries in our basic grid, for which the differences between the CR-CCSD(T) and full CI energies are between 3.0 and 3.1 millihartree. The 2–3 millihartree differences between the CR-CCSD(T) and full CI energies are observed only for $R_{Be-F} \geq 3.3$ bohr and $R_{H-F} \geq 4.0$ bohr. For the vast majority of the remaining nuclear geometries, the errors in the CR-CCSD(T) results are $\sim$1 millihartree ($\sim$0.027 eV) or smaller. As can be seen from figure 7(*c*), the PES obtained in the CR-CCSD(T) calculations is located slightly (usually, $\sim$1–2 millihartree or $\sim$0.027–0.054 eV) above the full CI PES and both PESs are virtually parallel to each other.

As shown in table 9, the stretching of the H–F bond has a much larger effect on the results of the standard CCSD and CCSD(T) calculations than the stretching of the Be–F bond. For example, when we stretch the H–F bond to 3.0–5.0 bohr and consider all Be–F separations, including $R_{Be-F} = 8.0$ bohr, the errors in the CCSD and CCSD(T) results are 13.163 and 9.690 millihartree (0.358 and 0.264 eV),

Downloaded At: 16:32 21 January 2011

respectively. When we stretch the Be–F bond to 3.1–5.0 bohr and consider all H–F separations, the errors in the CCSD and CCSD(T) results are much larger (16.287 and 27.887 millihartree or 0.443 and 0.759 eV, respectively). As shown in table 9, the CR-CCSD(T) method is a lot more robust in this regard. The errors in the CR-CCSD(T) results remain very small (< 0.085 eV) independent of the region of PES under consideration.

A direct comparison of figures 6(*c*) and 6(*d*) shows that the CR-CCSD(T) PES is virtually identical to the exact, full CI, PES, which makes the CR-CCSD(T) method an attractive new alternative for calculating PESs for exchange reactions involving the rearrangements of single chemical bonds. In particular, the CR-CCSD(T) approach eliminates an artificial maximum on the CCSD(T) PES at $R_{Be\text{-}F} \approx 4.5$ bohr and $R_{H\text{-}F} \approx 5.0$ bohr (cf. the contour line of 4.0 eV in figure 6(*a*)), which is a two-dimensional analogue of humps on the CCSD(T) potential energy curves describing unimolecular dissociations (cf. sections 3.2.2.1 and 3.2.2.2). In addition, the CCSD(T) PES allows for a formation of the BeF + H products at significantly lower energies than the full CI PES (cf. the thick contour lines corresponding to the energy of 2.9 eV in figures 6(*a*) and 6(*d*)). The product valley on the PES generated with the CR-CCSD(T) PES is shaped in almost exactly the same way as the product valley of the full CI PES (cf. the thick and thin contour lines corresponding to 2.9 and 3.0 eV, respectively, in figures 6(*c*) and 6(*d*)). The CCSD(T) method produces a well-pronounced saddle point on the PES for the collinear BeFH system (at $R_{Be\text{-}F} \approx 2.8$ bohr and $R_{H\text{-}F} \approx 3.5$ bohr; cf. figure 6(*a*)), which is not present on the exact, full CI, and CR-CCSD(T) PESs (cf. figures 6(*c*) and 6(*d*)). The absence of the saddle point on the full CI and CR-CCSD(T) PESs shown in figures 6(*c*) and 6(*d*) is a consequence of using a MIDI basis set, which is too small to provide a realistic representation of the transition state region (cf. [200–202]). This problem is remedied when the cc-pVTZ basis set is employed (cf. the discussion below).

Downloaded At: 16:32 21 January 2011

Interestingly enough, even the simple R-CCSD(T) approach provides a great deal of improvement in the poor description of PES offered by the CCSD and CCSD(T) methods. For example, the maximum error in the R-CCSD(T) results, relative to full CI, is 4.594 millihartree (0.125 eV), which should be compared with the 28.605 millihartree (0.778 eV) maximum error in the CCSD(T) results. The R-CCSD(T) method is somewhat more accurate than the CR-CCSD(T) approach (by 0.3–0.6 millihartree) when the internuclear distance in one of the two diatomics, HF or BeF, is close to the corresponding equilibrium bond length. The situation is reversed when we explore the entire PES, including regions where the H–F and Be–F bonds are stretched. We must, of course, keep in mind that the R-CCSD(T) approach ultimately breaks down when both H–F and Be–F distances become large (see figures 6(*b*) and 7(*b*)). As shown in figure 6(*b*), the R-CCSD(T) method does not completely eliminate an artificial maximum on the CCSD(T) PES at $R_{Be\text{-}F} \approx 4.5$ bohr and $R_{H\text{-}F} \approx 5.0$ bohr. Although there is a considerable improvement in the description of this region by the R-CCSD(T) approach, the CR-CCSD(T) approximation is much better in this regard, producing the PES whose topology is essentially identical to the topology of the exact, full CI, PES in all regions.

The calculations with the small basis set, such as MIDI, for which the exact, full CI results are available, provide great insights into the performance of new methods, but obviously, in practice, we use much larger basis sets. Typically, the most accurate PESs for chemical reactions that can be used in quantum or classical dynamical

Downloaded At: 16:32 21 January 2011

Table 9. Maximum values of the absolute errors in the CCSD, CCSD(T), R-CCSD(T) and CR-CCSD(T) energies, relative to the exact, full CI energies, for the ground-state PES of the collinear BeFH system, as described by the MIDI basis set. The errors are given in millihartree and (the values between parentheses) eV. The $R_{Be\text{-}F}$ and $R_{H\text{-}F}$ values are in bohr. The results are taken from [49].

		Maximum absolute error					
Method	All geometries	$R_{Be\text{-}F} \leq 3.1$	$3.1 < R_{Be\text{-}F} \leq 5.0$	$5.0 < R_{Be\text{-}F}$	$R_{H\text{-}F} \leq 3.0$	$3.0 < R_{H\text{-}F} \leq 5.0$	$5.0 < R_{H\text{-}F}$
CCSD	16.287 (0.443)	10.185 (0.277)	16.287 (0.443)	13.098 (0.356)	7.296 (0.199)	13.163 (0.358)	16.287 (0.443)
CCSD(T)	28.605 (0.778)	8.667 (0.236)	27.887 (0.759)	28.605 (0.778)	7.489 (0.204)	9.690 (0.264)	28.605 (0.778)
R-CCSD(T)	4.594 (0.125)	1.029 (0.028)	4.040 (0.110)	4.594 (0.125)	1.032 (0.028)	1.496 (0.041)	4.594 (0.125)
CR-CCSD(T)	3.122 (0.085)	1.645 (0.045)	3.122 (0.085)	2.436 (0.066)	1.323 (0.036)	2.995 (0.081)	3.122 (0.085)

Downloaded At: 16:32 21 January 2011

Table 10. Maximum values of the absolute errors in the CCSD, CCSD(T), R-CCSD(T) and CR-CCSD(T) energies, relative to the results of the MRCI(Q) calculations, for the ground-state PES of the collinear BeFH system, as described by the cc-pVTZ basis set. The errors are given in millihartree and (the values between parentheses) eV. The $R_{Be\text{-}F}$ and $R_{H\text{-}F}$ values are in bohr.

		Maximum absolute error					
Method	All geometries	$R_{Be\text{-}F} \leq 3.1$	$3.1 < R_{Be\text{-}F} \leq 5.0$	$5.0 < R_{Be\text{-}F}$	$R_{H\text{-}F} \leq 3.0$	$3.0 < R_{H\text{-}F} \leq 5.0$	$5.0 < R_{H\text{-}F}$
CCSD	41.782 (1.137)	23.541 (0.641)	28.168 (0.766)	41.782 (1.137)	23.541 (0.641)	31.005 (0.844)	41.782 (1.137)
CCSD(T)	120.140 (3.269)	17.161 (0.467)	23.101 (0.629)	120.140 (3.269)	16.229 (0.442)	29.183 (0.794)	120.140 (3.269)
R-CCSD(T)	19.516 (0.531)	5.384 (0.147)	5.801 (0.158)	19.516 (0.531)	4.938 (0.134)	4.929 (0.134)	19.516 (0.531)
CR-CCSD(T)	6.604 (0.180)	6.354 (0.173)	6.604 (0.180)	5.480 (0.149)	6.354 (0.173)	5.819 (0.158)	6.604 (0.180)

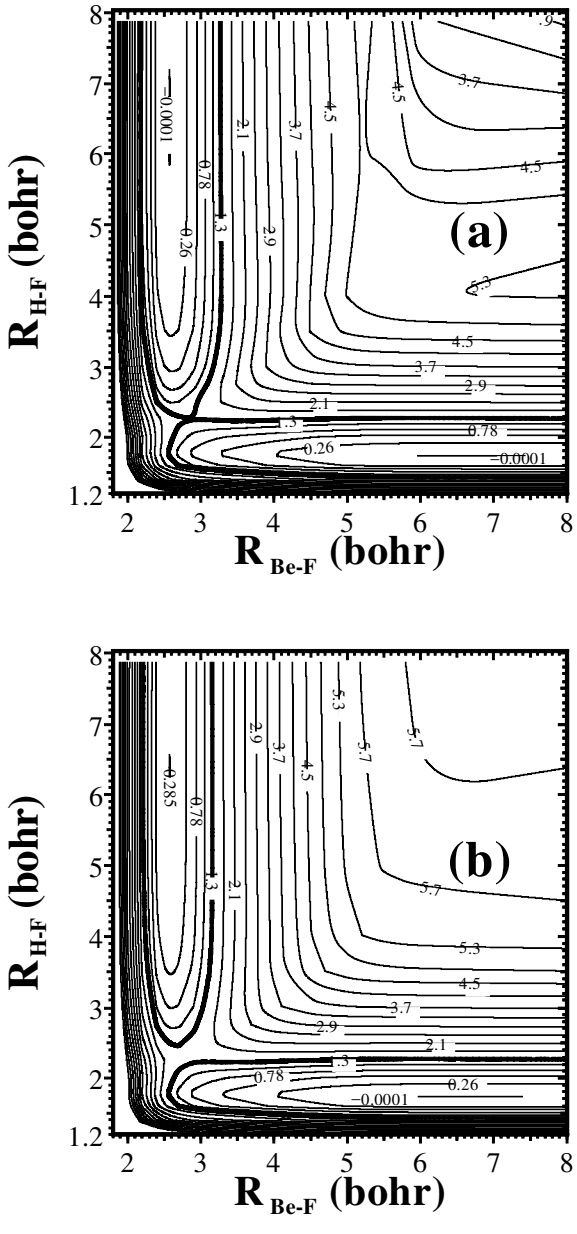

Figure 8. Contour plots of the ground-state PESs of the collinear BeFH system obtained in the (*a*) CCSD(T), (*b*) R-CCSD(T), (*c*) CR-CCSD(T) and (*d*) MRCI(Q) calculations with the cc-pVTZ basis set (this work; the details of these calculations and many additional calculations for several values of the Be–F–H angle will be reported elsewhere [210]). The Be–F and H–F distances, $R_{Be\text{-}F}$ and $R_{H\text{-}F}$, respectively, are in bohr. In each case, the energies E are reported in eV relative to the energy of the Be + HF reactants, defined by the nuclear geometry $R_{Be\text{-}F} = 8.0$ bohr and $R_{H\text{-}F} = 1.7325$ bohr. The thick contour line corresponding to $E = 1.3$ eV separates the region where the contour spacing is 0.26 eV from the region where the contour spacing is 0.4 eV. A few extra contour lines corresponding to $E = -0.0001$ eV (in (*a*)–(*d*)), 0.13 eV (in (*d*)), 0.285 eV (in (*b*)) and 0.3 eV (in (*c*)) have been added to indicate the presence of the potential wells in the reactant and product valleys.

Downloaded At: 16:32 21 January 2011

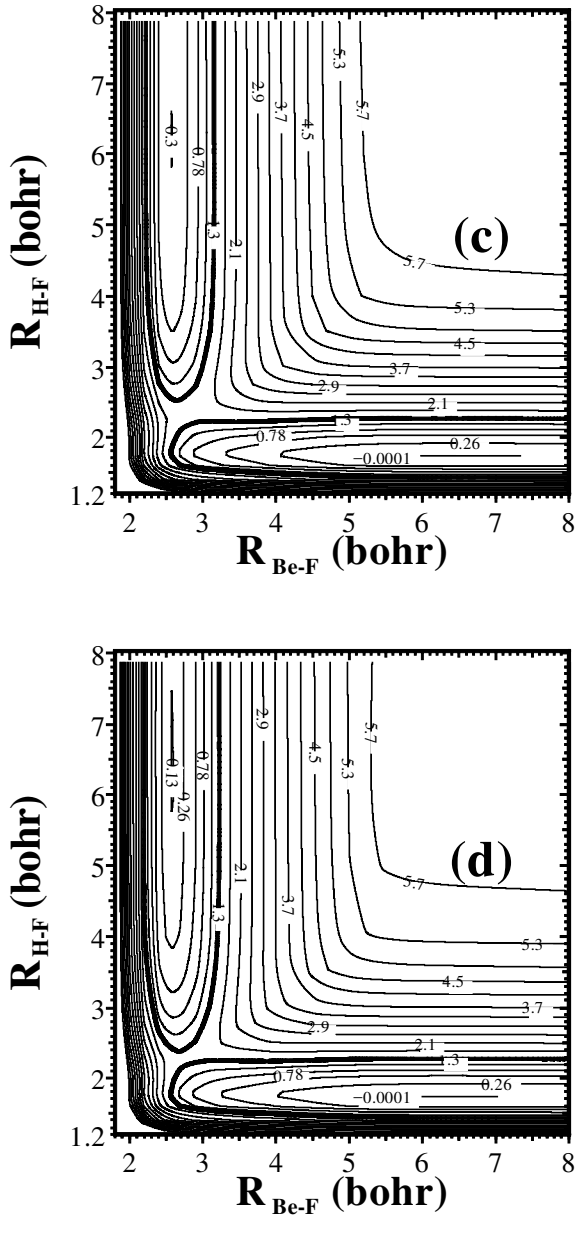

Figure 8(*c*) and 8(*d*).

simulations are generated with the MRCI method employing CASSCF orbitals and corrected for the effect of higher-than-doubly excited configurations from the multidimensional reference space by the quasi-degenerate Davidson corrections [164, 211–214]. We performed such calculations for the collinear BeFH system, using the cc-pVTZ basis set and the MRCI(Q) method of Knowles and Werner [180,181], as implemented in MOLPRO [179]. The details of these calculations and many additional calculations for several values of the Be–F–H angle will be reported

Downloaded At: 16:32 21 January 2011

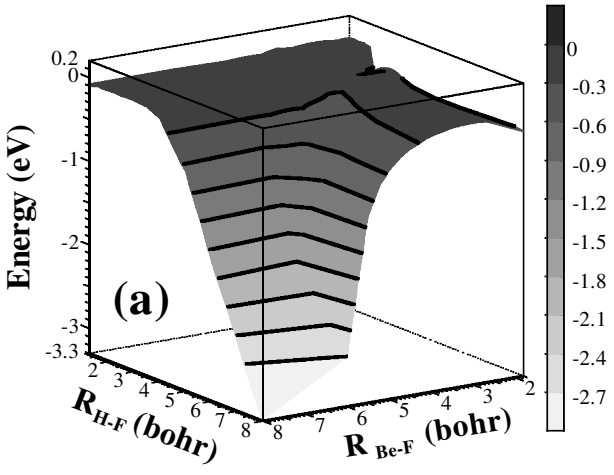

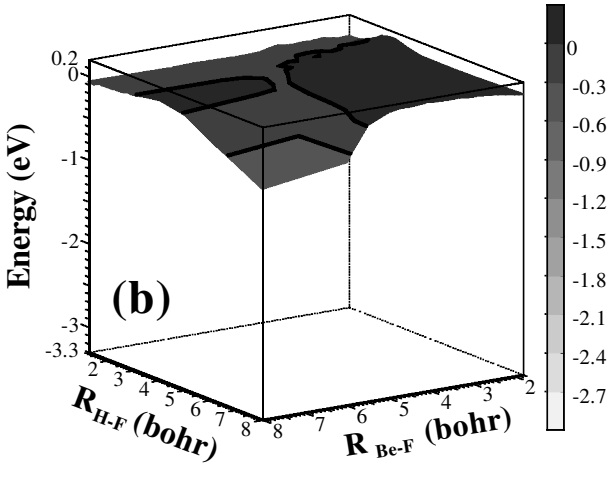

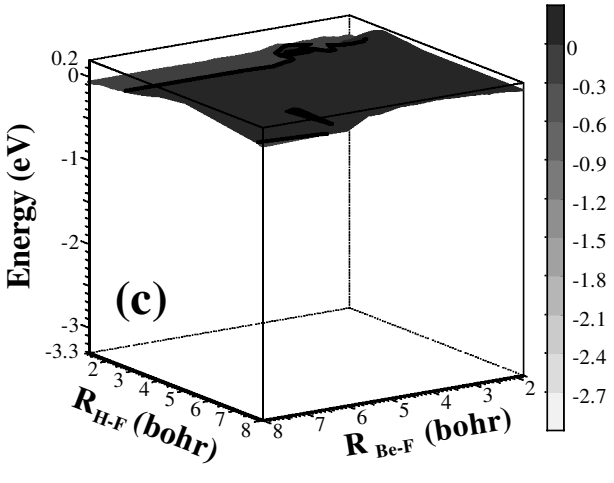

Downloaded At: 16:32 21 January 2011

elsewhere [210]. As mentioned earlier, eight electrons and eight valence orbitals were considered as active in those CASSCF-based MRCI(Q) calculations. It is interesting to examine whether the performance of the CR-CCSD(T) method in the calculations with the larger cc-pVTZ basis set is as good as it was in the calculations with the small MIDI basis set. Ideally, we would like to be able to obtain the PESs of the MRCI(Q) or similar quality with the ease of use of the CR-CCSD(T) approximation.

A comparison of the CCSD(T), R-CCSD(T), CR-CCSD(T) and MRCI(Q) PESs, shown in figures 8(*a*)–8(*d*), respectively, and a comparison of the errors in the CCSD, CCSD(T), R-CCSD(T) and CR-CCSD(T) calculations relative to the highly accurate MRCI(Q) results, shown in table 10 and figure 9, clearly demonstrate that the R-CCSD(T) and CR-CCSD(T) approaches provide remarkable improvements in the poor description of the ground-state PES of the BeFH system by the standard CCSD and CCSD(T) methods. For the cc-pVTZ basis set used here, the observed improvements are even more spectacular than the improvements obtained in the R-CCSD(T) and CR-CCSD(T) calculations employing the MIDI basis set. The CR-CCSD(T) method is particularly effective in this regard. As in the case of the calculations with the MIDI basis set, the CR-CCSD(T) approach using the cc-pVTZ basis set eliminates the unphysical features on the PES produced by the CCSD(T) method at intermediate and large stretches of the H–F and Be–F bonds. For example, the CCSD(T) PES creates a false impression of the existence of a well-pronounced barrier leading to the formation of the Be + F + H atomic products, which is an artifact of the CCSD(T) calculations (cf. the $R_{H\text{-}F} > 4.0$ bohr and $R_{Be\text{-}F} > 5.0$ bohr region on the CCSD(T), CR-CCSD(T) and MRCI(Q) PESs shown in figures 8(*a*), 8(*c*) and 8(*d*), respectively). In addition, the CCSD(T) PES allows for a formation of the BeF + H products at lower energies than the highly accurate MRCI(Q) PES (cf. the thick contour lines corresponding to the energy of 1.3 eV in figures 8(*a*) and 8(*d*)). Indeed, the very shallow, ~0.1–0.3 millihartree deep, van der Waals well in the product (BeF + H) valley is located on the CCSD(T) PES below the Be + HF reactants, which is wrong (cf. figures 8(*a*) and 8(*d*)), and the endothermicity of the Be + HF → BeF + H reaction of -0.2 kcal mol^{-1}, resulting from the CCSD(T) calculations, has the wrong sign, when compared with the MRCI(Q) endothermicity value of 3.2 kcal mol^{-1} or the MRDCI value reported by Aguado *et al.* [202] of 5.9 kcal mol^{-1}. Although the barrier on the CCSD(T) PES for the collinear Be + HF → BeF + H reaction of 30.0 kcal mol^{-1} is not unreasonable (the MRCI(Q) result is 31.1 kcal mol^{-1} and the MRDCI value reported by Aguado *et al.* [202] is 33.2 kcal mol^{-1}), we must keep in mind that the CCSD(T) PES has a completely wrong topology (cf. figures 8(*a*) and 8(*d*)). The CR-CCSD(T) method fixes the problems showing up in the standard CCSD(T) calculations. In particular, the CR-CCSD(T) approach produces a PES that has a correct topology, especially in the difficult BeF + H and Be + F + H regions, while giving quite accurate values of the endothermicity and energy barrier for the collinear Be + HF → BeF + H reaction. The CR-CCSD(T) endothermicity value of

Figure 9. The dependence of the differences between the (*a*) CCSD(T), (*b*) R-CCSD(T) and (*c*) CR-CCSD(T) energies and the MRCI(Q) energies (in eV) for the collinear BeFH system, as described by the cc-pVTZ basis set, on the H–F and Be–F internuclear separations, $R_{H\text{-}F}$ and $R_{Be\text{-}F}$, respectively (in bohr). For further details and more numerical data, see [210].

Downloaded At: 16:32 21 January 2011

6.6 kcal mol^{-1} and the CR-CCSD(T) value of the saddle-point energy of 32.2 kcal mol^{-1}, obtained with the cc-pVTZ basis set, are in considerably better agreement with the results of the MRCI(Q) and MRDCI [202] calculations than the aforementioned results for these quantities obtained with the standard CCSD(T) approach. The experimental estimate of the endothermicity for the Be + HF $\rightarrow$ BeF + H reaction, based on the experimental values of the dissociation energies of HF and BeF [177], is 14.8 kcal mol^{-1}, although it does not seem to us that the dissociation energy of BeF has been determined experimentally with great precision. Nevertheless, the CR-CCSD(T) value of the endothermicity for the Be + HF $\rightarrow$ BeF + H reaction of 6.6 kcal mol^{-1}, obtained with the cc-pVTZ basis set, is somewhat closer to the experimentally derived endothermicity value of 14.8 kcal mol^{-1} than the values resulting from the MRCI(Q) and MRDCI [202] calculations. The product (BeF + H) valley and the Be + F + H asymptotic region of the CR-CCSD(T) PES obtained with the cc-pVTZ basis set are shaped in almost exactly the same way as the product valley and the Be + F + H region of the MRCI(Q) PES. This can be best seen by comparing the thick contour lines corresponding to 1.3 eV and thin contour lines corresponding to 5.3 and 5.7 eV in figures 8(*c*) and 8(*d*). These contour lines have incorrect shapes when the CCSD(T) PES is examined (see figure 8(*a*)). In fact, the energy value of 5.7 eV above the reactants is never reached in the CCSD(T) calculations. Unlike in the MRCI(Q) and CR-CCSD(T) cases, the contour line corresponding to 5.3 eV on the CCSD(T) PES is located only in the narrow region of large Be–F and relatively small H–F distances.

Downloaded At: 16:32 21 January 2011

It is encouraging to observe the similarities between the CR-CCSD(T) and MRCI(Q) contour plots shown in figures 8(*c*) and 8(*d*). The excellent agreement between the CR-CCSD(T) and MRCI(Q) PESs and the considerable differences between the CCSD(T) and MRCI(Q) results for the cc-pVTZ model of BeFH can also be seen by examining the distribution of errors in the CR-CCSD(T) and CCSD(T) results relative to the MRCI(Q) data shown in figure 9 and table 10. As in the case of the MIDI basis set, the differences between the CCSD(T) and MRCI(Q) PESs obtained with the cc-pVTZ basis set are particularly large when the Be–F and H–F bonds are stretched. Those differences are greater (in absolute value) than 1 eV in the entire $R_{Be\text{-}F} \geq 5.5$ bohr and $R_{H\text{-}F} \geq 6.0$ bohr region. They are greater than 0.5 eV in the entire $R_{Be\text{-}F} \geq 5.0$ bohr and $R_{H\text{-}F} \geq 5.0$ bohr region. Finally, they are greater than 0.2 eV for almost all nuclear geometries from the $R_{Be\text{-}F} < 2.5$ bohr and $R_{H\text{-}F} \geq 2.5$ bohr region, for the majority of geometries from the $R_{Be\text{-}F} \geq 3.5$ bohr and $R_{H\text{-}F} \geq 3.5$ bohr region and for many geometries from the 2.5 bohr $\leq R_{Be\text{-}F} < 3.5$ bohr and $R_{H\text{-}F} \approx 3.0$ bohr region. The maximum difference between the CCSD(T) and MRCI(Q) energies of the collinear BeFH system, as described by the cc-pVTZ basis set, is 3.269 eV (120.140 millihartree; at $R_{Be\text{-}F} = R_{H\text{-}F} = 8.0$ bohr; cf. table 10), which clearly shows how serious the breakdown of the RHF-based CCSD(T) approximation can be in studies of chemical reactions. Similar remarks apply to the PES obtained in the CCSD calculations. For example, the differences between the CCSD and MRCI(Q) energies are greater than 0.5 eV in the entire $R_{Be\text{-}F} \geq 3.9$ bohr and $R_{H\text{-}F} \geq 4.0$ bohr region and for almost all geometries from the $R_{Be\text{-}F} < 3.9$ bohr and 2.5 bohr $\leq R_{H\text{-}F} < 4.0$ bohr region. As shown in table 10, the maximum difference between the CCSD and MRCI(Q) results is 1.137 eV (41.782 millihartree; at $R_{Be\text{-}F} = 6.0$ bohr and $R_{H\text{-}F} = 8.0$ bohr). Thus, the standard CCSD and CCSD(T) methods lead to huge errors relative to MRCI(Q)

when the ground-state PES of BeFH is examined. The only essential difference between the CCSD and CCSD(T) results is the fact that the PES obtained in the CCSD calculations is located above the MRCI(Q) PES, whereas the CCSD(T) PES is located below the MRCI(Q) PES.

The extremely large errors in the results of the CCSD and CCSD(T) calculations for the BeFH system employing the cc-pVTZ basis set should be confronted with the small errors in the results relative to MRCI(Q) obtained with the CR-CCSD(T) method. For example, there are no nuclear geometries for which the differences between the MRCI(Q) and CR-CCSD(T) energies exceed 0.2 eV (see table 10). There are relatively few points where the difference between the CR-CCSD(T) and MRCI(Q) energies is between 0.1 and 0.2 eV. Typically, the differences between the CR-CCSD(T) and MRCI(Q) energies for the collinear BeFH system, as described by the cc-pVTZ basis set, are of the order of 0.01–0.1 eV. In other words, the CR-CCSD(T) and MRCI(Q) PESs are virtually parallel and lie very close to each other (see figure 9(*c*)). This observation is in sharp contrast with a highly non-uniform distribution of differences between the CCSD(T) and MRCI(Q) energies and large errors in the CCSD(T) results relative to MRCI(Q) shown in figure 9(*a*). As in the case of the calculations with the MIDI basis set, the stretching of the H–F bond has a much larger effect on the results of the standard CCSD and CCSD(T) calculations than the stretching of the Be–F bond (see table 10). The CR-CCSD(T) method seems to be almost insensitive to which of the two bonds is being stretched.

Downloaded At: 16:32 21 January 2011

A comparison of the R-CCSD(T) and MRCI(Q) PESs on the one hand and the CCSD(T) and MRCI(Q) PESs on the other hand (all generated with the same cc-pVTZ basis set) confirms our earlier observation, based on the calculations with the MIDI basis set, that a great deal of improvement in the poor CCSD(T) results can already be achieved at the simple R-CCSD(T) level (cf. figures 8(*a*), 8(*b*) and 8(*d*); see also figures 9(*a*) and 9(*b*) and table 10). The maximum difference between the R-CCSD(T) and MRCI(Q) energies is 0.531 eV, which is a lot less than the 3.269 eV maximum difference between the CCSD(T) and MRCI(Q) energies. As a matter of fact, the differences between the R-CCSD(T) and MRCI(Q) energies rarely exceed 0.2 eV and there are regions on the ground-state PES of the cc-pVTZ BeFH system where the R-CCSD(T) results are somewhat better than the results of the CR-CCSD(T) calculations (cf. table 10). We must realize, however, that the R-CCSD(T) method breaks down when the Be–F and H–F bonds are significantly stretched (see figure 9(*b*); cf. also the contour lines corresponding to 5.7 eV in figure 8(*b*)). On the other hand, it is quite remarkable to observe the similarities between the R-CCSD(T) and MRCI(Q) PESs for the cc-pVTZ BeFH system (cf. figures 8(*b*) and 8(*d*)). The small differences between the R-CCSD(T), CR-CCSD(T) and MRCI(Q) PESs of the BeFH system, for which standard CCSD and CCSD(T) methods fail, clearly demonstrate that the renormalization of the standard (T) correction to the CCSD energy according to the prescription described in section 3.1 is a sound theoretical procedure that may enable us to study exchange chemical reactions of the general type: closed shell + closed shell $\rightarrow$ doublet + doublet with the ease of use characterizing the popular, RHF-based, CCSD(T) method.

Finally, it is interesting to examine the potential energy curves of the HF fragment obtained by considering one-dimensional cuts of the PES of BeFH corresponding to Be–F distances fixed at some very large value, such as 50 bohr. We have discussed those kinds of cuts in [49], where we reported the results of calculations with the MIDI basis set. Here, we focus on the one-dimensional cuts of

the PES of BeFH obtained with the cc-pVTZ basis set (see figure 10(*a*)). The resulting curves represent the HF system in the presence of the Be atom located at a large distance from the HF fragment. For the well-behaved methods, the resulting potential energy curves should be essentially identical to the potential energy curve of the isolated HF molecule. This is what we observe when we analyse the results of the CR-CCSD(T) and MRCI(Q) calculations (cf. figure 10(*a*)). In fact, the dissociation energy D_e of the HF molecule, extracted from the MRCI(Q) PES of BeFH by considering the one-dimensional cut corresponding to $R_{Be\text{-}F} = 50$ bohr, is 5.93 eV, in very good agreement with the experimental D_e value for HF of 6.12 eV [177, 197]. The CR-CCSD(T) value of D_e for the HF molecule, obtained in a similar manner by examining the one-dimensional cut of the CR-CCSD(T) PES of the BeFH system corresponding to $R_{Be\text{-}F}$ fixed at 50 bohr, is 6.09 eV, in excellent agreement with the MRCI(Q) and experimental dissociation energies of HF. As we can see, the presence of the Be atom has practically no effect on the excellent curve for the isolated HF molecule obtained with the CR-CCSD(T) approach (see figure 10(*a*); cf. also sections 3.2.2.1 and 3.2.2.2). In other words, although the CR-CCSD(T) method is not strictly size extensive (see section 3.4), the CR-CCSD(T) results seem to be approximately size extensive. The CCSD(T) method is strictly size extensive, so that the presence of the Be atom has no effect on the HF curve obtained with this approach. This means, however, that the poor performance of the standard CCSD(T) method for the potential energy curve of the isolated HF molecule propagates into the calculation for the BeFH system. This can be seen by examining the CCSD(T) PES of BeFH in the region of large Be–F distances (see figure 10(*a*); cf. also figure 8(*a*)). The potential energy curve of HF obtained by considering a one-dimensional cut of the CCSD(T) PES of BeFH corresponding to a Be–F distance fixed at 50 bohr has the same type of hump in the region of intermediate H–F distances as the CCSD(T) potential energy curve of the isolated HF molecule (cf. sections 3.2.2.1 and 3.2.2.2).

Downloaded At: 16:32 21 January 2011

Similar (but not identical) remarks apply to the one-dimensional cuts of the PES of the BeFH system corresponding to H–F distances fixed at some very large value (as before, we chose $R_{H\text{-}F} = 50$ bohr). Again, for the well-behaved theories, the resulting potential energy curves (shown for the cc-pVTZ basis set in figure 10(*b*)) should be essentially identical to the potential energy curve of the isolated BeF molecule. As shown in figure 10(*b*) (see also figure 8(*d*)), the MRCI(Q) method is a well-behaved method in this sense. The dissociation energy D_e of the BeF molecule, extracted from the MRCI(Q) PES of BeFH by considering the one-dimensional cut corresponding to $R_{H\text{-}F} = 50$ bohr, is 5.78 eV. The experimental value of D_e for BeF is 5.5 eV [177], in reasonable agreement with the MRCI(Q) result. The CR-CCSD(T) potential for the BeF molecule, obtained by examining the one-dimensional cut of the CR-CCSD(T) PES of the BeFH system corresponding to $R_{H\text{-}F} = 50$ bohr, is not as good as the MRCI(Q) potential, since there is a small hump on the resulting CR-CCSD(T) curve (see figure 10(*b*)). On the other hand, the overall improvement offered by the CR-CCSD(T) method in the region of PES of BeFH corresponding to the asymptotic values of $R_{H\text{-}F}$ is still quite remarkable, particularly if we realize how poor the results of the standard CCSD(T) calculations are in this region (cf. figure 10(*b*)). The potential energy curve of BeF, obtained by considering the one-dimensional cut of the CR-CCSD(T) PES of BeFH corresponding to $R_{H-F} = 50$ bohr, is in excellent agreement with the analogous MRCI(Q) curve up to $R_{Be\text{-}F} = 5.0$ bohr. At $R_{Be\text{-}F} \approx 5.5$ bohr, there is a small (a few millihartree) hump

Downloaded At: 16:32 21 January 2011

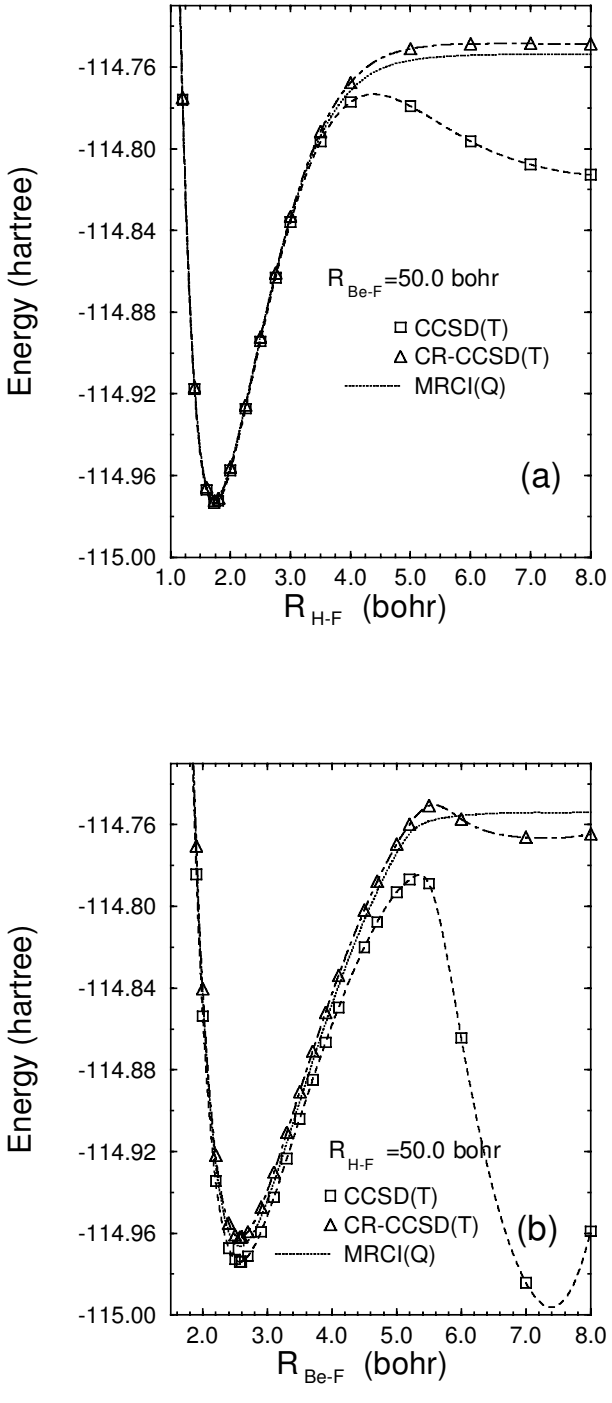

Figure 10. The (*a*) HF and (*b*) BeF potentials (energies in hartree, the H–F and Be–F separations, $R_{H\text{-}F}$ and $R_{Be\text{-}F}$, respectively, in bohr) obtained by considering the one-dimensional cuts of the ground-state PES of the collinear BeFH system, as described by the cc-pVTZ basis set, corresponding to fixed Be–F and H–F separations of 50.0 bohr. A comparison of the CCSD(T) (□), CR-CCSD(T) (△) and MRCI(Q) (dotted curves) results (all obtained in this work).

on the CR-CCSD(T) curve, which is a consequence of the fact that the $R_{Be\text{-}F} > 5.0$ bohr and $R_{H\text{-}F} = 50$ bohr region corresponds to a simultaneous dissociation of two single bonds, which cannot be perfectly described by the CR-CCSD(T) method. We would have to use the higher-level and more expensive CR-CCSD(TQ),b approach to eliminate or reduce significantly the small hump from the CR-CCSD(T) curve shown in figure 10(*b*). Interestingly enough, the dissociation energy for the BeF molecule, obtained by forming the difference between the CR-CCSD(T) energies at the maximum on the CR-CCSD(T) potential shown in figure 10(*b*), defining the hump at $R_{Be\text{-}F} \approx 5.5$ bohr, and at $R_{Be\text{-}F} = 2.5719$ bohr, corresponding to the equilibrium bond length of BeF, is 5.75 eV, in very good agreement with the experimental D_e value for the isolated BeF molecule. Thus, although the CR-CCSD(T) curve of BeF is not as good as the CR-CCSD(T) curve of HF shown in figure 10(*a*), the departure from size extensivity, observed by examining the CR-CCSD(T) energies of BeFH for $R_{H\text{-}F}$ fixed at 50 bohr, is still relatively small. We must realize that the strictly size-extensive CCSD(T) theory produces a completely unphysical potential for the BeF molecule in the BeF + H limit, with a well-pronounced hump for the intermediate values of $R_{Be\text{-}F}$ and a completely erroneous behaviour at the asymptotic values of the H–F and Be–F distances (see figure 10(*b*)).

Downloaded At: 16:32 21 January 2011

Before proceeding to the next section, where we describe the most recent quasi-variational and quadratic MMCC methods, let us summarize some of the findings discussed in sections 3.2.2.1–3.2.2.3. As shown in those three sections, the CR-CCSD[T] and CR-CCSD(T) methods are primarily designed to describe PESs involving single bond stretching or breaking (cf. [41–44, 46, 47, 49, 158]). We do not recommend applying the CR-CCSD[T] and CR-CCSD(T) approaches to multiple bond breaking. For example, if we want to study double bond breaking, we should resort to the CR-CCSD(TQ),x (x = a, b) methods [42, 47] (see section 3.2.2.1). The CR-CCSD(TQ),x methods should also provide further improvements in the results for single bond breaking [44, 46, 47] (cf. sections 3.2.2.1 and 3.2.2.2). Surprisingly enough, the CR-CCSD(TQ),x methods (particularly, the 'b' variant of the CR-CCSD(TQ) approximation) provide a reasonably good description of triple bond breaking, although the results for N_2 at large internuclear separations are not perfect [43, 47] (see table 5 and figure 2). Further improvements in the CR-CCSD(TQ),b results for triple bond breaking are obtained when we apply the completely renormalized CCSDT(Q) method [45, 47]. As already mentioned, an alternative solution to the problem of triple bond breaking is provided by the CI-corrected MMCC(2,6) method described in section 3.1, in which the judicious choice of active orbitals for the CISDtqph calculations (used to construct $|\Psi_0\rangle$ in the MMCC(2,6) formula, equation (58)), combined with the presence of the hextuply excited moments $\mathcal{M}_{\mathbf{IJKL}mn}^{ab\mathbf{CDEF}}(2)$ in the CISDtqph-corrected MMCC(2,6) energy expression, may tremendously help the results (see table 5 and figure 2). The CISDtqph-corrected MMCC(2,6) calculations require, however, that we define active orbitals, which is not the case when we use the CR-CCSD[T], CR-CCSD(T) and CR-CCSD(TQ),x methods. This leads to a very interesting question: Can we formulate the MMCC approximations that preserve the underlying philosophy of the CCSD(T), CCSD(TQ$_f$) and similar approaches, which is an idea of adding non-iterative corrections to the CCSD energies that do not require using external (CI-like) sources of $|\Psi_0\rangle$ or active orbitals, and yet obtain a virtually perfect description of triple bond breaking? The MMCC approximations that allow us to give an

affirmative answer to this question, referred to as the quasi-variational MMCC approaches, are described in the next section.

3.3. *The quasi-variational MMCC methods and their quadratic MMCC(2,4), MMCC(2,5) and MMCC(2,6) variants*

3.3.1. *Theory*

The fact that the CISDtqph-corrected MMCC(2,6) approach allows us to describe triple bond breaking suggests that in looking for the extensions of the CR-CCSD(T) and CR-CCSD(TQ) methods that might provide an excellent description of triple bond breaking one has to consider approximations that use the pentuply and hextuply excited moments of the CCSD equations, $\mathcal{M}^{abcde}_{ijklm}(2)$ and $\mathcal{M}^{abcdef}_{ijklmn}(2)$, respectively. In our initial attempt to design the desired method, we tried to extend the CR-CCSD(T) and CR-CCSD(TQ) approaches by combining the MMCC(2,6) approximation, defined by equation (58), with the MBPT(3)-like expressions for the wavefunction $|\Psi_0\rangle$. The MBPT(2)-like wavefunctions, defined by equation, (88) or (89), would not be sufficient, since they do not contain higher-than-quadruply excited components that must be present in the formula for $|\Psi_0\rangle$ if we are to benefit from the $\mathcal{M}^{abcde}_{ijklm}(2)$ and $\mathcal{M}^{abcdef}_{ijklmn}(2)$ contributions to the MMCC(2,6) energy expression. The MBPT(3) wavefunction is the lowest-order wavefunction that has the pentuply and hextuply excited contributions, which can be combined with the $\mathcal{M}^{abcde}_{ijklm}(2)$ and $\mathcal{M}^{abcdef}_{ijklmn}(2)$ moments to give the MMCC(2,6) correction $\delta_0(2,6)$. Thus, we constructed the appropriate MBPT(3)-like wavefunctions that could be used in the MMCC(2,6) calculations, but we have not succeeded in improving the CR-CCSD(TQ) results for triple bond breaking, reported in [43], with the resulting methods [161].

Downloaded At: 16:32 21 January 2011

Thus, a different approach to the extension of the CR-CCSD(T) and CR-CCSD(TQ) methods to the MMCC(2,6) case is called for if we want to obtain an excellent description of the entire PES involving triple bond breaking. We have recently suggested a new idea of exploiting the exponential, CC-like, forms of $|\Psi_0\rangle$ in equation (22) for the δ_0^{CCSD} correction to the CCSD energy, instead of the MBPT-like forms used in the CR-CCSD(T) and CR-CCSD(TQ) approaches. The CC-like functions $|\Psi_0\rangle$ should certainly be much more effective in introducing high-order terms into equation (22) than the finite-order MBPT expressions used in the existing CR-CCSD(T) and CR-CCSD(TQ) approaches. Moreover, the use of the exponential form of $|\Psi_0\rangle$ in equation (22) leads to strictly size-extensive results.

The simplest choice of wavefunction $|\Psi_0\rangle$ for calculating the correction δ_0^{CCSD}, equation (22), might be, of course, the CCSD wavefunction itself,

$$|\Psi_0^{\mathrm{CCSD}}\rangle = \mathrm{e}^{T_1+T_2}|\Phi\rangle. \tag{104}$$

Our tests indicate, however, that calculations of the correction δ_0^{CCSD} with $|\Psi_0\rangle = |\Psi_0^{\mathrm{CCSD}}\rangle$ do not lead to great improvements in the CCSD results. This is related to the fact that the CCSD wavefunction $|\Psi_0^{\mathrm{CCSD}}\rangle$, equation (104), does not bring any information about the connected triexcited clusters, which are very important in the calculations for all types of bond breaking. The approximate T_3 components (the $T_3^{[2]}$ cluster components defined by equation (65)) are present in the $|\Psi^{\mathrm{CCSD[T]}}\rangle$, $|\Psi^{\mathrm{CCSD(T)}}\rangle$ and $|\Psi^{\mathrm{CCSD(TQ),x}}\rangle$ wavefunctions, equations (63), (64), (88) and (89), defining the CR-CCSD[T], CR-CCSD(T) and CR-CCSD(TQ),x (x = a, b) approximations, and they play the essential role in providing significant improvements in the CCSD results offered by the completely renormalized CC approaches.

Thus, in defining the exponential form of $|\Psi_0\rangle$ for calculating the δ_0^{CCSD} correction, we must go beyond the CCSD approximation.

The simplest way to do it, while introducing the approximate T_3 clusters in a meaningful manner into $|\Psi_0\rangle$, is by considering the following wavefunction $|\Psi_0\rangle$ in equation (22) [161]:

$$|\Psi_0^{\mathrm{QVMMCC}}\rangle = \mathrm{e}^{\Sigma}|\Phi\rangle, \tag{105}$$

where

$$\Sigma = T_1 + T_2 + T_3^{[2]}, \tag{106}$$

with $T_3^{[2]}$ representing an MBPT(2)-like estimate of the T_3 cluster component defined by equation (65). Notice that operator Σ is an approximation to the exact cluster operator T, which is correct through the second-order of the MBPT wavefunction (T_1 and T_3 contribute, for the first time, in the second order and T_2 contributes, for the first time, in the first order; T_4, T_5, etc. do not contribute in the first two orders). We could, of course, contemplate more elaborate forms of the operator Σ in equation (105), but our numerical experience to date indicates that a simple form of Σ given by equation (106) is sufficient to provide excellent results for triple bond breaking.

Downloaded At: 16:32 21 January 2011

The use of the wavefunction $|\Psi_0^{\mathrm{QVMMCC}}\rangle$, equation (105), as $|\Psi_0\rangle$ in calculating the MMCC correction $\delta_0^{(\mathrm{A})}$, equation (9), with various forms of the cluster operator Σ, leads to the hierarchy of the quasi-variational (QV) MMCC approximations [161]. In this work, we focus on the most important type of QVMMCC approximation, in which the wavefunction $|\Psi_0^{\mathrm{QVMMCC}}\rangle$, with Σ defined by equation (106), is used to calculate the correction δ_0^{CCSD}, equation (22), which is subsequently added to the CCSD energy. Aside from the very high accuracy and the approximately variational and size-extensive description that the QVMMCC methods offer, the big advantage of all QVMMCC approaches is the fact that we do not have to select active orbitals in an *ad hoc* molecule-by-molecule manner, which characterizes all multireference approaches, in QVMMCC calculations. This remark applies, in particular, to the quadratic MMCC models discussed below, which represent a new class of computational 'black boxes' that are capable of providing a highly accurate description of multiple bond breaking.

The name 'quasi-variational MMCC approximations' originates from the fact that by inserting the wavefunction $|\Psi_0^{\mathrm{QVMMCC}}\rangle$ into the formula for the correction $\delta_0^{(\mathrm{A})}$, equation (9), or into the equivalent MMCC functional, equation (23), and by assuming that $\Sigma = T^{(\mathrm{A})}$, we obtain the expectation value of the Hamiltonian with the CC wavefunction $\mathrm{e}^{T^{(\mathrm{A})}}|\Phi\rangle$ [161]. Indeed, by replacing $|\Psi_0\rangle$ in equations (9) and (23) by $|\Psi_0^{\mathrm{QVMMCC}}\rangle$, equation (105), we obtain

$$\delta_0^{(\mathrm{A})}(\mathrm{QVMMCC}) = \sum_{n=m_{\mathrm{A}}+1}^{N} \sum_{j=m_{\mathrm{A}}+1}^{n} \langle\Phi|\mathrm{e}^{\Sigma^{\dagger}} Q_n\, C_{n-j}(m_{\mathrm{A}})\, M_j^{\mathrm{CC}}(m_{\mathrm{A}})|\Phi\rangle / \langle\Phi|\mathrm{e}^{\Sigma^{\dagger}}\mathrm{e}^{T^{(\mathrm{A})}}|\Phi\rangle \tag{107}$$

or (cf. equations (23) and (24))

$$\delta_0^{(\mathrm{A})}(\mathrm{QVMMCC}) = \langle\Phi|\mathrm{e}^{\Sigma^{\dagger}} H \mathrm{e}^{T^{(\mathrm{A})}}|\Phi\rangle / \langle\Phi|\mathrm{e}^{\Sigma^{\dagger}}\mathrm{e}^{T^{(\mathrm{A})}}|\Phi\rangle - E_0^{(\mathrm{A})}. \tag{108}$$

The corresponding QVMMCC energy, obtained by adding the $\delta_0^{(A)}(\mathrm{QVMMCC})$ correction to $E_0^{(A)}$, becomes

$$E_0^{\mathrm{QVMMCC}} \equiv E_0^{(A)} + \delta_0^{(A)}(\mathrm{QVMMCC}) = \langle \Phi | e^{\Sigma^\dagger} H e^{T^{(A)}} | \Phi \rangle / \langle \Phi | e^{\Sigma^\dagger} e^{T^{(A)}} | \Phi \rangle. \quad (109)$$

Clearly, the QVMMCC energy, equation (109), reduces to the expectation value of the Hamiltonian with the CC wave function $e^{T^{(A)}}|\Phi\rangle$ when $\Sigma = T^{(A)}$. In particular, if method A represents the standard CCSD theory and $\Sigma = T_1 + T_2$, the resulting QVMMCC energy, based on adding the correction (cf. equation (22))

$$\delta_0^{\mathrm{CCSD}}(\mathrm{QVMMCC}) = \sum_{n=3}^{N} \sum_{j=3}^{\min(n,6)} \langle \Phi | e^{\Sigma^\dagger} Q_n C_{n-j}(2) M_j^{\mathrm{CC}}(2) | \Phi \rangle / \langle \Phi | e^{\Sigma^\dagger} e^{T_1+T_2} | \Phi \rangle \quad (110)$$

to the CCSD energy, becomes equivalent to the expectation value of the Hamiltonian calculated with the CCSD wavefunction, which obviously is an upper bound to the exact ground-state energy. Although we do not want to use $\Sigma = T_1 + T_2$ in calculations of the MMCC correction $\delta_0^{\mathrm{CCSD}}(\mathrm{QVMMCC})$, equation (110) (as explained earlier, this does not lead to the desired improvements of the CCSD results owing to the absence of the connected triples in the corresponding wavefunction $|\Psi_0^{\mathrm{QVMMCC}}\rangle$), it is quite possible that the use of the operator Σ defined by equation (106) in calculations of $\delta_0^{\mathrm{CCSD}}(\mathrm{QVMMCC})$ gives energies that are, in the vast majority of cases, the upper bounds to the exact energies, even when multiple chemical bonds are broken. Numerical examples illustrating this statement are discussed in section 3.3.2.

Downloaded At: 16:32 21 January 2011

There is only one practical problem associated with the use of wavefunction $|\Psi_0^{\mathrm{QVMMCC}}\rangle$, equation (105), in calculations of the δ_0^{CCSD} corrections, namely the use of the exponential wavefunction $|\Psi_0^{\mathrm{QVMMCC}}\rangle$ requires that we consider all many-body terms in equation (22) or (110), including the N-body ones, where N is the number of electrons. Although this does not change the fact that the generalized moments of the CCSD equations, corresponding to projections of those equations on higher-than-hextuply excited configurations, vanish (so that the summation over j in equation (22) or (110) is still limited to the $j = 3$–6 terms in the QVMMCC theory), the full use of the exponential wavefunction $|\Psi_0^{\mathrm{QVMMCC}}\rangle$ requires that we deal with the full CI expansion of $|\Psi_0^{\mathrm{QVMMCC}}\rangle$ in calculating δ_0^{CCSD}. Since dealing with the full CI expansion of $|\Psi_0^{\mathrm{QVMMCC}}\rangle$ in equations (22) or (110) would lead to methods that are prohibitively expensive, at this time we decided to consider simple approximations, in which the power series expansion for $|\Psi_0^{\mathrm{QVMMCC}}\rangle$,

$$|\Psi_0^{\mathrm{QVMMCC}}\rangle = \sum_{k=0}^{N} \frac{\Sigma^k}{k!} |\Phi\rangle, \quad (111)$$

with Σ defined by equation (106), is truncated in equation (22) or (110) at a given power of Σ [161].

Two approximations are particularly important here, namely the linearized QVMMCC (LMMCC) model, in which

$$|\Psi_0^{\mathrm{QVMMCC}}\rangle \approx |\Psi_0^{\mathrm{LMMCC}}\rangle = (1 + \Sigma)|\Phi\rangle, \quad (112)$$

and the quadratic QVMMCC (QMMCC) model, in which

$$|\Psi_0^{\mathrm{QVMMCC}}\rangle \approx |\Psi_0^{\mathrm{QMMCC}}\rangle = (1 + \Sigma + \tfrac{1}{2}\Sigma^2)|\Phi\rangle, \quad (113)$$

where, in all practical calculations discussed in section 3.3.2, Σ is defined by equation (106). Cubic, quartic and other QVMMCC models based on truncating the power series expansion for $|\Psi_0^{\mathrm{QVMMCC}}\rangle$ are clearly possible, too. The motivation behind the LMMCC approximation stems from the success of the completely renormalized CCSD[T] and CCSD(T) methods, discussed in section 3.2, which utilize very similar expressions for $|\Psi_0\rangle$ that are linear in cluster amplitudes or their perturbative estimates. As a matter of fact, the LMMCC approach using Σ defined by equation (106) is equivalent to the CR-CCSD[T] method described in section 3.2 (see the discussion below).

In designing the QMMCC method, we were inspired by the recent work by Van Voorhis and Head-Gordon [215, 216] and, to a certain degree, by the earlier work on the so-called extended [64, 217–226] and expectation value [64, 227, 228] CC theories, in which products involving cluster operators and their Hermitian adjoints can be used to mimic the effect of higher-order clusters, such as T_4 (as is, for example, done in the factorized CCSD$(\mathrm{TQ_f})$ approach [20] and its renormalized and completely renormalized extensions discussed in section 3.2). Van Voorhis and Head-Gordon demonstrated that the variational CCD (CC with doubles) calculations, based on minimizing the expectation value of the Hamiltonian with the CCD wavefunction $\mathrm{e}^{T_2}|\Phi\rangle$, lead to a qualitatively correct description of triple bond breaking in N_2, eliminating, as one might expect, the non-variational collapse of the standard CCD theory at large internuclear separations [215]. As already mentioned, our QVMMCC approximations, based on using the asymmetric energy formula, equation (109), which resembles, to some extent, the expectation value of the Hamiltonian with the CC wavefunction, are expected to provide upper bounds to the exact energy in most cases, including the case of triple bond breaking (in fact, even the CR-CCSD(T) and CR-CCSD(TQ) methods provide upper bounds to the exact energy in cases involving single and double bond breaking [41, 42, 44, 46, 47, 49, 158]; cf. section 3.2.2). The only problem with using the expectation value of the Hamiltonian with the CC wavefunctions is the fact that the resulting energy expression is a non-terminating series in cluster components [4]. This problem prompted Van Voorhis and Head-Gordon to investigate the possibility of using the bi-variational approach of Arponen and Bishop, termed the extended CC (ECC) theory [217–226] (cf. also [64]), in calculations of PESs involving multiple bond breaking [216]. The ECC theory is obtained by imposing the stationary conditions for the asymmetric energy functionals [64, 217–226]

$$E(\Sigma, T) = \langle\Phi|\mathrm{e}^{\Sigma^\dagger}\mathrm{e}^{-T}H\mathrm{e}^{T}|\Phi\rangle = \langle\Phi|\mathrm{e}^{\Sigma^\dagger}\bar{H}|\Phi\rangle = \langle\Phi|[\mathrm{e}^{\Sigma^\dagger}(H\mathrm{e}^{T})_{\mathrm{C}}]_{\mathrm{C}}|\Phi\rangle, \qquad (114)$$

where $\bar{H} = \mathrm{e}^{-T}H\mathrm{e}^{T} = (H\mathrm{e}^{T})_{\mathrm{C}}$ is the similarity-transformed Hamiltonian, with respect to two independent cluster operators T and Σ or, more precisely, T and $\Sigma^\dagger$ (it should be noted that the MBPT analysis shows that the lowest-order estimates of T and Σ are identical, so that $\Sigma \approx T$ [64]). The advantage of equation (114) over the expectation value of the Hamiltonian with the CC wavefunction is the fact that $E(\Sigma, T)$ is a finite series in T and $\Sigma^\dagger$. Unfortunately, the power series expansions of the ECC functional $E(\Sigma, T)$ in terms of T and $\Sigma^\dagger$ contain relatively high powers of T and $\Sigma^\dagger$ that cause the ECC calculations to be prohibitively expensive, even at the lowest-order ECCD (ECC with doubles) level [64, 216]. For this reason, Van Voorhis and Head-Gordon decided to introduce the so-called QCCD (quadratic CCD) approximation, in which the power series expansion of $E(\Sigma, T)$, with $T = T_2$ and

Downloaded At: 16:32 21 January 2011

$\Sigma = \Sigma_2$, is terminated at quadratic terms in $\Sigma^\dagger$ [216]. The QCCD approximation is much less expensive than the full ECCD approach using higher powers of $\Sigma^\dagger$ and yet, as demonstrated by Van Voorhis and Head-Gordon [216], it leads to a qualitatively correct description of triple bond breaking in N_2, eliminating, in analogy to the variational CCD method [215], the non-variational collapse of the standard CCD theory at large internuclear separations [216].

Although our QMMCC energy expression, equation (109), is somewhat different from the ECC energy, equation (114), there are apparent similarities between both expressions. Thus, on the basis of the positive experience of Van Voorhis and Head-Gordon with their QCCD approximation, we decided to introduce the QMMCC approximation, in which we replace the complete power series expansion of $|\Psi_0^{\mathrm{QVMMCC}}\rangle$ in the QMMCC energy by $|\Psi_0^{\mathrm{QMMCC}}\rangle$, equation (113) (or $e^{\Sigma^\dagger}$ in equation (110)), by $(1 + \Sigma^\dagger + \frac{1}{2}(\Sigma^\dagger)^2$. As in the QCCD case, problems related to the use of the complete power series expansion for $|\Psi_0^{\mathrm{QVMMCC}}\rangle$ in the QMMCC energy expressions, including large costs of considering higher powers of $\Sigma^\dagger$ in the power series expansion of $e^{\Sigma^\dagger}$ in equation (110), are eliminated. The success of the QCCD model of Van Voorhis and Head-Gordon in providing the effectively variational and qualitatively (not quantitatively though) correct description of triple bond breaking in N_2, in spite of the bi-variational, rather than variational, character of the ECC theory, combined with the apparent similarity of the QMMCC, variational CC and ECC energy expressions, suggests that we should largely be able to eliminate the non-variational collapse of the standard CCSD method in describing triple bond breaking (cf. table 5 and figure 2) by replacing the complete QVMMCC model by the QMMCC approximation, in which cubic and other higher-order terms in $\Sigma^\dagger$ in equation (110) are neglected. Although the truncated QMMCC model is no longer strictly size extensive, the size inextensivity errors in the QMMCC calculations must be significantly smaller than the relatively small size inextensivity errors observed in the LMMCC-like calculations, such as CR-CCSD(T) (cf. section 3.4), owing to the presence of the quadratic $\frac{1}{2}\Sigma^2$ terms in equation (113).

Downloaded At: 16:32 21 January 2011

Let us now analyse the LMMCC and QMMCC approximations in greater detail. Because of our definition of the operator Σ, equation (106), which does not contain higher-than-triply excited clusters, the LMMCC model is fully equivalent to the CR-CCSD[T] approximation described in section 3.2. Indeed, the $|\Psi_0^{\mathrm{LMMCC}}\rangle$ wavefunction, equation (112), is identical to the $|\Psi^{\mathrm{CCSD[T]}}\rangle$ wavefunction defined by equation (63). In consequence, the LMMCC energy,

$$E_0^{\mathrm{LMMCC}} = E^{\mathrm{CCSD}} + \delta_0^{\mathrm{CCSD}}(\mathrm{LMMCC}), \tag{115}$$

where $\delta_0^{\mathrm{CCSD}}(\mathrm{LMMCC})$ is the value of δ_0^{CCSD}, equation (22), obtained with $|\Psi_0\rangle = |\Psi_0^{\mathrm{LMMCC}}\rangle$, equals [161]

$$\begin{aligned} E_0^{\mathrm{LMMCC}} &= E^{\mathrm{CCSD}} + \langle \Psi_0^{\mathrm{LMMCC}} | Q_3 M_3^{\mathrm{CC}}(2) | \Phi \rangle / \langle \Psi_0^{\mathrm{LMMCC}} | \mathrm{e}^{T_1+T_2} | \Phi \rangle \\ &= E^{\mathrm{CCSD}} + \langle \Psi^{\mathrm{CCSD[T]}} | Q_3 M_3^{\mathrm{CC}}(2) | \Phi \rangle / \langle \Psi^{\mathrm{CCSD[T]}} | \mathrm{e}^{T_1+T_2} | \Phi \rangle \\ &= E^{\mathrm{CR\text{-}CCSD[T]}}, \end{aligned} \tag{116}$$

where $E^{\mathrm{CR\text{-}CCSD[T]}}$ is the CR-CCSD[T] energy defined by equation (61).

The QMMCC approach, in which the operator Σ is defined by equation (106), is an improvement over the LMMCC or CR-CCSD[T] approximations, since, in addition to the linear terms in $\Sigma^\dagger$ that are already present in the LMMCC model,

we consider the quadratic $(\Sigma^\dagger)^2$ terms in equation (110). By truncating the power series expansion of $e^{\Sigma^\dagger}$ in equation (110) at the quadratic $(\Sigma^\dagger)^2$ terms, with Σ defined by equation (106), or, equivalently, by replacing the ground-state wavefunction $|\Psi_0\rangle$ in equation (22) for the $\delta_0^{\rm CCSD}$ correction by $|\Psi_0^{\rm QMMCC}\rangle$, equation (113) (this reduces the summation over n in equations (110) or (22) from $\sum_{n=3}^{N}$ to $\sum_{n=3}^{6}$), we obtain the following formula for the QMMCC energy [161]:

$$E_0^{\rm QMMCC} = E^{\rm CCSD} + \delta_0^{\rm CCSD}({\rm QMMCC}), \tag{117}$$

where

$$\delta_0^{\rm CCSD}({\rm QMMCC}) = N^{\rm QMMCC}/D^{\rm QMMCC}, \tag{118}$$

with the numerator

$$\begin{aligned} N^{\rm QMMCC} &= \sum_{n=3}^{6}\sum_{j=3}^{n}\langle\Psi_0^{\rm QMMCC}|Q_n\, C_{n-j}(2)\, M_j^{\rm CC}(2)|\Phi\rangle \\ &= \langle\Phi|[T_1^\dagger T_2^\dagger + (T_3^{[2]})^\dagger]M_3^{\rm CC}(2) \\ &+ [\tfrac{1}{2}(T_2^\dagger)^2 + T_1^\dagger(T_3^{[2]})^\dagger][M_4^{\rm CC}(2) + T_1 M_3^{\rm CC}(2)] \\ &+ T_2^\dagger(T_3^{[2]})^\dagger[M_5^{\rm CC}(2) + T_1 M_4^{\rm CC}(2) + (T_2 + \tfrac{1}{2}T_1^2)M_3^{\rm CC}(2)] \\ &+ \tfrac{1}{2}[(T_3^{[2]})^\dagger]^2[M_6^{\rm CC}(2) + T_1 M_5^{\rm CC}(2) + (T_2 + \tfrac{1}{2}T_1^2)M_4^{\rm CC}(2) \\ &+ (T_1T_2 + \tfrac{1}{6}T_1^3)M_3^{\rm CC}(2)]|\Phi\rangle \end{aligned} \tag{119}$$

and the denominator

$$\begin{aligned} D^{\rm QMMCC} &= \langle\Psi_0^{\rm QMMCC}|e^{T_1+T_2}|\Phi\rangle \\ &= 1 + \langle\Phi|T_1^\dagger T_1|\Phi\rangle + \langle\Phi|[T_2^\dagger + \tfrac{1}{2}(T_1^\dagger)^2](T_2 + \tfrac{1}{2}T_1^2)|\Phi\rangle \\ &+ \langle\Phi|[T_1^\dagger T_2^\dagger + (T_3^{[2]})^\dagger](T_1T_2 + \tfrac{1}{6}T_1^3)|\Phi\rangle \\ &+ \langle\Phi|[\tfrac{1}{2}(T_2^\dagger)^2 + T_1^\dagger(T_3^{[2]})^\dagger](\tfrac{1}{2}T_2^2 + \tfrac{1}{2}T_1^2T_2 + \tfrac{1}{24}T_1^4)|\Phi\rangle \\ &+ \langle\Phi|T_2^\dagger(T_3^{[2]})^\dagger(\tfrac{1}{2}T_1T_2^2 + \tfrac{1}{6}T_1^3T_2 + \tfrac{1}{120}T_1^5)|\Phi\rangle \\ &+ \langle\Phi|\tfrac{1}{2}[(T_3^{[2]})^\dagger]^2(\tfrac{1}{6}T_2^3 + \tfrac{1}{4}T_2^2T_1^2 + \tfrac{1}{24}T_1^4T_2 + \tfrac{1}{720}T_1^6)|\Phi\rangle. \end{aligned} \tag{120}$$

As we can see, the $T_2^\dagger(T_3^{[2]})^\dagger$ and $\frac{1}{2}[(T_3^{[2]})^\dagger]^2$ components, originating from the $(\Sigma^\dagger)^2$ quadratic terms, lead to the appearance of the $M_5^{\rm CC}(2)|\Phi\rangle$ and $M_6^{\rm CC}(2)|\Phi\rangle$ terms in equation (118). In consequence, the QMMCC energy expression involves the complete set of the generalized moments of the CCSD equations, including the pentuply and hextuply excited moments, $\mathcal{M}_{ijklm}^{abcde}(2)$ and $\mathcal{M}_{ijklmn}^{abcdef}(2)$, respectively. The presence of the $\mathcal{M}_{ijklm}^{abcde}(2)$ and $\mathcal{M}_{ijklmn}^{abcdef}(2)$ terms in the QMMCC energy formula should (and, in fact, does) help to obtain an excellent description of triple bond breaking.

The QMMCC energy correction $\delta_0^{\rm CCSD}({\rm QMMCC})$, equation (118), has a very interesting many-body structure, characterized by a highly non-standard selection of higher-order terms. Even if we ignore the presence of the $D^{\rm QMMCC}$ denominator in equation (118), which is characteristic to all MMCC expressions and which plays an important role in improving the results of the MMCC calculations in the bond-

Downloaded At: 16:32 21 January 2011

breaking region, an interesting combination of lower- and higher-order terms enters the numerator expression (119). On the one hand, in equation (119), the usual fourth-order-like terms of the $\langle\Phi|(T_3^{[2]})^\dagger (V_N T_2)_C|\Phi\rangle$ type, originating from the $\langle\Phi|(T_3^{[2]})^\dagger M_3^{CC}(2)|\Phi\rangle$ contribution and defining the non-iterative triples corrections $E_T^{[4]}$, equation (79), are combined with the fifth-order-type $E_{QQ}^{[5]}$ and $E_{TQ}^{[5]}$ terms, equations (98) and (101), respectively, that originate from $\langle\Phi|\frac{1}{2}(T_2^\dagger)^2 M_4^{CC}(2)|\Phi\rangle$ and $\langle\Phi|(T_3^{[2]})^\dagger M_3^{CC}(2)|\Phi\rangle$ and that define the non-iterative triples and quadruples (TQ) methods (see section 3.2.1; cf. also [174–176] for further information about the $E^{[5]}$ terms). On the other hand, there are several higher-order terms in equation (119) whose selection would not be easy to justify without using the underlying MMCC formalism. The familiar $E_T^{[4]}$, $E_{QQ}^{[5]}$ and $E_{TQ}^{[5]}$ terms, equations (79), (98) and (101), are combined in equation (119) with the selected higher-order terms, including, for example, the sixth-order-type $\langle\Phi|T_2^\dagger(T_3^{[2]})^\dagger T_2(V_N T_2)_C|\Phi\rangle$ terms, originating from $\langle\Phi|T_2^\dagger(T_3^{[2]})^\dagger T_2 M_3^{CC}(2)|\Phi\rangle$, or the eighth-order-type $\frac{1}{48}\langle\Phi|[(T_3^{[2]})^\dagger]^2 (V_N T_2^4)_C|\Phi\rangle$ terms, originating from $\langle\Phi|\frac{1}{2}[(T_3^{[2]})^\dagger]^2 M_6^{CC}(2)|\Phi\rangle$. The conventional order-by-order MBPT analysis, used to design the non-iterative CC approaches of the standard type, would never lead to equations of the type of equation (118) or (119). This once again demonstrates the fascinating new possibilities offered by the MMCC formalism: we can use the MMCC theory to formulate entirely new classes of non-iterative CC corrections, employing the non-standard selections of higher-order terms that can only be justified on the basis of the underlying many-body structure of the MMCC corrections $\delta_0^{(A)}$.

Downloaded At: 16:32 21 January 2011

The above equations (117)–(120) define the complete QMMCC theory (within the $\Sigma = T_1 + T_2 + T_3^{[2]}$ approximation). Since the QMMCC energy, equation (117), contains all generalized moments of the CCSD equations, including the $\mathcal{M}_{ijklmn}^{abcdef}(2)$ or $M_6^{CC}(2)|\Phi\rangle$ terms, the QMMCC method described by equations (117)–(120) is referred here to as the QMMCC(2,6) approximation. By neglecting the $\frac{1}{2}[(T_3^{[2]})^\dagger]^2$ terms in equation (119) (which is equivalent to reducing the summation over n in equation (119) to $\sum_{n=3}^{5}$) and by neglecting similar terms in equation (120), we obtain the QMMCC analogue of the MMCC(2,5) approximation, referred to as the QMMCC(2,5) method. The QMMCC(2,5) energy is defined as follows [161]:

$$E_0^{\mathrm{QMMCC}(2,5)} = E^{\mathrm{CCSD}} + \delta_0^{\mathrm{CCSD}}[\mathrm{QMMCC}(2,5)], \tag{121}$$

where

$$\delta_0^{\mathrm{CCSD}}[\mathrm{QMMCC}(2,5)] = N^{\mathrm{QMMCC}(2,5)}/D^{\mathrm{QMMCC}(2,5)}, \tag{122}$$

with

$$\begin{aligned} N^{\mathrm{QMMCC}(2,5)} &= \sum_{n=3}^{5}\sum_{j=3}^{n}\langle\Psi_0^{\mathrm{QMMCC}}|Q_n\, C_{n-j}(2)\, M_j^{CC}(2)|\Phi\rangle \\ &= \langle\Phi|[T_1^\dagger T_2^\dagger + (T_3^{[2]})^\dagger]M_3^{CC}(2) \\ &\quad + [\tfrac{1}{2}(T_2^\dagger)^2 + T_1^\dagger(T_3^{[2]})^\dagger][M_4^{CC}(2) + T_1 M_3^{CC}(2)] \\ &\quad + T_2^\dagger(T_3^{[2]})^\dagger[M_5^{CC}(2) + T_1 M_4^{CC}(2) + (T_2 + \tfrac{1}{2}T_1^2)M_3^{CC}(2)]|\Phi\rangle \end{aligned} \tag{123}$$

and

$$D^{\mathrm{QMMCC(2,5)}} = 1 + \langle\Phi|T_1^\dagger T_1|\Phi\rangle + \langle\Phi|[T_2^\dagger + \tfrac{1}{2}(T_1^\dagger)^2](T_2 + \tfrac{1}{2}T_1^2)|\Phi\rangle + \langle\Phi|[T_1^\dagger T_2^\dagger + (T_3^{[2]})^\dagger](T_1T_2 + \tfrac{1}{6}T_1^3)|\Phi\rangle + \langle\Phi|[\tfrac{1}{2}(T_2^\dagger)^2 + T_1^\dagger(T_3^{[2]})^\dagger](\tfrac{1}{2}T_2^2 + \tfrac{1}{2}T_1^2T_2 + \tfrac{1}{24}T_1^4)|\Phi\rangle + \langle\Phi|T_2^\dagger(T_3^{[2]})^\dagger(\tfrac{1}{2}T_1T_2^2 + \tfrac{1}{6}T_1^3T_2 + \tfrac{1}{120}T_1^5)|\Phi\rangle. \quad (124)$$

The main difference between the complete QMMCC or QMMCC(2,6) and QMMCC(2,5) approximations is in the fact that the QMMCC(2,5) method does not require the consideration of the $\mathcal{M}_{ijklmn}^{abcdef}(2)$ moments corresponding to projections of the CCSD equations on hextuply excited configurations. Interestingly (and surprisingly) enough, the absence of the $\mathcal{M}_{ijklmn}^{abcdef}(2)$ moments and the hextuply excited $\frac{1}{2}[(T_3^{[2]})^\dagger]^2$ terms in the QMMCC(2,5) energy expression has no detrimental effect on the results of QMMCC calculations for triple bond breaking in N_2, which, at least intuitively, should require an explicit consideration of hextuple excitations (cf. section 3.1.3).

In analogy to the QMMCC(2,5) approximation, we can also propose the QMMCC(2,4) and QMMCC(2,3) approaches. In the QMMCC(2,4) method, we neglect the $T_2^\dagger(T_3^{[2]})^\dagger$ terms in the QMMCC or QMMCC(2,6) energy expression, equation (117), in addition to the $\frac{1}{2}[(T_3^{[2]})^\dagger]^2$ terms that have already been neglected in constructing the QMMCC(2,5) approximation. Thus, the QMMCC(2,4) energy is calculated as follows:

$$E_0^{\mathrm{QMMCC(2,4)}} = E^{\mathrm{CCSD}} + \delta_0^{\mathrm{CCSD}}[\mathrm{QMMCC}(2,4)], \quad (125)$$

where

$$\delta_0^{\mathrm{CCSD}}[\mathrm{QMMCC}(2,4)] = N^{\mathrm{QMMCC(2,4)}}/D^{\mathrm{QMMCC(2,4)}}, \quad (126)$$

with

$$N^{\mathrm{QMMCC(2,4)}} = \sum_{n=3}^{4}\sum_{j=3}^{n}\langle\Psi_0^{\mathrm{QMMCC}}|Q_n\, C_{n-j}(2)\, M_j^{\mathrm{CC}}(2)|\Phi\rangle = \langle\Phi|[T_1^\dagger T_2^\dagger + (T_3^{[2]})^\dagger]M_3^{\mathrm{CC}}(2) + [\tfrac{1}{2}(T_2^\dagger)^2 + T_1^\dagger(T_3^{[2]})^\dagger][M_4^{\mathrm{CC}}(2) + T_1M_3^{\mathrm{CC}}(2)]|\Phi\rangle \quad (127)$$

and

$$D^{\mathrm{QMMCC(2,4)}} = 1 + \langle\Phi|T_1^\dagger T_1|\Phi\rangle + \langle\Phi|[T_2^\dagger + \tfrac{1}{2}(T_1^\dagger)^2](T_2 + \tfrac{1}{2}T_1^2)|\Phi\rangle + \langle\Phi|[T_1^\dagger T_2^\dagger + (T_3^{[2]})^\dagger](T_1T_2 + \tfrac{1}{6}T_1^3)|\Phi\rangle + \langle\Phi|[\tfrac{1}{2}(T_2^\dagger)^2 + T_1^\dagger(T_3^{[2]})^\dagger](\tfrac{1}{2}T_2^2 + \tfrac{1}{2}T_1^2T_2 + \tfrac{1}{24}T_1^4)|\Phi\rangle. \quad (128)$$

In the QMMCC(2,3) approximation, we would simplify the above equations further by neglecting the $[\frac{1}{2}(T_2^\dagger)^2 + T_1^\dagger(T_3^{[2]})^\dagger]$ quadruply excited terms in equations (127) and (128). Since this would lead to slightly modified CR-CCSD[T] or CR-CCSD(T) approximations, we do not consider the QMMCC(2,3) method in this work.

Downloaded At: 16:32 21 January 2011

We consider, however, the QMMCC(2,4) approach, since it allows us to understand the significance of the CR-CCSD(TQ) methods, when compared with the complete LMMCC and QMMCC models. The QMMCC(2,4) method can be viewed as a modified CR-CCSD(TQ),b approximation, in which there is only one quadratic term multiplying $[M_4^{CC}(2) + T_1 M_3^{CC}(2)]$ in the numerator of the MMCC(2,4) correction $\delta_0(2,4)$, namely the $\frac{1}{2}(T_2^{\dagger})^2$ term (cf. equations (90), (92) and (94) with equations (125)–(128)). The similarity of the QMMCC(2,4) and CR-CCSD(TQ),b methods becomes, in fact, transparent, when we analyse numerical examples (see section 3.3.2). The small differences between the CR-CCSD(TQ),b and QMMCC(2,4) methods, combined with the fact that the QMMCC(2,4) approach represents an approximation to the full QMMCC model and with the fact that the LMMCC and CR-CCSD[T] methods are equivalent, imply that the CR-CCSD(TQ),b approach described in section 3.2 can be regarded as an intermediate step between the less accurate LMMCC = CR-CCSD[T] or CR-CCSD(T) methods that work well for the single bond breaking and the highly accurate QMMCC(2,5) and QMMCC(2,6) approaches that work well for the single and multiple bond breaking. In other words, we can view the CR-CCSD(TQ),b and, to some extent, CR-CCSD(TQ),a approaches as the simplified QMMCC methods, in which the only quadratic term of the $\frac{1}{2}(\Sigma^{\dagger})^2$ type, originating from the presence of $e^{\Sigma^{\dagger}}$ in the QVMMCC energy formulas, equations (107) or (110), and included in the calculations, is the lowest-order $\frac{1}{2}(T_2^{\dagger})^2$ term. All other cluster-amplitude-dependent terms defining the CR-CCSD(TQ),b approximation are linear in T_1 and T_2. We can, in fact, observe the following accuracy patterns in calculations for bond breaking [161]:

$$\begin{aligned}\text{LMMCC} \equiv \text{CR-CCSD[T]} \lesssim \text{CR-CCSD(T)} < \text{CR-CCSD(TQ),b} \approx \text{QMMCC}(2,4) \\ < \text{QMMCC}(2,5) \lesssim \text{QMMCC}(2,6) \equiv \text{QMMCC} \lesssim \text{Full CI},\end{aligned} \tag{129}$$

which are a clear reflection of the above theoretical analysis.

We examine some of these patterns in the next section. All of our test calculations to date show that the CR-CCSD[T] and CR-CCSD(T) methods are the lowest-order QVMMCC formalisms, whose applicability is restricted to single bond breaking, whereas the QMMCC(2,5) and QMMCC(2,6) approaches can be regarded as the high-level QVMMCC approximations that are capable of describing all kinds of bond breaking, including the triple bond breaking in N_2. The CR-CCSD(TQ),b method or its QMMCC(2,4) counterpart represents the intermediate levels of the QVMMCC theory, which work very well for single and double bond breaking but which may fail to provide an accurate description of triple bond breaking. In other words, the CR-CCSD[T], CR-CCSD(T) and CR-CCSD(TQ),x (x = a, b) approaches can be regarded as 'black-box' methods that remove the failing of the standard CC approximations in situations involving single and double bond breaking. The QMMCC(2,5) and QMMCC(2,6) approaches can be viewed as the next generation of the completely renormalized CC methods that can provide an accurate description of single, double and even triple bond breaking.

3.3.2. *Examples of applications of the QMMCC method*

We begin the discussion of examples of the QMMCC calculations with the DZ model of the H_2O molecule, described, in detail, in section 3.1.2. Let us recall that, in this case, we are interested in improving the poor description of the simultaneous stretching or breaking of both O–H bonds by the standard CCSD, CCSD[T],

Downloaded At: 16:32 21 January 2011

CCSD(T) and CCSD(TQ_f) methods. We have already demonstrated that considerable improvements in the results of the standard CC calculations for the double dissociation of water can be obtained when we apply the CI-corrected MMCC methods (see sections 3.1.2 and 3.1.4, particularly tables 2 and 6). In this case, the CISDt-corrected MMCC(2,3) method or the CISDtq-corrected MMCC(2,4) approach seems to provide a sufficient level of improvement, reducing, for example, the larger negative errors in the CCSD[T], CCSD(T) and CCSD(TQ_f) results for $R = 2R_e$ (R is the O–H separation; R_e is the equilibrium O–H bond length) to relatively small, ~2 millihartree, positive errors. The CISDtqp-corrected MMCC(2,5) scheme and the CISDtqph-corrected MMCC(2,6) approach reduce those errors further, to 0.730 and 0.538 millihartree, respectively (cf. table 6), whereas the CR-CCSD[T], CR-CCSD(T) and CR-CCSD(TQ),x (x = a, b) methods offer the same level of improvement as the CI-corrected MMCC(2,3) and MMCC(2,4) approaches (cf. table 2). It is interesting to examine whether the QMMCC methods, which can be viewed as natural extensions of the CR-CCSD[T], CR-CCSD(T) and CR-CCSD(TQ),x approaches, preserving the 'black-box' character of the completely renormalized CC theories, are capable of providing further improvements.

A comparison of the QMMCC(2,4), QMMCC(2,5) and QMMCC(2,6) results for the DZ model of water with the results of the full CI calculations, CI-corrected MMCC(2,4), MMCC(2,5) and MMCC(2,6) calculations, and completely renormalized CCSD[T], CCSD(T) and CCSD(TQ) calculations is made in table 11. As expected (cf. the remarks at the end of section 3.3.1), the QMMCC(2,4) approach, defined by equation (125), provides results that are virtually identical to the very good CR-CCSD(TQ),x (x = a, b) results. The QMMCC(2,4) results are also similar to the results of the CISDtq-corrected MMCC(2,4) calculations. This is quite promising, since, unlike the CISDtq-corrected MMCC(2,4) theory, the QMMCC(2,4) method does not require selecting active orbitals. The complete QMMCC formalism, referred to as the QMMCC(2,6) method (cf. equation (117)), provides further improvements in the results, reducing the 2.005 millihartree error in the QMMCC(2,4) energy at the significantly stretched, $R = 2R_e$, geometry to 0.546 millihartree. The description of the double dissociation of the water molecule by the QMMCC(2,6) method is as good as the excellent description of this process by the CISDtqph-corrected MMCC(2,6) approach, which requires that we first perform the CISDtqph calculations (see table 11). It is quite remarkable that we can reduce the 1.790, 5.590 and 9.333 millihartree errors in the CCSD results at $R = R_e$, $1.5R_e$ and $2R_e$, respectively, to less than 0.7 millihartree by adding the *a posteriori* non-iterative QMMCC corrections, employing only T_1 and T_2 components, to CCSD energies.

What is even more remarkable is the fact that we can ignore the most expensive $\mathcal{M}^{abcde}_{ijklm}(2)$ and $\mathcal{M}^{abcdef}_{ijklmn}(2)$ moments in the complete QMMCC or QMMCC(2,6) energy formula, equation (117), without changing the excellent QMMCC(2,6) results. The errors in the QMMCC(2,6) results for the DZ model of water, obtained by zeroing the $\mathcal{M}^{abcde}_{ijklm}(2)$ and $\mathcal{M}^{abcdef}_{ijklmn}(2)$ moments, are as small as the tiny (<0.7 millihartree) errors in the results of the complete QMMCC(2,6) calculations, in which all generalized moments of the CCSD equations are included (see table 11). By ignoring the $\mathcal{M}^{abcde}_{ijklm}(2)$ and $\mathcal{M}^{abcdef}_{ijklmn}(2)$ moments of the CCSD equations in the QMMCC(2,6) energy expression, we are essentially preserving the simplicity and the relatively low cost of the CR-CCSD(TQ),b calculations. This means that we may be able to generate PESs corresponding to a simultaneous breaking of two single bonds, which will differ from the exact PESs by ~1 millihartree (perhaps even less), with an

Downloaded At: 16:32 21 January 2011

Table 11. A comparison of the QMMCC(2,4), QMMCC(2,5) and QMMCC(2,6) ground-state energies with the results of the full CI, standard CC, completely renormalized CCSD[T], CCSD(T) and CCSD(TQ), and CI-corrected MMCC(2,4), MMCC(2,5) and MMCC(2,6) calculations for the equilibrium and two displaced geometries of the H_2O molecule with the DZ basis set.[a]

Method	$R = R_e$[b]	$R = 1.5R_e$[c]	$R = 2R_e$[c]
Full CI	−76.157 866[b]	−76.014 521[c]	−75.905 247[c]
CCSD	1.790	5.590	9.333
CCSDT[d]	0.434	1.473	−2.211
CCSDTQ[e]	0.015	0.141	0.108
CR-CCSD[T][f]	0.560	2.053	1.163
CR-CCSD(T)[f]	0.738	2.534	1.830
CR-CCSD(TQ),a[f]	0.195	0.905	1.461
CR-CCSD(TQ),b[f]	0.195	0.836	2.853
MMCC(2,4)[g,h]	0.501	0.942	2.416
MMCC(2,5)[g,i]	0.421	0.584	0.730
MMCC(2,6)[g,i]	0.417	0.477	0.538
QMMCC(2,4)[j]	0.271	0.959	2.005
QMMCC(2,5)[j]	0.202	0.688	0.549
QMMCC(2,6)[j]	0.202	0.688	0.546
QMMCC(2,6) ($M_{ijklmn}^{abcdef}(2) = 0$)[j]	0.202	0.688	0.546
QMMCC(2,6) ($M_{ijklm}^{abcde}(2) = M_{ijklmn}^{abcdef}(2) = 0$)[j]	0.206	0.708	0.657

[a] The full CI total energies are in hartree. The CC, CI and MMCC energies are in millihartree relative to the corresponding full CI energy values.
[b] The equilibrium geometry and full CI result from [166].
[c] The geometry and full CI result from [167].
[d] From [22].
[e] From [25].
[f] The CR-CCSD[T], CR-CCSD(T) and CR-CCSD(TQ),a results from [42]. The CR-CCSD(TQ),b results obtained in the present work.
[g] The active space consisted of the $1b_1$, $3a_1$, $1b_2$, $4a_1$, $2b_1$ and $2b_2$ orbitals.
[h] From [48].
[i] From [171].
[j] From [161].

Downloaded At: 16:32 21 January 2011

effort comparable with (certainly not much greater than) that for the CR-CCSD(TQ),b calculations. On the basis of the results of the QMMCC calculations for water shown in table 11, we can conclude that the QMMCC method, in which the $\mathcal{M}_{ijklm}^{abcde}(2)$ and $\mathcal{M}_{ijklmn}^{abcdef}(2)$ moments are ignored, is definitely worth further exploration. We can also use the QMMCC(2,5) method, defined by equation (121), and obtain the results for the double dissociation of water that can only be matched by the excellent results of the full QMMCC (QMMCC(2,6)) or CISDtqph-corrected MMCC(2,6) calculations (see table 11). Our benchmark calculations for the water molecule clearly reflect the accuracy pattern described by equation (129).

As mentioned in the previous section, the primary motivation behind the QMMCC and other QVMMCC approximations is the need to improve the CR-CCSD(TQ) description of triple bond breaking. As shown in section 3.2.2.1, the

CR-CCSD(TQ),b approach provides great improvements in the poor description of the triple bond breaking in N_2 by the conventional CCSD, CCSD(T) and CCSD(TQ_f) approaches, but the 10–25 millihartree differences between the CR-CCSD(TQ),b and full CI energies at the intermediate and larger values of the N–N distance R, observed in the calculations for the DZ model of N_2 (described, in detail, in section 3.1.4), are not entirely satisfactory (see table 5 and figure 2). Moreover, it would be desirable if we could remove or, at the very least, reduce or shift away the ~4.9 millihartree hump on the CR-CCSD(TQ),b potential energy curve for the DZ model of N_2 (cf. section 3.2.2.1 and figure 2). We already know that the CISDtqph-corrected MMCC(2,6) approach provides the desired improvements in the description of triple bond breaking in N_2, reducing the 10–25 millihartree differences between the CR-CCSD(TQ),b and full CI energies at the intermediate and larger internuclear separations R to 4.0–4.5 millihartree (see section 3.1.4, particularly table 5 and figure 2). We must keep in mind, however, that the CISDtqph-corrected MMCC(2,6) approach requires that we select active orbitals for the CISDtqph calculations that are needed to construct wavefunction $|\Psi_0\rangle$ entering the MMCC(2,6) energy expression (58). In other words, although the CISDtqph-corrected MMCC(2,6) approach can be viewed as a non-iterative CC approximation that provides an excellent description of triple bond breaking, this method is not a pure 'black box' of the CCSD(T) or CCSD(TQ_f) type, since we must make some arbitrary decisions about active orbitals in order to carry out the related CISDtqph calculations (and these calculations increase the computer effort). We are very interested in developing 'black-box' equivalents of the highly successful CISDtqph-corrected MMCC(2,6) approach, in which it is sufficient to add the relatively simple non-iterative corrections to the CCSD energies, without relying on the *a priori* computed CI wavefunction $|\Psi_0\rangle$ that enters the MMCC expressions.

Downloaded At: 16:32 21 January 2011

Our test calculations for triple bond breaking in the DZ N_2 molecule demonstrate that at least some of the QMMCC methods satisfy the above criteria (see table 12 and figure 11). Clearly, all QMMCC approximations introduced in section 3.3.1 represent 'black-box' approaches, which solely rely on the T_1 and T_2 cluster components obtained in the CCSD calculations. At the same time, as shown in table 12 and figure 11, the QMMCC(2,6) and QMMCC(2,5) methods provide excellent results for triple bond breaking in the DZ N_2 molecule. As demonstrated in table 12, the complete QMMCC = QMMCC$(2,6)$ theory, based on equation (117), reduces the huge negative errors in the CCSD results for N_2 in the $R > 1.75R_e$ region and the non-negligible 13.517, 25.069 and 14.796 millihartree errors in the CR-CCSD(TQ),b results at $R = 1.75R_e$, $2R_e$ and $2.25R_e$ to 1.380, 6.230 and -3.440 millihartree, respectively. For smaller values of R, the errors in the QMMCC(2,6) results are ~1–2 millihartree (they are smaller than the errors resulting from the full CCSDT calculations). As shown in figure 11, the QMMCC = QMMCC$(2,6)$ potential for N_2 is virtually identical to the exact potential obtained with the full CI approach. The hump on the potential energy curve obtained with the QMMCC(2,6) method is considerably smaller than the hump on the CR-CCSD(TQ),b curve (cf. figure 11). In fact, the QMMCC(2,6) potential is a monotonically increasing function in the entire 2.068 bohr $\leq R \leq$ 4.35 bohr region ($R = R_e = 2.068$ bohr is the equilibrium bond length of N_2). The QMMCC(2,6) energies begin to decrease only when $R \approx 2.25R_e$, but even there the errors in the QMMCC(2,6) results, relative to full CI, are less (in absolute value) than 3.5 millihartree (cf. table 12 and figure 11). The dissociation energy D_e, obtained by

Downloaded At: 16:32 21 January 2011

Table 12. A comparison of the QMMCC(2,4), QMMCC(2,5) and QMMCC(2,6) ground-state energies with the results of the full CI, standard CC, completely renormalized CCSD(TQ) and CI-corrected MMCC(2,4), MMCC(2,5) and MMCC(2,6) calculations for a few internuclear separations R of the N_2 molecule with the DZ basis set.[a]

Method	$0.75R_e$	R_e[b]	$1.25R_e$	$1.5R_e$	$1.75R_e$	$2R_e$	$2.25R_e$
Full CI[c]	0.549 027	1.105 115	1.054 626	0.950 728	0.889 906	0.868 239	0.862 125
CCSD	3.132	8.289	19.061	33.545	17.714	−69.917	−120.836
CCSDT[d]	0.580	2.107	6.064	10.158	−22.468	−109.767	−155.656
CR-CCSD(TQ),a[c]	0.448	1.106	2.474	5.341	1.498	−40.784	−69.259
CR-CCSD(TQ),b[c]	0.451	1.302	3.617	8.011	13.517	25.069	14.796
MMCC(2,4)[e]	1.242	2.354	5.363	11.639	10.831	−16.086	−30.720
MMCC(2,5)[e]	1.220	2.089	3.527	5.493	1.631	−24.410	−39.124
MMCC(2,6)[e]	1.217	2.022	2.909	3.186	4.048	4.443	4.552
QMMCC(2,4)[f]	0.458	1.384	3.916	8.362	13.074	22.091	10.749
QMMCC(2,5)[f]	0.384	1.012	2.365	3.756	1.415	6.672	−2.638
QMMCC(2,6)[f]	0.384	1.012	2.373	3.784	1.380	6.230	−3.440
QMMCC(2,6) $(M_{ijklmn}^{abcdef}(2) = 0)$[f]	0.384	1.013	2.397	3.782	1.378	6.240	−3.418
QMMCC(2,6) $(M_{ijklm}^{abcde}(2) = M_{ijklmn}^{abcdef}(2) = 0)$[f]	0.387	1.040	2.533	4.317	2.062	4.674	−6.499

[a] The full CI total energies E, reported as $-(E + 108)$, are in hartree. The CC, MMCC and QMMCC energies are in millihartree relative to the corresponding full CI energy values. The lowest two occupied and the highest two unoccupied orbitals were frozen in correlated calculations.
[b] The equilibrium bond length, $R_e = 2.068$ bohr.
[c] From [43].
[d] From [45].
[e] From [171]. The active space consisted of the $3\sigma_g$, $1\pi_u$, $2\pi_u$, $1\pi_g$, $2\pi_g$ and $3\sigma_u$ orbitals.
[f] From [161].

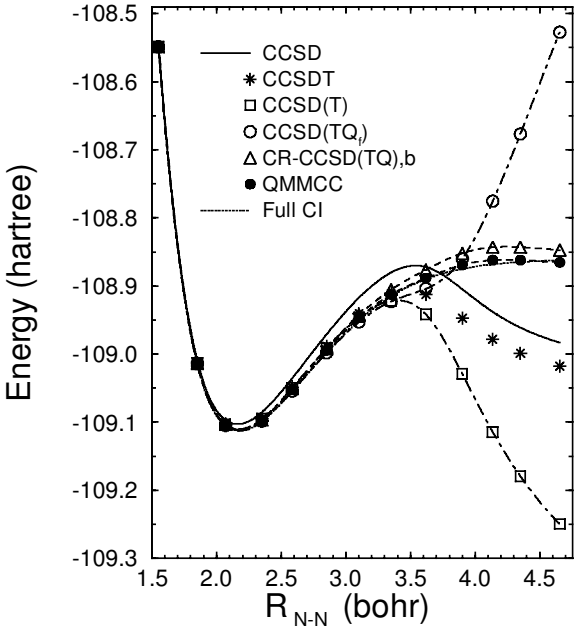

Figure 11. Potential energy curves for the DZ model of the N_2 molecule (energies in hartree and the N–N separation $R_{N\text{-}N}$ in bohr). A comparison of the results obtained with the QMMCC method (●) with the results of the CCSD (solid curve), CCSDT (*), CCSD(T) (□), CCSD(TQ_f) (○), CR-CCSD(TQ),b (△) and full CI (dotted curve) calculations (see [43, 161] for the original numerical data).

Downloaded At: 16:32 21 January 2011

forming the difference between the QMMCC(2,6) energies at $R = 4.35$ bohr and $R = R_e$, is 6.59 eV, in excellent agreement with the full CI value of D_e of 6.61 eV. Remarkably enough, the QMMCC(2,6) value of D_e is better than the D_e value obtained with the CISDtqph-corrected MMCC(2,6) theory (6.68 eV; cf. section 3.1.4). As demonstrated in figure 11 and table 12, the QMMCC(2,6) potential for N_2 is located above the exact, full CI, potential in the entire $R < 2.25R_e$ region, in spite of the apparently non-variational behaviour of the CCSD method at larger N–N separations. This clearly shows that the QMMCC theory is essentially a variational formalism which is capable of providing an excellent description for a large part of the N_2 potential.

On the basis of our experience with the CI-corrected MMCC methods, one might expect that lower-order QMMCC methods, such as QMMCC(2,5), should not work as well as the complete QMMCC(2,6) approximation at larger N–N separations (cf. section 3.1.4 for a discussion of the CI-corrected MMCC results for N_2; cf. also tables 5 and 12). Surprisingly enough, this is not the case. As shown in table 12, the QMMCC(2,5) method, defined by equation (121), which does not require the calculation of the hextuply excited $\mathcal{M}^{abcdef}_{ijklmn}(2)$ moments, provides the results of full QMMCC(2,6) quality. The QMMCC(2,5) approach reduces the large, 30–120 millihartree, unsigned errors in the CCSD results for N_2 in the $R \geq 1.5R_e$ region to 3.756 millihartree at $R = 1.5R_e$, 1.415 millihartree at $R = 1.75R_e$, 6.672 millihartree at $R = 2R_e$ and 2.638 millihartree at $R = 2.25R_e$. This should be confronted with the 24–39 millihartree errors in the CISDtqp-corrected MMCC(2,5) results in

the $2R_e \leq R \leq 2.25R_e$ region. What is perhaps even more surprising is the fact that we can ignore the most expensive $\mathcal{M}^{abcde}_{ijklm}(2)$ and $\mathcal{M}^{abcdef}_{ijklmn}(2)$ moments of the CCSD equations in the complete QMMCC or QMMCC(2,6) energy expression, equation (117), without changing the excellent QMMCC(2,6) results. The errors in the results of the QMMCC(2,6) calculations for N_2, in which the $\mathcal{M}^{abcdef}_{ijklmn}(2)$ moments are neglected, are practically identical to the very small errors resulting from the complete QMMCC(2,6) calculations (see table 12). There is a slight increase of errors when the $\mathcal{M}^{abcde}_{ijklm}(2)$ as well as the $\mathcal{M}^{abcdef}_{ijklmn}(2)$ moments are neglected, but the overall performance of the QMMCC(2,6) approximation, in which $\mathcal{M}^{abcde}_{ijklm}(2) = \mathcal{M}^{abcdef}_{ijklmn}(2) = 0$, is absolutely remarkable. For example, the QMMCC(2,6) potential obtained by zeroing $\mathcal{M}^{abcde}_{ijklm}(2)$ and $\mathcal{M}^{abcdef}_{ijklmn}(2)$ is a monotonically increasing function in the entire $R_e \leq R \leq 2R_e$ region. The QMMCC(2,6)($\mathcal{M}^{abcde}_{ijklm}(2) = \mathcal{M}^{abcdef}_{ijklmn}(2) = 0$) energies begin to decrease only when $R \approx 4.35$ bohr, but even there the errors in the QMMCC(2,6)($\mathcal{M}^{abcde}_{ijklm}(2) = \mathcal{M}^{abcdef}_{ijklmn}(2) = 0$) results are a few millihartree (see table 12). The dissociation energy D_e, obtained by forming the difference between the QMMCC(2,6)($\mathcal{M}^{abcde}_{ijklm}(2) = \mathcal{M}^{abcdef}_{ijklmn}(2) = 0$) energies at $R = 2R_e$ and $R = R_e$, is 6.54 eV, in very good agreement with the full CI D_e value of 6.61 eV. Similar calculations for the QMMCC(2,6)($\mathcal{M}^{abcdef}_{ijklmn}(2) = 0$) and QMMCC(2,5) methods give D_e values which are only slightly better than the QMMCC(2,6)($\mathcal{M}^{abcde}_{ijklm}(2) = \mathcal{M}^{abcdef}_{ijklmn}(2) = 0$) value of D_e (6.59 and 6.61 eV, respectively). As mentioned earlier, by neglecting the $\mathcal{M}^{abcde}_{ijklm}(2)$ and $\mathcal{M}^{abcdef}_{ijklmn}(2)$ moments of the CCSD equations in the QMMCC(2,6) calculations, we are largely preserving the cost of the CR-CCSD(TQ),b or QMMCC(2,4) calculations. Thus, we may be able to generate highly accurate PESs, corresponding to difficult cases of multiple bond breaking, which will differ from the exact PESs by at most a few millihartree, with the ease of use of the CR-CCSD(TQ),b or QMMCC(2,4) approximations by employing the QMMCC(2,6)($\mathcal{M}^{abcde}_{ijklm}(2) = \mathcal{M}^{abcdef}_{ijklmn}(2) = 0$) approach. If it turns out that this is not enough for some difficult applications, we can always resort to the higher-level QMMCC(2,5) theory or to the complete QMMCC(2,6) approximation.

Downloaded At: 16:32 21 January 2011

The successful description of triple bond breaking by the complete QMMCC(2,6) theory and its QMMCC(2,6)($\mathcal{M}^{abcde}_{ijklm}(2) = 0$), QMMCC(2,6)($\mathcal{M}^{abcde}_{ijklm}(2) = \mathcal{M}^{abcdef}_{ijklmn}(2) = 0$) and QMMCC(2,5) counterparts, combined with the common intuitions about the importance of pentuple and hextuple excitations in studies of triple bond breaking, suggests that the QMMCC methods must be capable of describing at least some effects due to higher-order T_5 and T_6 clusters. The highly factorized character of the QMMCC(2,6) and QMMCC(2,5) energy corrections, equations (118) and (122) (particularly the numerator terms $N^{\mathrm{QMMCC(2,6)}}$ and $N^{\mathrm{QMMCC(2,5)}}$, equations (119) and (123), respectively), suggests that those effects are being brought into the QMMCC calculations through some kind of factorization of the T_5 and T_6 energy contributions. If a future theoretical analysis could ever confirm this, this factorization of the T_5 and T_6 effects would be reminiscent of the factorization of the T_4 contributions exploited in the CCSD$(\mathrm{TQ_f})$ and CR-CCSD(TQ),x (x = a, b) methods. We are planning to explore this interesting aspect of the QMMCC theory in future papers.

The above examples clearly demonstrate that the new QMMCC theory enables us to preserve the 'black-box' character of the non-iterative CC methods, while providing us with a highly accurate description of ground-state PESs involving a breaking of single and multiple bonds. At this time, it seems to us that the

determination of the most expensive $\mathcal{M}^{abcdef}_{ijklmn}(2)$ moments of the CCSD equations, corresponding to the projections of these equations on the hextuply excited configurations, is a waste of computer time, since there is practically no difference between the QMMCC(2,6) results with and without these moments. We may even ignore the pentuply excited moments $\mathcal{M}^{abcde}_{ijklm}(2)$ and still obtain an excellent description of single and multiple bond breaking, as long as we retain the specific many-body structure of the QMMCC(2,6) and QMMCC(2,5) energy corrections, equations (118)–(120) and (122)–(124), respectively. As in the recent studies by Van Voorhis and Head-Gordon [216], the incorporation of the quadratic $(\Sigma^{\dagger})^2$ terms in equations (107) or (110) that bring various product terms involving the T and $T^{\dagger}$ components is the key to successful description of multiple bond breaking by the QMMCC formalism.

3.4. *Size extensivity of the MMCC methods: the approximate size extensivity of the CR-CCSD(T) approach*

As already mentioned in section 2.1, depending on the explicit form of the 'trial' wavefunction $|\Psi_0\rangle$ and depending on the approximations that are used to design the specific form of the non-iterative correction $\delta_0^{(A)}$, the results of the MMCC calculations for ground electronic states may not be strictly size extensive. This, in particular, applies to the CR-CCSD[T], CR-CCSD(T) and CR-CCSD(TQ) calculations. A similar remark applies to the CI-corrected MMCC calculations for excited states, in which the non-iterative corrections $\delta_K^{(A)}$ are added to the EOMCC energies. Since the issue of size extensivity is important from the point of view of applications, we address this issue here.

Downloaded At: 16:32 21 January 2011

First, let us clarify a few important points related to the issue of size extensivity in quantum-chemical calculations. Size extensivity is often defined as the absence of unlinked terms (diagrams) in the wavefunction and energy expressions. This is the definition adopted throughout the present work. The unlinked terms are evidently absent in the wavefunction and energy expressions defining the standard CC methods, including CCSD, CCSDT, CCSD(T), etc., by virtue of the linked and connected cluster (or diagram) theorems [229–233] that serve as a formal basis of all CC theories (cf., for example, [15, 18] for a thorough discussion and further historical remarks) and because of the use of the explicitly connected equations, such as equations (5) and (8), in the standard CC calculations. In consequence, the total CC energy always displays the correct dependence on the size of a given many-electron (e.g. molecular) system. For example, the total energy of a system composed of a number of non-interacting closed-shell atoms and molecules, obtained from any type of standard, closed-shell, CC calculation, equals the sum of energies of individual atoms and molecules constituting this system. This behaviour of CC energy is obviously very important when we go from one molecule to an ensemble of molecules. All standard CC theories will always provide us with the correct dependence of the total energy on the size of a molecular system, as described above. An example of the correct dependence of the CC energy on the size of the molecular system is shown in table 13, where we measure the size extensivity of the CCSD[T], CCSD(T), CR-CCSD[T] and CR-CCSD(T) energies by subtracting the sum of energies of two and three isolated glycine molecules (each glycine is a 40-electron system) from the energies of the glycine dimer and trimer consisting of the glycine molecules separated by a very large (200 bohr) distance. In this particular example, we used the glycine isomer GLY12, found by Jensen and Gordon [234], and

Table 13. The size extensivity calculations for the CCSD[T], CCSD(T), CR-CCSD[T] and CR-CCSD(T) methods. The energy of two or three glycine (GLY12 [234]) molecules is subtracted from the energy of the corresponding glycine dimer or trimer consisting of the glycine molecules separated by distance(s) of 200 bohr. The calculations were performed with the 6-31G basis set, assuming the AM1 structure of the GLY12 isomer of glycine [234], and using the CC programs implemented in GAMESS [158]. The units for energy are millihartree and (in parentheses) kcal mol^{-1}.

	CCSD[T]	CCSD(T)	CR-CCSD[T]	CR-CCSD(T)
$E(2\,\mathrm{GLY12}) - 2E(\mathrm{GLY12})$	$-5. \times 10^{-5}$ $(-3. \times 10^{-5})$	$-5. \times 10^{-5}$ $(-3. \times 10^{-5})$	3.872 32 (2.429 92)	3.488 68 (2.189 18)
$E(3\,\mathrm{GLY12}) - 3E(\mathrm{GLY12})$	-1.1×10^{-4} (-6.8×10^{-5})	-1.1×10^{-4} (-6.8×10^{-5})	10.043 39 (6.302 33)	9.078 22 (5.696 67)

the standard 6-31G basis set [235], as implemented in GAMESS [159], to perform the relevant calculations. All calculations were performed with the new CCSD[T], CCSD(T), CR-CCSD[T] and CR-CCSD(T) programs incorporated into the June 2002 release of GAMESS [158]. As expected, the standard CCSD[T] and CCSD(T) energies, which are based on the explicitly connected energy expressions, equations (81) and (82), provide the perfectly size-extensive description of a system of two and three non-interacting glycine molecules.

Downloaded At: 16:32 21 January 2011

The fact that all standard CC approximations provide a size-extensive description of many-electron systems, in the sense described above, does not necessarily imply that we can use them to describe the molecular fragmentation leading to chemical bond breaking. This paper is full of examples showing the failures of the standard CC approximations for various types of bond-breaking phenomena. Interestingly enough, many methods that are not size extensive, such as MRCI, which are based on using the energy expansions containing unlinked terms, provide a reasonable description of bond breaking. Thus, the relationship between size extensivity, as defined by the absence of unlinked terms (diagrams) in the energy and wavefunction expressions, and the ability of a given method to provide an accurate description of bond breaking, is not a simple one. This has already been demonstrated in figure 10(*a*), which shows the one-dimensional cut of the ground-state PES of the BeFH system in the Be + HF limit. The strict size extensivity of the standard CCSD(T) approach (i.e. the fully connected character of the CCSD(T) energy expression) implies, in this case, only one thing: the poor performance of the standard CCSD(T) method for the potential energy curve of the isolated HF molecule propagates into the calculation for the BeFH system. Another illustration of the same type is provided in figure 12(*a*), where we show the entire potential energy curve of the HF molecule, obtained in the CCSD(T) calculations, in the presence of one, three and five Ne atoms located at very large distances from HF and from one another (we used a separation of 100 bohr between the HF molecule and the nearest Ne atom, the next Ne atom is 200 bohr from HF, etc.; all calculations were performed using the DZ basis set [165]). In the perfectly size-extensive calculations, such as CCSD(T), the only effect that the Ne atoms can have on the energy of HF is changing this energy by the energy of the added Ne atoms. Thus, if we shift the potential energy curves for the dissociation of the HF molecule in the HF + nNe systems by the energies of the added Ne atoms, we must obtain the HF

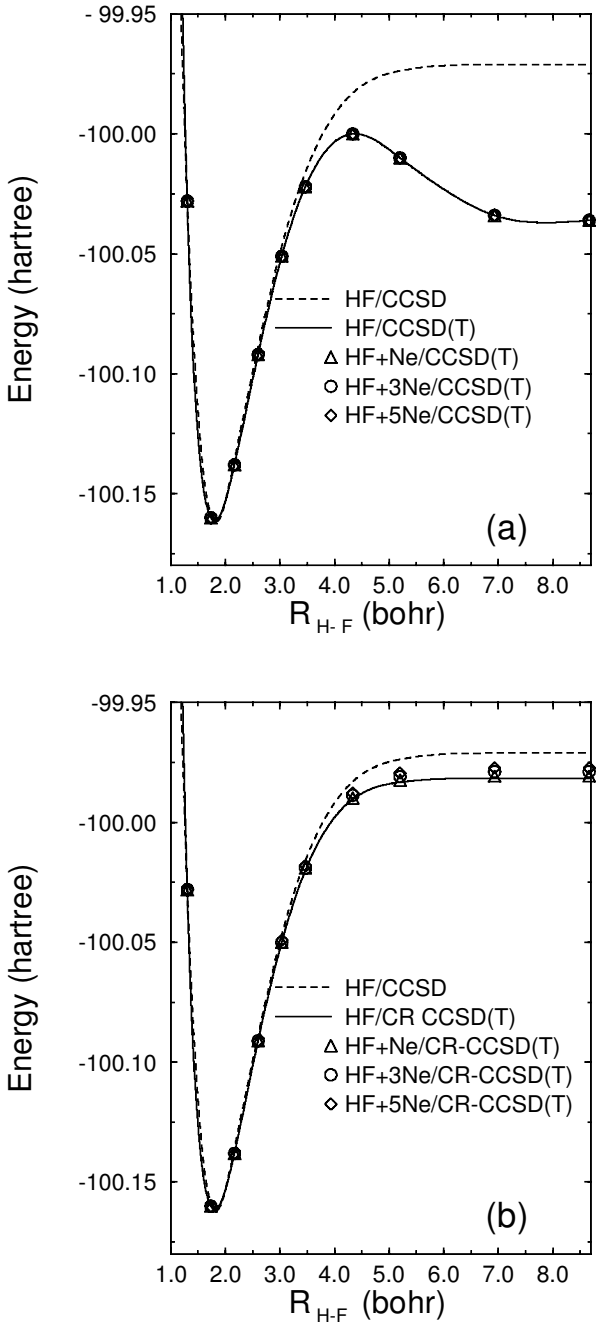

Figure 12. Potential energy curves of the HF molecule (energies in hartree, the H–F separation $R_{H\text{-}F}$ in bohr) in the presence of one (△), three (○) and five (◇) Ne atoms located at very large distances from HF and from one another (the Ne atom nearest to the HF molecule is separated from it by 100 bohr, the second, third, etc. Ne atoms are separated from HF by 200, 300, etc. bohr). The results of the (*a*) CCSD(T) and (*b*) CR-CCSD(T) calculations using the DZ basis set. The HF potentials corresponding to the HF + *n*Ne systems are shifted by the energies of the Ne atoms. The dashed curves represent the CCSD potential.

Downloaded At: 16:32 21 January 2011

potentials that coincide with one another, independent of the number of the added Ne atoms. This is exactly what we observe in the CCSD(T) calculations, whose results are shown in figure 12(*a*). Unfortunately, since the standard CCSD(T) approach fails to describe bond breaking in the isolated HF system, the analogous CCSD(T) curves for the HF + *n*Ne systems are as poor as in the case of a single HF molecule. As we can see, the absence of unlinked terms in the CCSD(T) energy expression does not help us to restore the correct description of the H–F bond breaking in the HF + *n*Ne systems.

In trying to understand this problem, we must, first of all, realize that standard CC methods can provide a correct description of a fragmentation process

$$\mathrm{XY} \rightarrow \mathrm{X} + \mathrm{Y} \tag{130}$$

only if the reference configuration $|\Phi_{\mathrm{XY}}\rangle$ of system XY factorizes into a product of references $|\Phi_{\mathrm{X}}\rangle$ and $|\Phi_{\mathrm{Y}}\rangle$ of subsystems X and Y in the X + Y limit (the only exception to this rule is provided by the exact, full CC or full CI, approach, which is, of course, rigorously size extensive, independent of the behaviour of $|\Phi_{\mathrm{XY}}\rangle$ in the X + Y limit). The RHF configuration, used as a reference in the spin-adapted CC calculations for singlet electronic states, does not separate correctly in the X + Y limit if X and Y are open-shell fragments. In consequence, all standard RHF-based CC methods fail to provide a correct description of the separation of the closed-shell system XY into open-shell fragments X and Y, in spite of the apparently connected character of the CC energy expressions. This is exactly what happens when the HF molecule dissociates into the H and F atoms or when the ethane molecule dissociates into two methyl radicals. Second, the importance of the terms 'linked', 'unlinked', 'connected', 'disconnected', etc. becomes less clear in a situation such as bond breaking, where the MBPT series, used to define all those terms, is no longer summable. For example, the MBPT expansion of the CCSD(T) energy contains only connected terms. Each of those connected terms has a correct size dependence, as shown in the calculations of the HF potential in the HF + *n*Ne systems. This does not mean, however, that those terms alone guarantee the correct description of bond breaking. It is, therefore, not unthinkable to have a situation where the selected unlinked terms in the MBPT energy expansion help to restore the correct behaviour of energy in the bond-breaking region. A good example of the behaviour of this type is provided by any limited CI method, including, for example, MRCISD. The selected unlinked terms present in the CI energies are ultimately responsible for the variational behaviour of the CI theory, independent of the nuclear geometry. If those terms are carefully selected, as is done in MRCISD, we can actually retain the variational and, simultaneously, fairly accurate description of PESs involving bond breaking. Without those unlinked terms, the MRCISD method could have suffered from the pathological (non-variational) behaviour characterizing the standard CC theories. Ideally, we would like to use a genuine MRCC formalism which is both accurate and has no unlinked diagrams in it (i.e. is rigorously size extensive), but there has not been much success in formulating a robust and relatively simple MRCC theory that could be routinely used in calculations of molecular PESs for all kinds of molecular systems.

Very similar remarks apply to various MMCC calculations, including the calculations employing the CR-CCSD(T) approach. All MMCC approximations are based on the asymmetric energy expressions defining the MMCC functionals, equations (23) or (35). The MMCC functionals and the resulting corrections $\delta_0^{(\mathrm{A})}$ or

Downloaded At: 16:32 21 January 2011

$\delta_K^{(A)}$ can provide the exact (and, thus, size-extensive) energies, when the wavefunctions $|\Psi_0\rangle$ or $|\Psi_K\rangle$ are exact. In fact, as mentioned in section 3.3.1, the ground-state corrections $\delta_0^{(A)}$, added to standard CC energies, can lead to perfectly size-extensive results as long as the wavefunctions $|\Psi_0\rangle$ have the CC-like exponential form. In general, however, we do not have to insist on strict size extensivity in defining the MMCC approximations, particularly if this immediately leads to new formal complications and large computer costs, since there may exist judicious choices of wavefunctions $|\Psi_0\rangle$ or $|\Psi_K\rangle$ that lead to approximately size-extensive methods while allowing us to obtain a very good description of bond breaking with a little computational effort and with an ease of use of the 'black-box' methods of the CCSD(T) type. For example, if a given choice of $|\Psi_0\rangle$ or $|\Psi_K\rangle$ in the MMCC energy formulae leads to energies that are very close to the exact, full CI, energies for a wide range of molecular applications, we can certainly hope that the resulting energies are also approximately size extensive. The introduction of selected unlinked terms into the MMCC energy expressions may help us to restore high accuracy at larger internuclear separations, which is completely lost if we insist on using the connected energy expansions defining the standard CC theories. Ideally, we would like to use size-extensive theories, which are defined by the fully connected energy expressions and which also break chemical bonds, but, if we have to choose between the strict size extensivity and the high accuracy at larger internuclear separations obtained at the low computer cost for a relatively wide range of molecular systems, we may as well decide to choose the latter option. In making this decision, however, we should always make sure that we fully understand the consequences of introducing unlinked terms into the energy expansions for calculations for larger many-electron systems.

Downloaded At: 16:32 21 January 2011

Let us illustrate those consequences by a few examples of calculations with the MMCC-based CR-CCSD(T) method. The CR-CCSD(T) energy expression, equations (62) or (70), is not fully connected; there are unlinked (in this case, disconnected) terms in the non-iterative energy correction $N^{\mathrm{CR(T)}}/D^{\mathrm{(T)}}$ leading to some size inextensivity errors (cf. the discussion below for further analysis). In table

Table 14. The departure from size extensivity in the CR-CCSD(T) calculations for the HF + *n*Ne systems, as a function of the H–F separation $R_{\mathrm{H\text{-}F}}$ (in multiples of the equilibrium bond length $R_e = 1.7328$ bohr) and the number of Ne atoms added to HF (*n*). The numbers in the table are the values of $\Delta E(\mathrm{HF} + n\mathrm{Ne})$, equation (131) (in millihartree), obtained with the DZ basis set, assuming that the Ne atom nearest to the HF molecule is separated from it by 100 bohr and assuming that the second, third, etc. Ne atoms are separated from HF by 200, 300, etc. bohr.

$R_{\mathrm{H\text{-}F}}$	$n = 1$	$n = 2$	$n = 3$	$n = 5$
R_e	0.077	0.215	0.411	0.963
$1.5R_e$	0.147	0.350	0.607	1.268
$2R_e$	0.351	0.746	1.183	2.172
$3R_e$	0.886	1.790	2.711	4.601
$4R_e$	1.020	2.053	3.099	5.223
$5R_e$	1.031	2.074	3.128	5.270

14 and figure 12(*b*), we show the results of the CR-CCSD(T) calculations of the entire potential energy curve of the HF molecule in the presence of from one to five Ne atoms located at a very large distance from HF and from one another (as in the analogous CCSD(T) calculation shown in figure 12(*a*), we used a separation of 100 bohr between the HF molecule and the nearest Ne atom; the next Ne atom is 200 bohr from HF, etc.; all calculations were performed with a DZ basis set [165]). As in figure 12(*a*), all HF potentials shown in figure 12(*b*) are shifted by the energies of the added Ne atoms, so that if a given quantum-chemical method employed in those calculations was strictly size extensive the resulting potential energy curves would coincide. The CR-CCSD(T) method is not strictly size extensive, so that the CR-CCSD(T) potential energy curves for the HF + *n*Ne systems, shifted by the energies of the Ne atoms, are not perfectly identical to one another. However, they virtually coincide, particularly in the equilibrium region and for smaller stretches of the H–F bond (H–F separations $R_{H\text{-}F}$ up to twice the equilibrium bond length in HF). Even for larger H–F separations, where the standard CCSD(T) method completely fails, the departure from the perfectly size-extensive behaviour in the CR-CCSD(T) calculations is on the order of a few millihartree. This can be seen in figure 12(*b*) and by analysing the results in table 14.

Downloaded At: 16:32 21 January 2011

The departure from the perfectly size-extensive description of the HF + *n*Ne systems by the CR-CCSD(T) approach can be measured by calculating the energy difference

$$\Delta E(\mathrm{HF} + n\mathrm{Ne}) = E^{\text{CR-CCSD(T)}}(\mathrm{HF} + n\mathrm{Ne}) - [E^{\text{CR-CCSD(T)}}(\mathrm{HF}) + nE^{\text{CR-CCSD(T)}}(\mathrm{Ne})] \qquad (131)$$

as a function of the internuclear separation $R_{H\text{-}F}$ and the number of added Ne atoms. As shown in table 14, adding one Ne atom (i.e. doubling the size of the system; the Ne atom has as many electrons as the HF molecule) produces results that differ from the perfectly size-extensive description by a fraction of a millihartree (1 millihartree at most), independent of the value of $R_{H\text{-}F}$. Even when we add five neon atoms (increasing the number of electrons from 10 in HF to 60 in the combined HF + 5Ne system), the size inextensivity error defined by equation (131) is 1–2 millihartree for $R_{H\text{-}F} \leq 2R_e$ and ~5 millihartree for $R_{H\text{-}F} = 5R_e$. As a matter of fact, the CR-CCSD(T) results for the much larger HF + 10Ne system are almost identical to the analogous results for the HF + 5Ne system shown in figure 12(*b*) and table 14. Clearly, the potential energy curves for the HF + *n*Ne systems resulting from the CR-CCSD(T) calculations are much better than the corresponding CCSD(T) curves shown in figure 12(*a*). For example, the CR-CCSD(T) method provides a very reasonable description of the asymptotic region, where the H–F distances become large, independent of the number of the added Ne atoms. The loss of accuracy in this region due to the lack of size extensivity of the CR-CCSD(T) method is very small compared with the magnitude of improvements in the poor CCSD(T) results that the CR-CCSD(T) method offers in the region of large $R_{H\text{-}F}$ values.

Very similar remarks apply to the HF + HF system, in which we examine the effect of adding an HF molecule, located at a very large distance (100 bohr) from the original HF molecule, on the potential energy curve of the original HF molecule. We studied several cases, characterized by the gradually increasing level of complexity, including the situation where the added HF molecule is at its equilibrium geometry, the situation where the added HF molecule is slightly stretched (by a factor of 1.5 or

less) and the situations where the added HF molecule is significantly stretched (by a factor of 2 or 3). Adding the HF molecule at its equilibrium geometry to the dissociating HF system is more or less equivalent to adding the closed-shell Ne atom, which is characterized by the relatively small correlation effects. However, adding the stretched HF molecule to the dissociating HF system is equivalent to adding a quasi-degenerate system characterized by a large degree of non-dynamic correlation.

In analogy to the HF + nNe systems, the departure from perfectly size-extensive behaviour of the CR-CCSD(T) energies of the HF + HF system can be assessed by calculating the energy difference

$$\Delta E[\mathrm{HF}(\mathrm{R_{H\text{-}F}}) + \mathrm{HF}(nR_e)] = E^{\mathrm{CR\text{-}CCSD(T)}}[\mathrm{HF}(\mathrm{R_{H\text{-}F}}) + \mathrm{HF}(nR_e)] - \{E^{\mathrm{CR\text{-}CCSD(T)}}[\mathrm{HF}(\mathrm{R_{H\text{-}F}})] + E^{\mathrm{CR\text{-}CCSD(T)}}[\mathrm{HF}(nR_e)]\} \quad (132)$$

as a function of the H–F separation $R_{\mathrm{H\text{-}F}}$ in the first HF molecule and the magnitude of the stretch of the H–F bond in the second (spectator) HF molecule (expressed in multiples of the equilibrium bond length R_e). In the perfectly size-extensive description, the total energy of the HF + HF system should always be equal to the sum of the energies of the isolated HF molecules having the same bond lengths as in the combined HF + HF system. Thus, the energy difference $\Delta E[\mathrm{HF}(\mathrm{R_{H\text{-}F}}) + \mathrm{HF}(nR_e)]$, equation (132), should be zero, independent of the H–F distances in both HF molecules (i.e. independent of $R_{\mathrm{H\text{-}F}}$ and n). As shown in table 15, where we report the values of $\Delta E[\mathrm{HF}(\mathrm{R_{H\text{-}F}}) + \mathrm{HF}(nR_e)]$ obtained with the DZ basis set [165], $\Delta E[\mathrm{HF}(\mathrm{R_{H\text{-}F}}) + \mathrm{HF}(nR_e)]$ is never zero for the CR-CCSD(T) method. However, adding the HF molecule at its equilibrium geometry or adding the slightly stretched HF molecule (stretched by a factor of 1.5) to the dissociating HF system introduces very small size inextensivity errors that range between 0.1 millihartree for $R_{\mathrm{H\text{-}F}} = R_e$ and 0.9–1.5 millihartree for $R_{\mathrm{H\text{-}F}} = 5R_e$ (see table 15). This should be compared with the 0.500 and 1.650 millihartree errors in the CR-CCSD(T) results at $R_{\mathrm{H\text{-}F}} = R_e$ and $5R_e$, respectively, for the isolated HF molecule

Downloaded At: 16:32 21 January 2011

Table 15. The departure from size extensivity in the CR-CCSD(T) calculations for the HF + HF system, as a function of the H–F separation $R_{\mathrm{H\text{-}F}}$ in the first HF molecule, for the selected values of the stretch of the H–F bond in the second HF molecule (nR_e; the H–F distances in both HF molecules are in multiples of the equilibrium bond length $R_e = 1.7328$ bohr). The numbers in the table are the values of $\Delta E[\mathrm{HF}(\mathrm{R_{H\text{-}F}}) + \mathrm{HF}(nR_e)]$, equation (132) (in millihartree), obtained with the DZ basis set, assuming that both HF systems are separated by 100 bohr.

$R_{\mathrm{H\text{-}F}}$	$n = 1$	$n = 1.5$	$n = 2$	$n = 3$
R_e	0.076	0.140	0.321	0.765
$1.5R_e$	0.140	0.254	0.573	1.334
$2R_e$	0.321	0.573	1.272	2.913
$3R_e$	0.765	1.334	2.913	6.859
$4R_e$	0.863	1.495	3.254	7.776
$5R_e$	0.870	1.507	3.291	7.946

and the much larger 53.183 millihartree error in the result of the standard CCSD(T) calculations for isolated HF with $R_{H-F} = 5R_e$ (see table 1). Adding the equilibrium or slightly stretched HF system to the dissociating HF molecule introduces the size inextensivity errors that are comparable to the small errors characterizing the CR-CCSD(T) calculations for the potential energy curve of HF and that are orders of magnitude smaller than the huge errors at larger values of $R_{H\text{-}F}$ produced by the standard CCSD(T) theory.

The situation slightly changes when we add the significantly stretched HF system to the dissociating HF molecule. In this case, the size inextensivity errors characterizing the CR-CCSD(T) results, as defined by $\Delta E[\mathrm{HF}(\mathrm{R_{H\text{-}F}}) + \mathrm{HF}(nR_e)]$, equation (132), are somewhat larger, particularly when $R_{H\text{-}F}$ is large (cf. the 7.946 millihartree size inextensivity error when $R_{H\text{-}F} = 5R_e$ and when the added HF molecule is stretched by a factor of 3, reported in table 15), but the overall performance of the CR-CCSD(T) method in describing bond breaking in HF in the presence of another HF molecule remains quite good (much better than in the CCSD(T) case). From the purely pragmatic point of view, we can definitely claim that the dissociation of one of the two HF molecules in the HF + HF system is correctly described by the CR-CCSD(T) approach. The somewhat larger values of $\Delta E[\mathrm{HF}(\mathrm{R_{H\text{-}F}}) + \mathrm{HF}(nR_e)]$, which we observe in the region of larger $R_{H\text{-}F}$ and n, are a consequence of the fact that the CR-CCSD(T) method cannot provide a highly accurate description of multiple bond breaking. The large R_{H-F} and n values in the definition of $\Delta E[\mathrm{HF}(\mathrm{R_{H\text{-}F}}) + \mathrm{HF}(nR_e)]$, equation (132), correspond to a simultaneous breaking of both H–F bonds in the HF + HF system, causing the errors in the CR-CCSD(T) results to grow to 7–8 millihartree (cf. table 15). We can always improve the results in cases like this and reduce the size inextensivity errors by switching to the higher-level CR-CCSD(TQ),b formalism or to the QMMCC theory described in section 3.3.

Downloaded At: 16:32 21 January 2011

As already mentioned, the approximate MMCC methods, including CR-CCSD(T), are not strictly size extensive, since all MMCC approximations are derived from the asymmetric energy expressions defining the MMCC functionals, equations (23) or (35), which we truncate before insisting on the fully connected structure of the resulting energy expressions. The MMCC functionals, equations (23) or (35), do not use the intermediate normalization exploited in the standard CC theory and this may lead to the introduction of the unlinked (disconnected) terms into the resulting energies. The disconnected terms in the MMCC energies are related primarily to the presence of the overlap denominators, such as the $\langle \Psi_0 | \mathrm{e}^{T^{(\mathrm{A})}} | \Phi \rangle$ denominator entering the formula for the ground-state correction $\delta_0^{(\mathrm{A})}$, equation (9). This can be seen by examining the basic equations of the CR-CCSD(T) method, in which we correct the CCSD energy with the completely renormalized triples correction of the MMCC(2,3) type.

Indeed, as shown in section 3.2.1, the CR-CCSD(T) formula can be given the following form (cf. equation (70)):

$$E^{\mathrm{CR\text{-}CCSD(T)}} = E^{\mathrm{CCSD}} + \delta^{\mathrm{CR(T)}}, \tag{133}$$

where

$$\delta^{\mathrm{CR(T)}} = N^{\mathrm{CR(T)}}/D^{(\mathrm{T})}, \tag{134}$$

with $N^{\mathrm{CR(T)}}$ and $D^{(\mathrm{T})}$ defined by equations (74) and (78), respectively. The CCSD method is rigorously size extensive, so it is sufficient to focus on the non-iterative

correction $\delta^{\mathrm{CR(T)}}$, equation (134), in our analysis. The numerator $N^{\mathrm{CR(T)}}$ is an explicitly connected quantity (moments $\mathcal{M}^{abc}_{ijk}(2)$ that enter the formula for $N^{\mathrm{CR(T)}}$ are connected), so that the value of $N^{\mathrm{CR(T)}}$ for system XY in the X + Y limit is the sum of the $N^{\mathrm{CR(T)}}$ values for subsystems X and Y,

$$N^{\mathrm{CR(T)}}(\mathrm{X}+\mathrm{Y}) = N^{\mathrm{CR(T)}}(\mathrm{X}) + N^{\mathrm{CR(T)}}(\mathrm{Y}), \tag{135}$$

if the reference configuration $|\Phi_{\mathrm{XY}}\rangle$ of system XY factorizes into a product of references $|\Phi_{\mathrm{X}}\rangle$ and $|\Phi_{\mathrm{Y}}\rangle$ of subsystems X and Y in the same limit. If $D^{(\mathrm{T})}$ was equal to 1, the correction $\delta^{\mathrm{CR(T)}}$ and the total CR-CCSD(T) energy were perfectly size extensive. However, the denominator $D^{(\mathrm{T})}$ is always greater than 1 (cf., for example, section 3.2.2.1 for examples of typical values of $D^{(\mathrm{T})}$). As shown earlier (cf. equations (85) and (86)),

$$D^{(\mathrm{T})} = 1 + \chi, \tag{136}$$

where

$$\chi = \langle \Phi | T_2^\dagger T_2 | \Phi \rangle + O(V_{\mathrm{N}}^4), \tag{137}$$

with $O(V_N^4)$ representing the fourth- and higher-order terms in perturbation V_{N}. Assuming that cluster amplitudes defining T_2 are relatively small, so that $\chi < 1$, we can write

$$\delta^{\mathrm{CR(T)}} = N^{\mathrm{CR(T)}}/(1+\chi) = N^{\mathrm{CR(T)}} - N^{\mathrm{CR(T)}}\chi + \cdots. \tag{138}$$

The first term in the many-body expansion of correction $\delta^{\mathrm{CR(T)}}$ is connected. However, the $N^{\mathrm{CR(T)}}\chi$ term and all higher-order terms in equation (138) are apparently disconnected, introducing the size inextensivity errors into the CR-CCSD(T) results. Assuming further that $\chi \ll 1$ and assuming that we can approximate χ by the leading $\langle \Phi | T_2^\dagger T_2 | \Phi \rangle$ term, we obtain

$$\chi(\mathrm{X}+\mathrm{Y}) \approx \chi(\mathrm{X}) + \chi(\mathrm{Y}), \tag{139}$$

so that

$$\begin{aligned}\delta^{\mathrm{CR(T)}}(\mathrm{X}+\mathrm{Y}) &\approx N^{\mathrm{CR(T)}}(\mathrm{X}+\mathrm{Y})[1-\chi(\mathrm{X}+\mathrm{Y})] \\ &\approx [N^{\mathrm{CR(T)}}(\mathrm{X}) + N^{\mathrm{CR(T)}}(\mathrm{Y})][1-\chi(\mathrm{X})-\chi(\mathrm{Y})] \\ &= N^{\mathrm{CR(T)}}(\mathrm{X})[1-\chi(\mathrm{X})] + N^{\mathrm{CR(T)}}(\mathrm{Y})[1-\chi(\mathrm{Y})] - \Delta,\end{aligned} \tag{140}$$

where

$$\Delta = N^{\mathrm{CR(T)}}(\mathrm{X})\chi(\mathrm{Y}) + N^{\mathrm{CR(T)}}(\mathrm{Y})\chi(\mathrm{X}). \tag{141}$$

Approximating corrections $\delta^{\mathrm{CR(T)}}$ for subsystems X and Y by the first two terms in expansion (138), we obtain

$$\delta^{\mathrm{CR(T)}}(\mathrm{X}+\mathrm{Y}) \approx \delta^{\mathrm{CR(T)}}(\mathrm{X}) + \delta^{\mathrm{CR(T)}}(\mathrm{Y}) - \Delta, \tag{142}$$

where Δ, equation (141), describes the departure from the perfectly size-extensive behaviour of the CR-CCSD(T) theory. Clearly, if the $D^{(\mathrm{T})}$ denominators for subsystems X and Y were both 1, so that the $\chi(\mathrm{X})$ and $\chi(\mathrm{Y})$ contributions vanished, the size inextensivity error Δ, equation (141), would be zero. This shows that the main reason for the departure from the perfectly size-extensive behaviour of the CR-

Downloaded At: 16:32 21 January 2011

CCSD(T) theory is the presence of the $D^{(T)}$ denominator in the CR-CCSD(T) energy expression.

The above analysis was based on the assumption that $\chi \ll 1$, which is true only when the T_1 and T_2 cluster amplitudes are small. In this case, the $D^{(T)}$ denominator is close to 1, so that it is rather unlikely that the effects of size inextensivity of the CR-CCSD(T) method are serious in situations of this type. The situation becomes more complicated in the bond-breaking region, where the $D^{(T)}$ denominators become large because of large T_1 and T_2 values. In this case, χ is always significantly greater than 1 (cf., for example, the examples discussed in section 3.2.2.1), so that it is quite difficult to predict how the denominator $D^{(T)}$ relates to the size inextensivity errors in the CR-CCSD(T) calculations. In order to obtain some insights into the role of the $D^{(T)}$ denominator in causing the size-inextensive behaviour of the CR-CCSD(T) theory, we decided to compare the actual values of $D^{(T)}$, resulting from the aforementioned calculations for the HF + nNe systems, in which we examined the dissociation of HF in the presence of the Ne atoms at a very large distance from HF, with the idealized values of $D^{(T)}$ that are defined by imposing a condition that the ideal correction $\delta^{CR(T)}$ (designated here as $\delta^{CR(T)}_{ideal}$) is rigorously size extensive.

Here is the procedure that we used to define the idealized values of $D^{(T)}$. In order to enforce the strict size extensivity on the completely renormalized triples correction $\delta^{CR(T)}$, so that

$$\delta^{CR(T)}_{ideal}(X + Y) = \delta^{CR(T)}_{ideal}(X) + \delta^{CR(T)}_{ideal}(Y) \tag{143}$$

in the non-interacting, X + Y, limit of system XY, we define the ideal denominator $D^{(T)}$ in this limit (designated as $D^{(T)}_{ideal}(X + Y)$) as follows:

$$D^{(T)}_{ideal}(X + Y) = \frac{N^{CR(T)}(X) + N^{CR(T)}(Y)}{N^{CR(T)}(X)/D^{(T)}(X) + N^{CR(T)}(Y)/D^{(T)}(Y)}. \tag{144}$$

On the basis of the fact that the numerator $N^{CR(T)}$ is an explicitly connected quantity, so that it satisfies equation (135), one can easily verify that the ideal completely renormalized triples correction

$$\delta^{CR(T)}_{ideal}(X + Y) \equiv N^{CR(T)}(X + Y)/D^{(T)}_{ideal}(X + Y) \tag{145}$$

satisfies the size extensivity condition (143), if $D^{(T)}_{ideal}(X + Y)$ is given by equation (144). Clearly, the ideal denominator $D^{(T)}_{ideal}(X + Y)$, equation (144), is defined in a rather artificial (and, hence, impractical) manner, which depends on the type of fragmentation a given system undergoes. It is useful, however, to consider this idealized form of the denominator $D^{(T)}$, equation (144), since we can calculate its values for a given molecular system consisting of non-interacting fragments X and Y (using the values of $N^{CR(T)}$ and $D^{(T)}$ for individual subsystems X and Y) and compare the results with the actual values of $D^{(T)}$ resulting from the CR-CCSD(T) calculations in the non-interacting, X + Y, limit. The above definition of $D^{(T)}_{ideal}(X + Y)$ applies to a fragmentation of a given system into two subsystems. This includes cases such as the fragmentation of the HF + Ne system into the isolated HF molecule (having the same H–F bond length as in the HF + Ne system) and Ne. If we have to deal with several non-interacting fragments, as is the case for the HF + nNe systems with $n > 1$, we have to generalize equation (144) by imposing the condition that the ideal correction $\delta^{CR(T)}$ of the entire system is a sum of corrections $\delta^{CR(T)}$ of all non-interacting fragments.

Downloaded At: 16:32 21 January 2011

We used equation (144) and its generalization to an arbitrary number of non-interacting fragments to analyse the dependence of the CR-CCSD(T) denominator $D^{(T)}$, and its idealized $D^{(T)}_{ideal}$ analogue leading to a perfectly size-extensive description, on the H–F separation in HF in the HF + nNe systems with several values of n. As in the case of the results reported in figure 12 and table 14, we used the DZ basis set. The behaviour of the actual and ideal denominators $D^{(T)}$ for the HF + nNe systems is shown in figure 13.

As we can see, all denominators $D^{(T)}$ and $D^{(T)}_{ideal}$ display the same general behaviour, i.e. they are close to 1 around the equilibrium H–F distance, $R_{H\text{-}F} = R_e = 1.7328$ bohr, while increasing their values (to 2.0–2.6) for large values of $R_{H\text{-}F}$. As mentioned in the earlier sections, this behaviour of denominators $D^{(T)}$ is typical for all MMCC calculations. In general, the $\langle \Psi_0 | e^{T^{(A)}} | \Phi \rangle$ denominators increase their values for stretched nuclear geometries, damping in this way the non-iterative corrections to standard CC energies due to higher-order clusters, which are always grossly overestimated by the conventional approaches of the CCSD(T) type. As shown in figure 13, the discrepancies between the actual and ideal denominators of the CR-CCSD(T) theory grow with the number of Ne atoms (i.e. with the system size). They also seem to be larger at larger values of $R_{H\text{-}F}$. All of this explains why the departure from perfect size extensivity is greater for the stretched nuclear geometries in HF and for more Ne atoms (see table 14 and figure 12(*b*); cf. also the discussion above). On the other hand, it is quite remarkable to observe that

Downloaded At: 16:32 21 January 2011

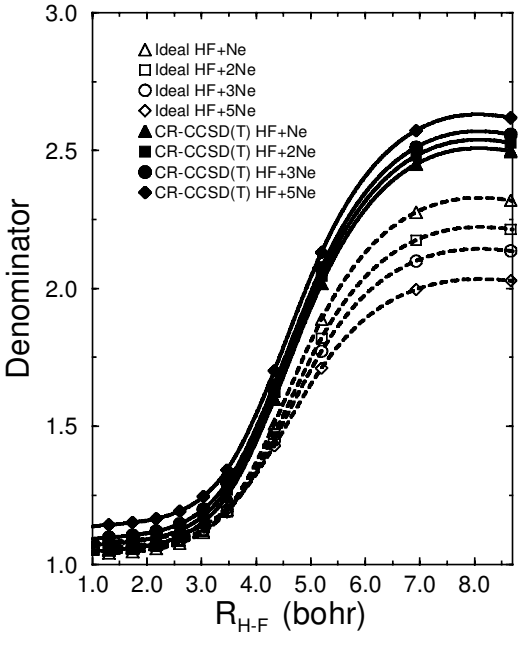

Figure 13. A comparison of the idealized values of the denominators $D^{(T)}$, equation (144), which are obtained by imposing a condition that the ideal CR-CCSD(T) correction $\delta^{CR(T)}$ is rigorously size extensive (dashed curves), with the actual values of the $D^{(T)}$ denominators used in the CR-CCSD(T) calculations, equations (78) or (86) (solid curves) for the HF + nNe systems with $n = 1$ (△ and ▲), $n = 2$ (□ and ■), $n = 3$ (○ and ●) and $n = 5$ (◇ and ◆). The results of the calculations with the DZ basis set.

there is only a 5–29% difference between the actual and ideal denominators in the CR-CCSD(T) calculations for the HF + *n*Ne system with $n = 5$, which is 6 times larger than the HF molecule (5% at $R_{H\text{-}F} \approx R_e$ and 29% at $R_{H\text{-}F} \approx 5R_e$). For cases involving fewer Ne atoms, those differences are even smaller. We must realize that, even in the case of the 29% difference between the actual value of $D^{(T)}$ and the $D^{(T)}$ value that would lead to a perfectly size-extensive description, the departure from size extensivity observed in the CR-CCSD(T) energy calculations is still relatively small, since $D^{(T)}$ enters only the non-iterative correction $\delta^{CR(T)}$, which is a correction to a much larger chunk of energy obtained in the size-extensive CCSD calculations. As shown in table 14, the 29% difference between the actual and ideal values of $D^{(T)}$ for the HF + 5Ne system with $R_{H\text{-}F} = 5R_e$ results in a relatively small, ~5 millihartree, size inextensivity error.

We can summarize the above discussion by stating that the CR-CCSD(T) and other renormalized and completely renormalized CC methods are not strictly size extensive, i.e. there are unlinked terms in the MBPT expansions of the corresponding energy expressions, largely because of the presence of the $\langle \Psi_0 | e^{T^{(A)}} | \Phi \rangle$ denominators in the formulae for corrections $\delta_0^{(A)}$. The presence of those denominators seems to have little or no effect on the description of bond breaking by the CR-CCSD(T) and other MMCC methods. Quite on the contrary, the PESs resulting from CR-CCSD(T) and other MMCC calculations are much better than those obtained with the standard CC methods of the CCSD(T) type, as amply documented in the earlier sections. On the other hand, lack of strict size extensivity of the CR-CCSD(T) and other MMCC methods may have an effect on the results of calculations for very large and extended systems. A lot depends here on the values of the T_1 and T_2 cluster amplitudes that are used to construct the MMCC corrections $\delta_0^{(A)}$. If they are small, then the $\langle \Psi_0 | e^{T^{(A)}} | \Phi \rangle$ denominators are close to 1, in which case the effects of size inextensivity of the approximate MMCC methods are negligible. If they are large, then the $\langle \Psi_0 | e^{T^{(A)}} | \Phi \rangle$ denominators become significantly greater than 1. They always become large in situations involving bond breaking. In this case, the $\langle \Psi_0 | e^{T^{(A)}} | \Phi \rangle$ denominators damp the unphysical values of the standard (T) and similar corrections at larger internuclear separations. However, the $\langle \Psi_0 | e^{T^{(A)}} | \Phi \rangle$ denominators may also acquire values which are significantly greater than 1 for very large many-electron systems. This can be seen by examining the explicit expressions for typical $\langle \Psi_0 | e^{T^{(A)}} | \Phi \rangle$ denominators, such as $D^{(T)}$, equation (78). As implied by equations (85) and (86) or (136), (137) and (139), the $D^{(T)}$ denominators increase in value with the size of a system, since the quantity $\chi = D^{(T)} - 1$ grows proportionally to the system size (cf. equation (139)). In the aforementioned example of the glycine molecule (the GLY12 isomer [234]) and its clusters (all described by the 6-31G basis set [235]), the denominator $D^{(T)}$ of the CR-CCSD(T) theory increases in value from 1.229 880 41 for a single glycine molecule (40 electrons) to 1.463 570 31 for two glycine molecules (80 electrons) and to 1.701 069 71 for three glycine molecules (120 electrons). It is possible that those values would be somewhat smaller if we optimized the geometry of the GLY12 isomer of glycine at the CR-CCSD(T) level (we used the geometry optimized by Jensen and Gordon [234] with the semiempirical AM1 approach), but this is not essential for this discussion; undoubtedly, the $D^{(T)}$ denominators grow with the system size. This means that for very large many-electron systems the $D^{(T)}$ and other $\langle \Psi_0 | e^{T^{(A)}} | \Phi \rangle$ denominators may artificially 'overdamp' the CR-CCSD(T) and other MMCC corrections $\delta^{(A)}$. We should note, however, that this implies that only the triples effect of the CR-CCSD(T) approach will be underestimated in

Downloaded At: 16:32 21 January 2011

calculations for systems with very large numbers of electrons. We must keep in mind that, in the CR-CCSD(T) case, the bulk of the correlation effects is still described by the size-extensive CCSD theory. In consequence, the departure from the perfectly size-extensive description in calculations for very large many-electron systems does not have to be big. This is shown in table 13, where we measure the size inextensivity error in the calculations for glycine clusters by subtracting the sum of energies of two and three isolated glycine molecules from the energies of the glycine dimer and trimer consisting of the glycine molecules separated by a very large distance. As one can see, in spite of the denominator value of 1.463 570 31 for the non-interacting glycine dimer, the departure from size extensivity in the CR-CCSD(T) calculations, measured by subtracting the sum of energies of the isolated glycine molecules from the energy of the dimer consisting of non-interacting glycine molecules, is only ~3 millihartree (2 kcal mol^{-1}). This should be compared with the total correlation energy of two non-interacting GLY12 molecules, which, according to the size-extensive CCSD(T) calculations with the 6-31G basis set, is −1.148 466 32 hartree (the CR-CCSD(T) method gives −1.136 768 10 hartree). The size inextensivity error amounts to 0.3% of the total correlation energy in this case. For a system consisting of three non-interacting glycine molecules, the departure from size extensivity in the CR-CCSD(T) calculations is ~9 millihartree (cf. table 13), which is only 0.5% of the total correlation energy of the glycine trimer. In other words, the size inextensivity of the CR-CCSD(T) method does not make it unusable for very large and extended systems. We may, for example, be interested in calculations of the bond breaking in a small polypeptide. The standard CCSD(T) method will provide size-extensive results, but they will be quite poor if we decide to study significantly stretched nuclear geometries or bond breaking. The CR-CCSD(T) approach will provide considerable improvements in the bond-breaking region with the ease of use and the relatively low cost of the CCSD(T) approach, although CR-CCSD(T) calculations will introduce small errors owing to lack of size extensivity of the CR-CCSD(T) method. We should always keep in mind that failures of the CCSD(T) method in the bond-breaking region are much more serious than the departures from perfect size extensivity observed in the CR-CCSD(T) calculations, as shown in the above examples. Moreover, we can always try to improve the results, reducing simultaneously the size inextensivity errors, by switching to higher-order MMCC theories, such as QMMCC. We will continue to study the consequences of size inextensivity in large molecule calculations by performing the CR-CCSD(T) and similar calculations for large systems consisting of 20–30 atoms and by comparing the results with the results of size-extensive multireference calculations, such as CASSCF or CASPT2. The results will be reported as soon as they become available.

There is another (still unexplored) possibility of improving the CR-CCSD(T) and other MMCC results in calculations for very large molecular systems (e.g. systems with over 20 atoms), if lack of size extensivity of the CR-CCSD(T) and other MMCC methods becomes a problem. As shown by Schütz and Werner [32, 34, 35] (cf. also [33]), the applicability of the standard CCSD(T) method can be extended to systems with ~100 atoms if we apply the local correlation formalism of Pulay and Saebø [29–31]. In this case, one combines an idea of localizing molecular orbitals and rewriting CC equations in a localized orbital basis with a concept of dividing the molecular space into different excitation domains. Those domains are used to introduce a hierarchy of pair and other excitations, so that, for example, the most

Downloaded At: 16:32 21 January 2011

numerous and, at the same time, the smallest multicentre excitations can be simply ignored in the calculations, ultimately leading to the CC algorithms that scale linearly with molecular size [32, 34, 35]. One can, therefore, contemplate a local CR-CCSD(T) approach, in which we use the idea of domains to separate the 'active site', where chemical bonds break or rearrange, from the remaining parts of the molecular system under study, where bond lengths remain close to their equilibrium values. This would make perfect sense in various applications of interest for biochemistry or biology, in which chemical changes, such as bond breaking or bond formation, usually have a local character, so that we can make a clear distinction between the chemically active site (an analogue of a solute molecule in a solution) and the remaining part of the molecule (solvent). The active site represents, in most cases, a relatively small molecular fragment, for which the CR-CCSD(T) method can provide an approximately size-extensive description, while allowing us to describe a breaking of single chemical bonds (if a given chemical change in an active site requires a consideration of multiple bond breaking, we can switch to one of the higher-level MMCC methods, such as CR-CCSD(TQ),b or QMMCC). The remaining part of a molecular system, where bonds are not rearranged, can be described by the local version of the standard CCSD(T) theory. Thus, after decomposing the molecule into an active site, where bonds are rearranged, and the remaining domains, where structural changes during a given chemical process are minimal, we could define the local CR-CCSD(T) correction $\delta_0^{\mathrm{CR(T),local}}$ of the entire molecular system under consideration as follows:

$$\delta_0^{\mathrm{CR(T),local}} = N^{\mathrm{CR(T)}}(\text{active site})/D^{(\mathrm{T})}(\text{active site}) + N^{(\mathrm{T})}(\text{other domains}), \quad (146)$$

thereby enforcing the approximately size-extensive behaviour of the resulting local variant of the CR-CCSD(T) theory numerically. In the above equation, we use a notation in which $N^{\mathrm{CR(T)}}(\text{active site})$ and $D^{(\mathrm{T})}(\text{active site})$ are the $N^{\mathrm{CR(T)}}$ and $D^{(\mathrm{T})}$ values calculated using the T_1 and T_2 cluster amplitudes of the active site only, whereas $N^{(\mathrm{T})}(\text{other domains})$ is, simply, the local version of the triples correction of the standard CCSD(T) method written for the rest of the molecule (cf. equation (84) for the original definition of $N^{(\mathrm{T})}$). We could, of course, extend this idea to other MMCC methods, such as CR-CCSD(TQ), should the need for the higher-level treatment (because, for example, of the presence of multiple bonds in the active site) arise. The above method of reducing or, perhaps, eliminating the potential problems related to size inextensivity of approximate MMCC methods, which has been inspired by our discussions with one of the principal contributors to local CC methodology, Dr Martin Schütz, has not yet been tested, but we believe that an extension of the CR-CCSD(T) and similar MMCC-based methods to very large systems along the lines described above is worth further exploration.

In the above discussion of the approximate size extensivity of the MMCC methods, we focused on the ground-state problem. The situation for excited states is slightly different, since the standard EOMCC methods, such as EOMCCSD, on which the excited-state MMCC approaches discussed in sections 2.2, 3.1.1 and 3.1.3 are based, are not size extensive. For example, there are disconnected terms in the EOMCCSD energy expression in the fourth order of perturbation theory [236–238]. This means that essentially all EOMCC or EOMCC-based methods, including, of course, the excited-state MMCC(2,3), MMCC(2,4) and other MMCC(m_A,m_B)

Downloaded At: 16:32 21 January 2011

approaches [77, 78], discussed in this work (cf. sections 2.2, 3.1.1 and 3.1.3), and the recently introduced SFCCSD and SFOD models [145, 146] that can be used to study single bond breaking [145, 146] and singlet–triplet gaps in diradicals [147] rely on the energy expressions having disconnected terms. On the other hand, the excited-state MMCC(m_A,m_B) methods satisfy the same additive separability conditions as the approximate EOMCC approaches that the MMCC(m_A,m_B) methods correct. For example, it has been demonstrated, first by Koch *et al.* [60] and later by others [238,239], that the EOMCCSD method is capable of correctly describing the separation of molecular excited states that correlate with the excited states of non-interacting fragments corresponding to a single excitation of one of the fragments, in spite of the presence of disconnected terms in the EOMCCSD energy expression. This means that, unlike the limited CI approaches, the lack of size extensivity of the standard EOMCCSD approach does not necessarily degrade the quality of the EOMCCSD results for large molecules (see an excellent discussion of this subject in [239]). Very similar remarks apply to all MMCC(2,m_B) approaches, including MMCC(2,3) and MMCC(2,4), as long as the wavefunction $|\Psi_K\rangle$ entering the formula for the non-iterative correction $\delta_K(2, m_B)$ (equation (46) with $m_A = 2$) has the same 'local excitation' structure as the corresponding solution of the EOMCCSD right eigenvalue problem [77]. The MMCC(2,m_B) approaches, which improve the EOMCCSD results, should actually provide a much better description of the separation of molecular excited states that correlate with the excited states of non-interacting fragments corresponding to a single excitation of one of the fragments than the EOMCCSD method.

Downloaded At: 16:32 21 January 2011

We should emphasize, however, that, in spite of these similarities, there is a major difference between the standard EOMCC and excited-state MMCC(m_A,m_B) methods. In the conventional EOMCC approaches, we can only hope that by increasing the excitation level m_A we reduce the error made in the calculations, but we do not have any non-trivial relationship with full CI that would provide us with additional guidance. In the excited-state MMCC(m_A,m_B) calculations, we are improving the results of the standard EOMCC calculations, such as EOMCCSD, by directly addressing the quantity of interest, i.e. $E_K - E_K^{(A)}$, where E_K is the full CI energy and $E_K^{(A)}$ is the energy of state $|\Psi_K\rangle$ resulting from a standard EOMCC calculation. Thus, the MMCC(m_A,m_B) results, albeit formally not size extensive, are much more accurate than the results of the standard EOMCC calculations. This automatically implies that the results of excited-state MMCC(m_A,m_B) calculations provide a significantly better description of the separation of molecular excited states into electronic states of non-interacting subsystems, even when the underlying EOMCC approximation is incapable of providing a correct description of this separation process. An example illustrating this statement has been provided in section 3.1.3, where we have shown, for example, that the MMCC(2,3) method restores the asymptotic degeneracy of the excited states of CH^+, which is broken by the EOMCCSD theory (see figure 1). We should also keep in mind that, in analogy to the ground-state CC methods, the additive separability of the standard EOMCC energies no longer holds if the reference configuration $|\Phi_{XY}\rangle$ of system XY does not factorize into a product of references $|\Phi_X\rangle$ and $|\Phi_Y\rangle$ of subsystems X and Y in the X + Y limit. This creates serious problems for the standard, spin-adapted, RHF-based, EOMCC methods, such as EOMCCSD, as shown in section 3.1.3 for the CH^+ system (see figure 1(*a*)). As in the case of the ground-state MMCC calculations,

the excited-state MMCC(m_A,m_B) methods, such as MMCC(2,3) or MMCC(2,4), employing the RHF configuration as a reference, are capable of providing a highly accurate description of the entire excited-state PESs, in spite of the apparent failure of the standard, RHF-based, EOMCC approximations to do the same.

4. Summary and future outlook

We have provided a comprehensive overview of the new approach to the many-electron correlation problem in atoms and molecules, termed the method of moments of coupled-cluster equations (MMCC). The principal idea of the MMCC formalism is that of the non-iterative energy corrections which, when added to the ground- and excited-state energies obtained in the standard CC and EOMCC calculations, such as CCSD or EOMCCSD, recover the exact, full CI, energies. The existence of the rigorous relationships between the standard CC or EOMCC energies and their exact, full CI, counterparts on which all MMCC approaches are based provides us with new ways of controlling the accuracy of *ab initio* quantum-chemical calculations. By directly addressing the quantities of interest, which are the differences between the full CI and CC or EOMCC energies in a given basis set, and by estimating those differences using the MMCC expressions, we can obtain results which are significantly better than the results of the standard CC calculations, such as CCSD, CCSD(T) or EOMCCSD. This is particularly true in quasi-degenerate situations, such as bond breaking, where the conventional arguments originating from MBPT, on which the standard non-iterative CC approximations are based, fail because of the divergent behaviour of the MBPT expansions at larger internuclear separations. This is also true for larger portions of PESs of excited states, which are very difficult to describe by the standard EOMCC theories, such as EOMCCSD.

Downloaded At: 16:32 21 January 2011

We have demonstrated that the MMCC formalism leads to a number of useful approximations, including the renormalized and completely renormalized CCSD(T) and CCSD(TQ) methods for the ground-state problem, the CI-corrected MMCC(m_A, m_B) approaches for the ground and excited states and the most recent QVMMCC methods, including QMMCC, which can be used to obtain excellent results for multiple bond breaking. The main theoretical concepts have been illustrated by examples of applications of approximate MMCC methods to ground- and excited-state PESs of several molecular systems. We have provided an overview of some of the material reported in the earlier original papers [41–46, 48, 49, 77, 78, 158] (cf. also [47, 97]) and discussed the most recent developments, such as the QVMMCC and QMMCC approaches [161] and the CI-corrected MMCC(2,5) and MMCC(2,6) methods [171]. We have also discussed new examples of applications of the MMCC methods, including the bond breaking in ethane and methyl fluoride, and the ground-state PES of the BeFH system, as described by the cc-pVTZ basis set [210]. Finally, for the first time ever, we have addressed the issue of size extensivity of the approximate MMCC methods, showing that the departure from strict size extensivity in the CR-CCSD(T) calculations is rather small, considering the crude nature of the approximations defining this approach. We will continue exploring this interesting issue in future papers.

We have clearly demonstrated that the MMCC theory provides us with a framework for designing 'black-box' approaches that can be used in accurate calculations of entire molecular PESs, or large portions of them, for a fraction of the effort associated with multireference calculations. This, in particular, applies to

the CR-CCSD(T) and CR-CCSD(TQ) approaches, which remove the pervasive failing of the standard CCSD(T) and CCSD(TQ_f) approximations at larger internuclear separations, while preserving the ease of use and the relatively low cost of the CCSD(T) and CCSD(TQ_f) calculations. As demonstrated in several calculations for actual molecular systems, the CR-CCSD(T) method is particularly well suited for PESs involving single bond breaking. If we need to study multiple bond breaking, we have to switch to the higher-level CR-CCSD(TQ) and QMMCC theories. An alternative approach to bond breaking is offered by the CI-corrected MMCC methods. They are somewhat more complicated than the CR-CCSD(T) and CR-CCSD(TQ) approaches, since they require that we perform additional CI calculations to generate trial wavefunctions $|\Psi_0\rangle$ or $|\Psi_K\rangle$ that enter the formulae for the MMCC energy corrections, but they are still fairly straightforward, compared with many other (e.g. multireference) methods, and they are relatively inexpensive. Another advantage of the CI-corrected MMCC methods is the ability to provide remarkable improvements in the EOMCC calculations for excited states, including complicated excited states dominated by double excitations and bond breaking in excited states.

Downloaded At: 16:32 21 January 2011

We have recently incorporated the renormalized and completely renormalized CCSD[T] and CCSD(T) methods in the GAMESS package [158]. We hope to be able to incorporate other methods, such as CR-CCSD(TQ),b or MMCC(2,3), in GAMESS in the future. This does not mean, however, that our effort ends there. Clearly, the MMCC formalism needs further development and testing. Among interesting formal problems that need to be addressed in the future are studies of the open-shell extensions of the (C)R-CCSD(T) (C)R-CCSD(TQ) and CI-corrected MMCC(m_A, m_B) methods. All methods described in this review allow us to study PESs for singlet electronic states, which separate into open-shell states of fragments into which a given molecular system dissociates. However, there are many applications in chemistry which involve PESs of doublet and triplet electronic states. The success of the CR-CCSD(T) and CR-CCSD(TQ) methods in describing reactive PESs and the apparent formal similarities between the standard and completely renormalized CCSD(T) and CCSD(TQ) approaches prompt the development of analytical derivatives for the CR-CCSD(T) and CR-CCSD(TQ) methods, so that we could, for example, locate transition states on molecular PESs without resorting to cumbersome numerical differentiation of the corresponding energies. The first and second analytical derivatives for the standard CCSD(T) method have already been formulated [240–244], which should facilitate analogous work on the analytical derivatives for the CR-CCSD(T) approach (some progress has already been made in this area and analytical first derivatives for the R-CCSD(T) approach have been formulated and implemented [245]).

The similarity of the standard and renormalized CC energy expressions should facilitate the development of the explicitly correlated (R12 [246–248]) variants of the R-CCSD(T) and CR-CCSD(T) approaches and their (TQ) extensions, which would be analogous to the existing CCSD[T]-R12 and CCSD(T)-R12 approaches [249–251]. The CC-R12 theory [249–251], in which the correlation cusp is treated via inclusion of terms that explicitly depend on the interelectronic distance r_{ij} in the CC wavefunction, is characterized by a much faster convergence to the complete basis set limit than the standard CC methods (cf., for example, [252–254]). The R12 extension of our renormalized and completely renormalized CCSD(T) and CCSD(TQ) approaches would enable us to study the complete basis set limits for

potential functions, vibrational spectra and other spectroscopic characteristics of molecular systems with a relatively small effort.

When discussing the approximate size extensivity of MMCC approaches, we have mentioned that it might be worthwhile to formulate the local extension of the CR-CCSD(T) and CR-CCSD(TQ) methods, based on the local correlation formalism of Pulay and Saebø [29–31]. The local variant of the standard CCSD(T) approach has already been formulated [32–35], enabling the CCSD(T) calculations for molecular systems with ~100 atoms [32, 34, 35]. The local variant of CR-CCSD(T), in which we would use the CR-CCSD(T) triples correction to describe the active centre and the standard triples correction of the CCSD(T) theory to describe the rest of a given molecular system, might help us to reduce the size inextensivity errors in the CR-CCSD(T) calculations for very large systems, while reducing the cost of the CR-CCSD(T) calculations by several orders of magnitude. Other potential CPU time savings in the CR-CCSD(T) and CR-CCSD(TQ) calculations might be obtained by employing the Laplace transform technique of Almlöf [255]. This technique has successfully been used by Scuseria and co-workers [256] to reduce the costs of the standard CCSD(T) calculations.

Downloaded At: 16:32 21 January 2011

Last, but not least, it would be very useful if we could further simplify the MMCC calculations for excited states by developing the excited-state extensions of the CR-CCSD(T) and CR-CCSD(TQ) methods. The CI-corrected MMCC(2,3) and MMCC(2,4) approaches discussed in sections 3.1.1 and 3.1.3 require that we run the CISDt or CISDtq calculations (or some other relatively inexpensive MRCI-like calculations) to produce the wavefunctions $|\Psi_K\rangle$ which appear in the MMCC(2,3) and MMCC(2,4) excited-state corrections to EOMCCSD energies, equations (49) and (50). Although the CISDt and CISDtq calculations are relatively inexpensive, they also require that we define active orbitals which correspond to excited electronic states of interest. These active orbitals are, in many cases, very easy to determine, but undoubtedly it would be much more convenient to be able to obtain the highly accurate corrections to EOMCCSD energies with the ease of use of the ground-state CCSD(T) or CR-CCSD(T) calculations, i.e. without performing any additional calculations. As explained in the Introduction, the existing non-iterative triples corrections to EOMCCSD or response CCSD excitation energies, including the corrections defining the EOMCCSD(T) [65], EOMCCSD($\tilde{\mathrm{T}}$) [66], EOMCCSD(T$'$) [66] and CCSDR(3) [70, 71] approaches, cannot be used in accurate calculations of larger portions of excited-state PESs or doubly excited states of systems with quasi-degenerate ground states.

In order to propose the excited-state analogue of the CR-CCSD(T) and CR-CCSD(TQ) methods, we must come up with intelligent guesses for excited-state wavefunctions $|\Psi_K\rangle$ that would rely solely on the information that can be extracted from the CCSD and EOMCCSD calculations, namely the T_1 and T_2 components of the CCSD cluster operator and the $R_{K,0}$, $R_{K,1}$ and $R_{K,2}$ components of the EOMCCSD excitation operator. In order for those guesses to be simple enough to enable calculations for larger systems, we must rely on the MBPT-like arguments, which are similar to the arguments that led to the discovery of the standard CCSD[T] and CCSD(T) triples corrections.

We have recently started testing an excited-state MMCC(2,3) formalism in which the wavefunction $|\Psi_K\rangle$ entering the MMCC(2,3) energy formula, equation (49), is defined in the following manner [257]:

$$|\Psi_K\rangle = \{R_{K,0} + (R_{K,1} + R_{K,0}T_1) + [R_{K,2} + R_{K,1}T_1 + R_{K,0}(T_2 + \tfrac{1}{2}T_1^2)] + [\tilde{R}_{K,3} + R_{K,2}T_1 + R_{K,1}(T_2 + \tfrac{1}{2}T_1^2) + R_{K,0}(T_1T_2 + \tfrac{1}{6}T_1^3)]\}|\Phi\rangle, \quad (147)$$

where

$$\tilde{R}_{K,3}|\Phi\rangle = \sum_{\substack{i<j<k \\ a<b<c}} \frac{\mathcal{M}^{abc}_{K,ijk}(2)}{\omega_K^{\mathrm{EOMCCSD}} - \langle \Phi^{abc}_{ijk}|(\bar{H}_1^{\mathrm{CCSD}} + \bar{H}_2^{\mathrm{CCSD}} + \bar{H}_3^{\mathrm{CCSD}})|\Phi^{abc}_{ijk}\rangle} |\Phi^{abc}_{ijk}\rangle, \quad (148)$$

with

$$\omega_K^{\mathrm{EOMCCSD}} = E_K^{\mathrm{EOMCCSD}} - E_0^{\mathrm{CCSD}} \quad (149)$$

representing the vertical excitation energy of the EOMCCSD theory, with T_1, T_2, $R_{K,0}$, $R_{K,1}$ and $R_{K,2}$ representing the relevant many-body components of the CCSD and EOMCCSD cluster and excitation operators and with $\bar{H}_n^{\mathrm{CCSD}}$ defining the n-body component of the CCSD similarity-transformed Hamiltonian. The wavefunction $|\Psi_K\rangle$, equation (147), is essentially equivalent to the truncated form of the $(R_{K,0} + R_{K,1} + R_{K,2} + \tilde{R}_{K,3})e^{T_1+T_2}|\Phi\rangle$ wavefunction, in which we neglect higher-than-triply excited configurations relative to reference $|\Phi\rangle$. As we will show elsewhere [257], the above formula for $|\Psi_K\rangle$ can be derived by analysing the approximate form of the EOMCCSDT eigenvalue problem.

We can view equation (147), with $\tilde{R}_{K,3}$ defined by equation (148), as an excited-state extension of the ground-state wavefunctions $|\Psi_0^{\mathrm{CCSD[T]}}\rangle$ and $|\Psi_0^{\mathrm{CCSD(T)}}\rangle$, equations (63) and (64), respectively, defining the CR-CCSD[T] and CR-CCSD(T) methods, in which the MBPT(2)-like triples $T_3^{[2]}|\Phi\rangle$ contribution is replaced by $\tilde{R}_{K,3}|\Phi\rangle$. The main difference between $T_3^{[2]}|\Phi\rangle$ and its excited-state $\tilde{R}_{K,3}|\Phi\rangle$ counterpart lies in the way we handle the perturbation theory denominators corresponding to triple excitations in each case. In equation (148), we use the diagonal part of the TT block of $\bar{H}^{\mathrm{CCSD}}$ instead of the standard sum of differences of orbital energies $(\varepsilon_i + \varepsilon_j + \varepsilon_k - \varepsilon_a - \varepsilon_b - \varepsilon_c)$ entering the three-body part of the MBPT reduced resolvent $R_0^{(3)}$. One can easily show that the only components of $\bar{H}^{\mathrm{CCSD}}$ that enter the diagonal part of the TT block of the CCSD similarity-transformed Hamiltonian are the one-, two- and three-body components [257] (see equation (148)). In equation (148), we also use the complete moments $\mathcal{M}^{abc}_{K,ijk}(2)$, instead of their lowest-order $\langle \Phi^{abc}_{ijk}|(V_NT_2)_C|\Phi\rangle$ estimates defining $T_3^{[2]}|\Phi\rangle$, equation (65), that are used to define the ground-state wavefunctions $|\Psi_0^{\mathrm{CCSD[T]}}\rangle$ and $|\Psi_0^{\mathrm{CCSD(T)}}\rangle$.

The details of the resulting MMCC(2,3) formalism, which essentially reduces to the CR-CCSD[T] or CR-CCSD(T) theory when $K = 0$, and which we call the completely renormalized EOMCCSD(T) (CR-EOMCCSD(T)) method, will be reported elsewhere [257]. As a matter of fact, we have not finished testing this 'black-box' variant of the excited-state MMCC(2,3) approach. However, we have already applied the new CR-EOMCCSD(T) method to excited states of the CH^+, N_2 and C_2 systems discussed in section 3.1.4. The preliminary results of our CR-EOMCCSD(T) calculations are shown in table 16. As we can see, the CR-EOMCCSD(T) approach reduces the large errors in the EOMCCSD results for states dominated by doubles (the $2\,^1\Sigma^+$, $1\,^1\Delta$ and $2\,^1\Delta$ states of CH^+ and the $1\,^1\Delta_g$ and $1\,^1\Pi_g$ states of C_2) as effectively as the CI-corrected MMCC(2,3) method (cf. the MMCC(2,3) results in table 3 with the CR-EOMCCSD(T) results in table 16). For the remaining states, which are dominated by singles and for which EOMCCSD is

Downloaded At: 16:32 21 January 2011

Table 16. A comparison of the CR-EOMCCSD(T), full CI and other CC results for the vertical excitation energies of CH^+, N_2 and C_2 (in eV).[a] The full CI values are the excitation energies. All other values are the deviations from the full CI results. The $n\,^1X$ energy is the excitation energy from the ground state ($1\,^1\Sigma^+$ for CH^+ and $1\,^1\Sigma_g^+$ for N_2 and C_2) to the nth singlet state of symmetry X.

Molecule	State	Full CI[a]	EOMCCSD	CC3[b]	EOMCCSDt[c,d]	EOMCCSDT[e]	CR-EOMCCSD(T)[f]
CH^+	$2\,^1\Sigma^+$	8.549	0.560	0.230	0.092	0.074	0.117
	$3\,^1\Sigma^+$	13.525	0.055	0.016	0.000	0.001	0.011
	$4\,^1\Sigma^+$	17.217	0.099	0.026	0.012	−0.002	0.025
	$1\,^1\Pi$	3.230	0.031	0.012	0.003	−0.003	0.007
	$2\,^1\Pi$	14.127	0.327	0.219	0.094	0.060	0.113
	$1\,^1\Delta$	6.964	0.924	0.318	0.057	0.040	0.027
	$2\,^1\Delta$	16.833	0.856	0.261	0.016	−0.038	−0.002
N_2[g]	$1\,^1\Pi_g$	9.584	0.081	0.033	0.029	0.009	0.128
	$1\,^1\Sigma_u$	10.329	0.136	0.007	−0.005	0.004	0.033
	$1\,^1\Delta_u$	10.718	0.180	0.009	0.001	0.008	0.053
	$1\,^1\Pi_u$	13.609	0.400	0.177	0.090	0.052	0.300
C_2[g]	$1\,^1\Pi_u$	1.385	0.089	−0.068	−0.047	0.034	−0.002
	$1\,^1\Delta_g$	2.293	2.054	0.859	0.285	0.407	0.283
	$1\,^1\Sigma_u^+$	5.602	0.197	−0.047	0.088	0.113	0.046
	$1\,^1\Pi_g$	4.494	1.708	0.496	0.075	0.088	0.054

[a] The full CI results and basis set for CH^+ taken from [168] (see also [79]). The full CI results and basis sets for N_2 and C_2 taken from [71]. The equilibrium bond lengths in CH^+, N_2 and C_2 are 2.137 13, 2.068 and 2.348 bohr, respectively.
[b] The CC3 results for CH^+ taken from [69]. The CC3 results for N_2 and C_2 taken from [71].
[c] From [75, 76, 81]. For N_2, the Cartesian d functions were used, instead of the spherical d functions that were used in the remaining calculations for this molecule.
[d] For CH^+, the active space consisted of the 3σ, $1\pi_x \equiv 1\pi$, $1\pi_y \equiv 2\pi$ and 4σ orbitals. For N_2, the active space consisted of the $3\sigma_g$, $1\pi_u$, $2\pi_u$, $1\pi_g$, $2\pi_g$ and $3\sigma_u$ orbitals. For C_2, the active space consisted of the $1\pi_u$, $2\pi_u$, $3\sigma_g$, $3\sigma_u$, $1\pi_g$ and $2\pi_g$ orbitals.
[e] From [76] (CH^+) and [81] (N_2 and C_2).
[f] From [257].
[g] The lowest-energy core orbitals, $1\sigma_g$ and $1\sigma_u$, were kept frozen.

Downloaded At: 16:32 21 January 2011

reasonably accurate, we usually observe the reduction of errors, from ~0.1–0.2 eV in the EOMCCSD case to ~0.01–0.05 eV in the CR-EOMCCSD(T) case. The mean absolute errors in the excitation energies corresponding to all seven states of CH^+, all four states of N_2 and all four states of C_2 listed in table 16 are 0.043, 0.129 and 0.096 eV, respectively. This is a lot better than the 0.407, 0.199 and 1.012 eV mean absolute errors in the EOMCCSD results and, with an exception of N_2, this is as good as the full EOMCCSDT description (see table 4). The mean errors in the excitation energies for CH^+ at two stretched geometries, $R_{C-H} = 1.5R_e$ and $R_{C-H} = 2R_e$, are 0.123 and 0.194 eV, respectively [257]. This is a reduction of errors in the EOMCCSD results almost by an order of magnitude. The results of the CI-corrected MMCC(2,3) and full EOMCCSDT calculations are somewhat better, but it is quite remarkable that the simple, 'black-box' type, CR-EOMCCSD(T) approach defined by equation (49), with $|\Psi_K\rangle$ defined by equation (147), can provide results of this high quality. There are some problems with obtaining a well-balanced description of the lowest $^1\Pi_u$ state of N_2 (cf. table 16), which means that we may have to modify the above formula for $|\Psi_K\rangle$, but it is already quite clear to us that we can use the MMCC(2,3) approximation as a vehicle towards the formulation of the

successful excited-state extension of the ground-state CR-CCSD(T) approach. Undoubtedly, the above preliminary CR-EOMCCSD(T) results for the excited states of CH^+, N_2 and C_2 are encouraging, but we have to make sure that we can obtain equally good results for other molecular systems, including larger molecules and larger basis sets. The CR-EOMCCSD(T) and similar approaches are currently under intense investigation by our group and further results of this effort will be reported as soon as they become available [257].

Acknowledgments

One of us (P.P.) would like to thank Professor Jeremy M. Hutson, an Editor of *International Reviews in Physical Chemistry*, for inviting him to write this review article. We would also like to thank Dr Martin Schütz for providing us with the CASPT2, MRCI and MRCI(Q) data for ethane and methyl fluoride that were used to prepare figures 3 (*c*) and 3 (*d*) and for stimulating discussions about the possibility of formulating local variants of the CR-CCSD(T) method. Finally, we would like to thank Dr Vladimir Špirko for his help with calculating the vibrational spectrum of F_2 presented in this paper (table 8). This work has been supported by the Department of Energy, Office of Basic Energy Sciences, SciDAC Computational Chemistry Program (Grant No. DE-FG02-01ER15228; awarded to P.P.). Additional support by the Alfred P. Sloan Foundation is gratefully acknowledged (P.P.).

Downloaded At: 16:32 21 January 2011

Appendix A. An elementary derivation of equation (9)

The ground-state MMCC theory and all MMCC approximations, including the CI-corrected MMCC methods for ground electronic states, the renormalized and completely renormalized CCSD[T], CCSD(T) and CCSD(TQ) approaches and the quasi-variational and quadratic CC methods discussed in this article, are based on equation (9). As mentioned in section 2.1, equation (9) was initially discovered as a byproduct of the more general studies of the mathematical relationships between multiple solutions of systems of nonlinear equations representing different standard CC approximations [41]. Shortly after the discovery of equation (9), Piecuch and Kowalski came up with another derivation of the same formula [42], which is based on applying the resolution of identity to the asymmetric energy expression defining the MMCC functional $\Lambda^{\rm CC}[\Psi]$, equation (23). This simple derivation of equation (9), which has originally been reported in appendix A of [42], is described here.

In order to derive equation (9), we first insert the resolution of identity,

$$P + \sum_{n=1}^{N} Q_n = 1, \tag{150}$$

where

$$P = |\Phi\rangle\langle\Phi| \tag{151}$$

is the projection operator onto the one-dimensional subspace spanned by the reference configuration $|\Phi\rangle$ and Q_n is the projection operator onto the subspace of the n-tuply excited configurations relative to $|\Phi\rangle$, into equation (23) defining the MMCC functional $\Lambda^{\rm CC}[\Psi]$. We obtain

$$\Lambda^{\mathrm{CC}}[\Psi] = \langle\Psi|P(H - E_0^{(\mathrm{A})})\mathrm{e}^{T^{(\mathrm{A})}}|\Phi\rangle / \langle\Psi|\mathrm{e}^{T^{(\mathrm{A})}}|\Phi\rangle + \sum_{n=1}^{N}\langle\Psi|Q_n(H - E_0^{(\mathrm{A})})\mathrm{e}^{T^{(\mathrm{A})}}|\Phi\rangle / \langle\Psi|\mathrm{e}^{T^{(\mathrm{A})}}|\Phi\rangle. \quad (152)$$

Since cluster operator $T^{(\mathrm{A})}$ is the excitation operator, so that $(T^{(\mathrm{A})})^{\dagger}$ and its powers annihilate $|\Phi\rangle$, we can rewrite the formula for the CC energy as follows (cf. equation (8)):

$$E_0^{(\mathrm{A})} = \langle\Phi|\mathrm{e}^{-T^{(\mathrm{A})}}H\mathrm{e}^{T^{(\mathrm{A})}}|\Phi\rangle = \langle\Phi|H\mathrm{e}^{T^{(\mathrm{A})}}|\Phi\rangle. \quad (153)$$

This implies that the first term on the right-hand side of equation (152) vanishes. Indeed,

$$\langle\Psi|P(H - E_0^{(\mathrm{A})})\mathrm{e}^{T^{(\mathrm{A})}}|\Phi\rangle / \langle\Psi|\mathrm{e}^{T^{(\mathrm{A})}}|\Phi\rangle = \langle\Psi|\Phi\rangle(\langle\Phi|H\mathrm{e}^{T^{(\mathrm{A})}}|\Phi\rangle - E_0^{(\mathrm{A})}) / \langle\Psi|\mathrm{e}^{T^{(\mathrm{A})}}|\Phi\rangle = 0, \quad (154)$$

so that

$$\Lambda^{\mathrm{CC}}[\Psi] = \sum_{n=1}^{N}\langle\Psi|Q_n(H - E_0^{(\mathrm{A})})\mathrm{e}^{T^{(\mathrm{A})}}|\Phi\rangle / \langle\Psi|\mathrm{e}^{T^{(\mathrm{A})}}|\Phi\rangle. \quad (155)$$

Downloaded At: 16:32 21 January 2011

By applying the well-known property of the CC exponential ansatz [3, 4, 15, 18, 41],

$$H\mathrm{e}^{T^{(\mathrm{A})}}|\Phi\rangle = \mathrm{e}^{T^{(\mathrm{A})}}(H\mathrm{e}^{T^{(\mathrm{A})}})_{\mathrm{C}}|\Phi\rangle = \mathrm{e}^{T^{(\mathrm{A})}}\bar{H}^{(\mathrm{A})}|\Phi\rangle, \quad (156)$$

where $\bar{H}^{(\mathrm{A})}$ is the similarity-transformed Hamiltonian of the CC theory, equation (6), it can be immediately shown that

$$Q_n H\mathrm{e}^{T^{(\mathrm{A})}}|\Phi\rangle = Q_n\sum_{j=0}^{n}(\mathrm{e}^{T^{(\mathrm{A})}})_{n-j}(H\mathrm{e}^{T^{(\mathrm{A})}})_{\mathrm{C},j}|\Phi\rangle = \sum_{j=0}^{n}Q_n(\mathrm{e}^{T^{(\mathrm{A})}})_{n-j}\bar{H}_j^{(\mathrm{A})}|\Phi\rangle, \quad (157)$$

where, in general, O_j represents the j-body component of operator O. Equation (156) can be easily obtained by multiplying $H\mathrm{e}^{T^{(\mathrm{A})}}|\Phi\rangle$ on the left by $\mathrm{e}^{T^{(\mathrm{A})}}\mathrm{e}^{-T^{(\mathrm{A})}} = 1$ and by realizing that the similarity-transformed Hamiltonian $\bar{H}^{(\mathrm{A})}$ can be identified with the connected product of H and $\mathrm{e}^{T^{(\mathrm{A})}}$ (see, for example, [15, 18, 41] for more information). Because of equation (8), the $j = 0$ term in the above summation gives the unlinked, energy-dependent, part of $Q_n H\mathrm{e}^{T^{(\mathrm{A})}}|\Phi\rangle$, namely $E_0^{(\mathrm{A})}Q_n\mathrm{e}^{T^{(\mathrm{A})}}|\Phi\rangle$. We can, therefore, rewrite equation (157) in the following form [41, 42]:

$$Q_n(H - E_0^{(\mathrm{A})})\mathrm{e}^{T^{(\mathrm{A})}}|\Phi\rangle = \sum_{j=1}^{n}Q_n(\mathrm{e}^{T^{(\mathrm{A})}})_{n-j}\bar{H}_j^{(\mathrm{A})}|\Phi\rangle = \sum_{j=1}^{n}Q_n C_{n-j}(m_{\mathrm{A}})M_j^{\mathrm{CC}}(m_{\mathrm{A}})|\Phi\rangle, \quad (158)$$

where $C_{n-j}(m_{\mathrm{A}})$ is the $(n-j)$-body component of $\mathrm{e}^{T^{(\mathrm{A})}}$, equation (10), and $M_j^{\mathrm{CC}}(m_{\mathrm{A}})|\Phi\rangle$ is defined by equation (11). In deriving equation (158), we used an obvious identity

$$\bar{H}_j^{(\mathrm{A})}|\Phi\rangle = Q_j\bar{H}^{(\mathrm{A})}|\Phi\rangle \equiv M_j^{\mathrm{CC}}(m_{\mathrm{A}})|\Phi\rangle. \quad (159)$$

It is worth noticing that since the zero-body contribution $(\mathrm{e}^{T^{(\mathrm{A})}})_0$ equals 1, the $j = n$ terms in equations (157) and (158) correspond to the connected component of

$Q_n H e^{T^{(A)}}|\Phi\rangle$, i.e. $Q_n(He^{T^{(A)}})_C|\Phi\rangle$. The remaining terms with $0 < j < n$ represent the linked, but disconnected, components of $Q_n He^{T^{(A)}}|\Phi\rangle$ (see [41] for further details).

The substitution of equation (158) into equation (155) gives the following result:

$$\Lambda^{CC}[\Psi] = \sum_{n=1}^{N}\sum_{j=1}^{n}\langle\Psi|Q_n\, C_{n-j}(m_A)\, M_j^{CC}(m_A)|\Phi\rangle/\langle\Psi|e^{T^{(A)}}|\Phi\rangle. \tag{160}$$

If we assume that the wavefunction $|\Psi\rangle$ in equation (160) is the exact, full CI, ground-state $|\Psi_0\rangle$, so that we can replace $\Lambda^{CC}[\Psi]$ by the energy difference $E_0 - E_0^{(A)} \equiv \delta_0^{(A)}$ (cf. equation (24)), we obtain

$$\delta_0^{(A)} = \sum_{n=1}^{N}\sum_{j=1}^{n}\langle\Psi_0|Q_n\, C_{n-j}(m_A)\, M_j^{CC}(m_A)|\Phi\rangle/\langle\Psi|e^{T^{(A)}}|\Phi\rangle. \tag{161}$$

Equation (161) is a general result, which is valid for any values of cluster amplitudes defining $T^{(A)}$. In practical applications of the MMCC theory, we assume, of course, that $T^{(A)}$ is obtained by solving the standard CC equations, equation (5). In other words, we impose a requirement that the generalized moments $\mathcal{M}_J^{CC,(j)}(m_A)$ with $j = 1, \ldots, m_A$ vanish. This immediately implies that (cf. equations (5), (11) and (12))

$$M_j^{CC}(m_A)|\Phi\rangle = 0, \qquad \text{for } j = 1, \ldots, m_A. \tag{162}$$

The substitution of equation (162) into equation (161) reduces the summations over n and j in equation (161) to $\sum_{n=m_A+1}^{N}\sum_{j=m_A+1}^{n}$, giving us the desired result, equation (9).

Downloaded At: 16:32 21 January 2011

Appendix B. An elementary derivation of equation (30)

The derivation of equation (30), which represents the generalization of equation (9) to all electronic states, is based on applying the resolution of identity to the functional $\Lambda^{EOMCC}[\Psi]$, equation (35) [77]. As pointed out in section 2.2, the $\Lambda^{EOMCC}[\Psi]$ functional gives us the exact value of the energy correction $\delta_K^{(A)}$, equation (1), when $|\Psi\rangle$ is replaced by the exact, full CI, state $|\Psi_K\rangle$ (see equation (36); let us recall that $K = 0$ corresponds to the ground state and the $K > 0$ values correspond to excited states). Thus, in deriving equation (30), it is sufficient to focus on the values of $\Lambda^{EOMCC}[\Psi]$ for $|\Psi\rangle = |\Psi_K\rangle$. As shown in [77], the derivation of equation (30) becomes very compact, when we base it on the following form of the resolution of identity:

$$P + Q^{(A)} + Q^{(R)} = 1, \tag{163}$$

where P and $Q^{(A)}$ are defined by equations (151) and (7), respectively, and

$$Q^{(R)} = \sum_{n=m_A+1}^{N} Q_n. \tag{164}$$

In analogy to the derivation of equation (9), we first premultiply $(H - E_K^{(A)})$ in the formula for $\Lambda^{EOMCC}[\Psi_K]$, equation (35), by $e^{T^{(A)}}e^{-T^{(A)}} = 1$ (cf. equation (156) in appendix A). Because of equation (36), we obtain

$$\delta_K^{(A)} = \Lambda^{EOMCC}[\Psi_K] = \langle\Psi_K|e^{T^{(A)}}(\bar{H}^{(A)} - E_K^{(A)})R_K^{(A)}|\Phi\rangle/\langle\Psi_K|R_K^{(A)}e^{T^{(A)}}|\Phi\rangle, \tag{165}$$

where $\bar{H}^{(A)}$ is the similarity-transformed Hamiltonian of the CC theory corresponding to $T = T^{(A)}$, equation (6). Next, we insert the resolution of identity, equation (163), before and after the leftmost $e^{T^{(A)}}$ in the numerator of equation (165) and utilize the fact that the EOMCC excitation operator $R_K^{(A)}$ satisfies equation (29). We obtain

$$\delta_K^{(A)} = \langle \Psi_K | (P + Q^{(A)} + Q^{(R)})\, e^{T^{(A)}} Q^{(R)} (\bar{H}^{(A)} - E_K^{(A)}) R_K^{(A)} | \Phi \rangle / \langle \Psi_K | R_K^{(A)} e^{T^{(A)}} | \Phi \rangle. \tag{166}$$

Since the projection operator $Q^{(R)}$, equation (164), involves the excited configurations with the excitation level higher than m_A, we can immediately write that

$$(P + Q^{(A)})\, e^{T^{(A)}} Q^{(R)} = 0. \tag{167}$$

Moreover, $R_K^{(A)}$ contains the many-body components $R_{K,n}$ with $n \leq m_A$, so that

$$Q^{(R)} R_K^{(A)} | \Phi \rangle = 0. \tag{168}$$

By inserting equations (167) and (168) into equation (166), we obtain

$$\delta_K^{(A)} = \langle \Psi_K | Q^{(R)} e^{T^{(A)}} Q^{(R)} (\bar{H}^{(A)} R_K^{(A)}) | \Phi \rangle / \langle \Psi_K | R_K^{(A)} e^{T^{(A)}} | \Phi \rangle. \tag{169}$$

The substitution of equation (164) into equation (169), combined with the fact that $Q_n e^{T^{(A)}} Q_j$ vanishes unless $j \leq n$ (recall that $T^{(A)}$ is the excitation operator), gives

$$\delta_K^{(A)} = \sum_{n=m_A+1}^{N} \sum_{j=m_A+1}^{n} \langle \Psi_K | Q_n\, e^{T^{(A)}} Q_j\, (\bar{H}^{(A)} R_K^{(A)}) | \Phi \rangle / \langle \Psi_K | R_K^{(A)} e^{T^{(A)}} | \Phi \rangle \tag{170}$$

or (cf. equation (31))

$$\delta_K^{(A)} = \sum_{n=m_A+1}^{N} \sum_{j=m_A+1}^{n} \langle \Psi_K | Q_n\, e^{T^{(A)}} M_{K,j}^{\mathrm{EOMCC}}(m_A) | \Phi \rangle / \langle \Psi_K | R_K^{(A)} e^{T^{(A)}} | \Phi \rangle, \tag{171}$$

which is the desired result, equation (30), if we realize that the only many-body component of $e^{T^{(A)}}$ that can enter $Q_n\, e^{T^{(A)}} M_{K,j}^{\mathrm{EOMCC}}(m_A) | \Phi \rangle$ is the $(n-j)$-body term $C_{n-j}(m_A)$, equation (10).

Downloaded At: 16:32 21 January 2011

References

[1] Coester, F., 1958, *Nucl. Phys.*, **7**, 421.
[2] Coester, F., and Kümmel, H., 1960, *Nucl. Phys.*, **17**, 477.
[3] Čížek, J., 1966, *J. chem. Phys.*, **45**, 4256.
[4] Čížek, J., 1969, *Adv. chem. Phys.*, **14**, 35.
[5] Čížek, J., and Paldus, J., 1971, *Int. J. quantum Chem.*, **5**, 359.
[6] Purvis III, G. D., and Bartlett, R. J., 1982, *J. chem. Phys.*, **76**, 1910.
[7] Urban, M., Noga, J., Cole, S. J., and Bartlett, R. J., 1985, *J. chem. Phys.*, **83**, 4041.
[8] Raghavachari, K., Trucks, G. W., Pople, J. A., and Head-Gordon, M., 1989, *Chem. Phys. Lett.*, **157**, 479.
[9] Scuseria, G. E., Scheiner, A. C., Lee, T. J., Rice, J. E., and Schaefer III, H. F., 1987, *J. chem. Phys.*, **86**, 2881.
[10] Scuseria, G. E., Janssen C. L., and Schaefer III, H. F., 1988, *J. chem. Phys.*, **89**, 7382.
[11] Lee, T. J., and Rice, J. E., 1988, *Chem. Phys. Lett.*, **150**, 406.
[12] Piecuch, P., and Paldus, J., 1989, *Int. J. quantum Chem.*, **36**, 429.
[13] Piecuch, P., and Paldus, J., 1990, *Theor. Chim. Acta*, **78**, 65.

[14] Piecuch, P., Toboła R., and Paldus, J., 1995, *Int. J. quantum Chem.*, **55**, 133.
[15] Paldus, J., 1992, *Methods in Computational Molecular Physics*, NATO Advanced Study Institute, Series B: Physics, Vol. 293, edited by S. Wilson and G. H. F. Diercksen (New York: Plenum), p. 99.
[16] Lee, T. J., and Scuseria, G. E., 1995, *Quantum Mechanical Electronic Structure Calculations with Chemical Accuracy*, edited by S. R. Langhoff (Dordrecht: Kluwer), p. 47.
[17] Bartlett, R. J., 1995, *Modern Electronic Structure Theory*, Part I, edited by D. R. Yarkony (Singapore: World Scientific), p. 1047.
[18] Paldus, J., and Li, X., 1999, *Adv. chem. Phys.*, **110**, 1.
[19] Crawford, T. D., and Schaefer III, H. F., 2000, *Rev. comp. Chem.*, **14**, 33.
[20] Kucharski, S. A., and Bartlett, R. J., 1998, *J. chem. Phys.*, **108**, 9221.
[21] Kállay, M., and Surján, P. R., 2001, *J. chem. Phys.*, **115**, 2945.
[22] Noga, J., and Bartlett, R. J., 1987, *J. chem. Phys.*, **86**, 7041; 1988, *J. chem. Phys.*, **89**, 3401 (erratum).
[23] Scuseria, G. E., and Schaefer III, H. F., 1988, *Chem. Phys. Lett.*, **152**, 382.
[24] Kucharski, S. A., and Bartlett, R. J., 1991, *Theor. Chim. Acta*, **80**, 387.
[25] Kucharski, S. A., and Bartlett, R. J., 1992, *J. chem. Phys.*, **97**, 4282.
[26] Oliphant, N., and Adamowicz, L., 1991, *J. chem. Phys.*, **95**, 6645.
[27] Piecuch, P., and Adamowicz, L., 1994, *J. chem. Phys.*, **100**, 5792.
[28] Musiał, M., Kucharski, S. A., and Bartlett, R. J., 2002, *J. chem. Phys.*, **116**, 4382.
[29] Pulay, P., 1983, *Chem. Phys. Lett.*, **100**, 151.
[30] Saebø, S., and Pulay, P., 1985, *Chem. Phys. Lett.*, **113**, 13.
[31] Saebø, S., and Pulay, P., 1993, *Annu. Rev. phys. Chem.*, **44**, 213.
[32] Schütz, M., 2000, *J. chem. Phys.*, **113**, 9986.
[33] Maslen, P. E., Lee, M. S., and Head-Gordon, M., 2000, *Chem. Phys. Lett.*, **319**, 205.
[34] Schütz, M., and Werner, H.-J., 2000, *Chem. Phys. Lett.*, **318**, 370.
[35] Schütz, M., 2002, *J. chem. Phys.*, **116**, 8772.
[36] Laidig, W. D., Saxe, P., and Bartlett, R. J., 1987, *J. chem. Phys.*, **86**, 887.
[37] Ghose, K. B., Piecuch, P., and Adamowicz, L., 1995, *J. chem. Phys.*, **103**, 9331.
[38] Piecuch, P., Špírko, V., Kondo, A. E., and Paldus, J., 1996, *J. chem. Phys.*, **104**, 4699.
[39] Piecuch, P., Kucharski, S. A., and Bartlett, R. J., 1999, *J. chem. Phys.*, **110**, 6103.
[40] Piecuch, P., Kucharski, S. A., and Špírko, V., 1999, *J. chem. Phys.*, **111**, 6679.
[41] Piecuch, P., and Kowalski, K., 2000, *Computational Chemistry: Reviews of Current Trends*, Vol. 5, edited by J. Leszczyński (Singapore: World Scientific), p. 1.
[42] Kowalski, K., and Piecuch, P., 2000, *J. chem. Phys.*, **113**, 18.
[43] Kowalski, K., and Piecuch, P., 2000, *J. chem. Phys.*, **113**, 5644.
[44] Kowalski, K., and Piecuch, P., 2001, *Chem. Phys. Lett.*, **344**, 165.
[45] Piecuch, P., Kucharski, S. A., and Kowalski, K., 2001, *Chem. Phys. Lett.*, **344**, 176.
[46] Piecuch, P., Kucharski, S. A., Špírko, V., and Kowalski, K., 2001, *J. chem. Phys.*, **115**, 5796.
[47] Piecuch, P., Kowalski, K., Pimienta, I. S. O., and Kucharski, S. A., 2002, *Low-Lying Potential Energy Surfaces*, ACS Symposium Series, Vol. 828, edited by M. R. Hoffmann and K. G. Dyall (Washington, DC: American Chemican Society), p. 31.
[48] Piecuch, P., Kowalski, K., and Pimienta, I. S. O., 2002, *Int. J. mol. Sci.*, **3**, 475.
[49] McGuire, M. J., Kowalski, K., and Piecuch, P., 2002, *J. chem. Phys.*, **117**, 3617.
[50] Lee, Y. S., and Bartlett, R. J., 1984, *J. chem. Phys.*, **80**, 4371.
[51] Lee, Y. S., Kucharski, S. A., and Bartlett, R. J., *J. chem. Phys.*, 1984, **81**, 5906; 1985, *J. chem. Phys.*, **82**, 5761 (erratum).
[52] Noga, J., Bartlett, R. J., and Urban, M., 1987, *Chem. Phys. Lett.*, **134**, 126.
[53] Trucks, G. W., Noga, J., and Bartlett, R. J., 1988, *Chem. Phys. Lett.*, **145**, 548.
[54] Kucharski, S. A., and Bartlett, R. J., 1989, *Chem. Phys. Lett.*, **158**, 550.
[55] Monkhorst, H., 1977, *Int. J. quantum Chem. Symp.*, **11**, 421.
[56] Sekino, H., and Bartlett, R. J., 1984, *Int. J. quantum Chem. Symp.*, **18**, 255.
[57] Dalgaard, E., and Monkhorst, H., 1983, *Phys. Rev.* A, **28**, 1217.
[58] Takahashi, M., and Paldus, J., 1986, *J. chem. Phys.*, **85**, 1486.
[59] Koch, H., and Jørgensen, P., 1990, *J. chem. Phys.*, **93**, 3333.

Downloaded At: 16:32 21 January 2011

[60] KOCH, H., JENSEN, H. J. AA., JØRGENSEN, P., and HELGAKER, T., 1990, *J. chem. Phys.*, **93**, 3345.
[61] GEERTSEN, J., RITTBY, M., and BARTLETT, R. J., 1989, *Chem. Phys. Lett.*, **164**, 57.
[62] COMEAU, D. C., and BARTLETT, R. J., 1993, *Chem. Phys. Lett.*, **207**, 414.
[63] STANTON, J. F., and BARTLETT, R. J., 1993, *J. chem. Phys.*, **98**, 7029.
[64] PIECUCH, P., and BARTLETT, R. J., 1999, *Adv. quantum Chem.*, **34**, 295.
[65] WATTS, J. D., and BARTLETT, R. J., 1995, *Chem. Phys. Lett.*, **233**, 81.
[66] WATTS, J. D., and BARTLETT, R. J., 1996, *Chem. Phys. Lett.*, **258**, 581.
[67] WATTS, J. D., and BARTLETT, R. J., 1994, *J. chem. Phys.*, **101**, 3073.
[68] KOCH, H., CHRISTIANSEN, O., JØRGENSEN, P., and OLSEN, J., 1995, *Chem. Phys. Lett.*, **244**, 75.
[69] CHRISTIANSEN, O., KOCH, H., and JØRGENSEN, P., 1995, *J. chem. Phys.*, **103**, 7429.
[70] CHRISTIANSEN, O., KOCH, H., and JØRGENSEN, P., 1996, *J. chem. Phys.*, **105**, 1451.
[71] CHRISTIANSEN, O., KOCH, H., JØRGENSEN, P., and OLSEN, J., 1996, *Chem. Phys. Lett.*, **256**, 185.
[72] LARSEN, H., OLSEN, J., JØRGENSEN, P., and CHRISTIANSEN, O., 2000, *J. chem. Phys.*, **113**, 6677; 2001, *J. chem. Phys.*, **114**, 10985 (erratum).
[73] HALD, K., JØRGENSEN, P., OLSEN, J., and JASZUŃSKI, M., 2001, *J. chem. Phys.*, **115**, 671.
[74] KOWALSKI, K., and PIECUCH, P., 2000, *J. chem. Phys.*, **113**, 8490.
[75] KOWALSKI, K., and PIECUCH, P., 2001, *J. chem. Phys.*, **115**, 643.
[76] KOWALSKI, K., and PIECUCH, P., 2001, *Chem. Phys. Lett.*, **347**, 237.
[77] KOWALSKI, K., and PIECUCH, P., 2001, *J. chem. Phys.*, **115**, 2966.
[78] KOWALSKI, K., and PIECUCH, P., 2002, *J. chem. Phys.*, **116**, 7411.
[79] KRYLOV, A. I., SHERRILL, C. D., and HEAD-GORDON, M., 2000, *J. chem. Phys.*, **113**, 6509.
[80] KUCHARSKI, S. A., WŁOCH, M., MUSIAŁ, M., and BARTLETT, R. J., 2001, *J. chem. Phys.*, **115**, 8263.
[81] PIECUCH, P., KOWALSKI, K., FAN, P.-D., and KUCHARSKI, S. A., *Theor. Chem. Acc.*, (in preparation).
[82] JEZIORSKI, B., and MONKHORST, H. J., 1981, *Phys. Rev.* A, **24**, 1668.
[83] JEZIORSKI, B., and PALDUS, J., 1988, *J. chem. Phys.*, **88**, 5673.
[84] MEISSNER, L., JANKOWSKI, K., and WASILEWSKI, J., 1988, *Int. J. quantum Chem.*, **34**, 535.
[85] PALDUS, J., PYLYPOW, L., and JEZIORSKI, B., 1989, *Many-Body Methods in Quantum Chemistry*, Lecture Notes in Chemistry, Vol. 52, edited by U. Kaldor (Berlin: Springer), p. 151.
[86] KUCHARSKI, S. A., and BARTLETT, R. J., 1991, *J. chem. Phys.*, **95**, 8227.
[87] BALKOVÁ, A., KUCHARSKI, S. A., MEISSNER, L., and BARTLETT, R. J., 1991, *Theor. Chim. Acta*, **80**, 335.
[88] BALKOVÁ, A., KUCHARSKI, S. A., and BARTLETT, R. J., 1991, *Chem. Phys. Lett.*, **182**, 511.
[89] PIECUCH, P., and PALDUS, J., 1992, *Theor. Chim. Acta*, **83**, 69.
[90] PALDUS, J., PIECUCH, P., JEZIORSKI, B., and PYLYPOW, L., 1992, *Recent Progress in Many-Body Theories*, Vol. 3, edited by T. L. Ainsworthy, C. E. Campbell, B. E. Clements and E. Krotschek (New York: Plenum), p. 287.
[91] PALDUS, J., PIECUCH, P., PYLYPOW, L., and JEZIORSKI, B., 1993, *Phys. Rev.* A, **47**, 2738.
[92] PIECUCH, P., and PALDUS, J., 1994, *Phys. Rev.* A, **49**, 3479.
[93] PIECUCH, P., and PALDUS, J., 1994, *J. chem. Phys.*, **101**, 5875.
[94] KOWALSKI, K., and PIECUCH, P., 2000, *Phys. Rev.* A, **61**, 052506.
[95] PIECUCH, P., and LANDMAN, J. I., 2000, *Parallel Comput.*, **26**, 913.
[96] KOWALSKI, K., and PIECUCH, P., 2001, *Chem. Phys. Lett.*, **334**, 89.
[97] KOWALSKI, K., and PIECUCH, P., 2001, *J. mol. Struct.: THEOCHEM*, **547**, 191.
[98] PIECUCH, P., and KOWALSKI, K., 2002, *Int. J. mol. Sci.*, **3**, 676.
[99] LINDGREN, I., and MUKHERJEE, D., 1987, *Phys. Rep.*, **151**, 93.
[100] MUKHERJEE, D., and PAL, S., 1989, *Adv. quantum Chem.*, **20**, 291.
[101] JEZIORSKI, B., and PALDUS, J., 1989, *J. chem. Phys.*, **90**, 2714.

Downloaded At: 16:32 21 January 2011

[102] Bernholdt, D. E., and Bartlett, R. J., 1999, *Adv. quantum Chem.*, **34**, 271.
[103] Jankowski, K., Paldus, J., Grabowski, I., and Kowalski, K., 1992, *J. chem. Phys.*, **97**, 7600; 1994, *J. chem. Phys.*, **101**, 1759 (erratum).
[104] Jankowski, K., Paldus, J., Grabowski, I., and Kowalski, K., 1994, *J. chem. Phys.*, **101**, 3085.
[105] Mahapatra, U. S., Datta, B., and Mukherjee, D., 1998, *Mol. Phys.*, **94**, 157.
[106] Mahapatra, U. S., Datta, B., and Mukherjee, D., 1999, *J. chem. Phys.*, **110**, 6171.
[107] Mach, P., Máşik, J., Urban, J., and Hubač, I., 1998, *Mol. Phys.*, **94**, 173.
[108] Máşik, J., and Hubač, I., 1999, *Adv. quantum Chem.*, **31**, 75.
[109] Pittner, J., Nachtigall, P., Čársky, P., Máşik, J., and Hubač, I., 1999, *J. chem. Phys.*, **110**, 10275.
[110] Hubač, I., Pittner, J., and Čársky, P., 2000, *J. chem. Phys.*, **112**, 8779.
[111] Sancho-Garcia, J. C., Pittner, J., Čársky, P., and Hubač, I., 2000, *J. chem. Phys.*, **112**, 8785.
[112] Pittner, J., Nachtigall, P., Čársky, P., and Hubač, I., 2001, *J. phys. Chem.* A, **105**, 1354.
[113] Nooijen, M., and Lotrich, V., 2001, *J. mol. Struct.: THEOCHEM*, **547**, 253.
[114] Nooijen, M., and Lotrich, V., 2000, *J. chem. Phys.*, **113**, 4549.
[115] Nooijen, M., and Bartlett, R. J., 1997, *J. chem. Phys.*, **106**, 6441.
[116] Nooijen, M., and Bartlett, R. J., 1997, *J. chem. Phys.*, **106**, 6449.
[117] Nooijen, M., and Bartlett, R. J., 1997, *J. chem. Phys.*, **107**, 6812.
[118] Nooijen, M., 2000, *J. phys. Chem. A*, **104**, 4553.
[119] Nooijen, M., and Lotrich, V., 2000, *J. chem. Phys.*, **113**, 494.
[120] Li, X., and Paldus, J., 1997, *J. chem. Phys.*, **107**, 6257.
[121] Li, X., and Paldus, J., 1998, *J. chem. Phys.*, **108**, 637.
[122] Li, X., and Paldus, J., 1998, *Chem. Phys. Lett.*, **286**, 145.
[123] Li, X., and Paldus, J., 1999, *J. chem. Phys.*, **110**, 2844.
[124] Li, X., and Paldus, J., 2000, *Mol. Phys.*, **98**, 1185.
[125] Li, X., and Paldus, J., 2000, *J. chem. Phys.*, **113**, 9966.
[126] Li, X., 2001, *J. mol. Struct.: THEOCHEM*, **547**, 69.
[127] Oliphant, N., and Adamowicz, L., 1991, *J. chem. Phys.*, **94**, 1229.
[128] Oliphant, N., and Adamowicz, L., 1992, *J. chem. Phys.*, **96**, 3739.
[129] Oliphant, N., and Adamowicz, L., 1993, *Int. Rev. phys. Chem.*, **12**, 339.
[130] Piecuch, P., Oliphant, N., and Adamowicz, L., 1993, *J. chem. Phys.*, **99**, 1875.
[131] Piecuch, P., and Adamowicz, L., 1994, *Chem. Phys. Lett.*, **221**, 121.
[132] Piecuch, P., and Adamowicz, L., 1995, *J. chem. Phys.*, **102**, 898.
[133] Ghose, K. B., and Adamowicz, L., 1995, *J. chem. Phys.*, **103**, 9324.
[134] Ghose, K. B., Piecuch, P., Pal, S., and Adamowicz, L., 1996, *J. chem. Phys.*, **104**, 6582.
[135] Adamowicz, L., Piecuch, P., and Ghose, K. B., 1998, *Mol. Phys.*, **94**, 225.
[136] Olsen, J., 2000, *J. chem. Phys.*, **113**, 7140.
[137] Krogh, J. W., and Olsen, J., 2001, *Chem. Phys. Lett.*, **344**, 578.
[138] Sherrill, C. D., Krylov, A. I., Byrd, E. F. C., and Head-Gordon, M., 1998, *J. chem. Phys.*, **109**, 4171.
[139] Krylov, A. I., Sherrill, C. D., Byrd, E. F. C., and Head-Gordon, M., 1998, *J. chem. Phys.*, **109**, 10669.
[140] Gwaltney, S. R., and Head-Gordon, M., 2000, *Chem. Phys. Lett.*, **323**, 21.
[141] Gwaltney, S. R., Sherrill, C. D., Head-Gordon, M., and Krylov, A. I., 2000, *J. chem. Phys.*, **113**, 3548.
[142] Gwaltney, S. R., and Head-Gordon, M., 2001, *J. chem. Phys.*, **115**, 2014.
[143] Gwaltney, S. R., Byrd, E. F. C., Van Voorhis, T., and Head-Gordon, M., 2002, *Chem. Phys. Lett.*, **353**, 359.
[144] Stanton, J. F., 1997, *Chem. Phys. Lett.*, **281**, 130.
[145] Krylov, A. I., 2001, *Chem. Phys. Lett.*, **338**, 375.
[146] Krylov, A. I., and Sherrill, C. D., 2002, *J. chem. Phys.*, **116**, 3194.
[147] Slipchenko, L. V., and Krylov, A. I., 2002, *J. chem. Phys.*, **117**, 4694.
[148] Bartlett, R. J., and Purvis III, G. D., 1980, *Phys. Scr.*, **21**, 255.
[149] Paldus, J., Čížek, J., and Takahashi, M., 1984, *Phys. Rev.* A, **30**, 2193.

Downloaded At: 16:32 21 January 2011

[150] PIECUCH, P., TOBOŁA, R., and PALDUS, J., 1996, *Phys. Rev.* A, **54**, 1210.
[151] PALDUS, J., and PLANELLES, J., 1994, *Theor. Chim. Acta*, **89**, 13.
[152] PERIS, G., PLANELLES, J., and PALDUS, J., 1997, *Int. J. quantum Chem.*, **62**, 137.
[153] STOLARCZYK, L., 1994, *Chem. Phys. Lett.*, **217**, 1.
[154] KANTOROVICH, L. V., and KRYLOV, V. I., 1958, *Approximate Methods of Higher Analysis* (New York: Interscience), p. 150.
[155] JANKOWSKI, K., PALDUS, J., and PIECUCH, P., 1991, *Theor. Chim. Acta*, **80**, 223.
[156] LI, X., and PALDUS, J., 2001, *J. chem. Phys.*, **115**, 5759.
[157] LI, X., and PALDUS, J., 2001, *J. chem. Phys.*, **115**, 5774.
[158] PIECUCH, P., KUCHARSKI, S. A., KOWALSKI, K., and MUSIAŁ, M., 2002, *Comput. Phys. Commun.*, **149**, 71.
[159] SCHMIDT, M. W., BALDRIDGE, K. K., BOATZ, J. A., ELBERT, S. T., GORDON, M. S., JENSEN, J. H., KOSEKI, S., MATSUNAGA, N., NGUYEN, K. A., SU, S. J., WINDUS, T. L., DUPUIS, M., and MONTGOMERY, J. A., 1993, *J. comput. Chem.*, **14**, 1347.
[160] LI, X., and PALDUS, J., 2002, *J. chem. Phys.*, **117**, 1941.
[161] PIECUCH, P., PIMIENTA, I. S. O., FAN, P.-D., and KOWALSKI, K., 2003, *Recent Progress in Electron Correlation Methodology*, ACS Symposium series, vol. XXX, edited by A. K. Wilson (Washington, DC: American Chemical Society), p. xxx, in press.
[162] BUENKER, R. J., and PEYERIMHOFF, S. D., 1974, *Theor. Chim. Acta*, **35**, 33.
[163] BUENKER, R. J., and PEYERIMHOFF, S. D., 1975, *Theor. Chim. Acta*, **39**, 217.
[164] BRUNA, P. J., and PEYERIMHOFF, S. D., 1987, *Adv. chem. Phys.*, **67**, 1.
[165] DUNNING, T. H., 1970, *J. chem. Phys.*, **53**, 2823.
[166] SAXE, P., SCHAEFER III, H. F., and HANDY, N. C., 1981, *Chem. Phys. Lett.*, **79**, 202.
[167] HARRISON, R. J., and HANDY, N. C., 1983, *Chem. Phys. Lett.*, **95**, 386.
[168] OLSEN, J., SÁNCHEZ DE MERÁS, A. M., JENSEN, H. J. AA., and JØRGENSEN, P., 1989, *Chem. Phys. Lett.*, **154**, 380.
[169] DUNNING JR., T. H., 1989, *J. chem. Phys.*, **90**, 1007.
[170] KENDALL, R. A., DUNNING JR., T. H., and HARRISON, R. J., 1992, *J. chem. Phys.*, **96**, 6796.
[171] PIMIENTA, I. S. O., KOWALSKI, K., and PIECUCH, P., unpublished results.
[172] MUSIAŁ, M., KUCHARSKI, S. A., and BARTLETT, R. J., 2000, *Chem. Phys. Lett.*, **320**, 542.
[173] MEISSNER, L., and BARTLETT, R. J., 2001, *J. chem. Phys.*, **115**, 50.
[174] BARTLETT, R. J., WATTS, J. D., KUCHARSKI, S. A., and NOGA, J., 1990, *Chem. Phys. Lett.*, **165**, 513.
[175] KUCHARSKI, S. A., and BARTLETT, R. J., 1986, *Adv. quantum Chem.*, **18**, 281.
[176] RAGHAVACHARI, K., POPLE, J. A., REPLOGLE, E. S., and HEAD-GORDON, M., 1990, *J. phys. Chem.*, **94**, 5579.
[177] HUBER, K. P., and HERZBERG, G., 1979, *Molecular Spectra and Molecular Structure*, Vol. 4, *Constants of Diatomic Molecules* (New York: Van Nostrand).
[178] COLBOURN, E. A., DAGENAIS, M., DOUGLAS, A. E., and RAYMONDA, J. W., 1976, *Can. J. Phys.*, **54**, 1343.
[179] AMOS, R. D., BERNHARDSSON, A., BERNING, A., CELANI, P., COOPER, D. L., DEEGAN, M. J. O., DOBBYN, A. J., ECKERT, F., HAMPEL, C., HETZER, G., KNOWLES, P. J., KORONA, T., LINDH, R., LLOYD, A. W., MCNICHOLAS, S. J., MANBY, F. R., MEYER, W., MURA, M. E., NICKLASS, A., PALMIERI, P., PITZER, R., RAUHUT, G., SCHÜTZ, M., SCHUMANN, U., STOLL, H., STONE, A. J., TARRONI, R., THORSTEINSSON, T., and WERNER, H.-J., MOLPRO, a package of *ab initio* programs designed by H.-J. Werner and P. J. Knowles, version 2002.1.
[180] WERNER, H.-J., and KNOWLES, P. J., 1988, *J. chem. Phys.*, **89**, 5803.
[181] KNOWLES, P. J., and WERNER, H.-J., 1988, *Chem. Phys. Lett.*, **145**, 514.
[182] ROOS, B. O., LINSE, P., SIEGBAHN, P. E. M., and BLOMBERG, M. R. A., 1982, *Chem. Phys.*, **66**, 197.
[183] ANDERSSON, K., MALMQVIST, P.-Å., ROOS, B. O., SADLEJ, A. J., and WOLIŃSKI, K., 1990, *J. phys. Chem.*, **94**, 5483.
[184] ANDERSSON, K., MALMQVIST, P.-Å., and ROOS, B. O., 1992, *J. chem. Phys.*, **96**, 1218.
[185] WOLIŃSKI, K., SELLERS, H. L., and PULAY, P., 1987, *Chem. Phys. Lett.*, **140**, 225.
[186] WOLIŃSKI, K., and PULAY, P., 1989, *J. chem. Phys.*, **90**, 3647.

Downloaded At: 16:32 21 January 2011

[187] Hirao, K., 1992, *Int. J. quantum Chem. Symp.*, **26**, 517.
[188] Hirao, K., 1992, *Chem. Phys. Lett.*, **190**, 374.
[189] Kozłowski, P. M., and Davidson, E. R., 1994, *J. chem. Phys.*, **100**, 3672.
[190] Kozłowski, P. M., and Davidson, E. R., 1994, *Chem. Phys. Lett.*, **222**, 615.
[191] Werner, H.-J., 1996, *Mol. Phys.*, **89**, 645.
[192] Rydberg, R., 1931, *Z. Phys.*, **73**, 376.
[193] Rydberg, R., 1933, *Z. Phys.*, **80**, 514.
[194] Klein, O., 1932, *Z. Phys.*, **76**, 226.
[195] Rees, A. L. G., 1947, *Proc. phys. Soc.*, **59**, 998.
[196] Piecuch, P., Kowalski, K., Kucharski, S. A., Musiał, M., and Špirko, V., unpublished results.
[197] Coxon, J. A., and Hajigeorgiou, P. G., 1990, *J. mol. Spectrosc.*, **142**, 254.
[198] Zemke, W. T., Stwalley, W. C., Coxon, J. A., and Hajigeorgiou, P. G., 1991, *Chem. Phys. Lett.*, **177**, 412.
[199] Zemke, W. T., Stwalley, W. C., Langhoff, S. R., Valderrama, G. L., and Berry, M. J., 1991, *J. chem. Phys.*, **95**, 7846.
[200] Schor, H., Chapman, S., Green, S., and Zare, R. N., 1978, *J. chem. Phys.*, **69**, 3790.
[201] Chapman, S., Dupuis, M., and Green, S., 1983, *Chem. Phys.*, **78**, 93.
[202] Aguado, A., Sanz, V., and Paniagua, M., 1997, *Int. J. quantum Chem.*, **61**, 491.
[203] Kuntz, P. J., and Roach, A. C., 1981, *J. chem. Phys.*, **74**, 3420.
[204] Roach, A. C., and Kuntz, P. J., 1981, *J. chem. Phys.*, **74**, 3435.
[205] Kuntz, P. J., and Schreiber, J. L., 1982, *J. chem. Phys.*, **76**, 4120.
[206] Garcia, E., and Lagana, A., 1985, *Mol. Phys.*, **56**, 629.
[207] Liu, X., and Murrell, J. N., 1991, *J. Chem. Soc., Faraday Trans.*, **87**, 435.
[208] Aguado, A., Sieiro, C., and Paniagua, M., 1992, *J. mol. Struct.: THEOCHEM*, **260**, 179.
[209] Huzinaga, S., Andzelm, J., Kłobukowski, M., Radzio-Andzelm, E., Sakai, Y., and Tatewaki, H., 1984, *Gaussian Basis Sets for Molecular Calculations* (Amsterdam: Elsevier).
[210] McGuire, M. J., Piecuch, P., and Kowalski, K., unpublished results.
[211] Paldus, J., 1983, *New Horizons of Quantum Chemistry*, edited by P.-O. Löwdin and B. Pullman (Dordrecht: Reidel), p. 31.
[212] Buenker, R. J., and Peyerimhoff, S. D., 1983, *New Horizons of Quantum Chemistry*, edited by P.-O. Löwdin and B. Pullman (Dordrecht: Reidel), p. 183.
[213] Bruna, P. J., Peyerimhoff, S. D., and Buenker, R. J., 1980, *Chem. Phys. Lett.*, **72**, 278.
[214] Jankowski, K., Meissner, L., and Wasilewski, J., 1985, *Int. J. quantum Chem.*, **28**, 931.
[215] Van Voorhis, T., and Head-Gordon, M., 2000, *J. chem. Phys.*, **113**, 8873.
[216] Van Voorhis, T., and Head-Gordon, M., 2000, *Chem. Phys. Lett.*, **330**, 585.
[217] Arponen, J. S., 1983, *Ann. Phys.*, **151**, 311.
[218] Arponen, J. S., Bishop, R. F., and Pajanne, E., 1987, *Phys. Rev.* A, **36**, 2519.
[219] Arponen, J. S., Bishop, R. F., and Pajanne, E., 1987, *Condensed Matter Theory*, **2**, 357.
[220] Bishop, R. F., Arponen, J. S., and Pajanne, E., 1989, *Aspects of Many-Body Effects in Molecules and Extended Systems*, Lecture Notes in Chemistry, Vol. 50, edited by D. Mukherjee (Berlin: Springer), p. 79.
[221] Bishop, R. F., and Arponen, J. S., 1990, *Int. J. quantum Chem. Symp.*, **24**, 197.
[222] Arponen, J. S., and Bishop, R. F., 1991, *Ann. Phys.*, **207**, 171.
[223] Bishop, R. F., Robinson, N. I., and Arponen, J. S., 1990, *Condensed Matter Theory*, **5**, 37,
[224] Bishop, R. F., 1991, *Theor. Chim. Acta*, **80**, 95.
[225] Arponen, J. S., 1997, *Phys. Rev.* A, **55**, 2686.
[226] Arponen, J. S., Bishop, R. F., and Pajanne, E., 1987, *Phys. Rev.* A, **36**, 2539.
[227] Bartlett, R. J., and Noga, J., 1988, *Chem. Phys. Lett.*, **150**, 29.
[228] Bartlett, R. J., Kucharski, S. A., Noga, J., Watts, J. D., and Trucks, G. W., 1989, *Many-Body Methods in Quantum Chemistry*, Lecture Notes in Chemistry, Vol. 52, edited by U. Kaldor (Berlin: Springer), p. 124.

Downloaded At: 16:32 21 January 2011

[229] BRUECKNER, K. A., 1955, *Phys. Rev.*, **100**, 36.
[230] GOLDSTONE, J., 1957, *Proc. R. Soc.* A, **239**, 267.
[231] HUBBARD, J., 1957, *Proc. R. Soc.* A, **240**, 539.
[232] HUBBARD, J., 1958, *Proc. R. Soc.* A, **243**, 336.
[233] HUBBARD, J., 1958, *Proc. R. Soc.* A, **244**, 199.
[234] JENSEN, J. H., and GORDON, M. S., 1991, *J. Am. Chem. Soc.*, **113**, 7917.
[235] HEHRE, W. J., DITCHFIELD, R., and POPLE, J. A., 1972, *J. chem. Phys.*, **56**, 2257.
[236] MEISSNER, L., and BARTLETT, R. J., 1991, *J. chem. Phys.*, **94**, 6670.
[237] MUKHOPADHYAY, D., MUKHOPADHYAY, S., CHAUDHURI, R., and MUKHERJEE, D., 1991, *Theor. Chim. Acta*, **80**, 441.
[238] MEISSNER, L., and BARTLETT, R. J., 1995, *J. chem. Phys.*, **102**, 7490.
[239] STANTON, J. F., 1994, *J. chem. Phys.*, **101**, 8928.
[240] SCUSERIA, G. E., 1991, *J. chem. Phys.*, **94**, 442.
[241] LEE, T. J., and RENDELL, A. P., 1991, *J. chem. Phys.*, **94**, 6229.
[242] WATTS, J. D., GAUSS, J., and BARTLETT, R. J., 1993, *J. chem. Phys.*, **98**, 8718.
[243] WATTS, J. D., GAUSS, J., and BARTLETT, R. J., 1992, *Chem. Phys. Lett.*, **200**, 1.
[244] GAUSS, J., and STANTON, J. F., 1997, *Chem. Phys. Lett.*, **276**, 70.
[245] STANTON, J. F., PIECUCH, P., and KOWALSKI, K., unpublished results.
[246] KUTZELNIGG, W., 1985, *Theor. Chim. Acta*, **68**, 445.
[247] KUTZELNIGG, W., and KLOPPER, W., 1991, *J. chem. Phys.*, **94**, 1985.
[248] KLOPPER, W., 1998, *The Encyclopedia of Computational Chemistry*, edited by P. v. R. Schleyer, N. L. Allinger, T. Clark, J. Gasteiger, P. A. Kollman and H. F. Schaefer III (Chichester: Wiley), p. 2351.
[249] NOGA, J., KUTZELNIGG, W., and KLOPPER, W., 1992, *Chem. Phys. Lett.*, **199**, 497.
[250] NOGA, J., and KUTZELNIGG, W., 1994, *J. chem. Phys.*, **101**, 7738.
[251] NOGA, J., KLOPPER, W., and KUTZELNIGG, W., 1997, *Recent Advances in Coupled-Cluster Methods*, Vol. 3, edited by R. J. Bartlett (Singapore: World Scientific), p. 1.
[252] MÜLLER, H., FRANKE, R., VOGTNER, S., JAQUET, R., and KUTZELNIGG, W., 1998, *Theor. Chem. Acc.*, **100**, 85.
[253] FRANKE, R., MÜLLER, H., and NOGA, J., 2001, *J. chem. Phys.*, **114**, 7746.
[254] NOGA, J., VALIRON, P., and KLOPPER, W., 2001, *J. chem. Phys.*, **115**, 2022.
[255] ALMLÖF, J., 1991, *Chem. Phys. Lett.*, **181**, 319.
[256] CONSTANS, P., AYALA, P. Y., and SCUSERIA, G. E., 2000, *J. chem. Phys.*, **113**, 10451.
[257] KOWALSKI, K., and PIECUCH, P., unpublished results.

Downloaded At: 16:32 21 January 2011